

Proceedings of the Eighteenth Annual Pacific Climate Workshop

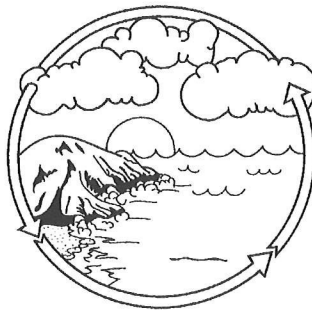
Asilomar Conference Grounds
Pacific Grove, California
March 18–21, 2001

Edited by
G. James West and Lauren D. Buffaloe

Technical Report 69
of the
Interagency Ecological Program for the
San Francisco Estuary

March 2002

PACLIM



Climate Variability
of the
Eastern North Pacific
and
Western North America

Single copies of this report may be obtained without charge from:

State of California
Department of Water Resources
P.O. Box 942836
Sacramento, CA 94236-0001

Proceedings of the Eighteenth Annual Pacific Climate Workshop

Asilomar Conference Grounds
Pacific Grove, California
March 18–21, 2001

Edited by
G. James West and Lauren D. Buffaloe

Technical Report 69
of the
Interagency Ecological Program for the
San Francisco Estuary

March 2002

PACLIM



Climate Variability
of the
Eastern North Pacific
and
Western North America

Contents

| | |
|--|------------|
| Authors | v |
| Acknowledgments | vii |
| Statement of Purpose | ix |
| Dedication | xi |
| Introduction | 1 |
| G. James West | |
| Summary | 3 |
| Mike Dettinger | |
| Holocene Ocean-Climate Variations in Alfonso Basin, Gulf of California, Mexico | 7 |
| Robert G. Douglas, Donn Gorsline, Alessandro Grippo, Ivette Granados, and Oscar Gonzalez-Yajimovich | |
| The Impacts of Current and Past Climate on Pacific Gas & Electric's 2001 Hydroelectric Outlook | 21 |
| Gary J. Freeman | |
| Snowfall Occurrence at Two Lee-Side Mountain Locations: Comparing the Sierra Nevada, California, and the Rocky Mountains, Colorado | 39 |
| Mark Losleben, Susan Burak, Robert E. Davis, and Karla Adami | |
| Primary Modes and Predictability of Year-to-Year Snowpack Variations in the Western United States from Teleconnections with Pacific Ocean Climate | 47 |
| Gregory J. McCabe and Michael D. Dettinger | |
| Response of High-Elevation Conifers in the Sierra Nevada, California, to 20th Century Decadal Climate Variability | 57 |
| Constance I. Millar, Lisa J. Graumlich, Diane L. Delany, Robert D. Westfall, and John C. King | |

| | |
|---|------------|
| The Modern Distribution of Midge Flies in Eastern Sierra Nevada, California, Lakes: Potential for Paleoclimatic Reconstruction | 61 |
| David F. Porinchu and Glen M. MacDonald | |
| Water Year 2001 in Northern California: Have the Good Years Ended? . . | 71 |
| Maurice Roos | |
| Major Flood Events of the Past 2,000 Years Recorded in Santa Barbara Basin Sediment | 83 |
| Arndt Schimmelmann, Carina B. Lange, and Hong-Chun Li | |
| The New Regimes: Fish Stories | 105 |
| Gary D. Sharp, James D. Goodridge, Leonid B. Klyashtorin, and Alexey V. Nikolaev | |
| Diatoms as Indicators of Freshwater Flow Variation in Central California | 129 |
| Scott W. Starratt | |
| Abstracts | 145 |
| Appendix A: Agenda | 187 |
| Appendix B: Poster Presentations | 195 |
| Appendix C: Participants | 199 |

Authors

Karla Adami
Mountain Research Station, INSTAAR
University of Colorado
Boulder, CO 30303

Susan Barak
Snow Survey Associates
P.O. Box 8544
Mammoth Lakes, CA 93546

Robert E. Davis
U.S. Army Engineering Research and
Development Center, USA-CRREL
72 Lyme Road
Hanover, NH 03755-1290

Diane L. Delany
U.S. Dept. of Agriculture Forest Service
Pacific Southwest Research Station
Albany, CA 94710

Michael D. Dettinger
U.S. Geological Survey
Scripps Institution of Oceanography, MS 0-224
9500 Gilman Drive
La Jolla, CA 92093

Robert G. Douglas
Dept. of Earth Sciences
University of Southern California
Los Angeles, CA 90089-0740

Gary J. Freeman
Pacific Gas & Electric Company
Room 1308, Mail code N13C
245 Market Street
San Francisco, CA 94105

Ivette Granados
Instituto Politenico Nacional
Centro de Interdisciplinario Ciencias Marinas
La Paz, Baja California Sur, Mexico 23000

Alessandro Grippo
Dept. of Earth Sciences
University of Southern California
Los Angeles, CA 90089-0740

Oscar Gonzalez-Yajimovich
Dept. of Earth Sciences
University of Southern California
Los Angeles, CA 90089-0740

James D. Goodridge
P.O. Box 750
Mendocino, CA 95460

Donn Gorsline
Dept. of Earth Sciences
University of Southern California
Los Angeles, CA 90089-0740

Lisa J. Graumlich
Mountain Research Center
Montana State University
Bozeman, MT 59717

John C. King
Laboratory of Tree-Ring Research
University of Arizona
Tucson, AZ 85721

Leonid B. Klyashtorin
Federal Institute for Fisheries and
Oceanography (VNIRO)
Moscow, Russia

Carina B. Lange
Scripps Institution of Oceanography
GRD and IOD
La Jolla, CA 92093

2001 PACLIM Conference Proceedings

Hong-Chun Li
Dept. of Earth Sciences
University of Southern California, Los Angeles
3651 Trousdale Parkway
Los Angeles, CA 90089-0740

Mark Losleben
Mountain Research Station, INSTAAR
University of Colorado
Boulder, CO 30303

Glen M. MacDonald
Dept. of Geography
University of California, Los Angeles
1255 Bunche Hall
Los Angeles, CA 90095

Gregory J. McCabe
U.S. Geological Survey
Denver Federal Center, MS-412
Denver, CO 80225

Constance I. Millar
U.S. Dept. of Agriculture Forest Service
Pacific Southwest Research Station
Albany, CA 94710

Alexey V. Nikolaev
Institute of Physics of the Earth Russian
Academy of Sciences
Moscow, Russia

David F. Porinchu
Dept. of Geography
University of California, Los Angeles
1255 Bunche Hall
Los Angeles, CA 90095

Arndt Schimmelman
Dept. of Geological Sciences
Indiana University
1001 East 10th Street
Bloomington, IN 47405-1405

Gary D. Sharp
Center for Climate/Ocean Resources Study
P.O. Box 2223
Monterey, CA 93940

Scott W. Starratt
U.S. Geological Survey
345 Middlefield Road
Menlo Park, CA 94025

(and) Dept. of Geography
University of California, Berkeley
Berkeley, CA 94720

Robert D. Westfall
U.S. Dept. of Agriculture Forest Service
Pacific Southwest Research Station
Albany, CA 94710

Acknowledgments

PACLIM workshops are produced by volunteers who always manage to put together a topically interesting and timely gathering of a wide range of research. The 2001 workshop had the largest number of participants, many for the first time, and continued a tradition started almost two decades ago by providing a forum for new ideas, information, and concepts.

For 2001, thanks go to the following institutions and people: USGS: Mike Dettinger, Program Chair; Long Beach City College: Janice Tomson, Meeting Organizer; University of Arizona, Laboratory of Tree-Ring Research: Malcolm Hughes and Robin Webb; NOAA-OAR-CDC: Henry Diaz; Scripps Institution of Oceanography: Dan Cayan, Program Chair Emeritus; USC: Lowell Stott; AGU: Sandra Williams.

Sponsorship and funding for the workshops come from a wide variety of sources. This year's PACLIM Workshop was sponsored by: U.S. Geological Survey Water Resources Division, Bill Kirby; U.S. Geological Survey Geological Research Division, Elliot Spiker; NOAA Office of Global Programs, Roger Pulwarty; CALFED Bay-Delta Science Program, Sam Luoma; American Geophysical Union, Sandra Williams; State of California Department of Water Resources, Barbara McDonnell.

For the fourth year, Mike Dettinger chaired and organized the meeting and maintained the web page. As she has done previously, Janice Tomson did a superb job of planning, organizing, and supervising the operation of the meeting—getting us there, getting us fed, watered, and roomed, and, with her Long Beach City College students, doing all the other numerous things that need to be done to make a successful meeting. Lucenia Thomas, USGS Water Resources Division, arranged travel and assisted in the meeting organization. Tom Murphree, Naval Postgraduate School, provided and set up the audio-visual equipment. The meeting moderators are also greatly acknowledged. Finally, we thank all our speakers and poster presenters (see Appendix A: Agenda) for their contributions and enthusiasm.

For the production and printing of the proceedings, thanks go once again to the California Department of Water Resources Interagency Ecological Program for the Sacramento-San Joaquin Estuary. The production of this volume was performed by my co-editor, Lauren Buffaloe, whom I thank for her special expertise and knowledge. Katherine West assisted in editing several of the papers.

The precedents for the 2001 volume were established by the previous editors of the PACLIM Proceedings: Dave Peterson (1984-88), with the able assistance of Lucenia Thomas; Julio Betancourt and Ana MacKay (1989-90); Kelly Redmond and Vera Tharp (1991-93); Caroline Isaacs and Vera Tharp (1994-96); Ray Wilson and Vera Tharp (1997); Ray Wilson and Lauren Buffaloe (1998); G. James West and Lauren Buffaloe (1999-2000).

G. James West
U.S. Bureau of Reclamation

Statement of Purpose

In 1984, a workshop was held on "Climatic Variability of the Eastern North Pacific and Western North America." From it has emerged an annual series of workshops held at Asilomar Conference Grounds at Pacific Grove, California, and the Wrigley Institute for Environmental Studies at Two Harbors, Santa Catalina Island, California. These annual meetings, which involve 80–100 participants, have come to be known as the Pacific Climate (PACLIM) Workshops, reflecting broad interests in the climatologies associated with the Pacific Ocean and western Americas in both the northern and southern hemispheres. Participants have included atmospheric scientists, hydrologists, glaciologists, oceanographers, limnologists, and both marine and terrestrial biologists. A major goal of PACLIM is to provide a forum for exploring the insights and perspectives of each of these many disciplines and for understanding the critical linkages between them.

PACLIM arose from growing concern about climate variability and its societal and ecological impacts. Storm frequency, snowpack, droughts and floods, agricultural production, water supply, glacial advances, stream chemistry, sea surface temperature, salmon catch, lake ecosystems, and wildlife habitat are among the many aspects of climate and climatic impacts addressed by PACLIM Workshops. Workshops also address broad concerns about the impact of possible climate change over the next century. From observed changes in the historical records, the conclusion is evident that climate change would have large societal impacts through effects on global ecology, hydrology, geology, and oceanography.

Our ability to predict climate, climate variability, and climate change critically depends on an understanding of global processes. Human impacts are primarily terrestrial in nature, but the major forcing processes are atmospheric and oceanic in origin and transferred through geologic and biologic systems. Our understanding of the global climate system and its relationship to ecosystems in the Eastern Pacific area arises from regional study of its components in the Pacific Ocean and western Americas, where ocean-atmosphere coupling is strongly expressed. Empirical evidence suggests that large-scale climatic fluctuations force large-scale ecosystem response in the California current and, in a very different system, the North Pacific central gyre. With such diverse meteorologic phenomena as the El Niño–Southern Oscillation and shifts in the Aleutian Low and North Pacific High, the eastern Pacific has tremendous global influences and particularly strong effects on North America. In the western US, where rainfall is primarily a cool-season phenomenon, year-to-year changes in the activity and tracking of North Pacific winter storms have substantial influence on the hydrological balance. This region is rich in climatic records, both instrumental and proxy. Recent research efforts are beginning to focus on better paleoclimatic reconstructions that will put present-day climatic variability in context and allow better anticipation of future variations and changes.

The PACLIM Workshops address the problem of defining regional coupling of multifold elements as organized by global phenomena. Because climate expresses itself throughout the natural system, our activity has been, from the beginning, multidisciplinary in scope. The specialized knowledge from different disciplines has brought together climatic records and process measurements to synthesize and understand the complete system. Our interdisciplinary group uses diverse time series, measured both directly and through proxy indicators, to study past climatic conditions and current processes in

this region. Characterizing and linking the geosphere, biosphere, and hydrosphere in this region provides a scientific analogue and, hence, a basis for understanding similar linkages in other regions and for anticipating the response to future climate variations. Our emphasis in PACLIM is to study the interrelationships among diverse data. To understand these interactive phenomena, we incorporate studies that consider a broad range of topics both physical and biological, time scales from months to millennia, and space scales from single sites to the entire globe.

Dedication



A number of individuals have been important in PACLIM Workshops. Jim Young was a friend, participant and benefactor to many PACLIM meetings. He will be missed.

Introduction

G. James West

The Eighteenth Annual PACLIM Workshop was held at the Asilomar Conference Grounds at Pacific Grove, California. After several years the workshop returned to its original site which has served well for conferences on climate of the eastern Pacific. Attended by more than 105 registered participants (see Appendix C, Participants), the workshop included 41 talks and an equal number of poster presentations. The talks consisted of a diverse range of issues ranging from decadal climate changes in the late Holocene, North American monsoon variability, and a wide range of climatically related topics for the eastern Pacific and western North America. On the first evening, Kelly Redmond gave his synthesis on the Western Winter of 2000-2001, Maury Roos presented his annual California Water Year report, Sam Luoma gave a perspective on CALFED's Science Program, and Gary Freeman and Ross Miller each presented information on California's energy system. Monday evening was given to poster presentations. Poster presentations were displayed throughout the entire meeting (see Appendix B, Poster Presentations). Tuesday evening's speakers, Doug Kennett and Dave Stahle, presented papers on climate and prehistoric populations on the California coast and on megadrought and megadeath in 16th century Mexico (the latter based on tree-ring and historical research), respectively.

All presenters were invited to expand their abstracts into a manuscript for inclusion in the Proceeding volume, and nearly all presentations are included in manuscript or abstract form. In this Proceedings volume, nine papers are presented full-length and two as an extended abstract. The abstracts submitted to the meeting are printed in a following section. The papers are not peer reviewed and editorial comments are generally limited to grammar, spelling, punctuation, and format. Editorial comments on the content on some submittals have been offered, but it is the responsibility of the author(s) for any errors of fact or logical inconsistencies.

Summary

Mike Dettinger

During the early 1990s (but echoing studies by S.T. Harding at the University of California, from as early as the 1930s), several lines of paleoclimate evidence in and around the Sierra Nevada Range have provided the water community in California with some real horror stories. By studying ancient tree stumps submerged in Lake Tahoe and Tenaya Lake, stumps that were emerging from Mono Lake during its recent decline, and stumps that were exhumed in the Walker River bed during the floods of 1997, paleoclimatologists like Scott Stine of California State University, Hayward, assembled a picture of epic droughts in the central Sierra Nevada during the medieval period. These droughts had to be severe to drop water levels in the lakes and rivers low enough for the trees to grow in the first place, and then had to last for hundreds of years to explain tree-ring counts in these sizeable stumps. Worse yet, the evidence suggested at least two such epic droughts, one ending close to 1100 and the other close to 1350. These epic droughts challenged paleoclimatologists, as well as modern climatologists and hydrologists, to understand and, ultimately, to determine the likelihood that such droughts might recur in the foreseeable future. The first challenge, however, was to verify that such droughts were more than local events and as extreme as suggested.

At this year's Pacific Climate (PACLIM) Workshop, held March 18–21, 2001, at Asilomar Conference Grounds, special sessions brought together scientists to compare paleoclimatic reconstructions of ancient droughts and pluvial (wet) episodes to try to determine the nature of decadal and centennial climate fluctuations in western North America, with emphasis on California. A companion session brought together modern climatologists to report on the latest explanations (and evidence) for decadal climate variations during the instrumental era of the 20th century.

PACLIM is an annual workshop that, since 1983, has brought together specialists from diverse fields, including physical, social, and biological sciences, to discuss and investigate climate and climate effects in the eastern Pacific and western America. This year's PACLIM was sponsored by the U.S. Geological Survey, NOAA Office of Global Programs, California Department of Water Resources, and, for the first time, the CALFED Science Program. In addition to the presentations summarized here, sessions at this year's PACLIM covered topics as varied as the North American monsoon system; recent economic and political effects of California's climate variations, including a presentation on climate and CALFED by Sam Luoma (U.S. Geological Survey, Menlo Park); and research into daily-to-seasonal weather variations. Information about this year's and next year's meetings can be found at <http://meteora.ucsd.edu/paclim/>.

Prehistoric Droughts and Floods

Recent developments and comparisons of paleoclimatic time series from a variety of sources and settings in the California region were an important focus of this year's PACLIM. Sediment layers from the offshore Santa Barbara Basin and Gulf of California; isotopic, chemical, and paleomagnetic signatures in cores from Pyramid Lake in northwestern Nevada; and tree rings from numerous

locales around the western states—along with many other paleomarkers from ocean sediments, marshes, and lakes, and other sources—were analyzed to develop high-resolution paleoclimate reconstructions (often cataloging year-by-year climate variations). The overall picture of decadal and centennial climate variations in California during the last several millennia that emerged from comparison of these various reconstructions is that long-term decades to centuries-long excursions of California's climate, and in particular, of its precipitation regimes, have indeed occurred in the not-too-distant past (for example, during medieval times).

For example, Larry Benson (USGS, Boulder, Colo.) reported that major oscillations in the water balance of Pyramid Lake have occurred irregularly but, on average, about every 150 years during the last 8,000 years. Among the paleodroughts that affected the lake were the medieval epic droughts inferred elsewhere in the Sierra Nevada. A major relocation of Anasazi populations in the Four Corners region occurred in the middle of the second of these prolonged droughty periods, which took place in the 1280s. Numerical simulations of the lake's water balance (as inferred from the geochemical variations in its sediments) suggest extended droughts could have involved greater than 30% reductions in the wetness of the Sierra Nevada, on average, over multidecade and even century time scales. Remarkably close, but quite independent, corroboration of many of these paleoclimatic changes came from Douglas Kennett's (California State University, Long Beach) report on the foraminifera and geochemistry of ocean sediments from the Santa Barbara Basin. The Santa Barbara Basin sediments indicate important sea-surface temperature variations along the California coast over the last several thousands of years that coincided with droughts and wet periods identified far inland in White Mountains bristlecone tree rings. Malcolm Hughes (The University of Arizona Laboratory of Tree-Ring Research) used new precipitation-sensitive tree-ring reconstructions, each over 1,000 years long, from around the West to show long-term droughts in exquisite detail. In the Southwest, the 1950s drought ranked as probably the most extensive intense decadal-scale drought in the last 1,000 years, but closer to home, the medieval droughts (especially the later one) were clearly evident in the tree rings. Similarly, Lisa Graumlich (Montana State University) found evidence of persistent (but not unbroken) drought conditions in 1,000-year tree-ring reconstructions from the Greater Yellowstone Region. David Meko (The University of Arizona Laboratory of Tree-Ring Research) and others showed evidence that the epic medieval droughts coincided with wet intervals farther north in Oregon, perhaps indicating persistent reroutings of storm tracks to the north of California during the drought periods.

Each of these climate reconstructions also included sustained, wetter-than-normal intervals of durations comparable, in some cases, to the epic droughts. Ominously, several of the climate reconstructions presented showed that the 20th century has yielded fewer droughts in California than in previous centuries. At the wet hydrologic extreme, past megafloods in coastal southern California were inferred from distinctive clay-rich layers in the Santa Barbara Basin. Megafloods occurred in A.D. 212, A.D. 440, and A.D. 1418, and A.D. 1650, according to Arndt Schimmelmann (Indiana University). To put these episodes in perspective, Schimmelmann noted that historical wet years have left no signs comparable to these prehistoric megafloods.

Overall, the comparisons of paleoclimate reconstructions presented at the workshop suggest epic droughts (decades and centuries long) did afflict central California during the last several millennia, including, in particular, the medieval droughts. The drought periods were vastly longer than we have experienced, but not necessarily more severe than historical droughts. There are tantalizing

suggestions of almost periodic recurrences of some of the inferred droughts, with periods ranging from 20 to 150 years and more. The general consensus from the PACLIM Workshop was that these droughts should not be envisioned as unbroken spells of uninterrupted dryness, but rather as extended intervals during which droughts were significantly more common. The "six-year" drought in California during the late 1980s and early 1990s may provide a much reduced model for such droughts; that drought was broken by a year of normal wetness at its midpoint and occurred despite year-to-year changes in the large-scale climate state (for example, El Niño conditions, La Niña conditions, and in-between conditions prevailed at various times during the course of this event). Thus it may be best to imagine that the epic droughts corresponded to long intervals with greater-than-normal propensities towards drought in California, quite possibly with droughts more persistent than usual. Thus these dry intervals probably reflect prolonged shifts to more droughty conditions rather than single "continuous droughts." Finally, Malcolm Hughes concluded that the various paleorecords presented at this year's PACLIM, along with many others, are now mature enough to support a major case study of one or both of the medieval droughts in far greater detail than has previously been possible. A wide range of paleoclimate indicators from the entire western North American region can now be brought together to provide constraints on the conditions, spatial extent, and persistence of those droughts, as well as compare these paleodroughts. Such comparisons would provide a much clearer depiction of epic droughts in California than is possible in a single workshop.

Modern Decades-long Climate Fluctuations

In an attempt to understand the climate mechanisms that might drive such long-term fluctuations, particularly in the Pacific Ocean basin and western Americas, several climatologists were asked to present some of the most recent views of decadal climate processes in the Pacific. Michael Evans (Harvard University) and Mark Lyford (University of Wyoming) used regional syntheses of paleoclimatic reconstructions to argue that the paleoclimatic versions of decadal and centennial climate variations form climate patterns that are recognizable in the modern climate system. Evans argued, in particular, that paleoclimatic reconstructions of decade-scale El Niño-Southern Oscillation (ENSO)-like climate variations show much the same pattern as that associated with current ENSO-like variations; furthermore, those variations are so symmetric around the equator in the Pacific Ocean basin that they must be of tropical origins. David Pierce (Scripps Institution of Oceanography) and Matthew Newman (Climate Diagnostics Center, Boulder, Colo.) used climate-model simulations and the last century of records of year-to-year and decadal climate variations to draw much the same conclusion: the decadal variations of Pacific, and thus western North American, climate witnessed during the last 50 years are driven by slow variations in the chaotic evolution of tropical Pacific ENSO episodes, with some amplification of the decadal parts by the long, slow responses of the extratropical Pacific Ocean to those year-to-year ENSO variations. In this view of the decadal variations of the Pacific climate, the decadal (and longer) climate spells are artifacts of slowly varying but essentially random variations of the global climate, termed "red-noise climates." The conclusions of these speakers reflect a growing belief among many climatologists that the so-called Pacific Decadal Oscillation (PDO) has its roots in the tropics, rather than reflecting independent climatic oscillations from the extratropical North Pacific. The PDO remains an interesting index to correlate to and reconstruct back through time; however the predictability of the PDO is limited.

Others at the workshop, notably David Keeling (Scripps Institution of Oceanography) and Alan Hunt (Pacific Northwest Laboratory), were more inclined to explain the long-term climate variations in terms of slow “external” forcings, like tidal mixing of the deep ocean, solar-irradiance variations, or greenhouse gas accumulations. At this workshop, the least popular among explanations of decadal climate variations were various, previously proposed extratropical ocean-air mechanisms. The chaotic-tropics versus external-forcings camps continue to debate the sources of decadal to centennial climate variability as this article is published (and probably for a long time to come).

Conclusion

This year’s PACLIM Workshop presented a picture of California’s long-term climatic history that includes significant epic “droughty” periods spanning hundreds of years, with water balance deficits as large as any we have suffered historically. Wetter-than-normal periods have also persisted at times in California prehistory, and extremely large floods during the last 2,000 years occasionally have left their marks offshore. Although competing plausible explanations for the origins of California’s long decadal to centennial paleoclimate variations have been offered, the origins remain uncertain—especially since it is not clear that we have ever seen even mild versions of this form of climate variation in our time in California. As a result, our ability to predict the recurrence of such disasters is minimal. We can, however, advise that such events have happened before and thus may happen again.

Holocene Ocean-Climate Variations in Alfonso Basin, Gulf of California, Mexico

Robert G. Douglas, Donn Gorsline, Alessandro Grippo, Ivette Granados,
and Oscar Gonzalez-Yajimovich

Abstract

Spectral analysis of a high-resolution sediment record from Alfonso Basin in the southern Gulf of California reveals decadal to millennial scale variations in sedimentation and biogenic production. Periods of variability occur at ca. 1480 yrs, 900 yrs, 350 yrs, 150 yrs and 100 yrs with a shift in the frequency of variability at about 3000 yrs B.P. Between 3000 and 7400 yrs B.P., climate in the Gulf was warmer and wetter with lower primary productivity. Sediments are terrigenous- and carbonate-rich with low amounts of organic carbon and biogenic silica. Periods of 150 and 350 years are related to productivity pulses. After 3000 yrs B.P., sediments are terrigenous- and organic-carbon rich with carbonate dissolution events with periodicities of 900+/- 50 years superimposed on the 350 yr events.

Introduction

Early studies of Holocene climate recognized a period of warm climate in the early Holocene and the cooling of the Little Ice Age (Denton and Karlen 1973), but the epoch was generally viewed as a time of warm and relatively stable climate. Recently developed paleoclimate records have changed this picture and show that Holocene climates were also unstable, punctuated by cooling events including the Little Ice Age, that appear to be part of a 1-2 kyr climate rhythm first detected in Dansgaard-Oeschger (D/O) and Heinrich events in the Pleistocene (Bond and others 1993; Bond and others 1999; DeMenocal and others 2000; Bard and others 2000). In the late Pleistocene (ca. 15-80 ka) climates were cold and unstable, oscillating rapidly between warm and cold states (Dansgaard and others 1993; Broecker, 1994; Bond and others 1997). The climate of the Holocene is emerging as one that differs more in the amplitude and rapidity of the variations rather than the style.

Modes of climate instabilities are best known from high-latitude ice core records and sediments in the North Atlantic basin, including the subtropics (Peterson and others 1991; DeMenocal and others 2000), but the extent to which they occur in the Pacific is still being assessed. One of the best high-resolution records is from Santa Barbara Basin, a mid-latitude site in the eastern Pacific, in which the D/O events correlate with the development of laminated sediments during brief anoxic events (Behl and Kennett 1996). In the Holocene portion of the core, variations in the laminated record are suggestive of sub-millennial scale events, but they are yet to be investigated.

In this study we investigate the timing, amplitude and nature of ocean-climate variability present in a high-resolution, laminated sediment record from Alfonso Basin in the Gulf of California. The emphasis is to document decadal to centennial scale variations that can link the millennial-scale

modes that can be resolved in typical ocean cores (Anderson 2001) to the annual to decadal-scale climate variability observed in the Modern ocean.

Alfonso Basin

Alfonso Basin is a small, closed depression (maximum depth 415 m) with an effective depth of about 350 m (Figure 1). Deep water entering the basin is drawn from low-oxygen intermediate water. Below 200 m the basin is suboxic to anoxic. Because of its location, near the junction of the Gulf and the open Pacific Ocean, the basin is a sensitive recorder of the monsoon-driven seasonal variations in the Gulf and the larger-scale climate circulation of the subtropical Pacific Ocean. Near the center of the basin a high accumulation rate (30-35 cm/Kyr) 2 m Kasten core, BAP96-CP, was collected which recovered most of the Holocene (7700 years B.P.). It was sampled at 1 cm intervals (approximately 35 year per sample) for biogenic and isotopic analyses and x-rayed to document the microfibrics and detailed stratigraphy.

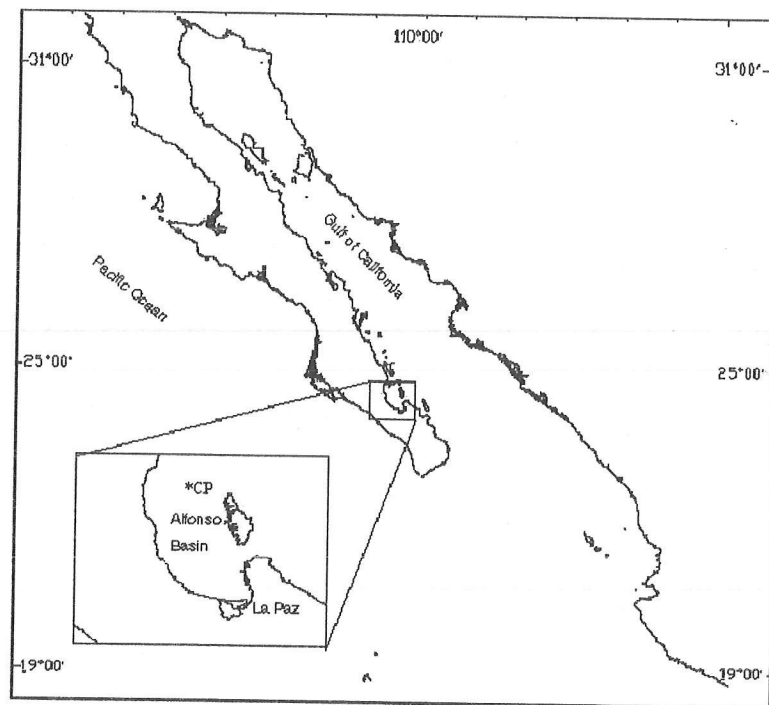


Figure 1 The southern portion of the Gulf of California showing the location of Alfonso Basin in La Paz Bay, north of the city of La Paz. The area is located at the edge of the subtropics and experiences both the monsoon driven seasonal variations of the Gulf and the general circulation of the subtropical eastern Pacific.

Climate, Biological Productivity, and Sedimentation

The Gulf of California is a marginal sea, nearly isolated from the adjacent Pacific Ocean and surrounded by arid lands. The region has a monsoon climate with seasonally reversing winds that

controls rainfall, surface circulation, and biological productivity (Figure 2). As a consequence, the seasonal pattern is strongly imprinted on the sediment record.

Modern Gulf Climatology

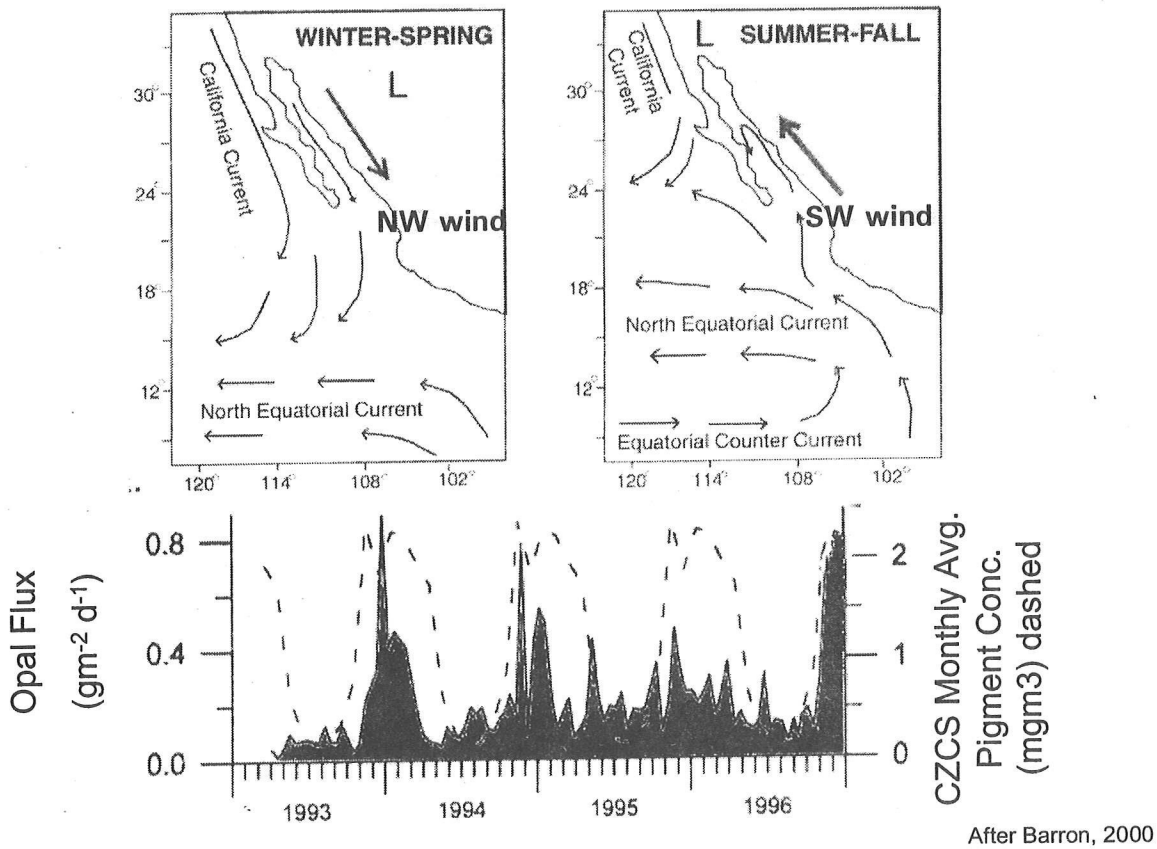


Figure 2 During the winter monsoon, strong winds from the northwest flow down the length of the Gulf, generating surface mixing and coastal upwelling. During the summer monsoon, the winds reverse and weak, southwest winds from the eastern tropical Pacific flow into the Gulf, introducing warm surface waters. Primary productivity in the Gulf is driven by the winds and is high in the winter-early spring and low during the summer-early fall (figure modified from Thunell 1996).

From late fall to early spring, strong northwesterly winds blow down the axis of the Gulf and generate strong coastal upwelling, especially along the eastern side. With the onset of the fall winds, sea surface temperatures cool and the thermocline breaks down allowing the development of a thick mixed layer. Mixing moves nutrient-rich deep waters into the photic zone. The upwelling and surface mixing generate eutrophic conditions and high biological productivity over much of the Gulf (Alvarez-Borrego and Lara-Lara 1991; Thunell 1996). The flux of skeletal debris to the bottom is correspondingly high. Coastal Zone Scanner images show the highest surface pigment concentrations (a proxy for productivity) are located in the middle and upper part of the Gulf between December and March (Thunell 1998). Diatoms and other siliceous phytoplankton dominate in the upwelled

waters. Productivity in the southern Gulf near Alfonso Basin is lower and sediment patterns indicate both silica and carbonate are exported to the bottom. Strong winds associated with the winter-spring monsoon transport eolian dust, which is an important source of the fine-grained terrigenous materials in slope and deeper basins (Baumgartner and others 1991).

In the summer-early fall, winds reverse and weak SE winds from the tropical eastern Pacific Ocean enter the Gulf. The warm surface waters generate a strong thermocline and stratify the water column. Surface waters become nutrient depleted, except for limited upwelling along the Baja peninsula (Alvarez-Borrego and Lara-Lara 1991; Pride and others 1999). Tropical surface waters extend well into the Gulf, especially during ENSO cycles. In the warm, oligotrophic waters calcareous plankton (Coccolithophorids and planktonic foraminifera) is abundant. In addition to the high production associated with the winter/spring upwelling, a distinctive diatom flora lives deep in the photic zone during summer months. As fall winds cool surface waters and the thermocline breaks down, mass sedimentation of these diatoms occurs as a "dump" to the bottom, the diatom mats forming thin lamina in the sediments (Kemp and others 2000). Tropical storms during the summer months and ENSO events account for most of the rainfall in the Gulf.

Sediment Record

Sediments from the floor of Alfonso basin are composed of laminated, terrigenous- (70% to 90%) and organic-carbon rich (5% to 7%), hemipelagic sediments accumulating as light and dark lamina, thin flood layers and turbidites. An individual lamina is typically 0.2- to 0.5-mm thick and includes conspicuous light-colored layers composed primarily of coccoliths or diatoms and dark-colored flood layers with coarse silt and organic debris. Turbidites are several millimeters to over a centimeter thick and contain displaced microfossils. Although oxygen values in the basin are very low, the central basin supports a micro- and meiofauna of tiny polychaetes, foraminifera, and other organisms that generate horizontal burrows 0.1 to 0.3 in diameter. The microburrows are a common feature and can disrupt or diffuse the boundaries of lamina but do not destroy the primary microfabric. Sediment mixing, if it occurs at all, is on a scale below 1 mm. In addition to the laminations, the sediments are banded, typically with clusters of laminations occurring as lighter or darker bands one to several centimeters thick. The bands are most conspicuous in the upper half of core CP.

In core CP, the calcium carbonate content is composed of coccoliths and foraminifera and is an imperfect proxy of plankton productivity. It varies from near zero to over 25%, with marked carbonate dissolution cycles in the upper 97 cm and carbonate maxima at 97 to 120 cm and below 200 cm (Figure 3). The increase in carbonate content below 97 cm is largely due to an increase in planktonic foraminifera. In Alfonso Basin (and the Gulf of California) the organic carbon flux (from plankton productivity) mediates carbonate dissolution and demand for bottom water oxygen. Sediments in Core CP with the highest carbonate dissolution correspond to the highest total organic carbon (TOC) content and lowest oxygen conditions (Douglas and others 2000). Samples were collected at 1 cm intervals, dried, weighed and the calcium carbonate content measured using a VIC Coulometrics CO₂ Analyzer. Replicate samples were run on a LECO Carbon/Carbonate Analyzer.

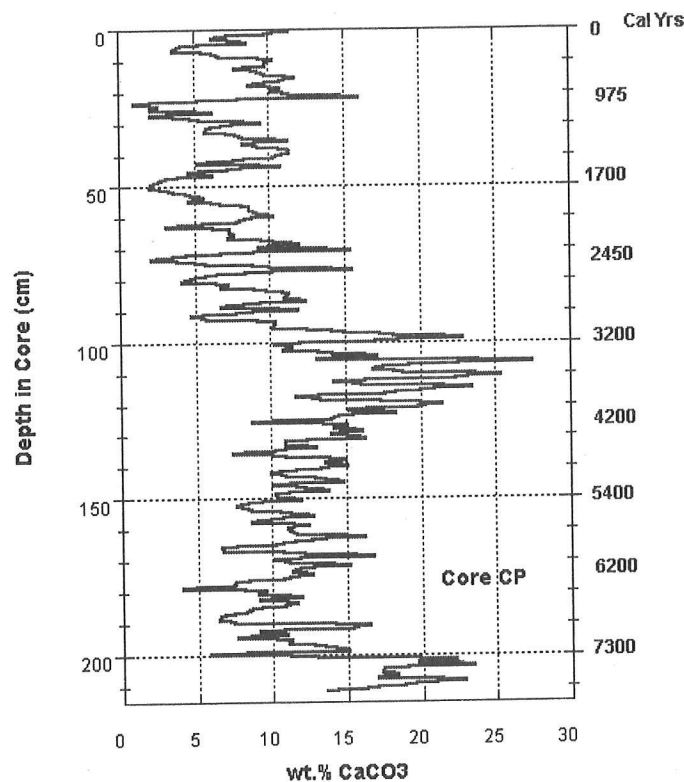


Figure 3 Down core calcium carbonate content in core BAP96-CP. The core was collected from near the center of Alfonso Basin, 386 m deep. Samples were taken at 1-cm intervals and analyzed on a VIC Coulometric CO₂ Analyzer. Replicate samples were run on a LECO Carbon/Carbonate Analyzer. Note the major change in carbonate content at 97 cm, about 3100 yrs B.P.

Age-Depth Model and Sedimentation Rates

Age-depth models for core BAP96-CP (hereafter referred to as core CP) were constructed using a combination of AMS radiocarbon dates, excess 210 Pb profiles and varve counts derived from gray-scale analysis.

Age control was established from AMS radiocarbon dates of foraminifera, which were converted to calendar years by applying a reservoir correction of 520±40 years (Stuvier and Reimer 1993, 1996) and the CALIB 4.3 radiocarbon program of Stuvier and others (2001). Dates at core intervals 0 to 1 cm, 120 to 121 cm and 211 to 212 cm are based on mixed planktonic species (mostly *Globorotalia menadrii*, *Pulleniatina obliquiloculata* and *Globigerina bulloides*). Radiocarbon dates for intervals 19 to 20 cm, 100 to 101 cm and 210 to 211 cm are based on mixed benthic species (Perez-Cruz 1999). The resulting age-depth profile forms a linear relationship ($r = 0.997$) and supports the observation from the X-radiograph stratigraphy that sedimentation was continuous below 5.5 cm.

Sedimentation rates were interpolated between calendar-calibrated radiocarbon dates and range from 0.32 mm/yr near the top of the core to 0.24 mm/yr below 120 cm (Figure 4).

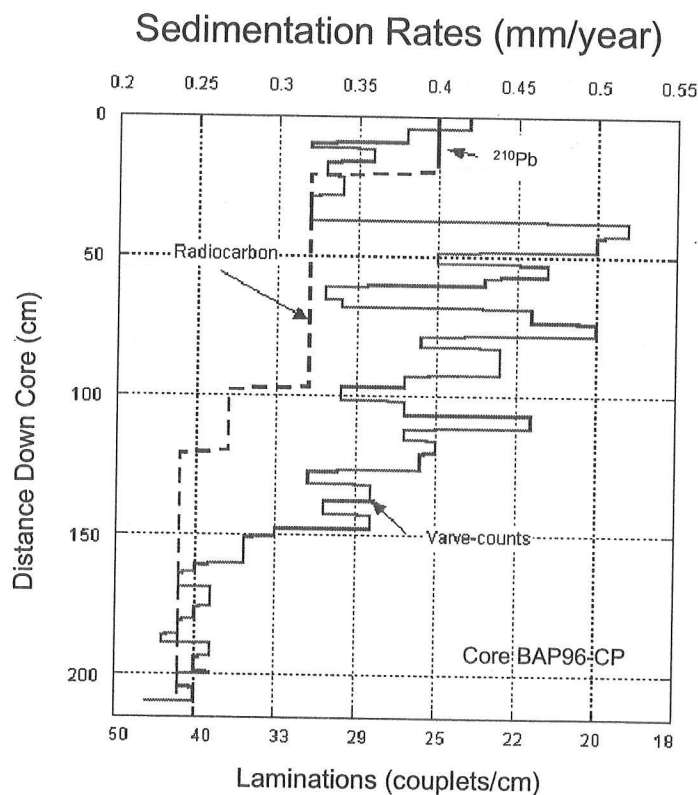


Figure 4 Sedimentation rates derived from radiocarbon based age-depth relationships, excess ^{210}Pb profiles and grayscale varve-counts. Rates are given in mm/year.

Uncorrected accumulation rates were calculated for the upper 20 cm of several basin floor cores, including kasten core CP, using excess ^{210}Pb and ^{137}Cs profiles. Core CP yielded a rate of 0.4mm/yr. Rates calculated for nearby box cores ranged from 0.35 to 0.5 mm/yr.

Core CP is intensely laminated but individual lamina are generally less than 0.3 mm in thickness and very difficult to count by eye and obtain acceptable results. To assist the counting, grayscale images were produced. One-cm thick slabs of sediment were X-radiographed and prints of the radiograph scanned at 600 dpi along one or more vertical profiles. The digitized scans were converted to pixel number and the files read using the NIH Image Program to produce a grayscale image. A pixel represented about 0.12 mm (less than 0.5 year). For each 5 cm interval of the core, the grayscale profiles were enlarged and the number of light-dark couplets manually counted. The counts were compared to the original radiograph to correct for artifacts such as fish bones, microburrows and flood or turbidite layers that might have influenced the digital scan and grayscale profile. Except in the most intensely laminated sections, small-scale horizontal burrows (0.1 to 0.3 mm in diameter) are common and can increase the apparent number of laminations per centimeter. For this reason, grayscale-based varve counts probably overestimated sedimentation rates.

In the upper 20 cm of the core, the grayscale analysis averaged about 25 light-dark laminations per cm, or 0.4 mm/couplet, identical to the accumulation rate based on the excess ^{210}Pb profile. We

conclude that the light-dark couplets are annual accumulations (varves). Below 20 cm, sedimentation rates vary in a cyclic fashion from 0.32 to 0.52 mm/yr and average 0.41 mm/yr, very close to modern rates. Below 150 cm, laminations are thinner, often disrupted and more difficult to discriminate. Also the record contains an increased number of flood and turbidite layers. Accumulation rates in this interval range between 0.23 to 0.27 mm/yr (Figure 4).

Considering the spacing of radiocarbon dates and that the core has been compacted due to dissolution of siliceous and carbonate debris, the rates based on the three methods are in reasonable agreement. Both the radiocarbon-based rates and varve-count rates indicate that below 150 cm, prior to 5200 yrs B.P., accumulation rates in Alfonso Basin were significantly lower.

In calibrating the spectral peaks derived for the laminated record for the entire core and the carbonate content, we have used the age-depth model based on radiocarbon-based calendar years, 0.27 mm/yr (37 yr/cm) (Table 2). For comparison, ages are also shown based on grayscale varve-count rates (0.4 mm/yr, which equals 25 yr/cm). In the analysis of higher frequencies in the intensely laminated intervals at 50 to 70 cm and 97 to 116, a sedimentation rate based on averaged varve-counts for the top 150 cm of 0.35 mm/yr (28 yr/cm) was used.

Spectral Analysis

Spectral analysis of variability was made of the laminated stratigraphy obtained from X-radiograph prints. In this manner a continuous millimeter-scale record of the entire core could be analyzed. The grayscale images, after digitizing and converting to pixel number, were exported to Analyseries 1.1© (Paillard and others 1996) to perform Fourier analysis. No filters were applied. The calculation of power spectra using the 2-p Multi-Tapered Method (MTM) yielded frequency peaks whose periodicity was converted to centimeters and to calendar years based on the age-depth models described above.

Because of the variations in sedimentation rate, density of the laminations, microburrows and flood layers in different sections of the core, spectral peaks were calculated for (1) the entire core, 0 to 212 cm (Figure 5); (2) the intervals of highest (0 to 150 cm) and lowest (150 to 212 cm) varve-count accumulation rates (Figures 6a, 6b), and (3) the two intervals with the most distinct and continuous laminations (type 2, see DeDiego and Douglas 1999) and fewest flood/turbidite layers (50 to 70 cm and 97 to 116 cm) (Figures 7a, 7b). The latter were made to examine spectra present at annual to decade scale variations in the laminated record. Power spectra were also calculated for the carbonate record of core CP using the MTM method (Figure 8).

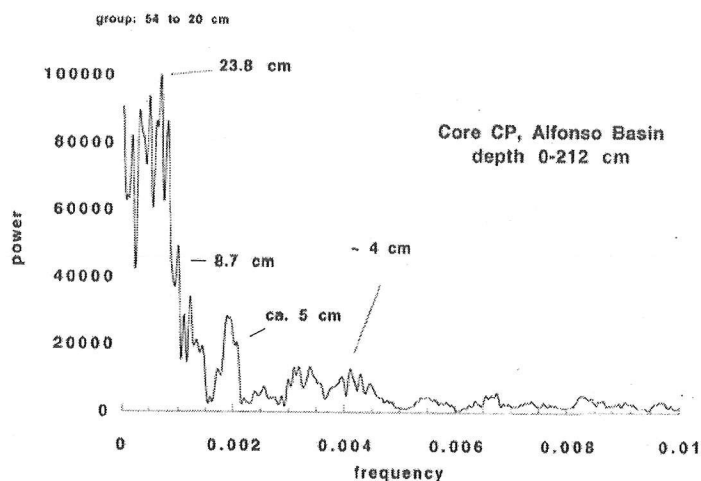
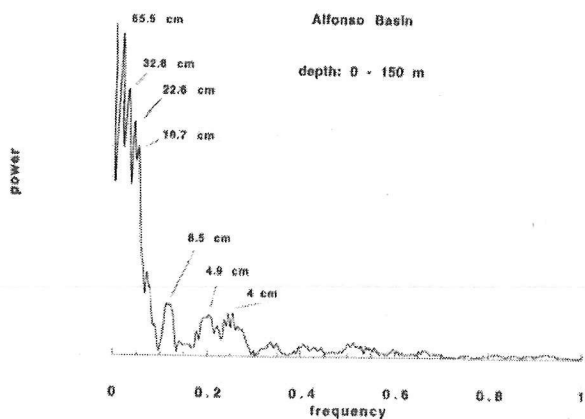
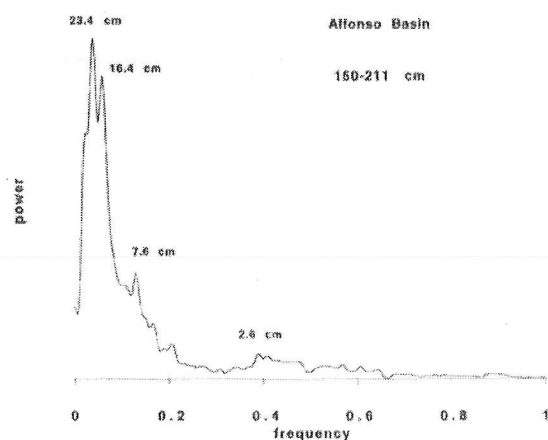


Figure 5 Power spectra calculated for the laminated sediment record, 0-212 cm. Spectral Analysis was of the laminated core stratigraphy obtained from grayscale conversion of X-radiograph prints.



A



B

Figure 6 Power spectra calculated for intervals of core CP with the highest and lowest varve-count sedimentation rates: (A) 0-150 cm interval with of varve-count sedimentation rates > 0.3 mm/yr; (B) 150-211 cm interval with varve-count based sedimentation rates < 0.27 mm/yr

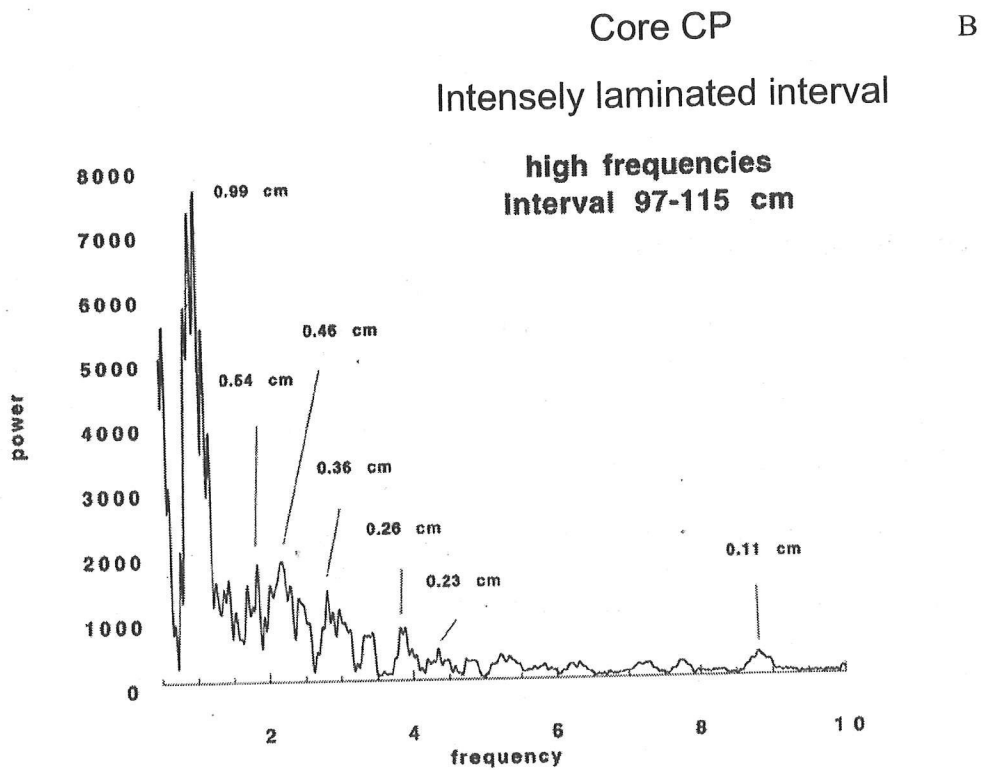
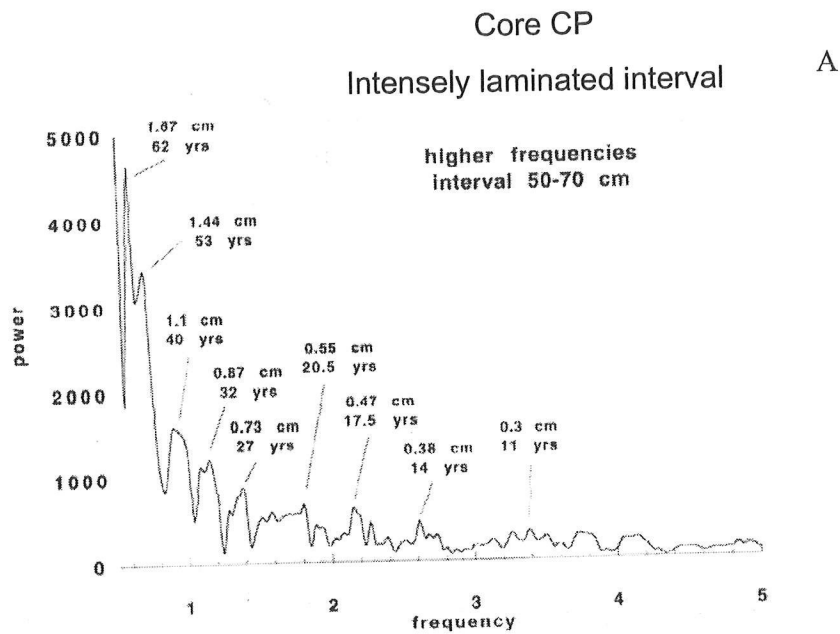


Figure 7 Power spectra for the two intervals with the most continuous and complete laminations (type 2 laminations; DeDiego and Douglas 1999) and few or no flood layers or turbidites: (A) 50-70 cm interval; (B) 96-115 cm interval

Analysis of the two most intensely laminated sections for higher frequency peaks yielded similar results. Although these variations occur at lower power, they are consistent and probably real. There are broad peaks, 4 to 6 years, 7 to 13 years and 20 to 41 years that are suggestive of the timing of ENSO events, sunspot variations and the North Pacific Oscillation. The latter, with a periodicity of 0.5 to 1 cm, corresponds to the banding observed in the core.

Carbonate Record

Significant fluctuations in the carbonate record occur at 950, 1550, 3100, 4300 and 7200 yrs B.P. The latter four appear to be related to the 1480 yr peak (40 cm) (Table 2). This is close to the 1500-yr climate rhythm observed in the intensity of the oxygen minimum zone in the Pacific margin of Baja California (Zheng and others (2001), the cooling events in the subtropical Atlantic (deMonocal and others 2000) and well known in the North Atlantic (Bond et al 1999). Two strong dissolution cycles occur in the core: one with a periodicity of about 900 ± 50 years (27 cm) that predominates in the upper part of the core, following the carbonate maximum at 3200 yrs B.P., and a second peak at 370 years (10 cm) that is strongest prior to 4300 yrs B.P. The latter is probably the same as the 8 cm peak identified from the laminated record, which we refer to as the 350 ± 50 yr period. The dissolution cycles are productivity driven and the second peak appears to be the same productivity pulses identified in the biogenic record in La Paz Basin (Bernal 2001). The other variability with power occurs at peaks of 5.7 cm and 4.3 cm and present periods of 150 ± 50 yrs.

Summary

Spectral analysis of carbonate content and sediment laminations reveals strong power concentrations at periods of ca. 1480, 90, 350, 150 and 100 years and possibly at decadal scales. The millennial scale variability matches the 1-2kyr climate rhythm of Bond et al. (1999). Centennial-scale variability is strong at about $900+/-50$ yrs, represented by the 23 to 27 cm peaks and at $350+/-50$ yrs, represented by the 8 cm and 10 cm peaks. The latter is the strongest event in the laminated and carbonate records.

The spectra peaks at 900 yrs, 350 yrs and 150 yrs are linked to productivity pulses that can be seen in carbonate dissolution cycles. Between 3000 and 7000 yrs B.P., microfossils, turbidites and flood layers and variations in the carbonate content suggest that the climate was warmer, wetter and primary productivity lower in the Gulf (Perez-Cruz 2000; Douglas and others 2001; Bernal 2001), in phase with similar climatic conditions elsewhere in low and mid latitudes (Steig 1999; Sandweiss and others 1999; Kerwin and others 1999; DeMoncal and others 2001). In Guaymas Basin, diatoms indicative of spring upwelling become the dominant floras (Sancetta 1995; Barron 2000). At roughly 3000 years B.P., climate in the Gulf became cooler, drier and more productive as the spring monsoon winds intensified. Climates appear also to have become more variable, especially in the last 1700 yrs.

Acknowledgements

We wish to thank Adolfo Molina Cruz (UNAM) and Enrique Nava Sanchez (CICIMAR-IPN), their graduate students and the crew of the R/V El Puma for assistance in collecting core BAP96-CP. AMS radiocarbon analyses were performed at the Livermore National Laboratory. Determinations of ^{210}Pb and ^{137}Cs were made by the Geochemistry Laboratory of the University of Southern California

under the direction of T-L. Ku. This work was supported by NSF grants INT-9908773 and OCE 0002250 and is part of a joint research program between the senior authors (University of Southern California) and Enrique Nava-Sanchez (*Centro Interdisciplinario de Ciencias Marinas-Instituto Politecnico Nacional (CICIMAR-IPN)*).

References

- Alvarez-Borrego S, Lara-Lara JR. 1991. The physical environment and primary productivity of the Gulf of California. *American Association of Petroleum Geologist Memior* 47:555–68.
- Anderson D. 2001. Attention of millennial-scale events by bioturbation in marine sediments. *Paleoceanography* 16:352–7.
- Barron J. 2000. Holocene paleoceanographic change at DSDP 480, Guaymas Basin, Gulf of California. EOS Transactions, Fall Meeting Supplement, Abstract.
- Bard E, Rostek F, Turon J-L, Gendreau S. 2000. Hydrological impact of Heinrich events in the subtropical Northeast Atlantic. *Science* 289:1321–4.
- Baumgartner T, Ferreira-Batrina V, Schrader H, Soutar A. 1991. Varve formation in the central Gulf of California: A reconsideration of the origin of the dark laminae from the 20th century varve record. *American Association of Petroleum Geologist Memior* 47:617–35.
- Behl R, Kennett J. 1996. Brief interstadial events in the Santa Barbara Basin, NE Pacific, during the past 60 kyr. *Nature* 379:243–6.
- Bernal F, Gladys R. 2001. *Registro Paleocanografico en los sedimentos laminados de la cuenca de la Paz, margen occidental del bajo Gofo de California* [PhD thesis]. Available from *Centro de Investigacion Cientifica y de Educacion Superior de Ensenada (CICESE)*, Ensenada, Mexico. 110 p.
- Bond G, Broecker W, Johnsen S, McManus J, Labeyrie L, Jouzel J, Bonani G. 1993. Correlations between climate records from North Atlantic sediments and Greenland ice. *Nature* 365:143–7.
- Bond G, Showers W, Cheseby M, Lotti R, Almasi P, P. deMenocal, P. Priore, H. Cullen, I. Hajadas and G. Bonani. 1997. A pervasive millennial-scale cycle in North Atlantic Holocene and Glacial climates. *Science* 278:1257-1266.
- Bond G, Showers W, Elliot M, Evans M, Lotti R, Hajadas I, Bonani G, Jonson S. 1999. The North Atlantic's 1-2 kyr climate rhythm: relation to Heinrich Events, Dansgaard/Oeschger Cycles and the Little Ice Age. In: Clark PU, Webb RS, Keigwin LD, editors. *Mechanisms of global climate change at millennial time scales*. Geophysical Monograph 112. Washington, DC: American Geophysical Union. p 35–58.
- Broecker W. 1994. Massive iceberg discharges as triggers for global climate change. *Nature* 372:421–4.
- Dansgaard W, Johnsen S, Clausen JB, Dahl-Jensen D, Gundestrup JW, Hammer C, Hvidberg CS, Steffensen J, Sveinbjordsdottir AE, Jouzel J, Bond G. 1993. Evidence for general instability of past climate from a 250-kyr ice core record. *Nature* 364:218–20.

- Denton GH, Karlen W. 1973. Holocene climatic variations-their patterns and possible causes. *Quat Res* 3:153–205.
- DeDiego T, Douglas R. 1999. Oxygen-related sediment microfabrics in modern “black shales,” Gulf of California, Mexico. *Journal of Foraminiferal Research* 29:453–64.
- Douglas R, Gorsline D, Grippo A. 2001. Late Holocene ocean-climate variations in Alfonso Basin, Gulf of California, Baja California, Mexico [abstract]. Presented in agenda for Eighteenth Annual Pacific Climate Workshop; 18–21 Mar 2001; Asilomar Conference Center, Pacific Grove, California.
- DeMenocal P, Ortiz J, Guilderson T, Sarnthein M. 2000. Coherent high and low latitude climate variability during the Holocene warm period. *Science* 288:2198–202.
- Kemp AE, Pike J, Pearce R, Lange C. 2000. The “fall dump”—a new perspective on the role of a “shade flora” in the annual cycle of diatom production and export flux. *Deep-Sea Research* 47:2129–54.
- Kerwin M, Overpeck J, Webb R, DeVernal A, Kind D, Healy R. 1999. The role of oceanic forcing in mid-Holocene Northern hemispheric climatic change. *Paleoceanography* 14:200–10.
- Paillard D, Labeyrie L, Yiou P. 1996. Macintosh program performs time-series analysis. *EOS Trans* 77:379.
- Perez-Cruz L. 2000. Paleooceanographic study of the Holocene through laminated sediments from the Bay of La Paz [PhD dissertation]. *Universidad Nacional Autonoma de Mexico*, Mexico City. 140 p.
- Peterson L, Overpeck J, Kipp N, Imbrie J. 1991. A high-resolution late Quaternary upwelling record from the anoxic Cariaco Basin, Venezuela. *Paleoceanography* 6:99–120.
- Pride C, Thunell R, Sigman D, Keigwin L, Altabet M, Tappan E. 1999. Nitrogen isotopic variations in the Gulf of California since the last deglaciation: response to global climate change. *Paleoceanography* 14:397–409.
- Sancetta C. 1995. Diatoms in the Gulf of California: seasonal flux patterns and the sediment record for the last 15,000 years. *Paleoceanography* 10:67–84.
- Sandweiss D, Maasch K, Anderson D. 1999. Transition in the mid-Holocene. *Science* 283:499–500.
- Steig E. 1999. Mid-Holocene climate change. *Science* 286:1485–7.
- Stuvier M, Reimer P. 1993. Extended ^{14}C database and revised CALIB radiocarbon calibration program. *Radiocarbon* 35:215–30.
- Thunell R. 1996. Plankton response to physical forcing in the Gulf of California. *J Plankton Res* 18:2017–26.
- Thunell R. 1998. Seasonal and annual variability in particle fluxes in the Gulf of California: a response to climatic forcing. *Deep-Sea Research* 45(Part 1):2059–83.
- Zheng Y, van Geen A. 2001. Millennial and centennial periodicity of fluctuations in the intensity of the oxygen minimum zone off Baja California margin during the Holocene. *EOS Transactions* 82(20), Spring Meeting Supplement, Abstract 0S41A-09, 2001.

The Impacts of Current and Past Climate on Pacific Gas & Electric's 2001 Hydroelectric Outlook

Gary J. Freeman

Introduction

California is currently experiencing the challenge of meeting energy shortages. Both the lack of normal precipitation this year to date and the low elevation freezing levels associated with this year's December and January storms have left PG&E's reservoirs at, and in some cases below their normal minimum winter operating levels. There is increased impact and risk of energy shortages in California during years when both the northwest's Columbia River Basin and California experience unusually dry conditions together. That is the case this year. The northwest is experiencing a much below normal year in terms of precipitation with very limited energy available to send into California. Available water from surface reservoirs for hydroelectric generation is currently limited for PG&E. The reservoirs will remain at winter minimum levels until either sufficient rainfall occurs or spring snowmelt runoff begins in April. During late December, January, and early February, approximately 65% of PG&E's January hydroelectric generation daily average of 22 GWh (all PG&E hydro sources), came from springs in the Pit/McCloud, Cow/Battle, and Lake Almanor watersheds. The remaining approximately 35% hydroelectric generation was mostly from surface storage draw down. Since about 46% of PG&E's normal year hydro generation comes from watersheds with significant aquifer outflow, the state of the aquifers as a reflection of past climatic variation is an important part of PG&E's hydroelectric energy picture. For the 2001 calendar year, aquifer outflow, mostly of springs, are anticipated to provide PG&E a relatively "firm" annual output this year in excess of 5,400 GWh, about 1,400 MW daily peaking capability, and nearly 3 million acre-feet (maf) of firm water regardless of current climatic dryness. The springs in northern California have increased in sustained outflow during the past several wetter than average years beginning with 1995. However they may now be about to begin a multi-year decline possibly the result of piezometric head dropping up slope of several large springs, which provide outflow to the river. The outflows from these aquifers reveal both short term cycling and long term trending. During very dry years, this contribution of past climatic wetness assumes an increased relative contribution to both sustained energy production and water availability for inflow to Lake Shasta, which drains into the Sacramento River.

California's Energy Problems

Following AB 1890, California's public utilities entered an era of preparing for deregulation (Brulte 1996). The unforeseen problems have been numerous and include transmission constraints, the unending rate freeze for utilities, a rapidly growing and changing load profile, large and uncertain expense related to siting difficulties and the environmental approval process, high energy prices, and a whole multitude of other influencing factors that have contributed to the current situation of energy shortages in California (Tison 2001).

Where and How Does Hydroelectric Generation Fit

Hydroelectric generation has historically provided about 20% of California's electric energy (Booth, 2001). A large portion of that hydro production normally is sent into California through the Intertie, which connects the northwest to California. Water Year 2001 is dry both in California and the Pacific Northwest. There has been little hydro energy available from the Pacific Northwest this year. While there appears to be a weak correlation between wetness and dryness in the Pacific Northwest and that in California, it is far from a given that both regions will be dry at the same time (Freeman 2000). However such is the case this year; both regions have experienced much drier than average conditions to date.

Value of Hydroelectric Generation in the Overall Power Mix

Hydroelectric powerhouses, even during reasonably dry conditions, are able to meet peak energy demands on very short notice. Hydroelectric generation is renewable. When compared with other sources of the generation mixes, PG&E's hydro generation is a relatively low cost source of energy production, with most of its powerhouses built several years ago. Depending upon water availability, a primary limitation becomes one of sustaining peak generation. In dry years in the absence of sufficient reservoir storage, water must be held back and used in a conservative manner that meets a reduced share of peaking needs.

Variability in PG&E's Hydroelectric Generation Availability

PG&E's hydroelectric system spans the Sierra Nevada and southern Cascades from Mt. Shasta and Goose Lake in northern California to the Kern River in the southern Sierra Nevada. There is a single powerhouse in the Coast Range, which uses water from the Eel River east of Willits. South of Lake Almanor on the North Fork Feather River, monthly hydroelectric generation from the Sierra Nevada's mostly granite watersheds is highly dependent on seasonal precipitation and the freezing levels of winter storms. PG&E has 99 storage reservoirs. Most PG&E reservoirs are relatively small in respect to their contributing drainage area. Therefore because a significantly large proportion of remaining seasonal weather uncertainty remains at the end of each calendar year, nearly all of the PG&E storage reservoirs in the Sierra Nevada are lowered to their winter minimum operating levels by about December 31 of each year. PG&E's one large reservoir, Lake Almanor (1,142,964 acre-foot capacity), which bridges the transition between Sierra granite and southern Cascade High Basin Volcanics makes up about 48% of PG&E's entire surface water storage. Lake Almanor is relatively large in terms of storage capacity in comparison to the lake's relatively small contributing headwater drainage area. While most of the PG&E reservoirs' water replenishment is from snowfall, rainfall frequently occurs at the lower elevations both to a limited drainage area immediately up slope of most reservoirs and to the side-water branches that contribute to the lower reaches of the rivers below many of the storage reservoirs. December through March rains are an important source for providing generation availability during months following early winter reservoir draw down.

Some reservoirs such as Bass Lake (east of Fresno), Bucks Lake, and Lake Almanor on the North Fork Feather River above Lake Oroville are deliberately held to relatively high levels at year-end to accommodate a variety of socioeconomic needs beyond that of hydroelectric energy production. Other limitations to energy production are routine scheduled facility outages for maintenance and a

number of “forced” or unscheduled outages that occur throughout the year often from unanticipated mechanical failure or from other unforeseen needs. There are also instream releases that are made to accommodate the river environment for fish, amphibians, vegetation, sediment transport, and recreational use.

The Climate Situation in 2001

Following a wet October, California has experienced significantly below normal seasonal precipitation to date. The Pacific Northwest has likewise experienced very dry winter conditions. Storm fronts to date have been generally much cooler than normal with snow rather than rainfall occurring at relatively low elevations. PG&E’s reservoirs were drawn down to their winter minimums almost a month earlier than normal in order to best accommodate California’s energy shortages. Normally some reservoir inflow occurs from rainfall during December through February in the Sierra Nevada watershed. That did not occur this season.

California’s climate for the Sierra Nevada and southern Cascades starting with 1987.

- 1987 through 1992 was significantly drier than average
- 1993 was wet; 1994 was dry
- 1995 through 1999 was wet
- 2000 was about average, wetter in the north and drier in the south
- 2001 is dry to date

The Ground Water Picture for the Southern Cascades

Five years of above average precipitation following six years of below normal precipitation quickly restored aquifer outflow from volcanic watersheds (mostly from springs) to their maximum observed rate of flow. To successfully track, study, and forecast the baseflow component from these watersheds, four times the August through October combined unimpaired runoff value was used to represent the stable annual baseflow component for PG&E’s southern Cascade watersheds. Snow melts almost 2 to 4 weeks earlier in the Pit River than further south in the higher Sierra watersheds. With deep, porous volcanic soils, this early snowmelt leaves the August through October period mostly as an unbiased indicator of total calendar year baseflow, basically unaffected from earlier storm or snowmelt increases in flow. A few of the months within that three-month period required normalization due to thunderstorms and other intense rainfall events that caused interflow, and possibly some overland flows, to reach the river.

Using the above approach for defining baseflow, PG&E made the following assumptions regarding aquifer outflow from the many springs and from ground water, which provide the relatively stable baseflow component for flow in the McCloud and Pit rivers.

- About 38% of PG&E’s Long-Term Annual Hydro Generation is provided from aquifer outflow of the volcanic basalts (Figure 1), mainly through some of the largest springs in the United States (Alt and Hyndman 2000; Planert and Williams 1999). During dry years, the relative percentage may increase to 50% or greater of PG&E’s total annual hydro generation output.

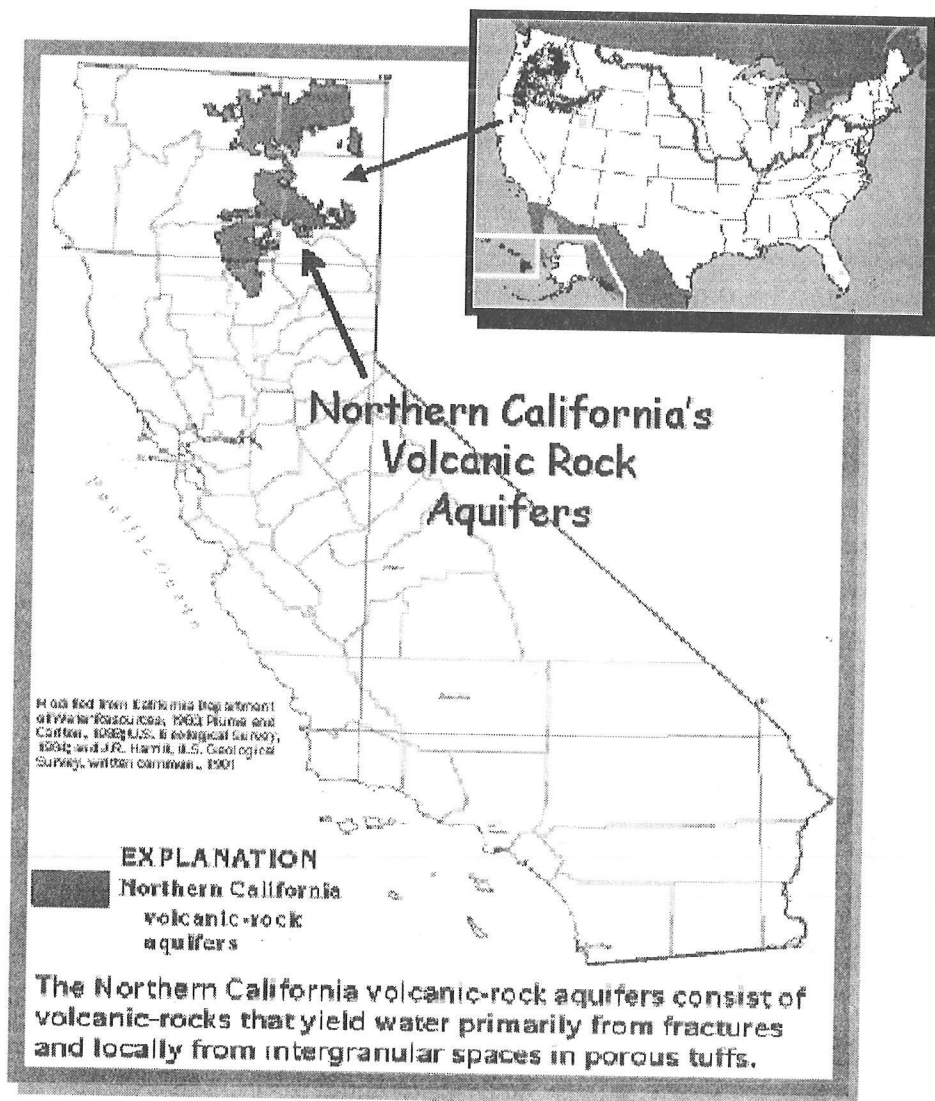


Figure 1 Northern California's volcanic rock. Source: California Department of Water Resources and U.S. Geological Survey.

- When the annual baseflow is analyzed as a time series that is smoothed with a 3-year centered-moving average, there appears to be both a short term 14-16 year cycling and a much longer long term drain-and-fill trend observed for 1907 through 1958, lasting 52 years. Short successive dry year periods tend to quickly rebound if followed by a series of wet years. However, the prolonged period of below average precipitation such as occurred during the dry years of 1907 through the early 1930s required about 28 years for the springs to fully recover back to the earlier high outflow rates experienced during the 5-7 year period immediately following 1900 (Figure 2).

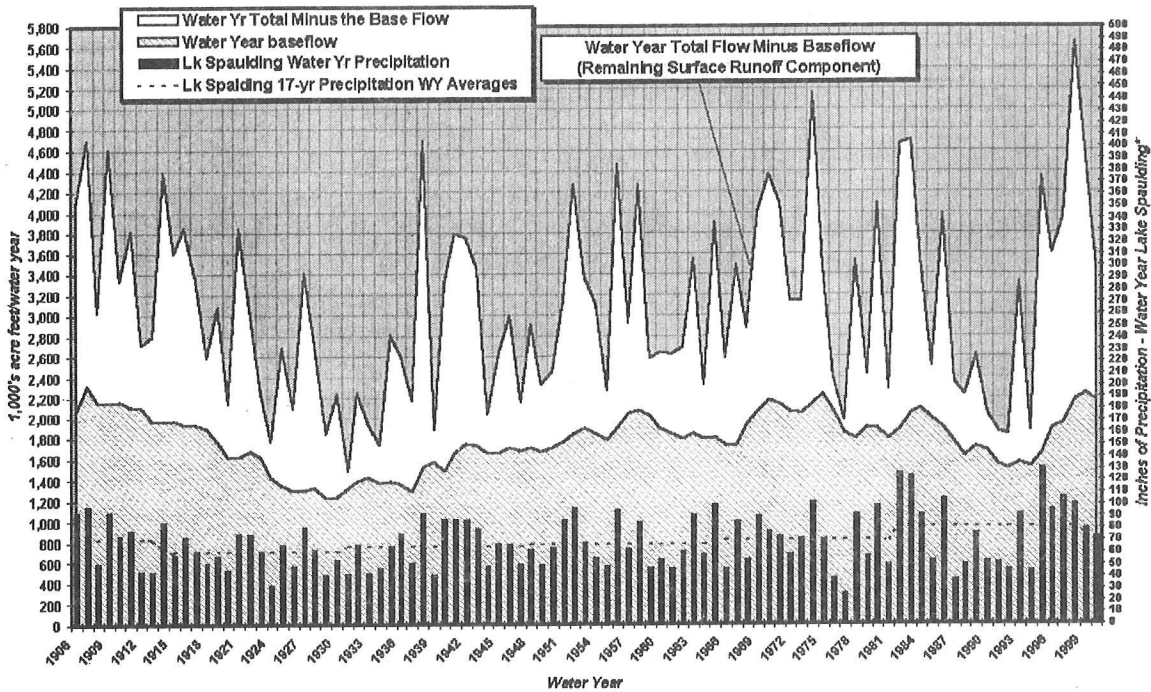


Figure 2 The Pit River annual unimpaired inflow to Lake Shasta for 1906 through 2000. Each year's total runoff is divided into both its annual baseflow component (bottom portion) topped by the more variable partial contribution of each year's seasonal precipitation, which is in excess of infiltration and evapotranspiration.

- This short term cycling and the longer-term net discharge and net recharge trends exert a significant effect on both water availability for Lake Shasta and for PG&E's Pit River hydroelectric generation output. During a normal year, based on the historic past 29 years, the Pit River makes up about 33% of PG&E's total hydro generation mix with about 28% of that generation calculated to come from the McCloud and Pit River aquifer outflow, most of which consists of precipitation of past years. The fall flows in the Pit and McCloud rivers are a resonating blended echo of the area's past climate in terms of precipitation. Some of the water may have traveled underground for many years before surfacing either at springs that feed into the Pit and McCloud Rivers or appearing within the bed of the channel. For example, one may visually observe water emerging in Burney Creek channel about 1/3 mile upstream of Burney Falls, a tributary to the Pit River. Starting with a dry river bed, within that 1/3 mile reach, there is approximately 150 cubic feet per second (cfs) flowing directly below the falls. A similar phenomenon exists on various tributaries to the Deschutes River in Oregon (Bastasch 1998). Without continuous sustained net balanced recharge to the aquifers from normal variance about a wet-period mean, the aquifer outflow rate after a couple years goes into a relatively rapid decline, which, if lasting long enough, has been observed to take almost three decades to restore springs to their original maximum flow rate. This creates droughts in water availability to the Pit and McCloud rivers, which drain into Lake Shasta, which in turn tends to create a sort of mini-drought sometimes out of synchronization with current climate conditions. This was most

recently observed in 1993, when base flow remained below normal in spite of the very wet year overall.

Short-Term Cycling

As illustrated in Figure 3, an approximate 14-16 year cycle appears in most time series plots of the unimpaired volcanic baseflow component. The long-term record tends to average about a 15-year mean, therefore in this paper the 14-16 year periodicity and 15-year periodicity are used interchangeably. With the lag in pressure transmissivity between wet and dry years, it is almost as if the baseflow itself produces a natural moving average smoother, possibly dampening and smoothing the annual year-to-year precipitation variance. The observed lag in resulting outflow from the aquifers is relatively stable from month to month, which supports using aquifer outflow cycles as input for predicting over one-third of PG&E's hydro generation several years in advance. There is an observed approximate 16% range in annual generation movement within the short 14-16 year oscillatory periods for the 1972-2001 thirty-year mean annual Pit and McCloud River baseflow.

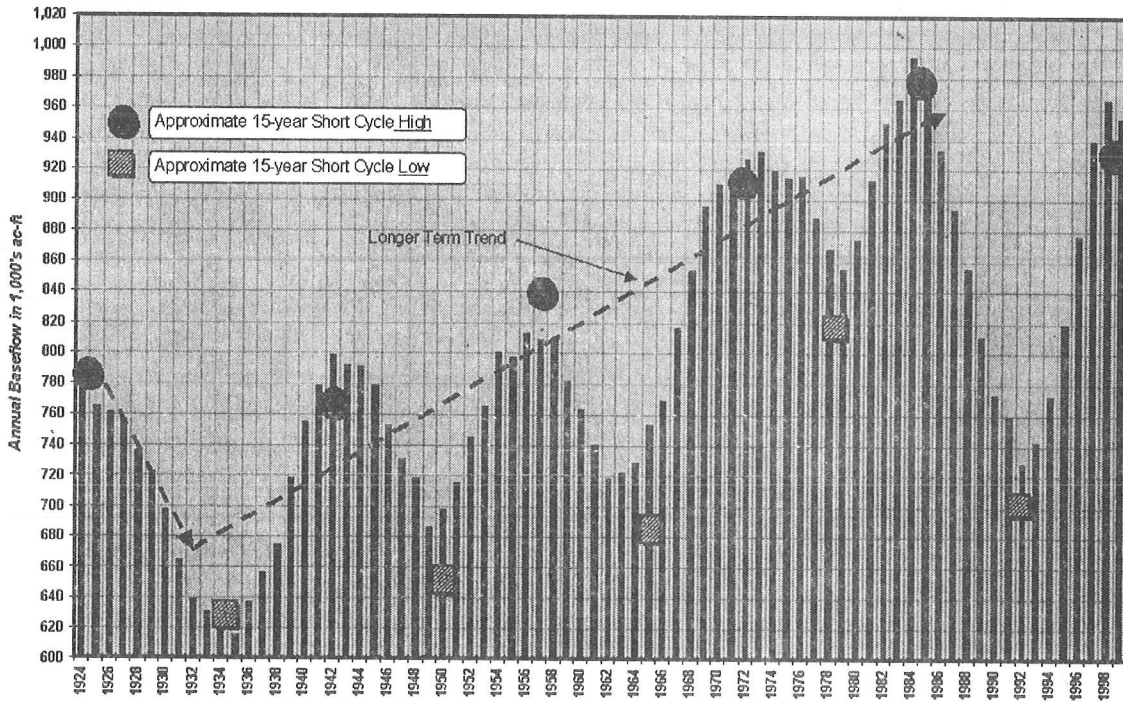


Figure 3 Fall River's annual unimpaired baseflow in thousand acre-feet for the 80-year period, 1922 through 2001. A centered 5-year moving average smoother was applied. Seventy-five years of smoothed data are shown. Fall River's return to maximum baseflow rates required about 50 years (1935 through 1984). This is 22 years longer than the Pit River as a whole, which required only 28 years for return to near maximum baseflow rates. Fall River is a major baseflow contributing tributary to the Pit River.

This year, while currently experiencing a dry seasonal outlook in terms of precipitation, the current energy short situation is continuing to benefit from the increased flow and generation benefits that come from being within three years of the 1998 peak outflow rate of the short term cycle. After starting a gradual decline in 1999, aquifer outflow rates from the northern California aquifers are anticipated to continue decreasing during the next 3-4 years, before baseflows begin a return toward increased rates of flow. The short-term flow cycles have been tracked back to about 1907 when flow data first began being collected on a regular basis. The cause for 14-16 year baseflow cycling likely lies in a similar cycling length, which appears to occur in the long-term precipitation record. An observed 14-16 year periodicity in precipitation appears in the 75-year long-term record for PG&E's 16-station precipitation index as well as for the Lake Spaulding climate station located in the central Sierra Nevada along Highway 80. Lake Spaulding's record extends back to 1894, providing a good mountain station for observing short term cycling over time. While an autocorrelation done on the Lake Spaulding water year precipitation extending back to 1894 does not provide significant forecast correlation in terms of a year's precipitation amount, the approximate 15-year periodicity appears quite strong in terms of a persistent climatic echo over time (Figure 4). No attempt is made here to address causative factors for precipitation cycles, such as possibly resulting from decadal type oscillation. Cycling in the annual precipitation record and the Pacific Decadal Oscillation is being researched and explored in terms of cause by a number of different scientists (Cayan 1998; Diaz 1995; Taylor 1995, 1999).

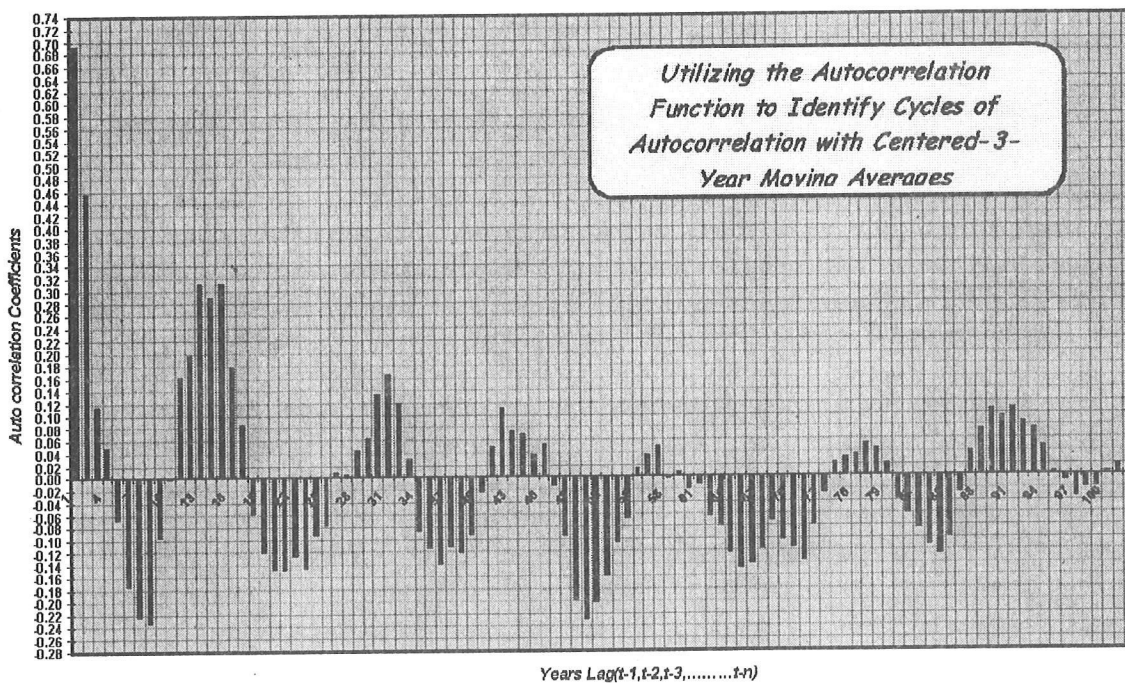


Figure 4 An autocorrelation performed on the centered 3-year moving average water year precipitation record for the Lake Spaulding climate station in the Central Sierra along Hwy 80. While the specific ACF does not produce a significant predictor in terms of precipitation amount, the approximate 15-year cycle readily reveals itself. The cycling correlates closely with northern California's aquifer 1-2 year outflow lagged response.

Aquifer Outflow and the Current Energy Crisis

With reservoirs other than Lake Almanor being at their winter minimum carryover storage and almost no rain-generated inflows, about 65% of PG&E's January and February 2001 hydro electric generation was produced from groundwater or aquifer outflow. About 3 maf of runoff into Lake Shasta will come from aquifer outflow/springs this year. This aquifer outflow water through PG&E's Pit River powerhouses is anticipated to produce almost 3,600 GWh or almost 33% of our total forecasted PG&E hydrogeneration this year with about 1,400 MW daily peaking ability, enough energy to meet the needs of more than 1 million family homes. While its contribution begins to decline over several months, a dry year next year, regardless of its severity, will still provide about 85% of the 2001 hydrogeneration from baseflow or about 3,000-3,100 GWh from the Pit-McCloud aquifer outflow. Three additional very dry years beyond 2002 would push the firm dependable annual contribution down to about 2,100 GWh; an amount similar to both the estimated 1924 and 1992 calculated actual baseflow contribution. Based on a review of the 1907-1930 period, it appears that beyond six dry years, longer-term effects to the ground water may begin.

Effects of Climate Change on Aquifer Outflow

While it may seem speculative to make assumptions with regard to defining climate cycles of wetness or dryness from baseflow response, the Pit and McCloud River aquifers appear to react to periods of wetness and dryness with a slightly delayed response, somewhat similar in manner to a moving average type statistic. The effects of precipitation variance on runoff during any given season is buffered in a decayed manner by the effects of wetness from previous years.

Extended Periods of "Net Groundwater Discharge" and "Net Groundwater Recharge"

The extended dry "net discharge period" observed to start in 1907 was followed by an extended "net recharge period" before baseflow rates returned to their earlier maximum outflow rates. Because the 1907 through 1958 (52 years) period took up such a large portion of the available historical record, it seems almost impossible to speculate beyond the short-term cycle, which is currently in a decline mode, to speculate whether or not we are now entering another longer-term downward trend which may once again require a long refill period. The 28-year net recharge period, 1931 through 1958, followed 24 years of declining baseflow or net discharge during the 1907 through 1930 period (Figure 5; Figure 6). When compared with long-term precipitation records for climate station located at Canyon Dam, there is a corresponding mean difference for the two periods of 5.21 inches with period mean of 33.55 inches for the net discharge period and 38.76 inches for the net recharge period.

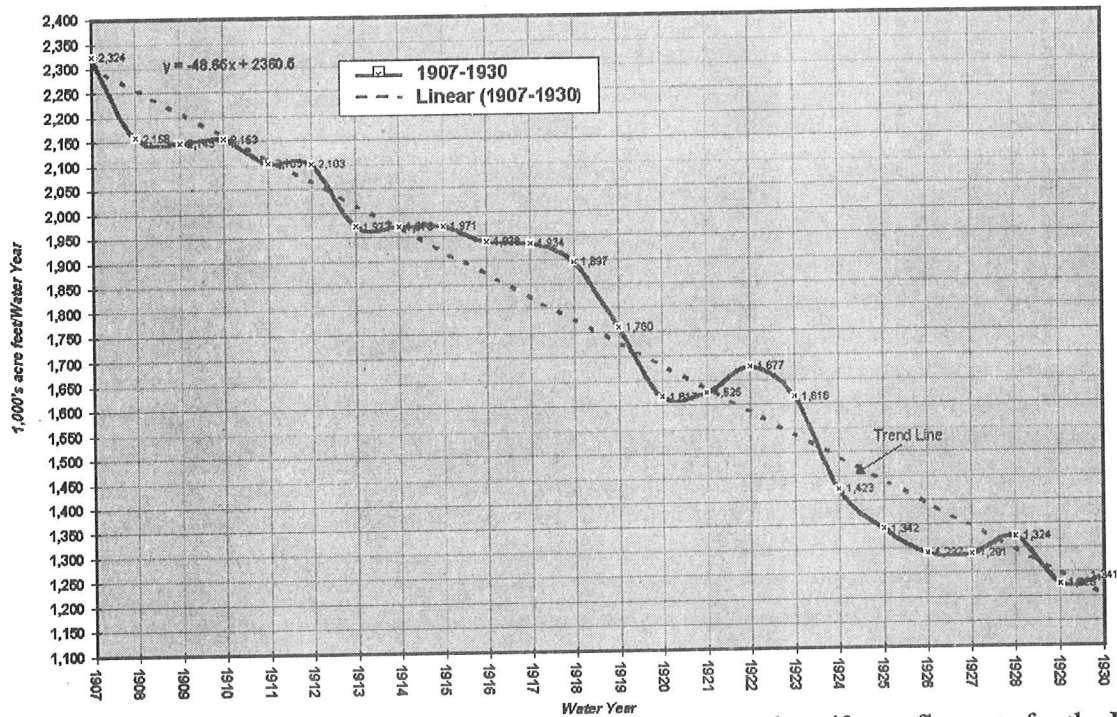


Figure 5 The 24-year (1907–1930) “decline” from maximum observed aquifer outflow rate for the Pit River unimpaired water year baseflow component of inflow to Lake Shasta

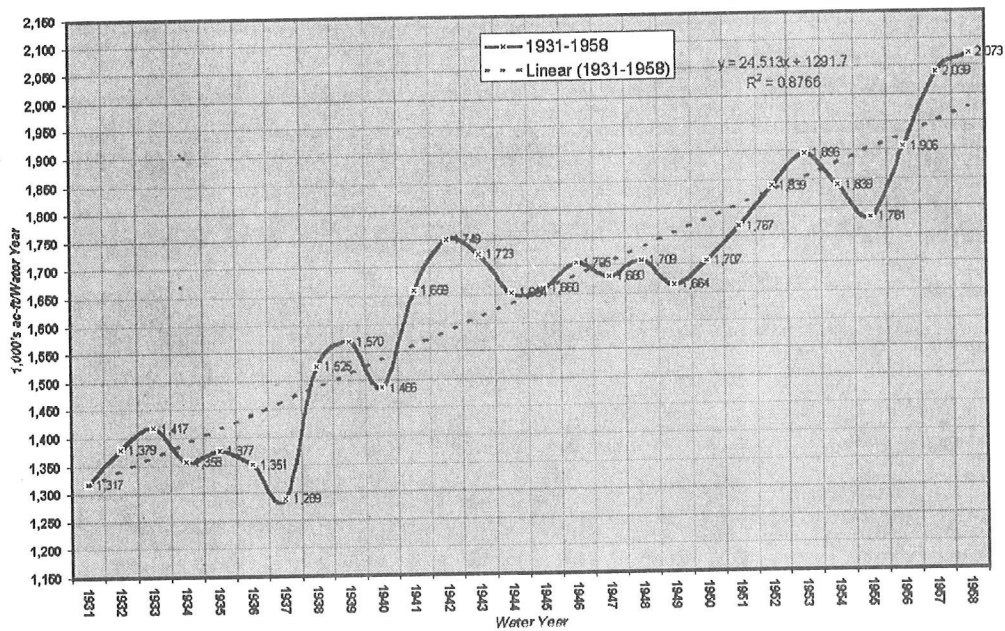


Figure 6 The 28-year (1931–1958) “climb” back to near-maximum aquifer outflow rate for the Pit River unimpaired water year baseflow component of inflow to Lake Shasta. This return to higher outflow rates follows the 24-year (1907–1930) decline from the prolonged dry period as shown in Figure 5.

52 Years of Reduced Baseflows

The aquifer outflow rate for the Pit River's unimpaired runoff to Lake Shasta was at the observed maximum annual flow rate of approximately 2.35 maf from 1901 through 1906. However, the 24-year period from 1907 through 1930 was characterized by mostly below normal precipitation. As a result of declining aquifer outflow, the annual accumulated 24-year departure from that of the 1906-1907 baseflow rates totaled a negative 11 maf in outflow by 1931. During the 1931 through 1958 recharge period (28 years) approximately another 16 maf was absent from the Pit River inflow to Shasta. In 1958 aquifer outflow rates were restored to about 93% the earlier 1906-1907 high rate of 2,225,000 maf per year. This 52-year period of below maximum aquifer outflow rates between 1907 and 1958 created an extended negative departure from the earlier full aquifer outflow rates for the Pit River. Since the Pit River is tributary to the Sacramento River, the effect was slightly over a half century of less than full baseflow availability (approximately negative 27 maf when compared with the maximum observed baseflow such as during the period just prior to 1907 and similar to that recently reached in 1998) from the northern volcanic drainage available for inflow to Lake Shasta for that period. Using the current hydroelectric capacity, hydroelectric generation production for the Pit River hydroelectric project was simulated back to the first of the century. Two equal length 44-year periods consisting of 1914-1957 and 1958-2001 were compared for the Pit River. The simulated difference was a 26,000 GWh reduction in energy for the earlier period compared with the mean baseflow rates experienced during the second half of the 20th century (Figure 7). A drop in average flow rate of 510 cfs occurred over a 23-year period, 1908 through 1930. In terms of annual flow quantity, this equated to a drop from approximately 2,225,000 maf per year in 1908 to 1,240,000 maf per year in 1930.

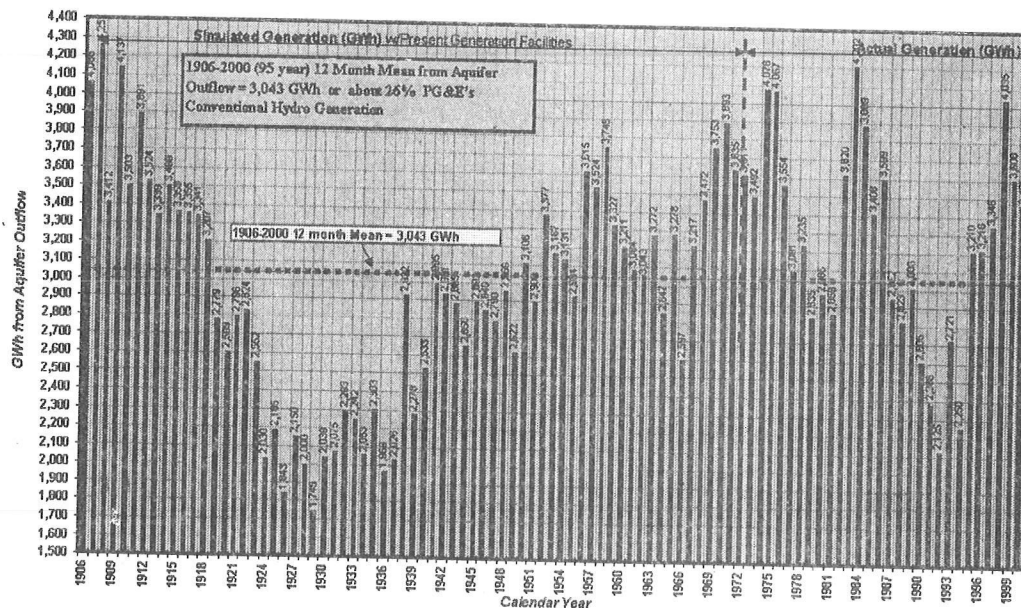


Figure 7 PG&E's Pit River annual calendar year hydroelectric generation from northern California's Pit and McCloud River aquifer outflow (springs). The 1906-1971 period was simulated based on historic baseflows passed through the current hydroelectric system. Water is imported from the McCloud River to the Pit River through the McCloud-Iron Canyon Tunnel.

From 1907 through 1930, precipitation was below average (Figure 8). While the drier period may hint at a possible low point in an approximately 95-100 year cycle, the data analyzed in this study is insufficient to draw any conclusions regarding the existence of a long-term cycle.

Lake Spaulding Water Year Discrete 15-Year Average Precipitation Groupings

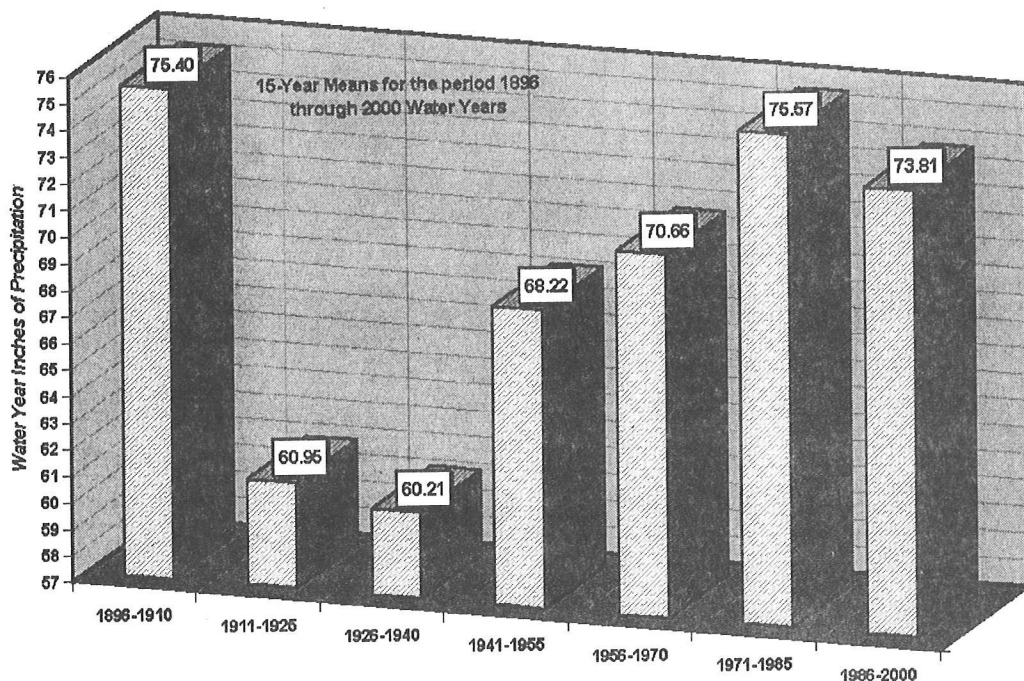


Figure 8 Water year precipitation shown as 15-year means. The mean precipitation (60.58 inches) for the 30-year period 1911 through 1940 vs. the mean precipitation (74.69 inches) of the 30-year period 1971 through 2000 readily illustrates the wetness of the latter period.

Recent Years

More recently, based on the recent six-year (1987-1992) consecutively dry period, the six-year average seasonal drop in accumulated precipitation for the Pit 5 PH climate station was 50.93 inches or 37.30 inches less than the prior 7-year (1981-1986) average of 88.23 inches. For the McCloud River at Shasta, the cumulative six-year annual decline in baseflow quantity from the preceding period was 1,596 thousand acre-feet (taf) for the six-year cumulative precipitation decline of 217.33 inches. The decline during the 1987-1992 net discharge period equates to 1,596 taf/217.33 inches or -7,340 af loss in baseflow for each inch decrease in precipitation at Pit 5 PH.

The following six years (1993-1998) was an unusually wet period. The net recharge was calculated to have an approximate 86% recovery factor or an accumulated 1,646,290 af increase above the earlier six-year total. The net recharge period equates to 6,310 af increase in baseflow for each inch net increase in precipitation.

The Long Term Hydrological Balance

A mass balance approach was used to analyze the hydrology for the Pit River. The long-term historic runoff record was used with the long-term precipitation average for Pit 5 PH. The calculations assume that the long term average recovery factor for ratio of runoff to precipitation for the Pit River Basin is the same as calculated for the McCloud Basin. The annual long-term average runoff for the Pit River Basin was calculated to be 3,107,000 af unimpaired runoff. To calculate a water balance, the 1906-2001 96-year Lake Spaulding mean annual precipitation record of 73.50 inches per water year average was used to extend the Pit 5 PH record back in time.

The long-term average water balance was calculated by first separating the aquifer outflow or baseflow component from the total river unimpaired outflow to Lake Shasta. It was then assumed that the remaining portion of the total annual runoff was from the non-baseflow component. For the Pit River unimpaired inflow to Lake Shasta, the average quantity of water per inch precipitation at Pit 5 PH was calculated to be 67,200 af.

The following average long-term mass balance was compiled:

- 26.58 inches of precipitation or 36.3% of the annual precipitation is computed from the recharge/discharge balance as aquifer outflow or baseflow. This annual component equates to 1,785 taf.
- 19.72 inches of precipitation or 26.9% of the annual precipitation is computed as unimpaired runoff from the current year's precipitation and is runoff other than baseflow. This annual component equates to 1,325 taf.
- 26.95 inches of precipitation or 36.8% of the annual precipitation is computed as evapotranspiration and is not available for river flow. This annual component equates to about 1,811 taf.

For example, one can assume that for a very dry year like 1977, with 34.92 inches of precipitation for the water year at Pit 5 PH, the normal full long-term average annual evapotranspiration component of Pit 5 PH of 1,811 taf (26.95-inch equivalent) is exceeded by 7.97 inches. The 1977 water year non-baseflow runoff was compiled as 1.88 inches or 126 taf. Since the observed baseflow component of the Pit River for the 1977 water year was 1,848 taf, then the remaining 6.09-inch balance of precipitation, equivalent to 409 taf of recharge for the twelve-month period was approximately 1,439 taf short; in other words, 1977 experienced a net discharge from the aquifer reserves of approximately 1,439 taf or the Pit 5 PH precipitation equivalent of 21.4 inches.

Possibilities for Precipitation Enhancement

PG&E is exploring ways to use and manage this aquifer storage for increasing hydroelectric generation. The Pit/McCloud River aquifers may provide a unique opportunity to enhance precipitation during wet years, store the added water underground with little if any evapotranspiration, and enjoy the availability of additional baseflow during dry years. Since PG&E's Pit River hydroelectric project has relatively large forebays, any increases to baseflow would provide additional water for hydroelectric production, most of which can be used for additional hours of

peaking. Additional baseflow provides increased inflow to the rivers; after its use to increase hydroelectric production, the water flows into Lake Shasta and the Sacramento River providing increased freshwater supply available for Delta outflow.

Since, even in the driest years, naturally produced precipitation appears sufficient to meet nearly all evapotranspiration demand, most of the remainder is available for aquifer recharge and overland flow. If one assumes that most of the enhanced precipitation over the headwater drainage would become 100% available for infiltration and aquifer recharge, then it can be assumed that one inch at Pit 5 PH will have the effect of adding approximately 67,200 af/inch to baseflow in the Pit River Basin and approximately 17,400 af/inch to baseflow for the McCloud River inflow to McCloud Reservoir for a combined total aquifer recharge potential of 84,560 af/inch of additional precipitation. For reasonableness, it seems likely that unforeseen losses will occur and that a factor of 90% (0.90 times the 84,560 af) would be a more reasonable calculation. If a reasonable increase in precipitation is 5%, then 0.05 times 73.25 inches per year equates to 3.66 inches per year.

- McCloud River water:

$$[(17,400 \text{ af/yr/in})(3.66 \text{ in})(1,343 \text{ KWh/af})]0.90 \div 1,000,000 \text{ KWh/GWh} = 77 \text{ GWh/yr}$$

- Pit River water:

$$[(67,180 \text{ af/yr/in})(3.66 \text{ in})(1,600 \text{ KWh/af})]0.90 \div 1,000,000 \text{ KWh/GWh} = 354 \text{ GWh/yr}$$

Total potential generation for a 5% increase in precipitation over the Pit and McCloud river basins is equivalent to an increase of 431 GWh/year peaking energy. This would provide approximately 575 additional hours (24 days) per year of new energy at 750 MW by extending peaking time on existing powerhouses. Shasta Dam with its large reservoir and powerhouse would also likely benefit from a 5% annual increase in inflow (300 taf) and consequent increased hydro generation amounting to an additional 85 Gwh/year. There are five 125 MW units at Shasta Dam (three of the five units have been recently upgraded to 142 MW, but at the time of this writing, the upgraded capacity has not yet been released for service at the higher capacity rating) (USBR 2001). The five 125 MW units could generate approximately 135 additional hours at a full combined capacity of 625 MW.

PG&E Annual Hydroelectric Generation Oscillation

PG&E's annual total calendar year hydro generation appears to oscillate in synchronization with the groundwater in a somewhat predictable pattern (Figure 9). With the single exception of Lake Almanor, the remaining storage reservoirs are relatively small. Typically the smaller reservoirs empty and fill each year. PG&E's Lake Almanor however, contains about 48% of its PG&E's usable storage capacity. The effects of annual precipitation variance on this large body of water frequently requires a multi-year operational response to restore the reservoir resulting in lagged response to those years with annual runoff in terms of variance of the mean annual inflow. The combined lagged effect of retaining operational control over Lake Almanor and the aquifer outflow lag is sufficient to dampen typical weather variance creating an oscillating system generation pattern with a possible 14-16 year periodicity. While the 30-year record appears to follow the 14-16 yr cycle observed for baseflow and precipitation, the record period is too short to make any valid conclusions about whether or not the generation cycle actually exists. If additional records in the future reveal that there is a valid 14-16 year cycle, then this cyclic pattern may be predictable in terms of a 3-year moving average several

years in advance with reasonable success. While the moving average effect for three or more years appears predictable with reasonable success, it's much more difficult to predict the effect of weather variance on the following year's generation. The effects of any given year's precipitation appear to be reflected through pressure changes on spring outflow, which lag 2-3 years. For Lake Almanor, one or more large years which fill the lake may require 1-3 years to return it to lower levels; the opposite effect is true for the effects of successive dry years, in which case it may require a refill period lasting 1-3 years. Lake Almanor and Cow-Battle creeks are likewise spring fed from aquifers formed within the flood basalts.

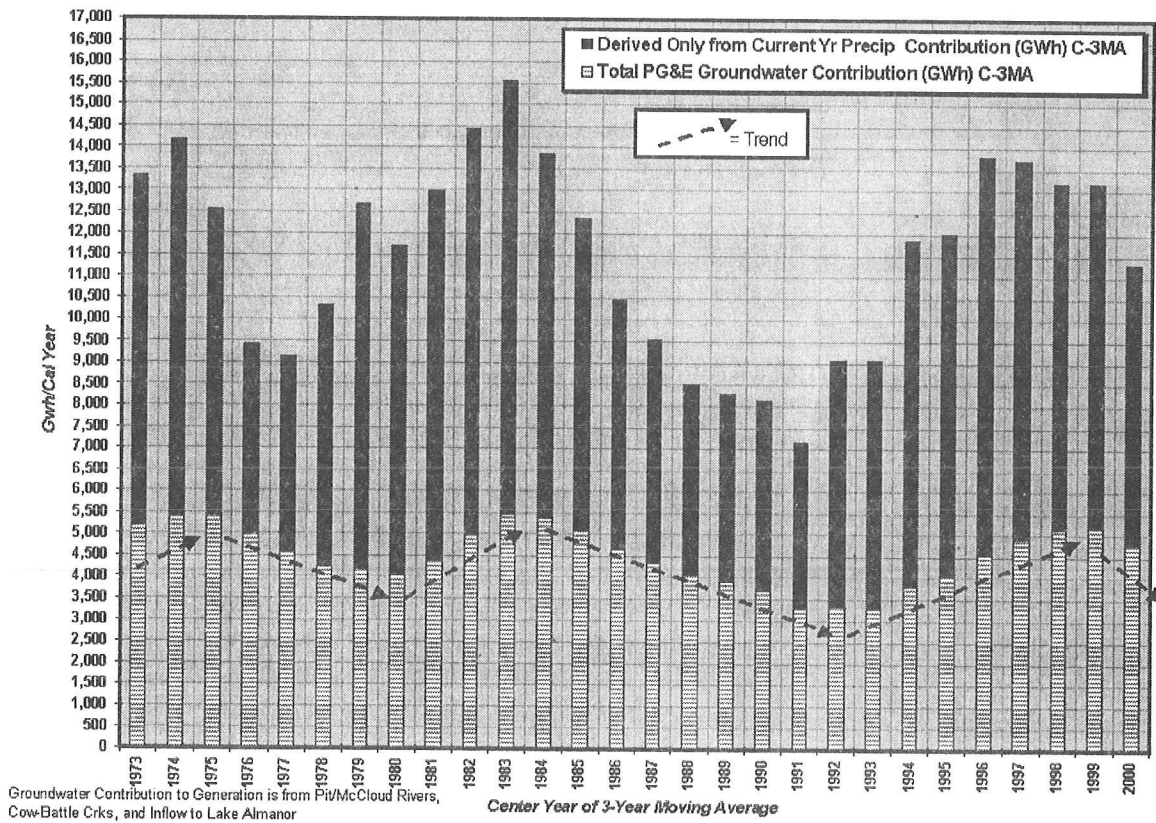


Figure 9 PG&E's Conventional Hydro Generation charted with a centered 3-year moving average for the 30-year period (1972-2001) (28 years shown). In addition to showing what may turn out to be an approximate 14-15 year periodicity, the 38% proportion of PG&E's hydroelectric energy from lagged volcanic baseflow (crosshatched base portion of columns) is readily apparent.

The Observed Effect of Climate on Rates of Aquifer Outflow

The buffering effects on hydroelectric generation of annual baseflow and Lake Almanor's large storage capacity not only lag current seasonal climate variance, but likely also reflect the smoothed lag of accumulated variance from the long-term historic precipitation mean. Baseflow response, during the net recharge phase, tends to echo and double in both time and quantity the effect of any longer term variance drift in precipitation variance from the long-term average. As such, the net discharge

flow reduction of approximately 11 maf from the aquifer decay in observed baseflow rate for the Pit River at Lake Shasta during the 24-year (1907-1930) period was echoed in continued sub maximum baseflow during the following 1931-1958 28-year net recharge period. The overall loss in baseflow during this 52-year period was about 27 maf in terms of the difference from the maximum identified baseflow rate or an amount equivalent to almost 95% of the capacity of Lake Mead (28.5 maf). The 52-year period of decreasing then increasing baseflow rate such as occurred with the 1907 through 1957 period provides an excellent opportunity to compare the precipitation record with baseflow and reflect on what changes in precipitation availability for the half century period may lead to the observed long term reduction in baseflow from northern California's volcanic aquifers.

The effect of baseflows on defining PG&E's dependable capacity cannot be ignored. For example both 1924 and 1977 were the two driest years during the 20th century for Lake Spaulding in the central Sierra Nevada. 1977 was 6.66 inches drier than 1924 and for that reason and because of its more recent occurrence is often chosen to represent PG&E's dependable capacity. However if one compares baseflow in the Pit River for 1977 with that for 1924, 1977 had 425,000 af more baseflow. For the Pit River, which normally makes up about 33% of PG&E's long-term average year generation, 1931 was significantly drier than 1977 in terms of dependable capacity from available water. The consequence of experiencing a 1931 baseflow case with 1977 annual precipitation would have likely reduced PG&E's overall 1977 hydro generation by an additional 15%.

What Lies Ahead?

While there is no crystal ball that provides sufficient skill level for predicting next year's hydrogeneration or precipitation, certain likelihood's tend to reveal themselves for the next 12 to 15 years and possibly beyond, especially when analyzed as a moving average of three or more years. The baseflow cycle took a downward turn beginning with 1999 (a much drier-than-normal 2001 water year brought the fifth driest year since 1926 in terms of precipitation for PG&E's 16-station precipitation index) and Lake Almanor will be reduced to or possibly slightly below normal end-of-year carryover storage for 2001. The likely effect is that through about 2005, there is sufficient net deficits accumulating in PG&E's hydro producing resources that the 2-3 year associated lag will likely see the moving 3-year grouping of years' total system generation continue to decline, then begin a return to progressively higher levels of generation for the remainder of the 7-year part of the cycle through about 2012. Whether or not there will be a return to an extended below normal period such as was experienced beginning in 1907 is impossible to determine at this time. While a possible 94-100 year type cycling may exist, the available data is insufficient to draw any conclusions other than to appreciate that a long-term 52-year period of reduced baseflow from the Pit and McCloud river aquifers occurred during the last century and it seems reasonable to assume that similar long-term trends will recur. An extension of the Lake Spaulding climate record back beyond its 1894 start seems to hint at an orderly progression of precipitation change which may tend to repeat itself over a period lasting 94-100 years; however, the record is too short and too limited in terms of mountain stations to draw any valid conclusions.

Conclusions

Northern California's volcanic aquifers provide PG&E and the State of California with a unique resource, one that buffers the effect of California's large precipitation variability in terms of runoff for those watersheds that overlie the volcanic basalts. For PG&E, during extended dry periods, the sustained baseflow from springs represents an increased proportion of the hydro generation resource potential. Normally baseflow over the long-term record represents about 38% of PG&E's hydrogeneration. During 1977, a very dry year for California, baseflow from northern California's volcanic aquifer-fed springs supplied approximately 58% of PG&E available hydro generation, increasing PG&E's total hydro generation that year by approximately 3,514 GWh. The large aquifers on the Pit-McCloud watersheds exhibit both a short-term oscillation of 14-16 years and, for the period studied, a single 52-year extended period of reduced outflow rates during which phases of net discharge and net refill were revealed. During the extended 1907 through 1958 period, approximately 27 maf in accumulated baseflow reduction from the maximum sustained flow rate took place. In terms of today's facilities on the Pit River, that would equate to an approximate 25,000 GWh loss of energy if the same situation occurred with today's hydroelectric system in place. If the current observed periodicity holds as during past years, the 2002-2005 outlook for baseflow from northern California's springs can be anticipated to continue its decline, possibly hinting that while any given year may be close to or above average, the average of the next four years of accumulated precipitation for northern California is likely to be less than the recent 40-year accumulated average (1961-2000). If another extended dry period should eventually occur, as with the 1907-1930 period, then once again we could experience 40-50 years of baseflow below the maximum aquifer rates.

References

- Alt D, Hyndman DW. 2000. Roadside geology of northern and central California. Montana: Mountain Press. 369 p.
- Bastasch R. 1998. Waters of Oregon. Corvallis (OR): Oregon State University Press. 278 p.
- Booth W. 2001. States locked into western grid face severe energy test. Available via the Internet at http://www.greenspun.com/bboard/q-and-a-fetch-msg.tcl?msg_id=004 Vol. Accessed on Aug 19 2001. The Washington Post Company.
- Brulte J. 1996. Fact sheets on AB 1890 from the Office of Governor Pete Wilson—deregulation of the electrical industry. Available via the Internet at <http://eerr.notes.org/california/ab1890factsheet.htm>. Accessed on Aug 19 2001.
- Cayan DR, Dettinger MD, Diaz HF, Graham NE. 1998. Decadal variability of precipitation over Western North America. *J Climatology* 11:3148-66.
- Diaz HF, Anderson CA. 1995. Precipitation trends and water consumption related to population in the southwestern United States: a reassessment. *Water Resources Research* 31:713-20.
- Freeman GJ. 2000. Comparison of Sacramento Valley Runoff Index with Columbia River Basin runoff. Pacific Gas & Electric Company. Unpublished internal files.

Planert M, Williams JS. 1999. Groundwater atlas of the United States—Segment 1: California Nevada, major aquifers, northern California volcanic-rock aquifers. Figure 137. U.S. Geological Survey.

Taylor GH. 1995. Long term precipitation cycles in Portland. Available via the Internet at http://www.ocs.orst.edu/reports/PDX_precip.html. Accessed on Aug 2 2001.

Taylor GH, Hannan C. 1999. The climate of Oregon—from rain forest to desert. Corvallis (OR): Oregon State University Press. 211 p.

Tison R. 2001. The true cause of California's energy crisis, energy-tech on-line. Available via the Internet at http://energy-tech.com/issues/html/we0102_001.html. Accessed on Aug 19 2001.

[USBR] U.S. Bureau of Reclamation. 2001 Shasta power plant. Available via the Internet at <http://www.usbr.gov/power/data/sites/shasta/shasta.htm>. Accessed on Aug 19 2001.

Snowfall Occurrence at Two Lee-Side Mountain Locations: Comparing the Sierra Nevada, California, and the Rocky Mountains, Colorado

Mark Losleben, Susan Burak, Robert E. Davis, and Karla Adami

Introduction

Snowfall occurrence, snowpack, and the relevant atmospheric circulation conditions in the Sierra Nevada and the Rocky Mountains are quantified and compared for three winter seasons, 1996-1999. The study sites are Mammoth Mountain, California, and Niwot Ridge, Colorado. Their latitudes and elevations are similar, and both are on the lee sides of their respective mountain ranges, but Mammoth is much closer to the Pacific Ocean, whereas Niwot is a more continental site.

Daily data is analyzed for differences and similarities in atmospheric circulation associated with snowfall occurrence, and the relationships to the El Niño-Southern Oscillation (ENSO) phases are discussed. Each season in this study occurs during a different phase. The 1998-99 season was during a cold phase (La Niña), the 1997-98 season was during a warm phase (El Niño), and the 1996-97 season was neutral, neither warm nor cold. The warm and cold seasons are classified as “strong” events by the Western Regional Climate Center (2001).

Site Locations

Mammoth Mountain, California is on the lee slope of the Sierra Nevada at latitude 37°N, longitude 119°W, and an elevation of 2835 m. It is in a more maritime climate; it is warmer and moister than Niwot Ridge.

Niwot Ridge, Colorado is at latitude 40°N, longitude 105°W, and at an elevation of 3048 m. It is on the lee slope of the Rocky Mountains, and in a more continental climate—colder, drier, and windier, than Mammoth.

Data

Snowfall data was collected at the Mammoth and Niwot sites on a daily event basis, and recorded as snow water equivalent.

NCAR/NCEP Reanalysis Geopotential Height Data was used to compute the daily circulation indices and synoptic weather patterns at the 700 mb and 850 mb levels for each day when snowfall occurred or did not occur.

Analysis

Each day in each winter season was classified as with or without snow at both sites. At each site each day was objectively classified as one of 27 possible synoptic weather types. Four circulation indices were also computed at two atmospheric levels, 700 mb and 850 mb, at both sites. A full explanation of this grid based classification scheme is given in Losleben and others (2000). The grid points used are shown on Figure 1. The circulation indices of the two sites were compared, and the significance levels of the different means were determined using *t*-test analysis. The synoptic weather types at each site were compared using frequency analysis of snow and no snow conditions.

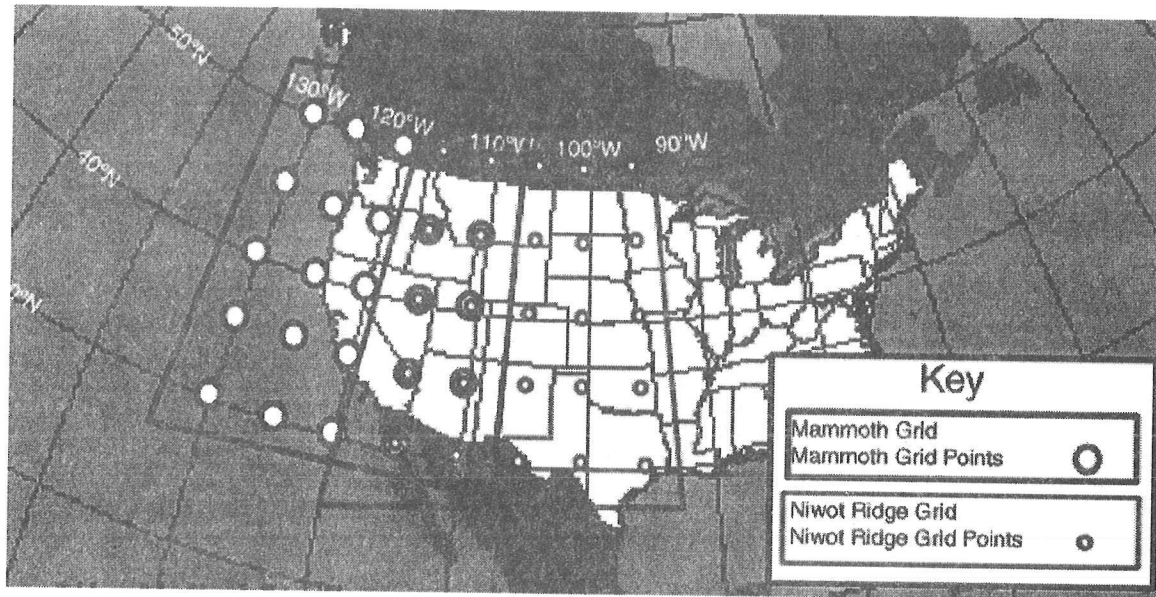


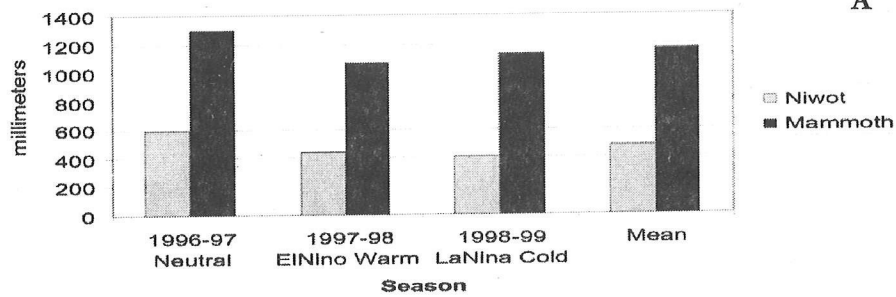
Figure 1 Niwot and Mammoth sites, located at the center of the red and blue grids, respectively. The circulation classifications, indices and synoptic patterns, are computed using these respective grid points.

Results

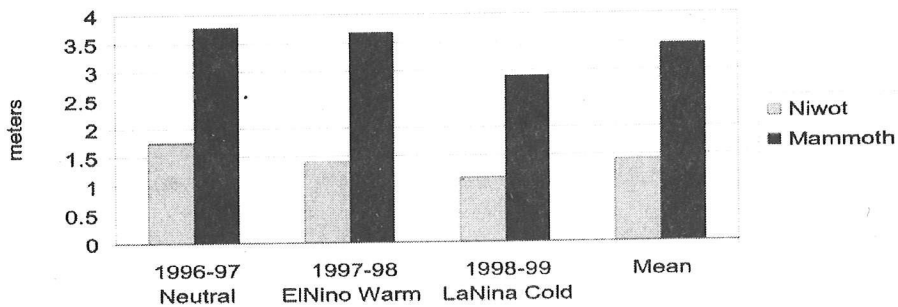
General Conditions

Precipitation. Mammoth snow water equivalent and snowpack was 2.4 times greater than at Niwot (Figures 2a, 2b), but the Mammoth snow season was 37% shorter compared to Niwot (Figure 2c). The seasonality of snowfall was also different. Snow fell at Mammoth primarily from December through February, but the Niwot snowfall season often included October and November, with the heaviest snowfalls in March and April.

**Precipitation Season Totals at Mammoth and Niwot
1996-97, 1997-98, 1998-99**



**Maximum Snowpack at Mammoth and Niwot
1996-97, 1997-98, 1998-99**



**Snow Season Length at Mammoth and Niwot
1996-97, 1997-98, 1998-99**

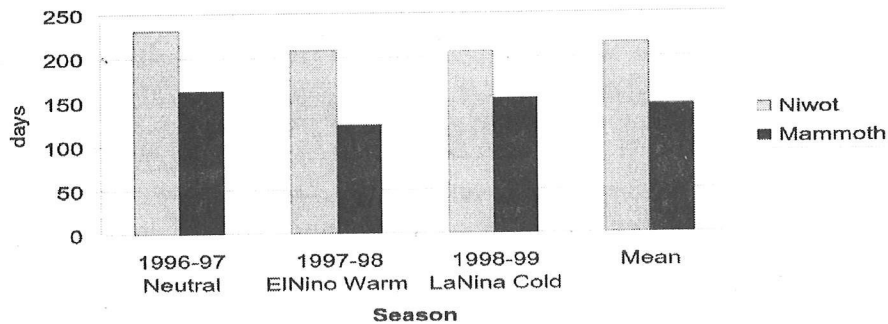


Figure 2 (A) Seasonal precipitation (mm) at Niwot and Mammoth; (B) maximum snowpack depth (m) at Niwot and Mammoth; (C) length of snowfall season (days) at Niwot and Mammoth

Weather Patterns for Snow and No-Snow Occurrence. Weather types associated with snowfall were also more diverse at Mammoth than at Niwot (Figures 3a, 3b). Generally, Mammoth snowfall occurred most frequently during the strong zonal westerly weather pattern, but southwesterly and cyclonic weather patterns also brought snow. No-snow periods occurred with northwesterly and anticyclonic weather patterns.

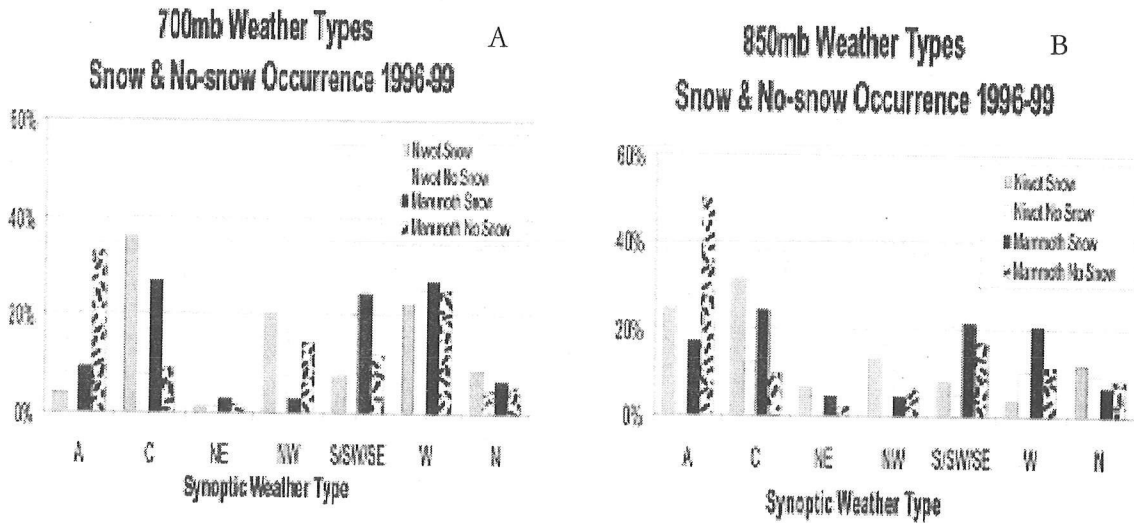


Figure 3 (A) Frequency of occurrence of daily synoptic patterns of all days with, or without, snowfall from the beginning of the 1996-97 season to the end of the 1998-99 season, at the 700 mb height, at Niwot and Mammoth. (B) Same as in Figure 3a, but at 850 mb height. "A" is anticyclonic, "C" is cyclonic, "NE" is northeast, "NW" is northwest, "S" is south, "SW" is southwest, "SE" is southeast, "W" is west, "N" is north.

Niwot snowfall occurred most frequently with cyclonic weather patterns passing south of the site. No-snow periods occurred during zonal, westerly weather patterns, and high pressure conditions.

Inter-Seasonal Variability

Synoptic Weather Type. At Mammoth, the most snow fell with the western weather type during the 1996-97 season (neutral phase), with the southwesterly type during the 1997-98 season (warm phase), and with the cyclonic type during the 1998-99 season (cold phase) (Figure 4a).

At Niwot, snowfall was most often associated with the cyclonic weather type, and secondly with the northwest type, during all three seasons. The association between snowfall and the north type increased in 1997-98 (warm phase) season, and with the westerly type in the 1998-99 season (cold phase) (Figure 4a).

Wind Direction. Wind directions associated with snowfall changed between the seasons (Figures 5a, 5b, 5c). At Mammoth, snowfall was most often associated with west winds in 1996-97, with southwest and west winds in 1997-98 and with west winds in 1998-99, but southwest winds were a strong second in this season. No-snow periods occurred with northwest winds, except during the 1997-98 season (warm ENSO phase).

At Niwot, snow fell with west and north-west winds in 1996-97, with northwest winds in 1997-98, and with west winds in 1998-99.

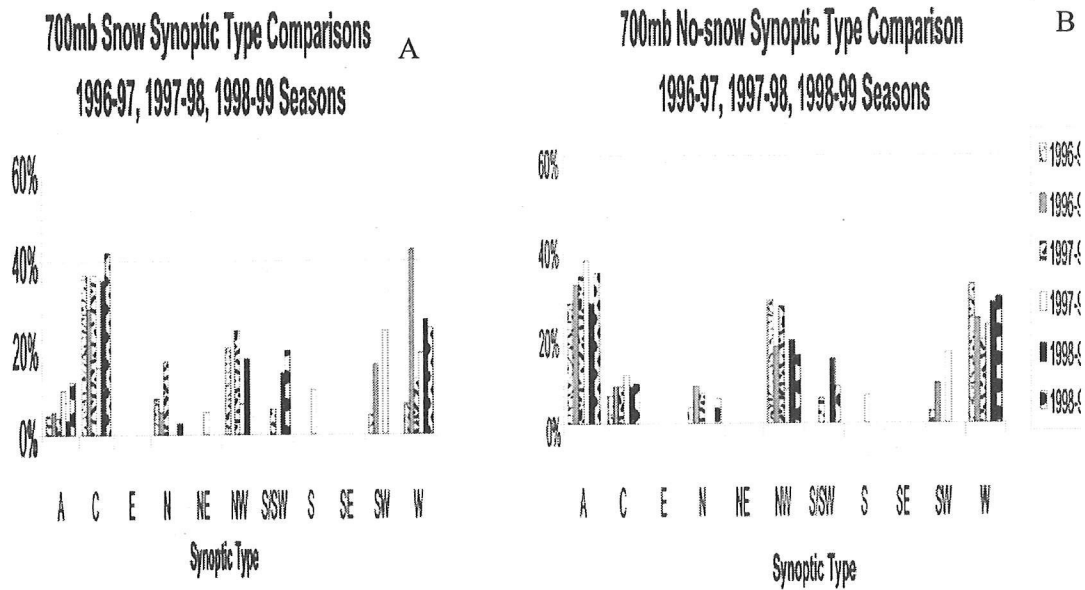


Figure 4 (A) Seasonal frequency of occurrence of daily synoptic types for all days with snow (A) and no snow (B), at Niwot and Mammoth at 700 mb height

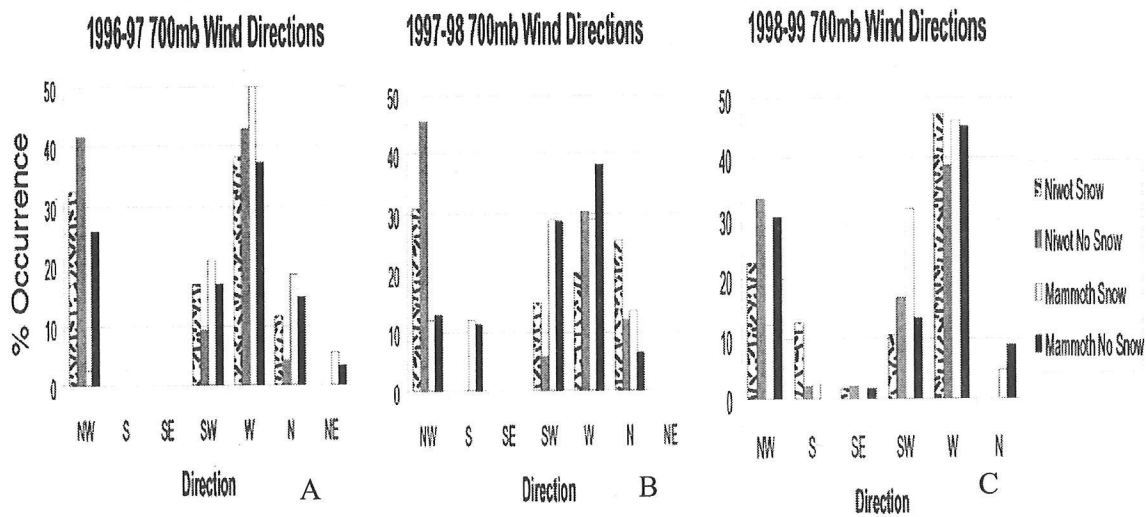


Figure 5 (A-C) Seasonal frequency of daily wind direction for days with, or without, snow at Niwot and Mammoth at 700 mb height

Circulation Indices. Clearly, vorticity (Z) was the most consistently significant index related to snowfall at both sites. This relationship held independently of ENSO phase (Figure 6). Regarding the relationships to the other indices, snowfall at Niwot was fairly insensitive to changes with ENSO phase, in contrast to the case at Mammoth. At Mammoth, the south (S) circulation index was a significantly important snowfall indicator in the 1998-99 season (cold phase), in contrast to the 1997-98 season (warm phase) when it was completely insignificant. During the 1996-97 (neutral phase) season, it was a marginally significant indicator. Force (F) was insignificant during the 1998-99 season (cold phase), but became marginally significant during the 1996-97 and 1997-98 seasons (warm and neutral phases).

At Niwot, there were no significant changes in index values from season to season (Figure 6). Whether significant or not, some interesting patterns emerge in the index relationships with snow and no-snow periods at the two sites (Figures 7a, 7b). For example, snow and the south (S) index are positively related at Mammoth, and negatively related at Niwot in all three seasons. Also, the vorticity index (Z) is positively related to snow occurrence and negatively related to no-snow occurrence.

| Index | 1996-97 Neutral ENSO Phase | | | | 1997-98 Warm ENSO Phase | | | | 1998-99 Cold ENSO Phase | | | |
|-------|----------------------------|--------------|---------|--------------|-------------------------|--------------|---------|--------------|-------------------------|--------------|---------|--------------|
| | Niwot | | Mammoth | | Niwot | | Mammoth | | Niwot | | Mammoth | |
| | Trend | Significance | Trend | Significance | Trend | Significance | Trend | Significance | Trend | Significance | Trend | Significance |
| S | >N | 85.70% | >S | 2.34% | <N | 62.80% | >S | 72.80% | less N | 22.40% | >S | 0.20% |
| W | <W | 23.60% | >W | 7.30% | <W | 14.20% | <W | 43.30% | <W | 80.80% | >W | 66.20% |
| F | <F | 81.80% | >F | 1.16% | <F | 70.80% | >F | 1.86% | >F | 14.60% | >F | 50.80% |
| Z | >Z | 0.00% | >Z | 0.00% | >Z | 0.00% | >Z | 0.00% | >Z | 0.00% | >Z | 0.00% |

denotes a significant or notable value

Figure 6 Significance levels of the circulation indices means of “days with snowfall” and “days without snowfall,” as a function of ENSO phase, at Niwot and Mammoth. The trends indicated for each index are from the perspective that snow will occur. Example: At Mammoth, during the 1998-99 season, the relationship between snowfall and the S index is positive (vector flow from the south), and this relationship is statistically significant at the 99.8% level. “S” is the north-south flow vector, “W” is the east-west flow vector, “F” is the force of these flow vectors, and “Z” is the vorticity, or cyclonicity, of flow.

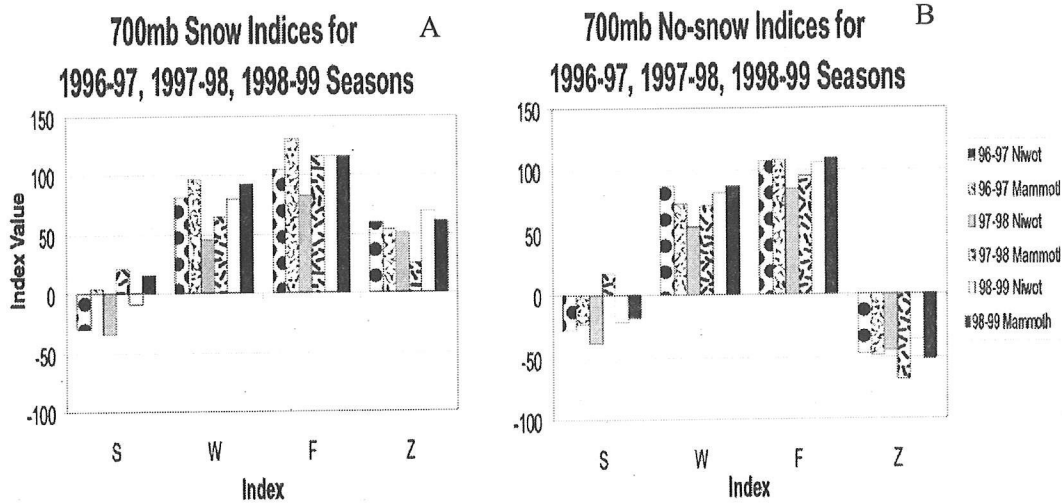


Figure 7 Seasonal separation of the circulation index values for all days with snow (A) and no snow (B), at Niwot and Mammoth at 700 mb height. Negative values indicate the opposite direction or condition. Example: At Niwot, snow occurrence in all three seasons, is related to a negative S index value, or a northerly flow vector. The situation at Mammoth is exactly the opposite, in that snow occurrence is related to a positive S index, or south flow vector, for all three seasons.

Discussion

The data suggests snowfall conditions are less variable at Niwot compared to Mammoth for the three seasons of this study. However, the differences between these three seasons, at each site, provide possible clues to the effects of ENSO phases on snowfall occurrence and related synoptic patterns. So, if the ENSO phase effect is robust at these sites (no small assumption, to be sure), Mammoth snowfall is clearly effected by ENSO phase, but the influence at Niwot is dubious in comparison.

At Mammoth, the south index was a significant snowfall indicator during the La Niña winter, and force became insignificant. According to synoptic classification, greater snowfall was associated with the westerly weather type in the neutral phase, the southwestern type during El Niño, and the cyclonic type during La Niña.

At Niwot snowfall was primarily associated with the cyclonic type, and secondarily, with the northwest type in all ENSO phases, but during La Niña, the westerly and southwesterly types also brought snow.

Summary

Although the winter season length at Mammoth was 37% shorter than that at Niwot, precipitation and snowpack at Mammoth was 2.4 times more.

Evaluation of atmospheric circulation at 700 and 850 mb heights shows that generally, Mammoth snowfall occurrence was about equally split between westerly, cyclonic, and southerly synoptic types, unlike at Niwot where snowfall was associated with cyclonic and northwest types.

Analysis of circulation indices showed that increased vorticity (Z) dominated as the most significant indicator of snowfall at both sites. Increased force (F) and south (S) indices were also important at Mammoth.

No snow conditions were associated with the anticyclonic type at both sites, as well as with north and northwest types at Mammoth.

References

Losleben MV, Pepin N, Pedrick S. 2000. Relationships of precipitation chemistry, atmospheric circulation, and elevation at two sites on the Colorado Front Range. *Atmospheric Environment* 34:1723–37.

Western Regional Climate Center. 2001. Information available via the Internet at <http://www.wrcc.dri.edu/enso/ensodef.html>. Accessed in 2001.

Primary Modes and Predictability of Year-to-Year Snowpack Variations in the Western United States from Teleconnections with Pacific Ocean Climate

Gregory J. McCabe and Michael D. Dettinger

Introduction

April 1 snowpack is the primary source of warm-season streamflow for most of the western United States (US) and thus represents an important source of water supply (Gray and Male 1981; McCabe and Legates 1995; Serreze and others 1999; Clark and others 2001). An understanding of climate factors that influence the variability of this water supply, and thus predictability, is important for water resource management. In this study, principal-component analysis is used to identify the primary modes of April 1 snowpack variability in the western US. Relations between these modes of variability and indices of Pacific Ocean climate [i.e. the Pacific Decadal Oscillation (PDO) and NINO3 sea-surface temperatures (SSTs)] are examined. Because these atmospheric/oceanic conditions change slowly from season to season, the observed teleconnections may be useful to forecast April 1 snowpack using data describing the Pacific Ocean climate in the previous fall and summer seasons, especially in the northwestern US.

Snowpack Variability

April 1 snowpack water-equivalent depth (April 1 snowpack) observations from 323 sites in the western US are used in this study to represent seasonal snowpack accumulations. At most snowcourse locations in the western US, the snow water equivalent on the ground reaches its peak at about April 1 (McCabe and Legates 1995; Serreze and others 1999; Clark and others 2001) and has been found to be highly correlated with annual streamflow in nearby rivers (McCabe 1996). The 323 sites used here all have complete records for the 50-year period from 1941 to 1990 (Figure 1).

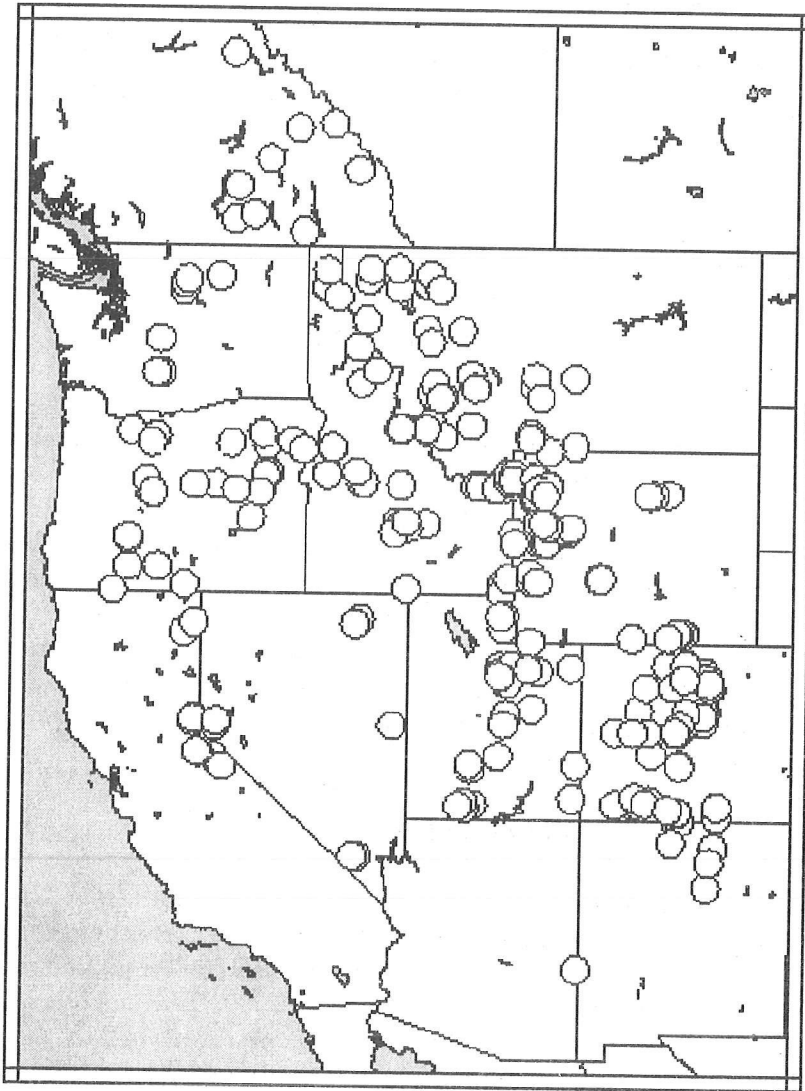


Figure 1 Snowcourses in the western United States used in this analysis

Modes of Snowpack Variability

A principal components analysis of the snowpack data yields two dominant components that explain 61% of the total variance in the snowpack data; the first component (PC1) explains 45%, and PC2 explains 16%. The loadings of PC1 on the raw April 1 snowpack data are positive and statistically significant for most of the 323 sites analyzed (Figure 2). This indicates that about half of the year-to-year variation of April 1 snowpack in the western US takes the form of co-variation. The loadings of PC2 form a pattern of statistically significant positive loadings in the southwestern US and statistically significant negative loadings in the northwestern US (Figure 2). This loading pattern is similar to the ENSO signal found in seasonal precipitation anomalies in the western US (Redmond and Koch 1991; Cayan and Webb 1992; Dettinger and others 1998).

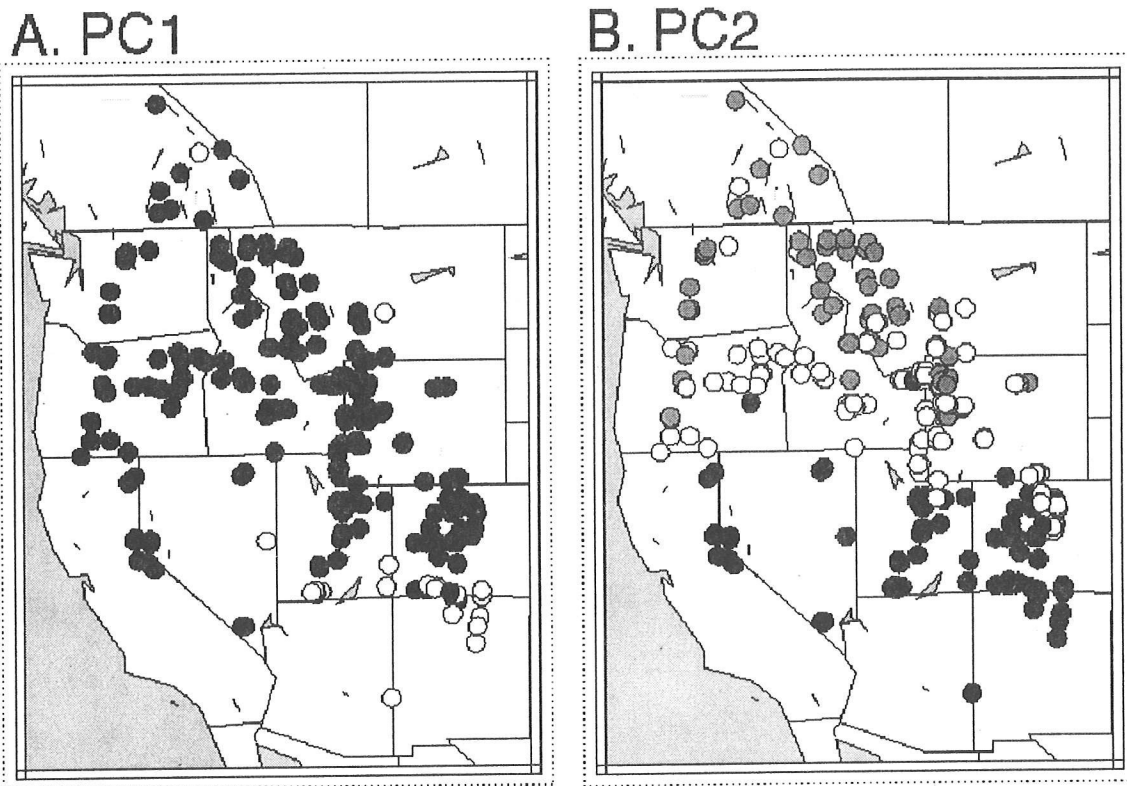


Figure 2 Loadings of April 1 snowpack for 323 snowcourses in the western United States on the first two principal components (PC1 and PC2) from a principal components analysis of the April 1 snowpack data for 1941-1990. Black dots indicate statistically significant (at a 95% confidence level) positive loadings, gray dots indicate statistically significant negative loadings, white dots indicate loadings that are non-statistically significant.

The time series of scores for PC1 indicate a large amount of year-to-year variability (Figure 3), with a notable shift from negative values to pre-dominantly positive values early in the period of record (around 1950); PC2 also exhibits considerable year-to-year variability, but is most notable for its many negative values through most of the series until 1977, when a switch to positive values occurred (Figure 3).

A comparison of the PC time series with winter Pacific Ocean climate indices (e.g. the Pacific Decadal Oscillation (PDO) and NINO3 SSTs) indicate that PC1 is most closely correlated to PDO, whereas PC2 is equally correlated with PDO and NINO3 (Table 1). This is an interesting result in that many previous studies have focused on ENSO indices as the primary large-scale driving force for the hydroclimate of the western US.

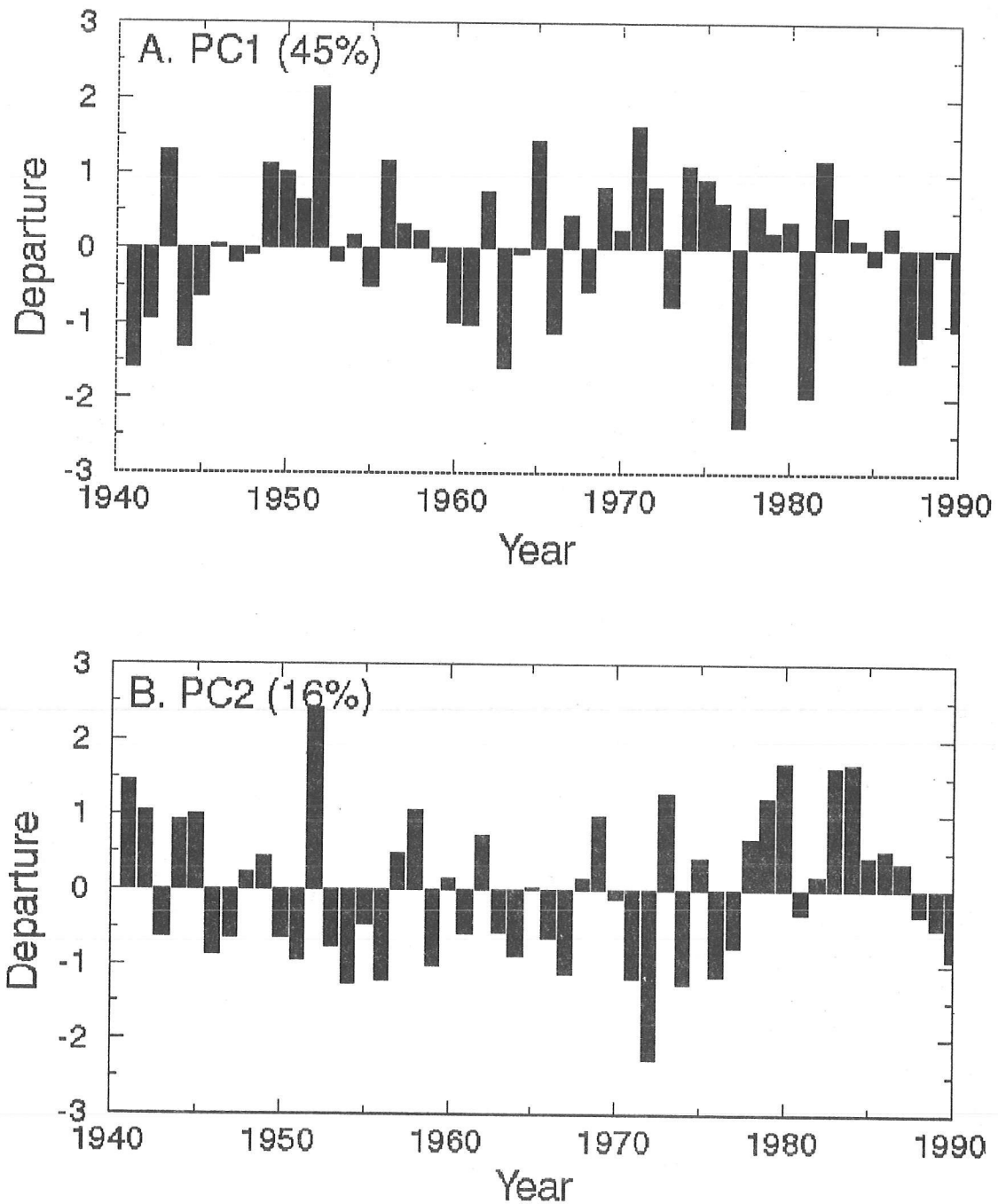


Figure 3 Time series of component scores for the first two components (PC1 and PC2) from a principal components analysis of April 1 snowpack data for 323 snowcourses in the western US for 1941-1990

Table 1 Correlations between the first two components (PC1 and PC2) from a principal components analysis of April 1 snowpack in the western US (1941-1990) and winter (November through March) PDO and NINO3 sea-surface temperatures

| | <i>Winter PDO</i> | <i>Winter NINO3</i> |
|-----|-------------------|---------------------|
| PC1 | -0.62 | -0.29 |
| PC2 | 0.44 | 0.45 |

Atmospheric Circulations

To investigate the atmospheric connections between the Pacific climate indices and the snowpack PCs, as well as to further document the correspondence between Pacific climate modes and the two snowpack PCs, correlations between each of these variables and fields of atmospheric pressure were examined. Presumably, if PC1 represents important effects of PDO on April 1 snow-pack, then these two variables should be associated with similar atmospheric pressure anomalies. The atmospheric signatures of each of the variables were identified by correlating the individual variables with gridded winter 700 hectoPascal (hPa) height anomalies (Figure 4).

Correlations between winter PDO multiplied by -1 and 700 hPa heights form a pattern that is very similar to the correlation pattern produced using PC1 scores (Figures 4A and 4C). Because PDO is negatively correlated with PC1, PDO was multiplied by -1 for easy comparison with PC1. The similarity in the correlation fields reflects shared atmospheric signatures and suggests a physical link between the two. The PDO corresponds to changes in atmospheric circulations that are translated into snowpack anomalies in the western US. In general, negative snowpack anomalies in the western US are associated with positive PDO. Furthermore, correlations between winter PDO and 500hPa storminess indicate that when the PDO is positive, storm tracks are reduced along the west coast of North America from Alaska to as far south as at least California (Figure 5A). Positive PDO is also associated with enhanced storminess in the central North Pacific (Figure 5A).

The correlation pattern for PC2 and 700hPa heights is more similar to that produced using NINO3 than the pattern produced using PDO (Figures 4B and 4D). This suggests PC2 may be more indicative of ENSO effects rather than of PDO effects on snowpack.

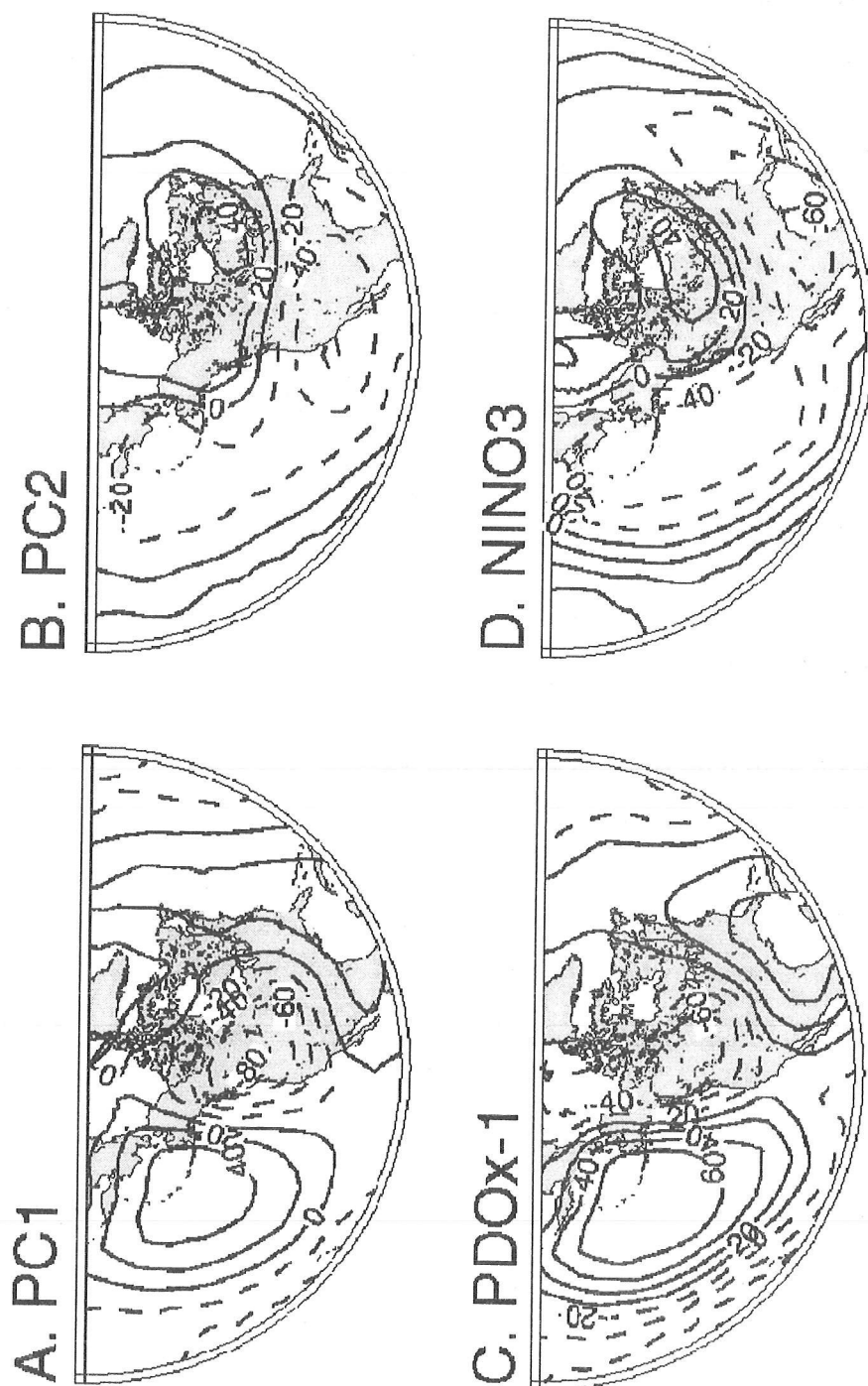


Figure 4 Correlations (times 100) between winter (November through March) 700-hectoPascal heights and component scores from (A) the first (PC1), and (B) the second (PC2) principal components from a principal components analysis of April 1 snowpack data for 323 snowcourses in the western US for 1941-1990, (C) winter Pacific Decadal Oscillation (PDO) multiplied by -1, and (D) winter NINO3 sea surface temperatures. PDO was multiplied by -1 for comparison with the other time series analyzed. The solid isolines indicate positive correlations and the dashed isolines indicate negative correlations. The contour interval is 20, and the first solid isoline is the zero correlation line.

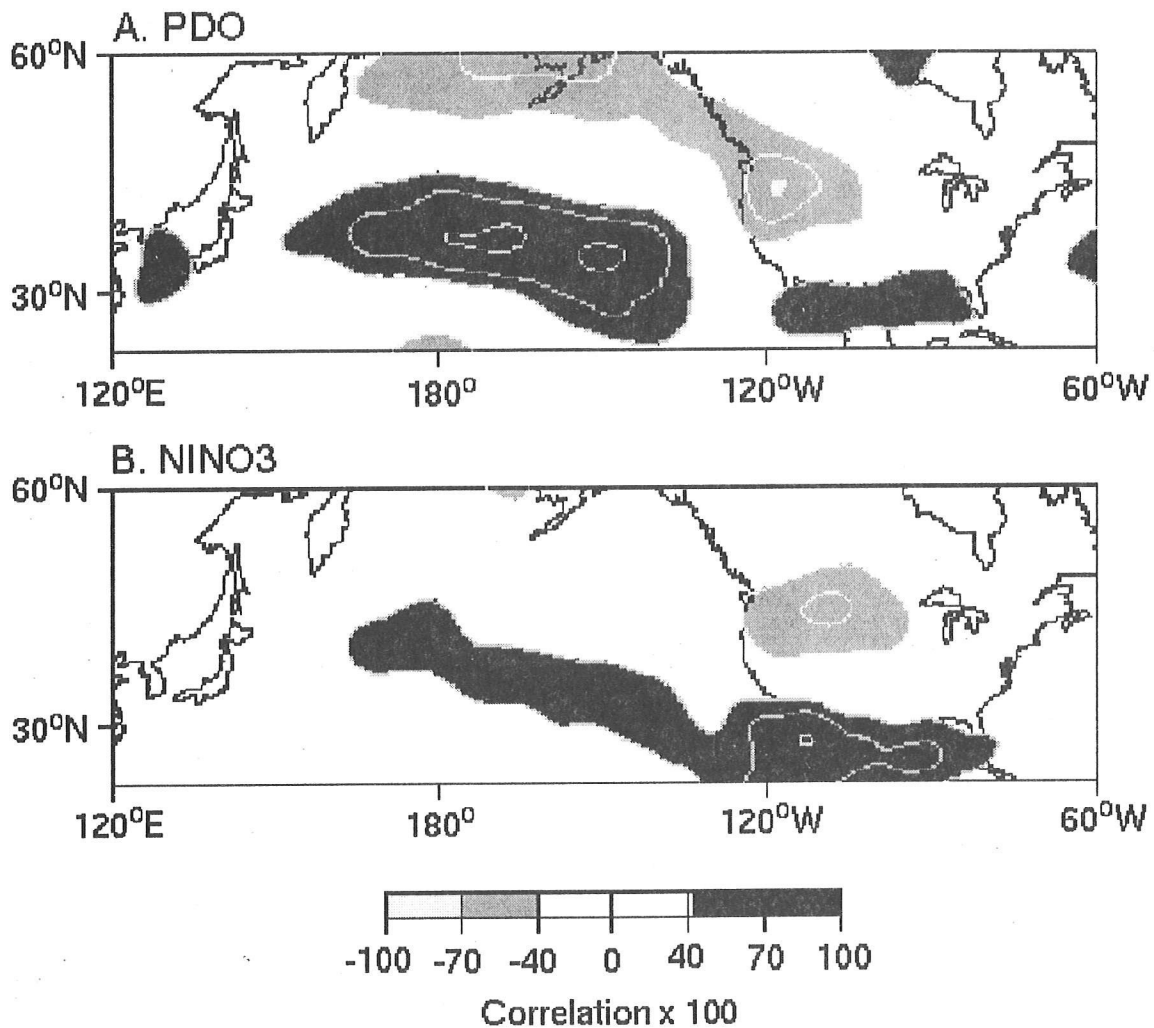


Figure 5 Correlations (times 100) between November-March mid-tropospheric storminess (500-hectoPascal (hPa) atmospheric pressure level) and the corresponding (A) PDO and (B) NINO3 SSTs, 1949-1990. Storminess is defined here as the anomalous monthly standard deviation of 2- to 8-day band-pass filtered daily 500 hPa heights from the NCAR/NCEP reanalysis. The first contour is 40 and the contour interval is 20. Contours that are significantly different from zero at a 99% confidence level are shaded (the shading interval is 30).

Potential for Seasonal Forecasts

Significant correlations between the snowpack PCs (i.e. PC1 and PC2) and the Pacific climate indices (i.e. PDO and NINO3) indicate that a large fraction of the variability of April 1 snowpack in the western US mirrors interannual and interdecadal variations of indices of Pacific Ocean climate. These correlations, together with the fact that these SST based indices evolve slowly, suggest that the current state of Pacific Ocean climate may provide a basis for forecasting April 1 snowpack several seasons in advance.

Correlations between April 1 snowpack and PDO and NINO3 (not shown) suggest predictive relations between snowpack and antecedent seasonal values of Pacific climate indices. Redmond and Koch (1991) and McCabe and Dettinger (1999) have shown statistically significant relations between antecedent summer/fall ENSO and PDO conditions and winter precipitation in the western US. To examine the predictability of April 1 snowpack using summer/fall PDO and NINO3, regressions were performed with April 1 snowpack as the dependent variable and summer/fall PDO and/or NINO3 as independent variables.

As a first approximation of the “best” predictor of April 1 snowpack for each of the stations, the r^2 values resulting from the regressions with PDO, with NINO3, and with PDO and NINO3 together were compared (Figure 6). This analysis indicated that PDO is the “best” predictor of April 1 snowpack for 79 (24%) of the 323 snowcourses. PDO and NINO3 together were the “best” predictors for 25 (8%) of the 323 snowcourses, and NINO3 alone was the “best” predictor for only 16 (5%) of the snowcourses analyzed. These snowcourses form the subset at which useful predictions can be made. The snowcourses with statistically significant forecast relations are located mostly in the northwestern US. Of the stations with statistically significant predictive relations, PDO and/or NINO3 predict readily useful fractions of April 1 snowpack variations (e.g., more than 25% of variance) for about 70 (22%) of all stations. These stations are exclusively in the northwestern US and southwestern Canada.

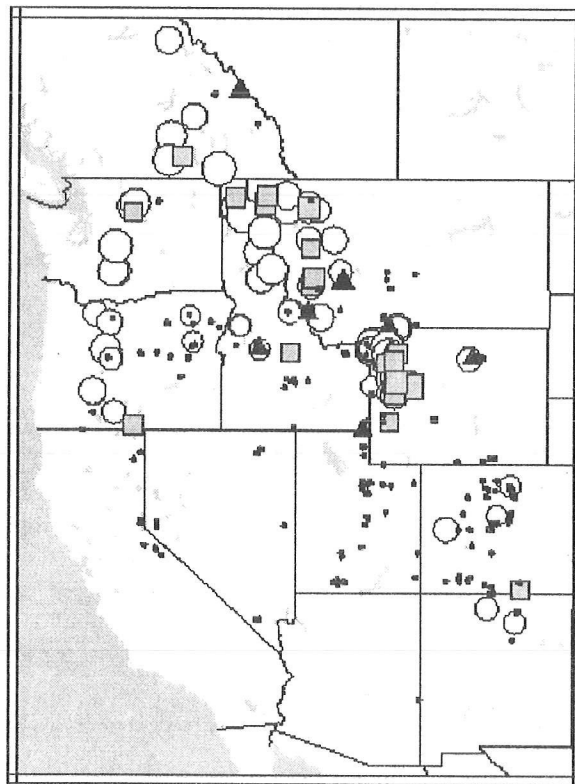


Figure 6 The “best” summer/fall predictor of April 1 snowpack. PDO, white circles; NINO3, black triangles; PDO and NINO3 together, gray squares; no good predictor, small black dots. Symbol size indicates the magnitude of the regression coefficient of determination.

Implications and Conclusions

The majority of the year-to-year variations (over 61%) of April 1 snowpack in the western US can be explained by two principal components. The first component explains 45% of the total variability in April 1 snowpack and is highly correlated with PDO. The second component explains 16% of the variability in April 1 snowpack and is correlated with NINO3 SSTs. These results indicate that year-to-year variations of the PDO index, a measure of the North Pacific Ocean climate (largely in response to ENSO), is the primary driving force of variability in April 1 snowpack in the western US. Thus, methodologies for forecasting April 1 snowpack variations should include PDO, and not just ENSO, variability. In part, this reflects the northern bias of these snowpack data. The southwestern US, where ENSO may be particularly important, is somewhat under-represented in the snowcourse data sets. Also, the dominant role of PDO in the present analysis reflects the reliability of PDO as a measure of how ENSO (and other influences) actually affects the North Pacific Ocean/North American sector in any given winter. Not all ENSOs are alike in their North American influences; PDO measures and incorporates the most important ENSO-to-ENSO differences. Because these atmospheric/oceanic conditions change slowly from season to season, the observed teleconnections may be useful to forecast April 1 snowpack using data describing the Pacific Ocean climate in the previous fall and summer seasons, especially in the northwestern US.

Notably, snowpack variations in the western US have a strong interannual, and a modest inter-decadal, character. The ability of the linear methods employed here to predict snowpack variations using PDO have therefore been contingent upon use of seasonal PDO values without any prior filtering. Indeed, in this unfiltered form, PDO reflects important ENSO episodes along with the slower decadal character of the North Pacific climate. Thus, PDO arguably is as much a measure of how the various individual ENSO episodes affected the North Pacific Ocean, and by extension North America, as it is a measure of interdecadal processes in the extratropical Pacific. Given the greater proximity of the North Pacific PDO index to western North America and its tendency to reflect the strongest ENSO variations, it is reasonable that it out-performs the ENSO indices when predicting snowpack in the western US.

References

- Clark MP, Serreze MC, McCabe GJ. 2001. The historical effect of El Nino and La Nina events on the seasonal evolution of the montane snowpack in the Columbia and Colorado River basins. *Water Resources Research* 37:741–57.
- Cayan DR, Webb RH. 1992. El Nino/Southern Oscillation and streamflow in the western United States. In: Diaz HF, Markgraf V, editors. *El Nino: historical and paleoclimatic aspects of the Southern Oscillation*. Cambridge (UK): Cambridge University Press. p 29–68.
- Dettinger MD, Cayan DR, Diaz HF, Meko D. 1998. Seasonal and interannual variations of atmospheric CO₂ and climate. *Tellus* 50B:1–24.
- Gray DM, Male DH. 1981. *Handbook of snow*. New York (NY): Pergamon Press.
- Mccabe GJ, Legates DR. 1995. Relationships between 700 hPa height anomalies and 1 April snowpack accumulations in the western USA. *Int J Climatol* 15:517–30.

2001 PACLIM Conference Proceedings

- McCabe GJ. 1996. Effects of winter atmospheric circulation on temporal and spatial variability in annual streamflow in the western United States. *J Hydrol Sci* 41:873-87.
- McCabe GJ, Dettinger MD. 1999. Decadal variations in the strength of ENSO teleconnections with precipitation in the western United States. *Int J Climatol* 19:1399-1410.
- Redmond KT, Koch RW. 1991. Surface climate and streamflow variability in the western United States and their relationship to large scale circulation indices. *Water Resources Research* 27:2381-99.
- Serreze MC, Clark MP, Armstrong RL, McGinnis DA, Pulwarty RS. 1999. Characteristics of the western US snowpack from SNOTEL data. *Water Resources Research* 35:2145-60.

Response of High-Elevation Conifers in the Sierra Nevada, California, to 20th Century Decadal Climate Variability

Constance I. Millar, Lisa J. Graumlich, Diane L. Delany, Robert D. Westfall, and John C. King

Extended Abstract

Trees in high-elevation ecosystems of the central Sierra Nevada, California showed complementary 20th century responses in four independent studies of forest growth. Annual growth rates of horizontal branches in treeline *Pinus albicaulis* doubled, from 0.9 cm/yr to 2.0 cm/yr between 1900-1996, with accelerated growth from 1920-1945 and from 1984-1996. Since 1900, *P. albicaulis* has progressively invaded formerly persistent snow-covered slopes below treeline as snow fields melted earlier in summer. Invasion accelerated during 1920-1945 and 1976-1999. Vertical extension of branches ("flags") in otherwise shrubby, treeline *P. albicaulis* and invasion of montane meadows by *P. contorta* occurred in single dominant pulses from 1945-1976. These ecological responses, unassociated with local conditions or land use, correlate with 20th century patterns of global warming and multidecadal phases of the Pacific Decadal Oscillation (PDO), corroborating that PDO is both detectable and has biotic effects in this region of California. Proper attribution of cause and effect to climate rather than human impacts of overgrazing and fire suppression is important also to wildland management.

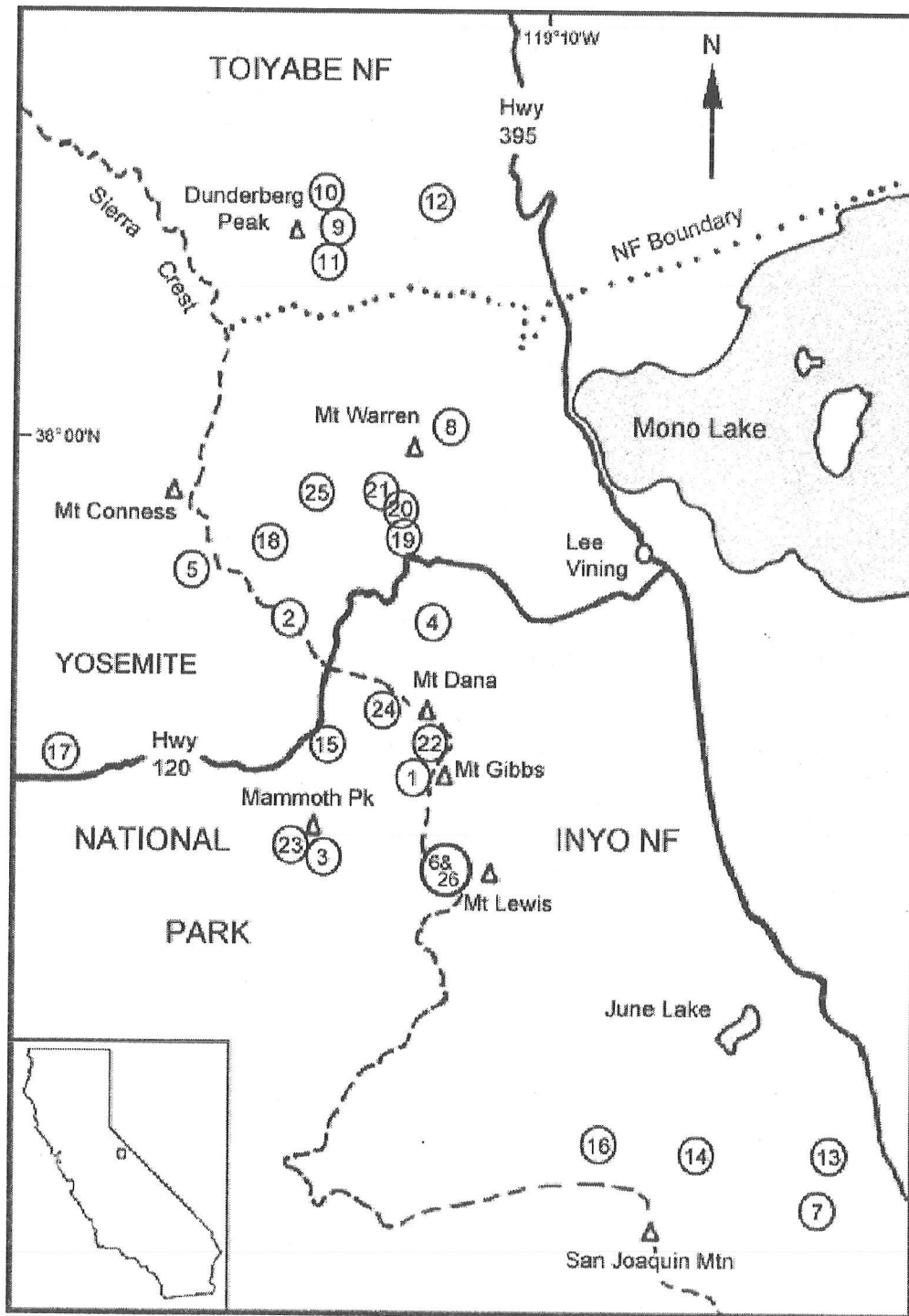


Figure 1 Locations of 26 study sites in the central Sierra Nevada, California, USA for horizontal branch growth (sites 1-6), snow field invasion (sites 7-12), meadow invasion (sites 13-21), and vertical leader release (sites 22-26) studies

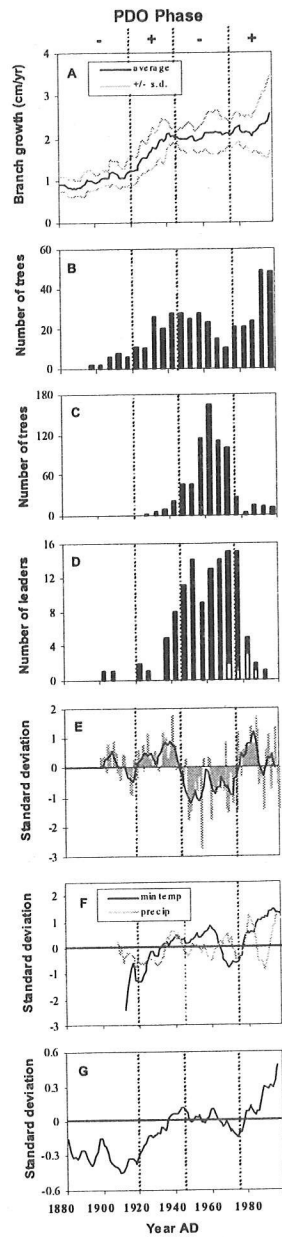


Figure 2 Growth dynamics from 1880-2000 of high elevation pines in central Sierra Nevada, CA, USA and 20th century climate records. A. Five-year running average annual horizontal branch growth (with standard deviations) of krummholz *Pinus albicaulis* at six treeline sites. B. Number of *P. albicaulis*, *P. monticola*, and *P. contorta* trees invading six high-elevation snow field slopes. C. Number of vertical leaders (branches) in krummholz *P. albicaulis* at five treeline sites. White bars are dead leaders; all others were alive in 1996. D. Number of *P. contorta* trees invading nine upper-montane meadow sites. E. Pacific Decadal Oscillation (PDO) indices with 5-year running average (modified from Mantua and others 1997). F. Five-year running average deviations in instrumental records of minimum monthly temperatures and annual precipitation at Yosemite Valley, CA, elev. 1250 m (1907-2000) (WRCC, 2001) G. Deviations from average Northern Hemisphere surface air temperatures (redrawn from Jones and others 1999). Plot data in A-D are pooled over plots and sites in each study.

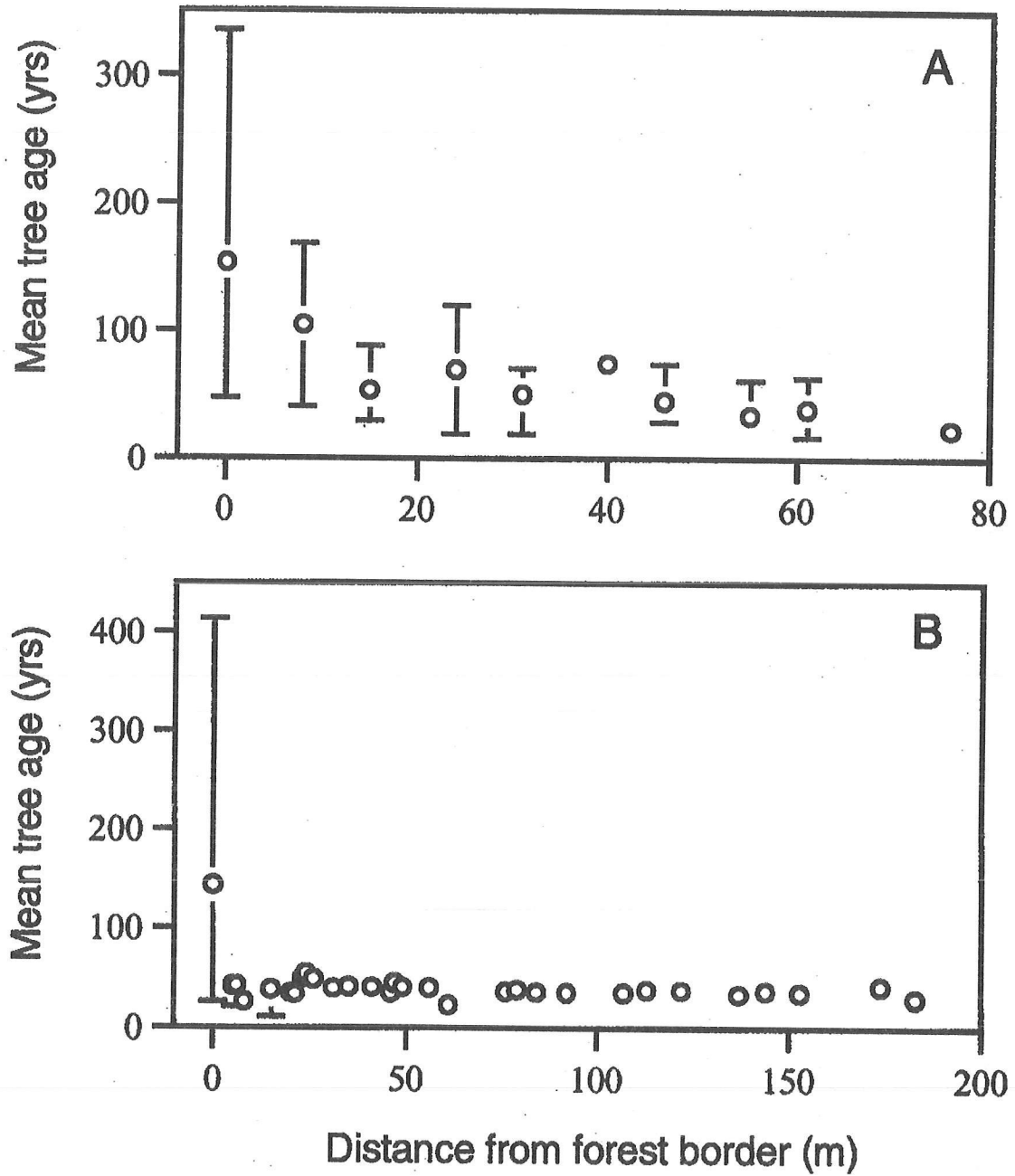


Figure 3 Mean spatial distribution and ages (with standard deviations) in 1999 of conifers invading forest openings in the Sierra Nevada, CA, USA. Plot data are pooled over all transects within each of nine meadow and six snow field sites. A. Invasion into snow field slopes by *Pinus albicaulis*, *P. monticola*, and *P. contorta*. B. Invasion into meadows by *P. contorta*.

The Modern Distribution of Midge Flies (Chironomidae; Insecta: Diptera) in Eastern Sierra Nevada, California, Lakes: Potential for Paleoclimatic Reconstruction

David F. Porinchu and Glen M. MacDonald

Introduction

We are using the remains of aquatic insects, specifically midge flies (Chironomidae), preserved in the lake sediment of small, climatically sensitive Sierra Nevada lakes to reconstruct the late-glacial and early Holocene temperature regime for the region.

Chironomids are non-biting midge flies belonging to the order Diptera. They are ubiquitous and frequently the most abundant insect found in freshwater ecosystems. Midge flies have three characteristics that are useful in paleoecological studies; they have relatively short lifecycles, the adults are mobile, and the larvae possess chitinous head capsules (Figure 1). The chitinized larval head capsules of midge flies are readily preserved in lake sediment and therefore are easily recovered and identified (Figure 2). The mobility of adult midge flies along with their short life cycle allow them to respond to climate change very quickly; as a result, midge flies are likely to have distributions in equilibrium with climate (Walker and MacDonald 1995).

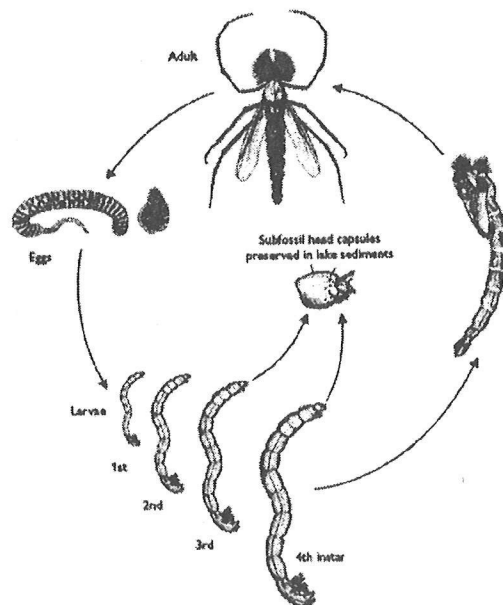


Figure 1 Lifecycle of midge flies. In temperate regions lifecycle takes approximately 1 year to complete (from Brodersen and Anderson 2000).

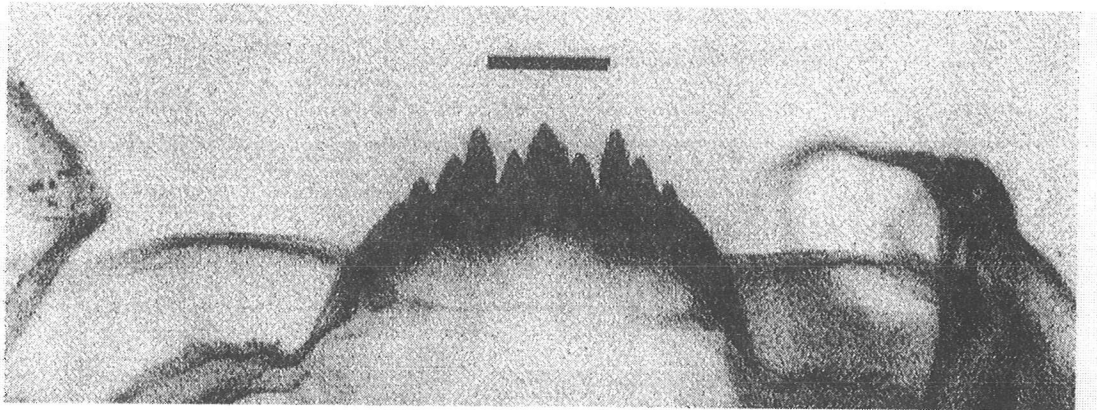


Figure 2 Photomicrograph of a sub-fossil midge fly (*Chironomus*) head capsule. Scale bar is 50 μm .

The use of midge flies in paleolimnology has a long history. In the early 20th century lake classification schemes describing lake ontogeny and trophic status were developed based on chironomid community composition. Recent research has also demonstrated the value of using chironomids as a proxy source of paleoclimatic data (Walker and others 1991a; Levesque and others 1993; Cwynar and Levesque 1995; Brooks and Birks 2000; Porinchu and Cwynar, forthcoming). It has long been known that chironomids are sensitive to lake water temperature and that individual taxa have differing tolerances to surface lake water temperature. However, it is the recent development of robust and ecologically meaningful statistical methods (weighted averaging regression and calibration) that has led to the dramatic increase in the number of paleolimnological studies using chironomids as a proxy for past environmental conditions (Birks 1998). Further reading describing the use of chironomids in paleoecology and paleoclimatology can be found in Walker (1995).

Methods

We are using a paleolimnological approach to reconstruct the nature of past climate change in the eastern Sierra Nevada. Paleolimnology is a multidisciplinary and integrative science that uses the physical, chemical, and biological information preserved in lake sediments to reconstruct past environmental conditions. The remains of aquatic organisms, i.e. lacustrine fossils, properly interpreted, can provide a sensitive and detailed history of the physical, limnological and climatic changes that occurred at a site over time (Smol and others 1991, 1995; MacDonald and others 1993; Moser and others 1996).

Quantitative paleolimnological reconstructions involve two steps; (1) establishing calibration or transfer functions and (2) using the transfer functions to infer past climatic conditions from fossil assemblages (Figure 3). The first step requires the development of a surface sediment calibration set or "training-set" (Moser and others 1996; Smol and others 1995). The most recently deposited sediment within a lake (the upper-most 0.5 to 1.0 cm) is referred to as surface sediment and it represents the sediment that has accumulated in the lake basin over the last few years (<10 yrs) (Holmes and others 1989).

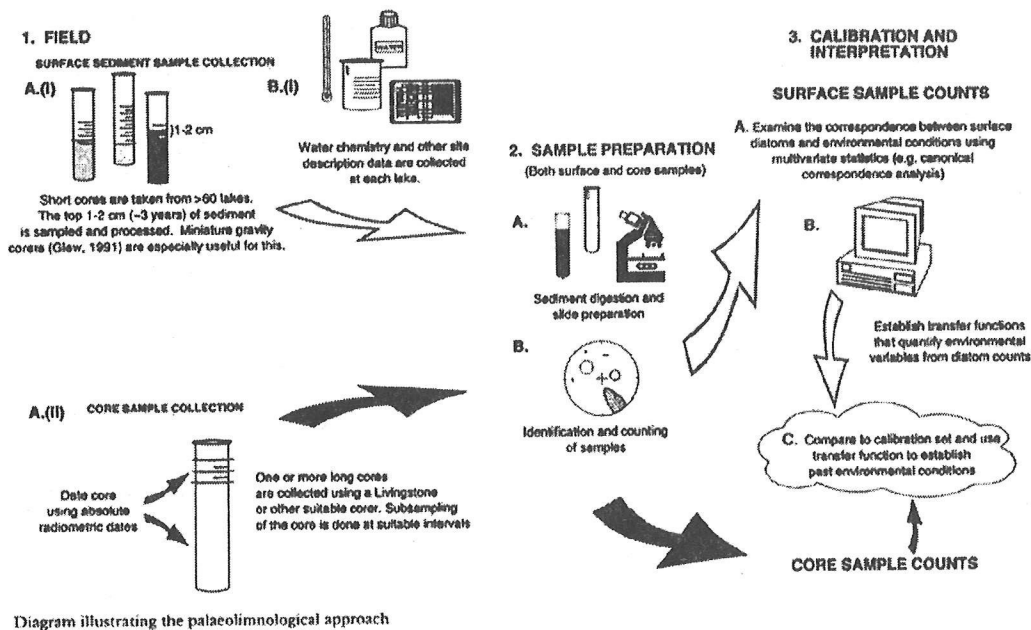


Diagram illustrating the paleolimnological approach (from Moser and others 1996)

During surface sediment collection, measurements of physical and limnological variables are made and samples for water chemistry analyses are collected. Variables measured in the field include lake temperature, lake depth, pH, Secchi depth, conductivity and salinity. Water samples collected in the field are later analyzed for trace metal concentrations, dissolved organic carbon, chlorophyll *a* and nutrients. Other variables of interest include catchment size, composition of surrounding vegetation, pedology, geology, and local and regional climate data (Moser and others 1996).

The surface sediment is processed and the remains of the biological proxies of interest (e.g. diatoms, Cladocera, chironomids) are identified and enumerated. Multivariate statistical techniques are used to identify which of the measured environmental variables are important in influencing species distribution within the calibration dataset lakes. The relationship between a specific environmental variable and species distribution is quantified in the form of a transfer function (mathematical formula that expresses the value of an environmental variable as a function of species composition data). This transfer function can then be applied to late-Quaternary biological assemblages to reconstruct past environmental conditions (Figure 3).

Field

Samples of water and surface sediment were recovered from 50 lakes along an elevation gradient in the central, eastern Sierra Nevada. The lakes that were sampled for the surface sample 'training-set' were located between Bridgeport, California, and Bishop, California (Figure 4). The east slope of the Sierra Nevada is much steeper than the west slope and as a result, it has more sharply defined environmental, vegetation, and climatic gradients.

Sierra Nevada Study Site

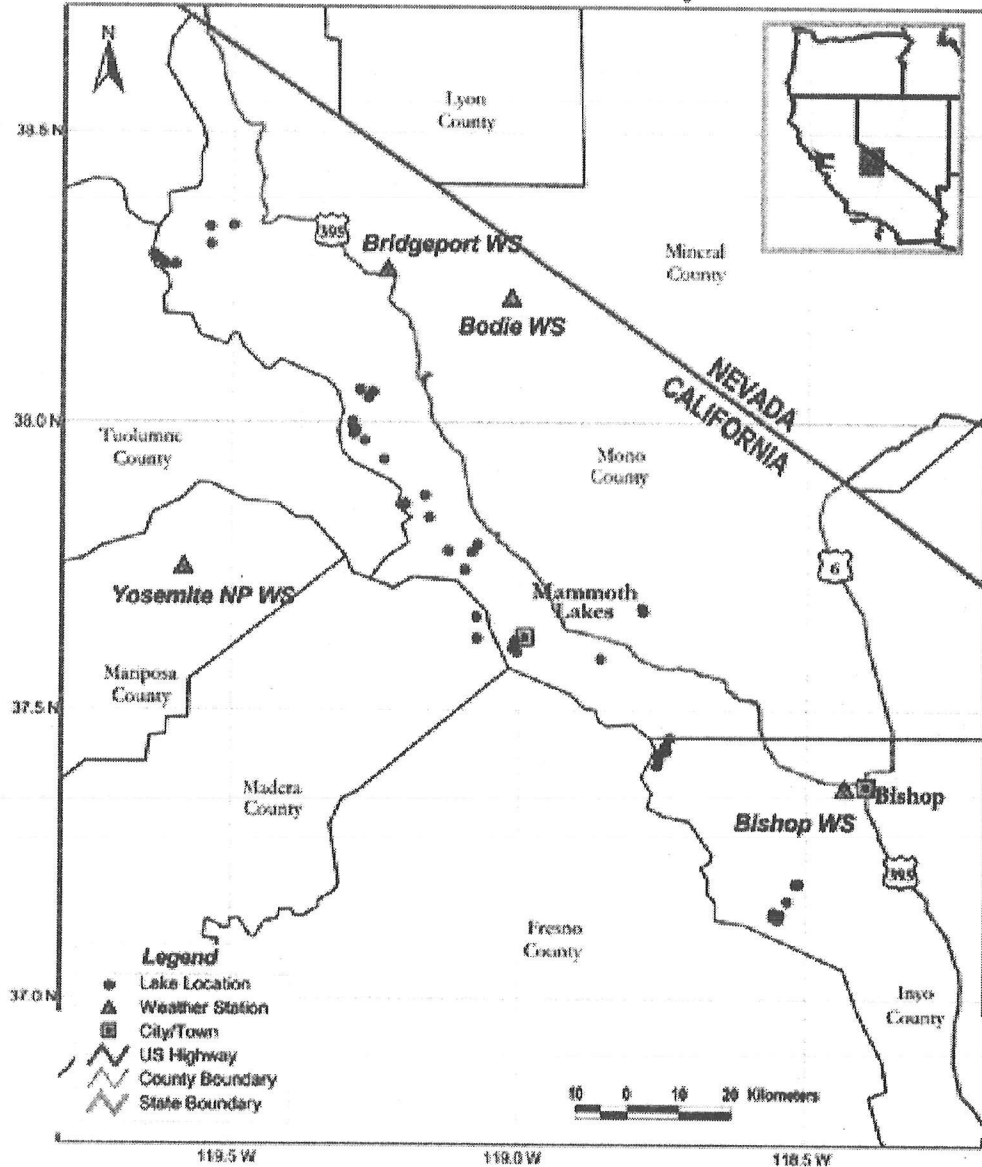


Figure 4 Location of the 50 lakes sampled for the calibration dataset

The lakes sampled for the calibration dataset were between 2.0 m and 40.0 m in depth, spanned an altitudinal gradient of approximately 1300 m and had a surface lake-water temperature gradient of approximately 9 °C. The majority of lakes sampled were small (1 to 10 ha) and closed basin. They spanned five broad vegetation zones; sage-brush scrub, pinyon-pine western juniper woodland, Jeffrey pine woodland, montane forest, and sub-alpine forest.

Sediment was recovered from the approximate center of each lake using a Glew mini-corer (1991) deployed from an inflatable raft. The Glew mini-corer is a gravity corer that allows recovery of lake surface sediment with minimum disturbance of the mud-water interface. Three sets of replicate samples were obtained from each lake. The top 1 cm of sediment was immediately removed and stored in Whirl-paks® for later analyses. Measurements of physical, chemical and biological variables that are thought to be ecologically important for chironomids were made at each lake. Measurement of physical variables, e.g. temperature, specific conductance, and pH were made at each lake during surface sediment collection. Water samples for water chemistry analyses were collected 0.5 m below the surface (water chemistry analyses were carried out at the National Laboratory for Environmental Testing in Burlington, Canada). Co-ordinates for the lakes were obtained using a Magellan Global Positioning System (GPS) and the appropriate 1:24,000 USGS topographic maps. The vegetation surrounding individual lakes was determined by ground observation.

Laboratory

Chironomid analysis followed standard procedures as outlined in Walker (1987). A minimum of 2 ml of sediment was deflocculated in a heated (30 °C) in 5% KOH solution for 30 minutes. The material was then sieved through a screen with 95 µm meshes. The sediment retained by the sieve was rinsed with distilled water and backwashed into a beaker. A Bogorov plankton counting tray was used to examine aliquots of the solution. Head capsules were sorted and handpicked with the aid of a Wild® 5X dissection microscope at 50X.

Chironomid head capsules that consisted of either the entire mentum or greater than half the mentum were counted as one head capsule. Head capsules consisting of half the mentum were enumerated as half a head capsule. Head capsules consisting of less than half the mentum were not enumerated. The specimens were permanently mounted on slides in Permount® and identified at 400X, generally to genus. Identifications were based predominantly on Wiederholm (1983), Walker (1988), and Oliver and Roussel (1983).

Numerical

Redundancy analysis (RDA), a constrained ordination technique, was used to explore the relationships that exist between the midge assemblages in the surface sediment and specific physical, chemical and environmental variables (ter Braak 1995). In other words, RDA was used to determine which of the measured physical and limnological variables had a statistically significant influence on the species composition of the chironomid fauna in the lakes studied. Canonical co-efficients, approximate *t*-tests, intra-set correlations, and the ratio of the 1st constrained eigenvalue (λ_1) to the 2nd unconstrained eigenvalue (λ_2) were used to identify which of the measured environmental variables would be good candidates for quantitative reconstruction purposes (Lotter and others 1997; Olander and others 1999; Laroque and others, forthcoming).

Results

Midge fly remains were found in the sediment of 45 of the 50 lakes sampled; these remains were identified and enumerated, which enabled a determination of the modern distribution of midge flies in eastern Sierra Nevada lakes. Redundancy analysis with forward selection identified surface water temperature, depth, Fe and Mg as the environmental variables that had a statistically significant and independent effect on the species composition of the chironomid fauna in the lakes studied. Correlation co-efficients, intra-set correlations, and approximate *t*-tests suggest that depth is strongly correlated with axis 1, while water temperature is strongly related to axis 2. The results of the RDA indicate that lake depth and water temperature are both strongly correlated to the species composition of the chironomid communities in Sierran lakes and that these two environmental variables can be successfully modeled. A more detailed description of the results will soon be available in a forthcoming publication.

Discussion

Earlier work has demonstrated that chironomid community composition is, in large part, a function of the summer temperature of surface lake waters. Most of the quantitative research relating chironomids to climate has been carried out in Maritime Canada, the Swiss Alps and Fennoscandia (Walker and others 1991b; Lotter and others 1997; Olander and others 1999; Laroque and others, in press). Published studies relating the distribution of chironomids to the physical and chemical limnology of lakes in the western United States is limited. This is the first attempt at quantifying the modern relationship between chironomids and climate in the Sierra Nevada.

Redundancy analysis demonstrated that four of the measured environmental variables, water temperature, depth, Fe and Mg, explained a statistically significant and independent amount of variation in the chironomid assemblages. Canonical coefficients, intra-set correlations and approximate *t*-tests indicate that water temperature is strongly related to distribution of chironomids along the elevational transect. Redundancy analysis using surface water temperature as the sole explanatory variable indicated that a high ratio of the 1st constrained axis (λ_1) to the 2nd unconstrained eigenvalue (λ_2) exists, suggesting that a transfer function for water temperature could be developed. We are in the process of refining a transfer function relating chironomid community composition to surface water temperature. Initial results from the model suggest that this transfer function may be applied to the late-Quaternary lake sediment recovered from the eastern Sierra to reconstruct past changes in the temperature regime for the region.

During the summer of 2000, we recovered late-Quaternary sediment cores from Barrett Lake (37°35'45", 119°00'30") in the Mammoth Lakes region of the eastern Sierra Nevada. Barrett Lake is a small (approximately 3 ha), mid-elevation site (2816 m) located in subalpine forest. Huber and Rinehart (1965) indicate that Barrett Lake lies along a contact of Cretaceous granite with Triassic-Jurassic metavolcanics (Anderson 1990). The surficial deposits present in the area have been described as belonging to the Hilgard stage of glaciation (Curry 1969). Barrett Lake is currently a warm (surface water temperature = 19.4 °C), dilute (conductivity = 0 mS), circumneutral (pH = 6.85), eutrophic (total phosphorous = 38.0 mg/L) lake. It is located just above the upper altitudinal limit of *Abies magnifica* (red fir) and near the lower altitudinal limit of *Tsuga mertensiana* (mountain hemlock). Also present around the lake are *Pinus flexilis* (limber pine) and *P. murrayana* (Anderson

1990). The lake itself is comprised of two basins; we recovered our cores from the southeast basin in 6.08 m of water.

We obtained a date of $11,900 \pm 65$ ^{14}C yr BP on basal sediment from Barrett Lake. High-resolution Loss-on-Ignition (LOI) analysis on the late-glacial portion of the Barrett Lake core revealed a dramatic reversal in lacustrine organic carbon accumulation during the late-glacial period (Figure 5). This reversal occurs between approximately 10,000 yr BP and 11,000 yr BP and is correlative with the Younger Dryas. Identification and enumeration of the sub-fossil chironomid remains preserved in the late-glacial portion of the sediment is underway. We are hoping to apply the chironomid-based transfer function for surface water temperature to the late-glacial chironomid assemblages contained within this core to reconstruct changes in the temperature regime for the eastern Sierra Nevada.

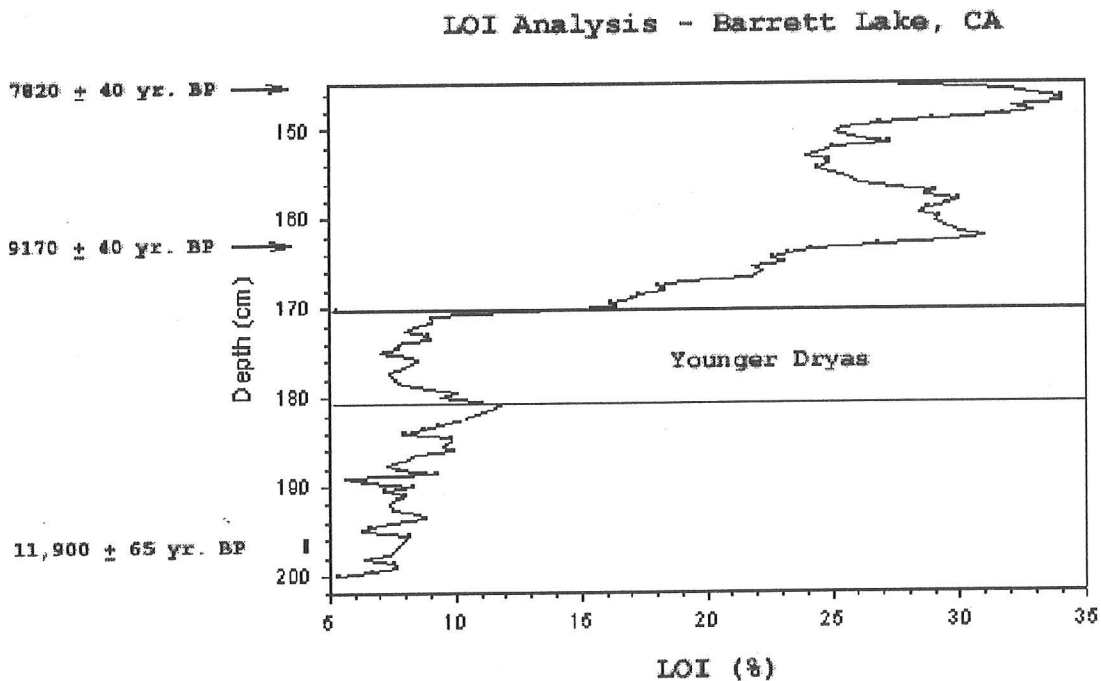


Figure 5 Loss-on-Ignition (LOI) analysis of late-glacial lake sediment from Barrett Lake, Mammoth Lakes region, California

References

- Anderson RS. 1990. Holocene forest development and paleoclimates within the central Sierra Nevada, California. *J Ecol* 78:470–89.
- Birks HJB. 1998. Numerical tools in paleolimnology—progress, potentialities, and problems. *J Paleolimnol* 20:307–22.

- Brodersen KP, Andersen NJ. 2000. Subfossil insect remains (Chironomidae) and lake-water temperature inference in the Sisimiut-Kangerlussuag region, southern West Greenland. *Geology of Greenland Survey Bulletin* 186:78–82.
- Brooks SJ, Birks HJB. 2000. Chironomid-inferred late-glacial and early-Holocene mean July air temperature for Kråkenes Lake, western Norway. *J Paleolim* 23:77–89.
- Curry RR. 1969. Holocene climatic and glacial history of the central Sierra Nevada, California. In: Schumm SA, Bradley WC, editors. *United States contributions to Quaternary Research*. Geological Society of America Special Paper 123:1–47.
- Cwynar LC, Levesque AJ. 1995. Chironomid evidence for late-glacial climatic reversals in Maine. *Quat Res* 43:405–13.
- Glew J. 1991. Miniature gravity corer for recovering short sediment cores. *J Paleolim* 5:285–7.
- Holmes RW, Whiting MC, Stoddard JL. 1989. Changes in diatom-inferred pH and acid neutralizing capacity in a dilute, high elevation, Sierra Nevada lake since AD 1825. *Freshwater Biology* 21:295–310.
- Huber NK., Rinehart CD. 1965. Geologic map of the Devil's Postpile Quadrangle, Sierra Nevada, California. GQ 437. Washington, DC: U.S. Geological Survey.
- Larocque I, Hall RI, Grahn E. Forthcoming. Chironomids as indicators of climate change: a 100-lake training set from a subarctic region of northern Sweden (Lapland). *Journal of Paleolimnology*.
- Levesque AJ, Mayle F, Walker IR, Cwynar LC. 1993. A previously unrecognized late-glacial cold event in eastern North America. *Nature* 361:623–6.
- Levesque AJ, Cwynar LC, Walker IR. 1997. Exceptionally steep north-south gradients in lake temperatures during the last deglaciation. *Nature* 385:423–6.
- Lotter AF, Birks HJB, Hofmann W, Marchetto A. 1997. Modern diatom, cladocera, chironomid and chryso-phyte cyst assemblages as quantitative indicators for the reconstruction of past environmental conditions in the Alps 1 Climate. *J Paleolim* 18:395–420.
- MacDonald GM, Edwards TWD, Moser KA, Pienitz R, Smol JP. 1993. Rapid response of treeline vegetation and lakes to past climate warming. *Nature* 93:243–6.
- Moser KA, MacDonald GM, Smol JP. 1996. Applications of freshwater diatoms to geographical research. *Prog Phys Geogr* 20:21–52.
- Olander H, Birks HJB, Korhola A, Blom T. 1999. An expanded calibration model for inferring lakewater and air temperatures from fossil chironomid assemblages in northern Fennoscandia. *The Holocene* 9:279–94.
- Oliver DR., Roussel ME. 1983. The insects and arachnids of Canada. Part II: the genera of larval midges of Canada-Diptera: Chironomidae. *Ag Can Publ* 1746:1–263.
- Porinchi DF, Cwynar LC. Forthcoming. Late-Quaternary history of midge communities and climate from a tundra site near the lower Lena River, Northeast Siberia. *Journal of Paleolimnology*.

- Smol JP, Walker IR, Leavitt PR. 1991. Paleolimnology and hindcasting climatic trends. *Verhandlungen Internationale Vereinigung für Theoretische und Angewandte Limnologie* 24:1240–6.
- Smol JP, Cumming BF, Douglas MSV, Pienitz R. 1995. Inferring past climatic changes in Canada using paleolimnological techniques. *Geoscience Canada* 21:113–8.
- ter Braak CJF. 1995. Ordination. In: Jongman RHG, ter Braak CFJ, van Tongeren OFR, editors. *Data analysis in community and landscape ecology*. Cambridge (UK): Cambridge University Press. p 91-169.
- Walker IR. 1987. Chironomidae (Diptera) in paleoecology. *Quat Sci Rev* 6:29–40.
- Walker IR. 1988. Late-Quaternary paleoecology of Chironomidae (Diptera: Insecta) from lake sediments in British Columbia [PhD dissertation]. Available from Simon Fraser University. 204 p.
- Walker IR. 1995. Chironomids as indicators of past environmental change. In: Armitage PD, Cranston PS, Pinder LCV, editors. *The Chironomidae: biology and ecology of non-biting midges*. New York (NY): Chapman & Hall. p 405–22.
- Walker IR, MacDonald GM. 1995. Distributions of Chironomidae (Insecta: Diptera) and other freshwater midges with respect to treeline, Northwest Territories, Canada. *Arctic and Alpine Research* 27:258–63.
- Walker IR, Mott RJ, Smol JP. 1991a. Alleröd-Younger Dryas lake temperatures from midge fossils in Atlantic Canada. *Science* 253:1010–2.
- Walker IR, Smol JP, Engstrom DR, Birks HJB. 1991b. An assessment of Chironomidae as quantitative indicators of past climate change. *Can J Fish Aquat Sci* 48:975–87.
- Walker IR, Levesque AJ, Cwynar LC, Lotter AF. 1997. An expanded surface-water paleotemperature inference model for use with fossil midges from eastern Canada. *J Paleolim* 18:165–78.
- Wiederholm T, editor. 1983. Chironomidae of the Holarctic region. Keys and diagnoses. Part I—Larvae. *Entomologica Scandinavica Supplement* 19:457 p.

Water Year 2001 in Northern California: Have the Good Years Ended?

Maurice Roos

Abstract

For the second water season in a row, precipitation and snowpack accumulation from October through December were far below normal in northern California. In 2000, the season was saved by a 60-day wet period from mid-January to mid-March. No two years are alike and although some recovery was expected during the second half of the wet season this year, it was unlikely that the large lag in precipitation on January 1, 2001, would be made up. January was still substantially below average in the month, although the southern portion of California had good rains. February was a good month at 120% of average precipitation and it did improve the water supply outlook. But it was not wet enough in northern California to make up for previous month shortfalls and in March, at 70% of average precipitation for the month, the dry look of the water year resumed. Reservoir carryover storage from the previous water year on October 1 was about 10% above average, which helped cushion shortfalls in runoff and water supply in 2001.

Introduction

The main portion of this paper will be a review of where California stood on water supply for year 2001. Parameters to be presented and compared include precipitation, snowpack, runoff, and in-state reservoir storage. At the end will be a short review of California's electric energy situation.

Water year 2001 started out with cooler than average eastern tropical Pacific sea surface temperatures. It was not as cold as the preceding two La Niña years and the cool anomaly was forecasted to fade later in the winter. However, the cool anomaly actual increased during the winter in the mid Pacific, so we had every reason to expect a typical La Niña pattern—dry in the Southwest and wet in the Pacific Northwest. Based on the preceding two years, Northern California would be near average, perhaps slightly above. That did not happen; instead the winter looked more like an El Niño pattern, with the best seasonal precipitation percentages in the south and dry in the north (which extended into the Pacific Northwest).

Precipitation percentages increased from north to south and decreased as one went from the coast inland. Except in the north, the lowlands and deserts were relatively wet and the Sierra Nevada and North Coast dry. The northeastern portion of California was quite dry—especially the northeastern Klamath River and North Lahontan areas. The one northern mountain area that approached normal rain and snow was on the divide between the upper Sacramento and Trinity rivers above Shasta Dam and Trinity reservoir. Runoff forecast percentages there as of April 1 were in the 70s. Eventual actual April through July runoff was 72% for Shasta Lake and 61% at Trinity, compared to a statewide total of about 55%. The following figures, one on precipitation (Figure 1), the other on snowmelt runoff for 2001 (Figure 2), show the statewide details.

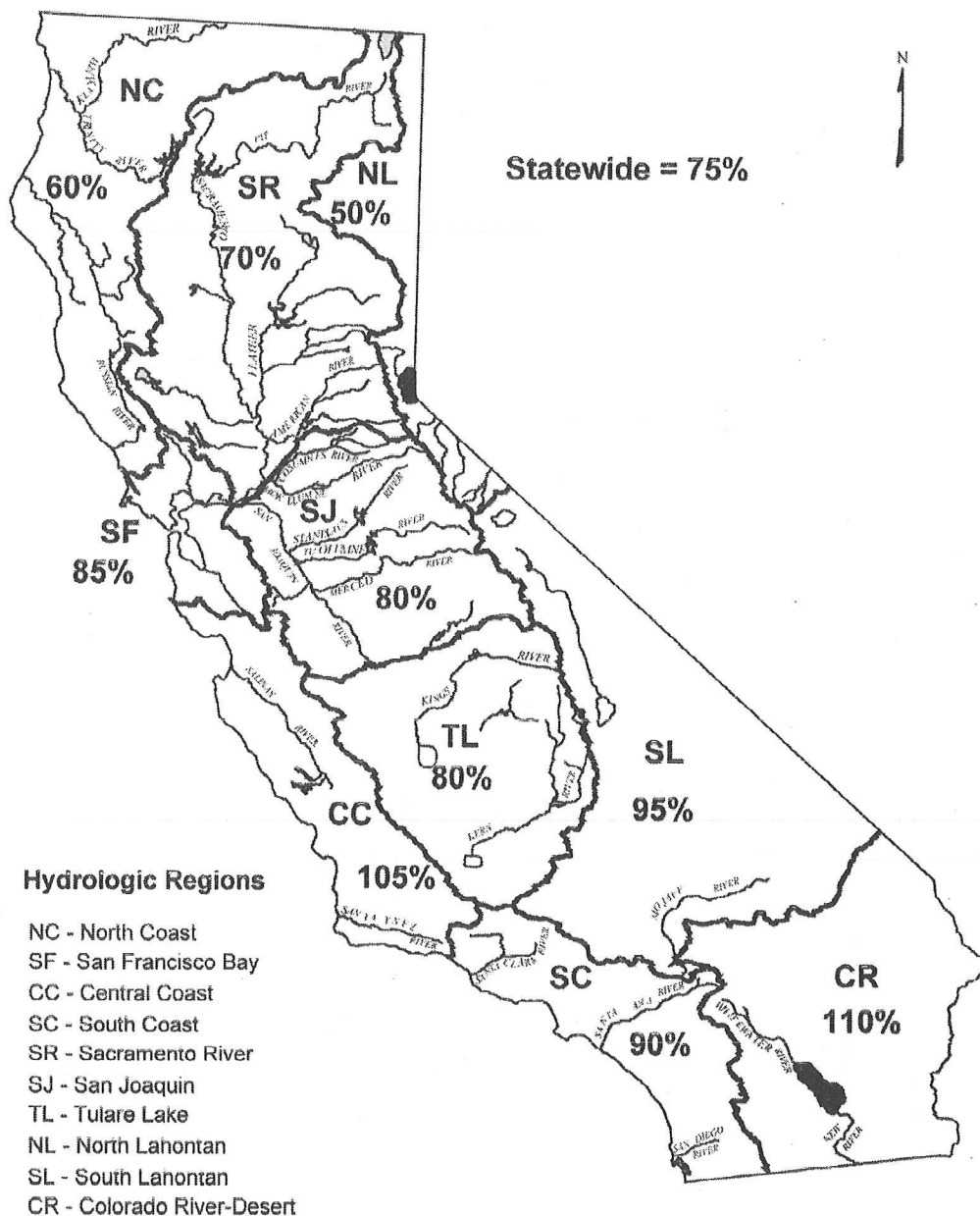


Figure 1 Water Year 2001 (October 1, 2000, through September 30, 2001) precipitation in percent of average

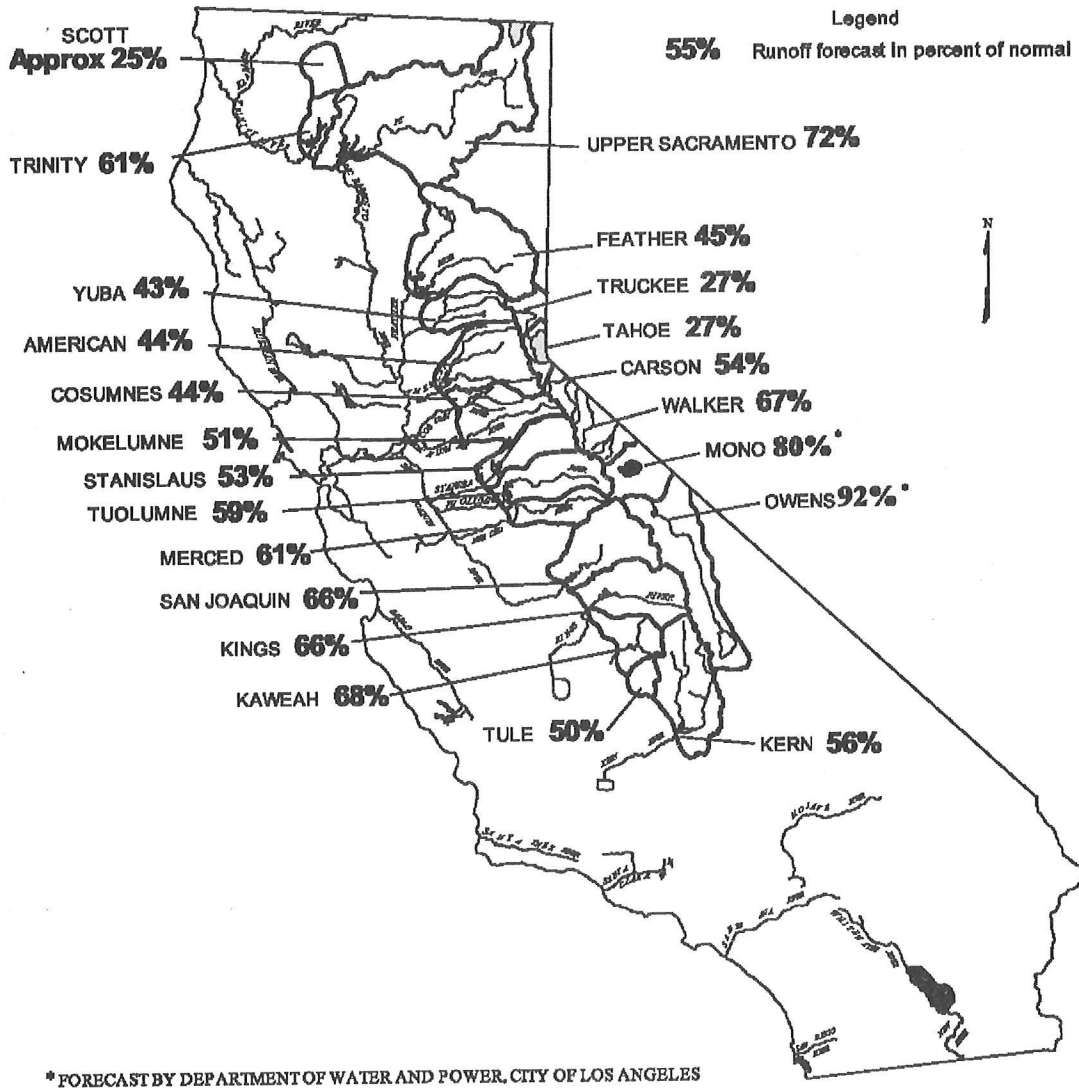


Figure 2 Estimated actual April-July unimpaired runoff for Water Year 2001.

Mountain Precipitation and Snowpack

We spend quite a bit of effort monitoring northern Sierra precipitation and snowpack because this is related quite closely to water supplies of the two major water projects, the Central Valley Project (CVP) and the State Water Project (SWP). The third and fourth charts (Figures 3 and 4) are northern Sierra precipitation, a monthly bar chart and an accumulated precipitation chart. The bar charts show how far below average December has been the last three years. This season November was also quite dry whereas the previous year was near average, and in the year before (1998-1999), November was above average. The net result was that as we entered January, the current season was further behind than the previous two years and on a track which could make Water Year 2001 an extremely dry season, perhaps beginning a drought. January was a little better, but still well below average, which stimulated drought preparations and the appointment of a drought response coordinator (Jeanine Jones of DWR).

The three-panel snow chart (Figure 5) shows the lag quite well, with partial recovery in February and resumption of the dry trend in March. Some snowpack melting started near the end of March; melting slowed during April until near the end of the month, then accelerated into May. On May 1, the overall snowpack stood at 65% of average. By that time the Sacramento region snowpack water content was less than half normal. The remainder of the season was quite dry with above average temperatures in May and somewhat above average temperatures in June. By late summer, the mountain watersheds were extremely dry and some strong wildfires occurred. Summer temperatures dropped significantly below normal in July and August, which eased concerns about a potential electrical power shortage.

Seasonal stream runoff since October 1 was low—only about 50% statewide by the end of the water year compared to 95% one year ago. Sacramento River runoff was slightly over half average at 54% (Figures 6 and 7) The statewide average was pulled down by poor runoff conditions in the normally wet North Coast region, which ran only about 35% of average. We also had one of the bigger floods in history on the Santa Ynez River in Santa Barbara County. On March 5 and 6, 2001, the river rose over eight feet above flood stage at the Narrows station near Lompoc, California, as major spills up to 21,800 cubic feet per second occurred at the upstream Cachuma Reservoir.

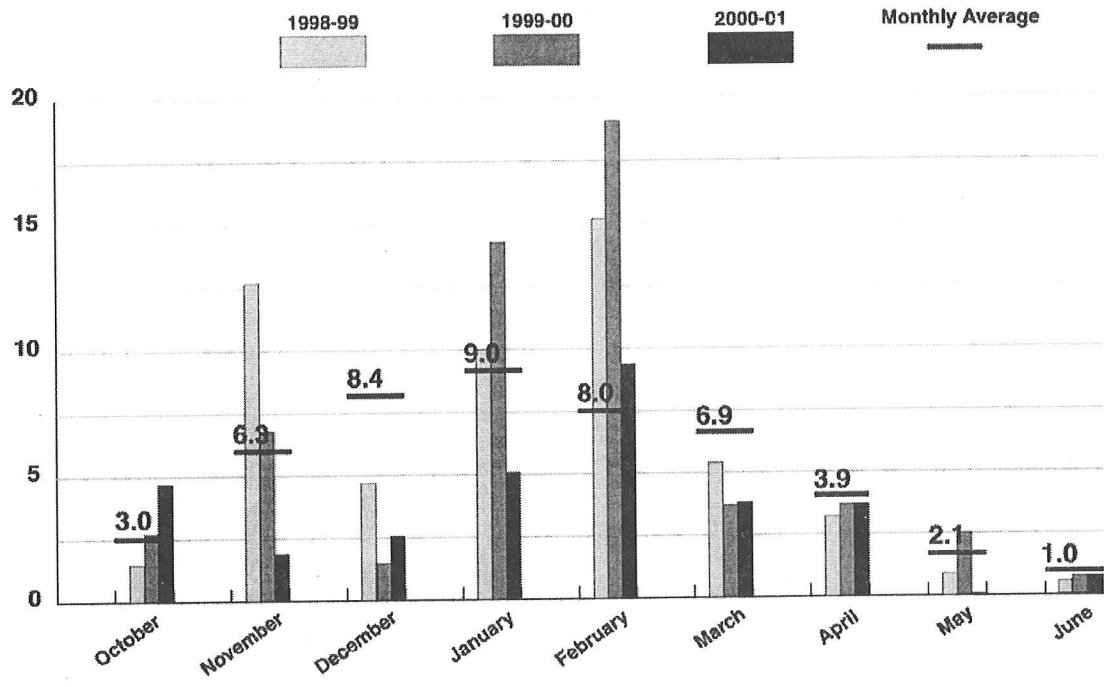


Figure 3 Northern Sierra precipitation in inches

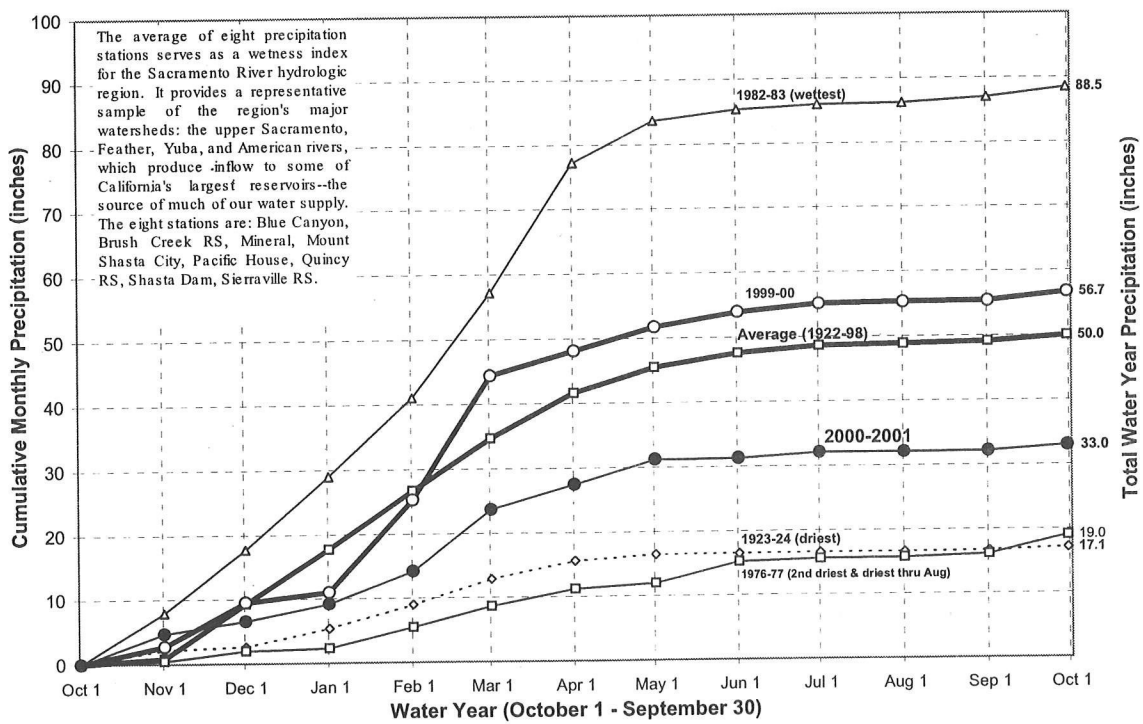


Figure 4 Northern Sierra precipitation, 8-station index, for Water Year 2001

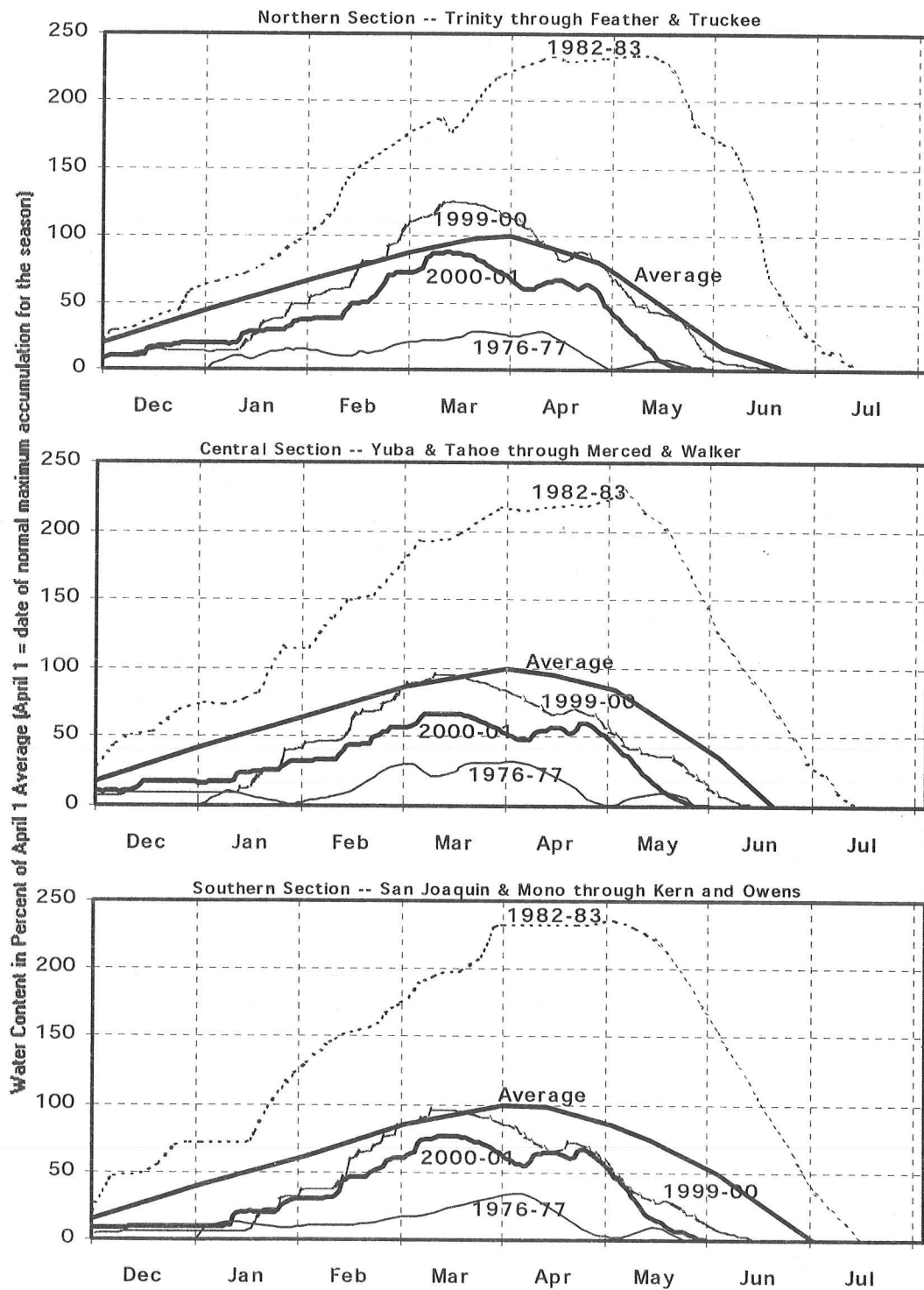


Figure 5 Snowpack water content in percent of April 1 average. April 1 is date of normal maximum accumulation for the season.

Sacramento River System Runoff In Million Acre Feet

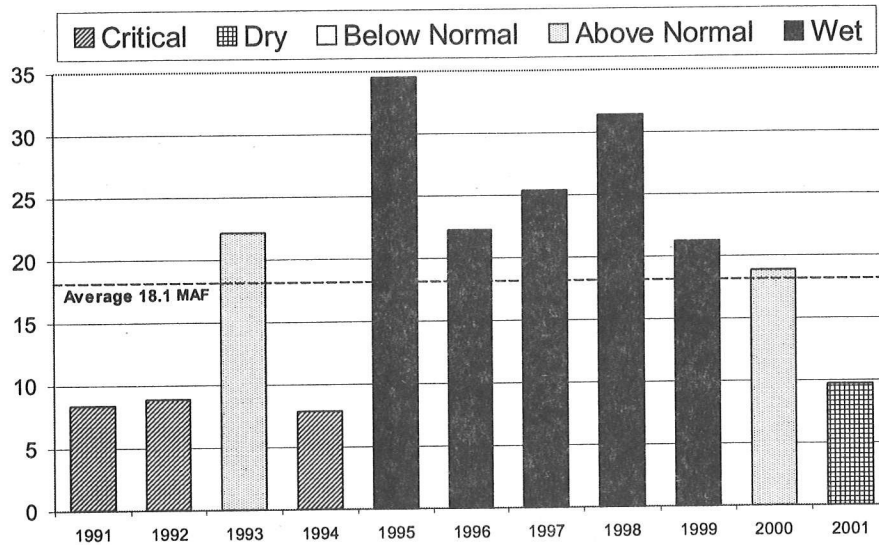


Figure 6 Runoff in million acre-feet for the Sacramento River system

San Joaquin River System Runoff In Million Acre-Feet

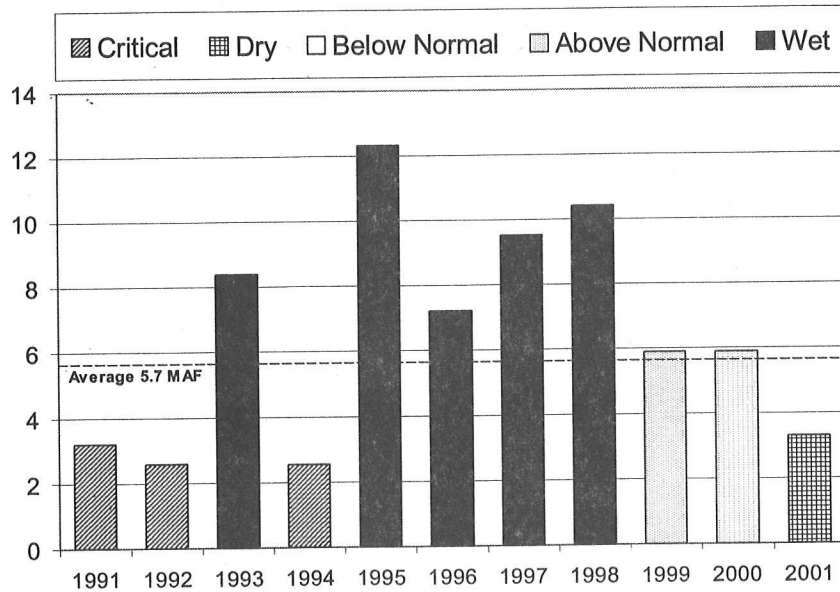


Figure 7 Runoff in million acre-feet for the San Joaquin River system

Snowmelt runoff, that is April through July runoff, was about 55% of average, slightly ahead of water year percentages. The snowpack seems to have peaked at about 80% in mid-March when a couple of weeks of relatively warm sunny weather started the melting—two weeks earlier than average. The April through July runoff (Figure 2) shows the distribution by watershed. The lowest figures are in the Tahoe Truckee area. But the Klamath River inflow to Upper Klamath Lake was also poor at around 40%.

Reservoir storage (Figure 8) started out 10% over average last fall and closed the water year at around 88% on September 30, still above the 70 to 75% level threshold for declaring drought. The normal early summer gain was muted this year but carryover helped meet the water needs of many folks. In addition to shortages in the north and northeast (especially the upper Klamath River area) the big deficits were in the CVP and SWP service area. The CVP delivered only 52% (including an October adjustment) to their San Joaquin Valley project agricultural customers in 2001. North of the Delta CVP agricultural deliveries were 60% but water rights holders, both north and south of the Delta, received full allotments. The SWP only delivered 39% of its entitlements. Full Colorado River supplies were available because of extensive storage even though runoff was 50% below average.

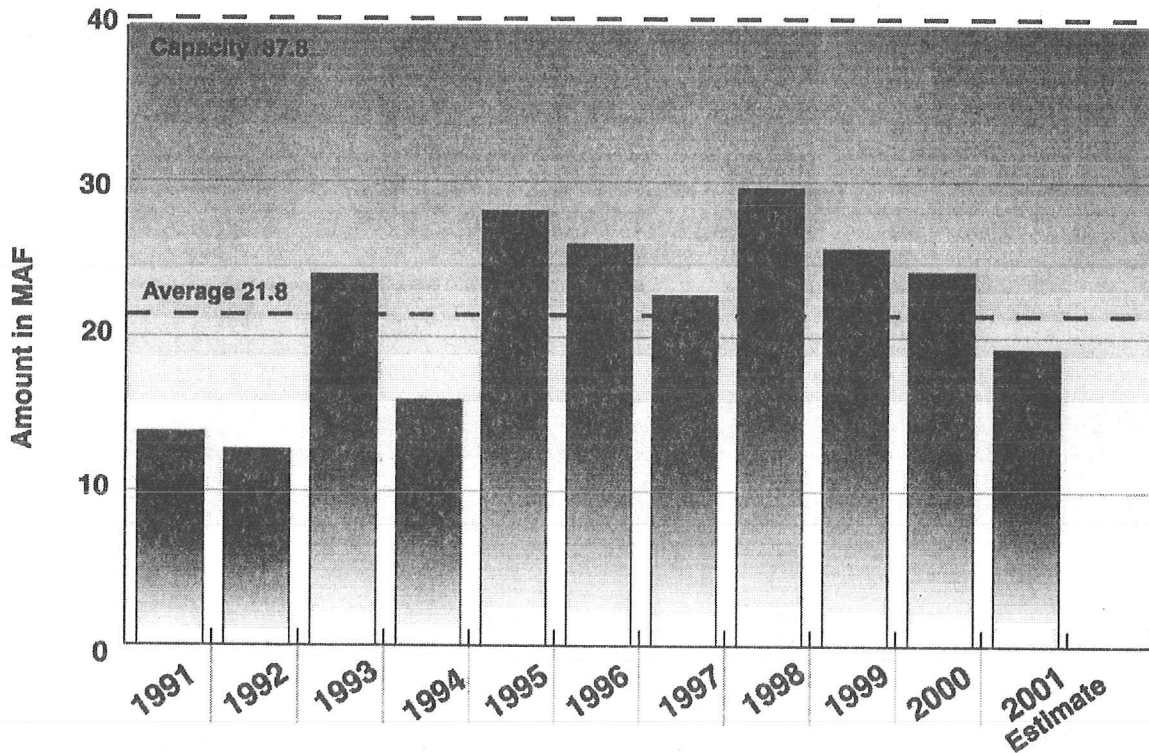


Figure 8 Storage of 156 major in-State reservoirs on October 1 in million acre-feet

Table 1 Water year data in percent of average (unless noted)

| <i>Water Year</i> | 2001 | 2000 | 1999 | 1998 | 1997 | 1996 | 1995 | 1994 |
|-----------------------------|--------|--------|--------|--------|--------|--------|--------|--------|
| Statewide | | | | | | | | |
| Precipitation | 75 | 100 | 95 | 170 | 125 | 110 | 165 | 65 |
| April 1 Snowpack | 60 | 100 | 110 | 160 | 75 | 95 | 175 | 50 |
| Runoff | 50 | 95 | 110 | 175 | 145 | 125 | 180 | 40 |
| Reservoir storage, Sept. 30 | 89 | 111 | 118 | 136 | 104 | 120 | 130 | 73 |
| Reservoir storage, maf | (19.4) | (24.2) | (25.6) | (29.6) | (22.7) | (26.0) | (28.1) | (15.9) |
| Regional | | | | | | | | |
| Northern Sierra Precip. | 66 | 113 | 110 | 165 | 138 | 123 | 171 | 64 |
| 8 Station Index, inches | (33.0) | (56.7) | (54.8) | (82.4) | (68.7) | (61.3) | (85.4) | (31.8) |
| Sacramento River | 54 | 104 | 117 | 174 | 141 | 123 | 191 | 43 |
| Unimpaired runoff, maf | (9.8) | (18.9) | (21.2) | (31.4) | (25.4) | (22.3) | (34.5) | (7.8) |
| San Joaquin River | 57 | 103 | 104 | 183 | 167 | 127 | 216 | 45 |
| Unimpaired runoff, maf | 3.2 | (5.9) | (5.9) | (10.4) | (9.5) | (7.2) | (12.3) | (2.5) |

We have had six good water years in a row in northern California, so the string of good years was bound to end sometime. Hopefully next year will be better and we will not slide into another drought.

Electrical Power Concerns

There is a lot of interest in California's electric power situation. Many know the Department of Water Resources has become the purchaser of some 30% or more of the electricity for the State since the two major private utilities and the Independent System Operator (ISO) no longer had credit in January. I'd like to present a few charts to give some background and perspective as I see it. DWR was a player in the deregulated market because we both generate and consume electric power with the State Water Project. But the scale of the early power-purchasing program was probably 10 to 20 times what we were used to and was a sudden, very large load on staff. It now appears the power purchasing assignment for the State may last a while, probably for years.

The following charts (Figures 9, 10, and 11) illustrate where our electricity comes from and how it is used. The biggest source is natural gas at nearly one-third. Hydro (counting small plants less than 50 MW) is a little less than one-fourth of our energy supply, and this figure includes a substantial contribution from the Pacific Northwest. (In-state hydro energy provides around 15% of the total usage, ranging from about 10% in dry years to 20% in wetter years.) For capacity (Figure 10) the mix is a little different: hydro and natural gas are larger fractions. After a hiatus of 10 to 15 years, new power plants are underway or planned for construction—perhaps 5,000 MW this year. But almost all these plants are based on natural gas, putting a lot of eggs in one basket. With cooler than normal

midsummer temperatures and peak summer electricity conservation, we squeaked through the summer. However, because of the dry year, California hydro may have been short by 25% or so in energy and probably some in capacity. The weather so far in the Pacific Northwest was also very dry which cut the amount of power normally available from there during the summer. Normally, the Pacific Northwest furnishes nearly 10% of our energy.

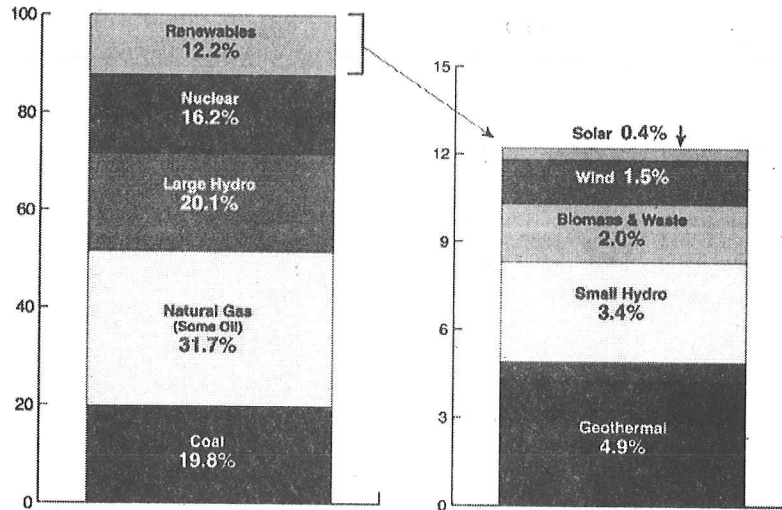


Figure 9 Sources of 1999 California net system electricity. Total = 239 billion KWh

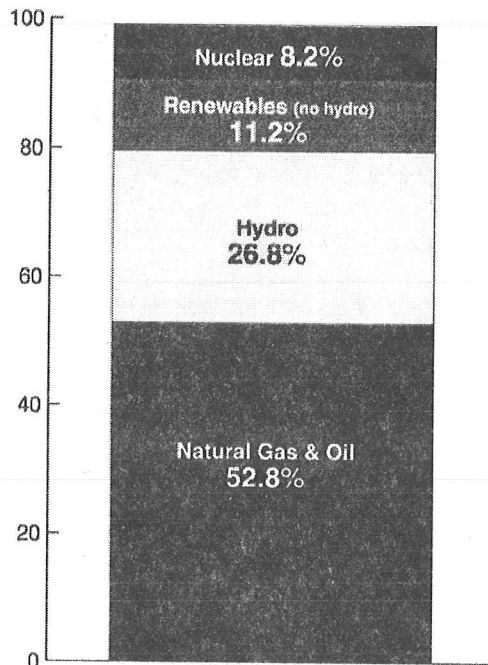


Figure 10 California electric MW capacity, 1999. Total = 52,600 MW.

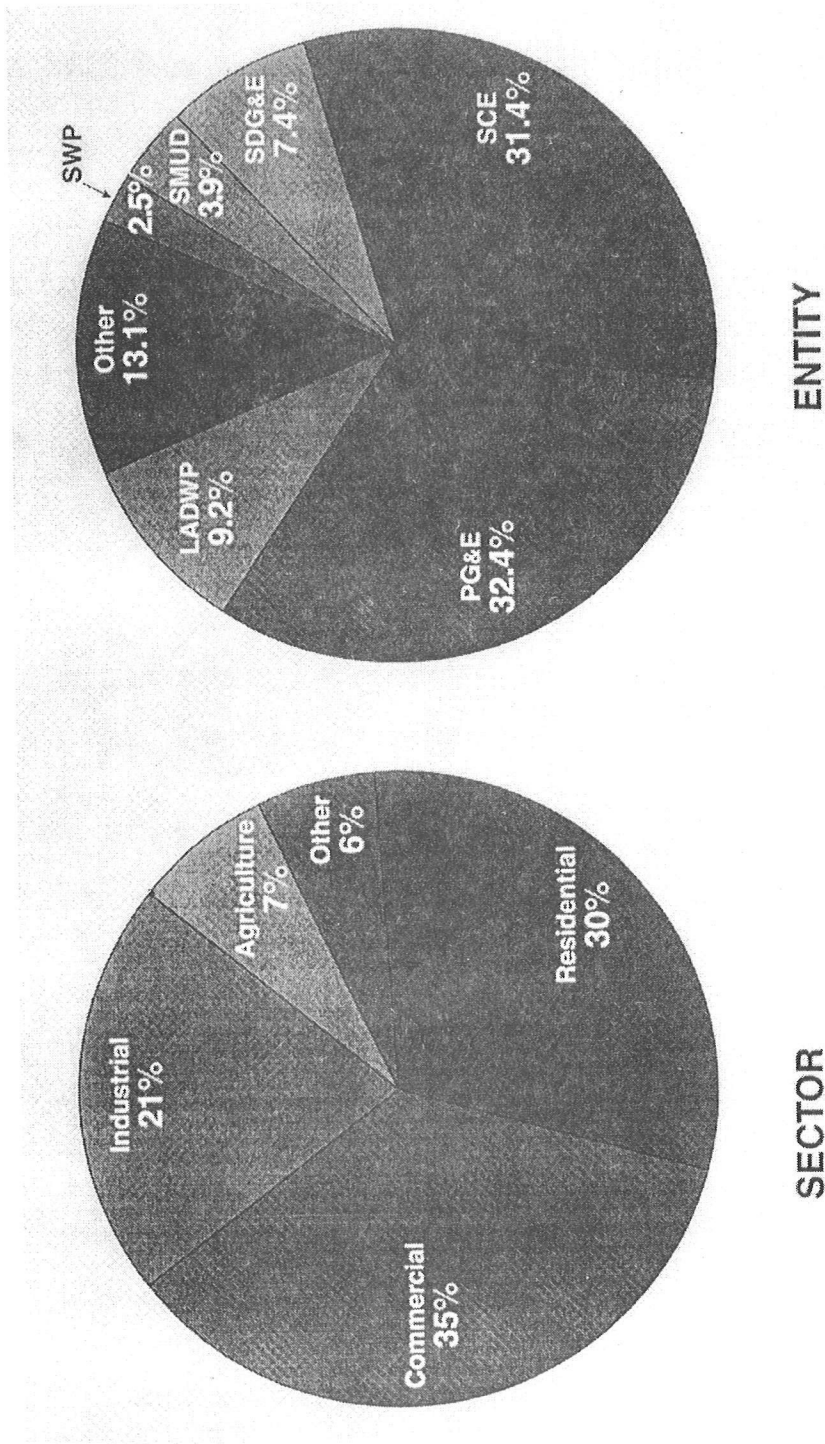


Figure 11 shows where electric power was used in 1999, the last year data was available when this talk was presented

Major Flood Events of the Past 2,000 Years Recorded in Santa Barbara Basin Sediment

Arndt Schimmelmann, Carina B. Lange, and Hong-Chun Li

Introduction

Every few hundred years the culmination of extreme regional precipitation in Southern California produces flooding that dramatically increases transport of fine-grained sediments into California's offshore basins. Conspicuous gray, clay-rich flood deposits in the predominantly olive, varved Holocene sediment record in the central Santa Barbara Basin (SBB) offer a paleoclimatic record of Southern California flood events in the Ventura River and Santa Clara River catchments. The last extreme flood occurred about A.D. 1605 and correlates well with a multitude of other climatic anomalies worldwide, coinciding with a brief, sharp cooling that compressed the world's atmospheric circulation patterns towards the equator (Schimmelmann and others 1998). Here we collect new corroborating evidence for the ca. 1605 event and report on five earlier major SBB flood events, in ca. A.D. 212, 440, 603, 1029, and 1418 that seem to correlate with supraregional climate changes, cultural transitions in South America and the Caribbean, and may be influenced in their temporal distribution by a ca. 208-year cycle of solar activity.

Methods

Piston core "6P" from the center of the SBB (34° 14.3'N, 120° 05.1'W) provided new sediment slabs for an almost continuous series of X-radiographic images covering the past ca. 6,000 years. For much of the past 2,000 years we also have available parallel X-radiographic records from other piston, gravity, and box cores that are closely correlated with 6P. Counting of the annual varves down-core provided a chronology with an estimated accuracy of ± 20 years at the A.D. 1000 level and ± 50 years at the A.D. 1 level. Seven foraminifera-based radiocarbon ages are in good agreement with our varve-count chronology within the past 2000 years (B. Roark, Lynn B. Ingram, and Doug J. Kennett, personal communications).

Gray layers of core 6P were examined with light and electron microscopy. The identification of finer-grained, gray flood deposits, in contrast to coarser-grained, gray turbidites, followed the methods and description given in Schimmelmann and others (1998). Grain-size analysis was also performed using light microscopy. Only prehistoric flood deposits with a thickness of ≥ 2 mm are considered in this study.

All ages refer to calendar years A.D. Without accurate dating to ± 1 year of flood deposits and other paleoclimatic evidence, our potential correlations among events and our interpretation of individual SBB floods must in many cases remain hypothetical. In particular, it is difficult to prove a causal connection between climatic events and prehistoric volcanic eruptions (Sadler and Grattan 1999).

Results and Discussion

The six major prehistoric flood deposits of the past 2000 years are discernible in all high-resolution sediment records of the central SBB, albeit with thicknesses that differ between cores and individual locations (Figure 1). Conservative estimates for the accuracy of the varve-count ages of the six prehistoric gray flood deposits are A.D. 1605 ± 5 yr, 418 ± 10 yr, 1029 ± 20 yr, 603 ± 35 yr, 440 ± 40 yr, and 212 ± 50 yr.

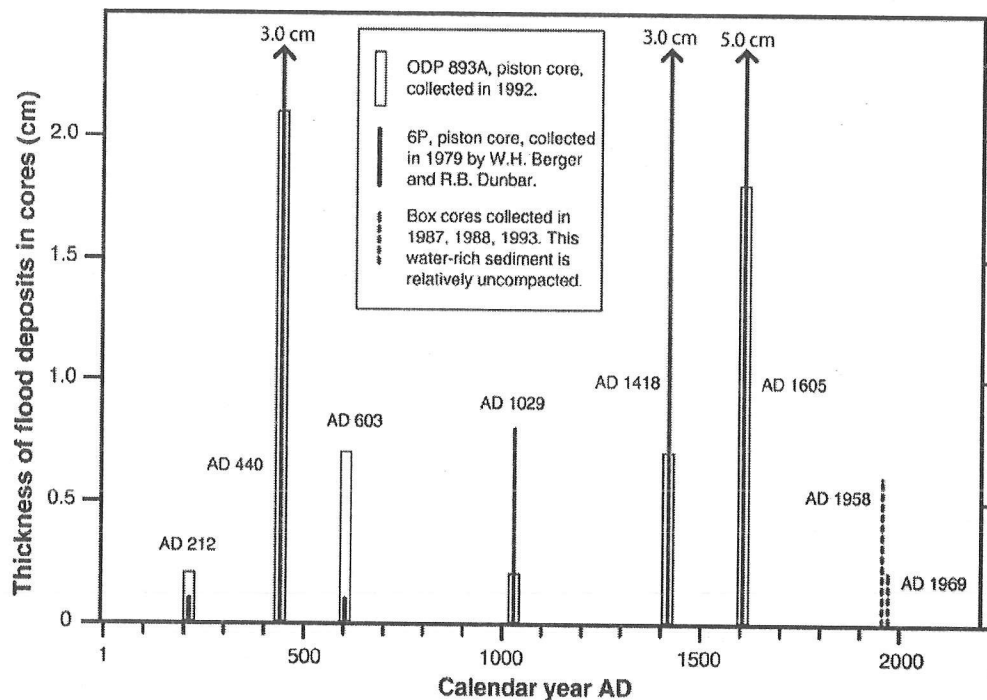


Figure 1 The six major prehistoric gray flood deposits of the past 2,000 years in the central Santa Barbara Basin express varying thicknesses in different cores. Recent flood deposits of the 20th century appear with inflated thickness because their young sediment is relatively uncompacted and contains much pore water.

The 1969 flood (Figure 1; further discussed in Schimmelmman and others 1998) demonstrates that occasional severe runoff in Southern California may occur within natural climatic variance, without assistance by either strong El Niño precipitation (for example, the 1958 flood layer) or by volcanic cooling-induced changes in atmospheric circulation (for example, the ca. 1605 flood layer; Schimmelmman and others 1998, 1999). The historic 20th century floods, however, all seem small in comparison to many prehistoric floods (Figure 1). We believe that the large thicknesses of some flood layers, especially around 440 and 1418, call for extraordinary climatic conditions that affected not only Southern California, but likely also a much wider region. Paleoclimatic evidence for widespread anomalies and events is collected in Tables 1-1 through 1-6 for the six time slices for which SBB flood deposits are documented during the past two millennia. Perturbations in global atmospheric circulation can manifest themselves by floods in one region and by drought in another. To a lesser extent the same consideration is valid for temperature anomalies. We caution that

temporal correlation does not necessarily imply common causation, and that the dating accuracy of paleoclimatic evidence degrades with increasing age. Nevertheless, the large matrices of evidence permit the formulation of reasonable hypotheses for several flood events. Not all listed evidence necessarily correlates with SBB flood deposits, and some SBB floods may represent merely local weather extremes. Our discussion starts with the ca. 1605 SBB flood and proceeds back in time.

A.D. 1605 ± 5 yr. Schimmelmann and others (1998) assembled much regional and global evidence for rapid, intense cooling around 1605, with an equatorward shift of prevailing wind patterns and associated storm tracks. Atmospheric cooling in the wake of the eruption of the Peruvian volcano Huaynaputina in 1600 is a likely cause (references in Schimmelmann and others 1999; Zielinski 2000), although another, unidentified volcanic eruption at about the same time may have been decisive for the magnitude of paleoclimatic anomalies in the Northern Hemisphere (Gervais and MacDonald 2001). The severity of flooding in Southern California may have been exacerbated by El Niño conditions, and the large thickness of the flood layer was in part caused by a preceding drought that left the soil vulnerable to erosion (Schimmelmann and others 1998). Table 1-1 lists 29 additional corroborating multidisciplinary lines of evidence for the global disturbance of atmospheric circulation in the first decade of the 17th century.

Table 1-1 Paleoclimatic evidence for 1605 ± 5 yr that may correlate with occurrences of six major flood layers in Santa Barbara Basin over the last 2000 years. All ages are in calendar years AD. The numerous data sources listed earlier by Schimmelmann and others (1998) for the ca. 1605 volcanic cold spell and Southern California wet period and flood are not repeated here.

| <i>Time period (yr AD)</i> | <i>Descriptions of paleoclimatic evidence; source of data</i> |
|---|--|
| ~1601 | Review of the Huaynaputina eruption and its climatic aftermath; Zielinski 2000. |
| 1601 | Strong volcanic signal in Antarctic ice core; Delmas and others 1992. |
| ~1600 | Abrupt and severe decline of mean late-season temperature at a timberline site in the Sierra Nevada; 1604 very cold; Scuderi 1993. |
| ~1604-1610 | Extreme decline of July temperatures in Idaho reaching absolute minimum temperature in 857 yr record; Biondi and others 1999. |
| ~1600 | Relatively cold near-surface water in Santa Barbara Basin, via planktonic foraminifera; Field and Baumgartner 2000. |
| ~1602-1605 | Athabasca region fairly cold April to August, ~1602-1605, based on tree-rings; Luckman and others 1997. |
| ~1600 | Evidence points to wet interval in North Dakota lakes; Fritz and others 2000. |
| 1601 | Coldest summer of the last millennium on the Northern Hemisphere; Jones and others 1998. |
| 1601 | Coldest year in Ostfriesland, Germany, within time period 1590-1612; Glaser 1995. |
| Early 1600s (¹⁴ C-dated) | Wet interval in Owens Lake, followed by lower lake level ~ 1615; Li and others 2000; Fig. 2-C. |

Table 1-1 Paleoclimatic evidence for 1605 ± 5 yr that may correlate with occurrences of six major flood layers in Santa Barbara Basin over the last 2000 years. All ages are in calendar years AD. The numerous data sources listed earlier by Schimmelmann and others (1998) for the ca. 1605 volcanic cold spell and Southern California wet period and flood are not repeated here.

| <i>Time period (yr AD)</i> | <i>Descriptions of paleoclimatic evidence; source of data</i> |
|--------------------------------|---|
| ~1600-1610 | Unusually cold in Subarctic Québec, based on tree-rings; Wang and others 2001. |
| ~1600 | Preponderance of narrow tree rings in Canadian Rockies ~1600; Luckman 1997. |
| ~1600 | Cold shortly after 1600 in Mongolia, based on tree-rings; D'Arrigo and others 2001. |
| 1601 | Cold summer shown in many European tree-ring data; Briffa and others 1999. |
| ~1600 | Precipitous drop of nitrate concentration in Guliya ice core to record low levels, suggesting sun's influence (Wang and others 2000), but Lean (2000) reconstructed no major change in solar irradiance 1600-1630. |
| ~1600 | Cooling in New Zealand, based on tree-rings; D'Arrigo and others 1998. |
| ~1602-1605 | Cold springs/summers in coastal Gulf of Alaska, based on tree-rings; Wiles and others 1998. |
| ~1605 | South African stalagmite suggests cool, dry conditions; Holmgren and others 1999. |
| ~1600 | Greenland ice sheet bore hole temperatures show very cold temperatures; Dahl-Jensen and others 1998. |
| ~1600 | Glacier advances in Greenland; Geirsdóttir and others 2000. |
| ~1600 | Cold weather in northeast China; Hong and others 2000. |
| ~1600-1610 | Drought in northern Nigeria, Tarhule and Woo 1997. |
| ~1550 (¹⁴ C-dated) | Fragmentation of Amazonian rainforest due to drought (Meggers, 1994), and cultural changes affecting Precolumbian populations in the Caribbean (Meggers, 1996), possibly in connection with rare "mega-El Niño" events. |
| ~1601 | Very cold growing season in eastern Norway, based on tree-rings; Kalela-Brundin 1999. |
| 1601 | Kola peninsula, Russia, 403-year tree-ring record shows very cold summer temperature; Gervais and MacDonald 2001. |
| ~1600 | Eastern Canadian Arctic varved lake record shows cold summers; Moore and others 2001. |
| 1606-1612 | The driest 7-year episode in 770 years, recorded in northeastern Virginia tree rings; Stahle and others 1998. |
| ~1600 | Dramatic decrease in Scottish mean annual precipitation; Baker and others 2000; Fig. 2-G |
| ~1605 | Extreme summer warmth at Dome Summit South, Antarctica; Morgan and van Ommen 1997. |

Between Floods of ~1605 and ~1419. The period 1468 to 1580 had the second highest drought frequency of the past 2000 years in the Sierra Nevada (Hughes and Brown 1992).

A.D. 1419 ± 10. This SBB flood event correlates with Southern and Central California regional records of increased contemporaneous wetness, and also with reports of climatic change at about the same time elsewhere (Table 1-2). Ice cores from both hemispheres indicate an abrupt global reorganization of atmospheric circulation around 1400 (Kreutz and others 1997), at a time widely considered to mark the beginning of the Little Ice Age (glaciation had started earlier in some regions surrounding the North Atlantic; Grove 2001). A large increase in flood magnitude is reported for the upper Mississippi at the transition to the Little Ice Age (Knox 1993). The various global paleoclimatic temperature and precipitation responses feature distinct regional differences, but most temperature records suggest cooling in the early 15th century. One factor for this predominant cooling may have been decreasing solar irradiance (Beer and others 2000), yet oceanographic mechanisms for triggering the LIA have been proposed (for example, Broecker 2000). No ice-core evidence can be cited in support of short-term volcanic cooling 1350-1450 (Zielinski 2000), and the uncertainty in varve-count dating of ±10 years of the flood deposit discourages correlation with specific historical accounts of El Niño occurrences (Quinn 1999). Eltahir and Wang's (1999) nilometer-based El Niño reconstruction features a low El Niño frequency around 1418. The majority of evidence in Table 1-2 is consistent with an SBB flood occurring during the late 1410s to early 1420s.

Table 1-2 Paleoclimatic evidence for 1418 ± 10 yr. Notes as in Table 1-1.

| <i>Time period (yr AD)</i> | <i>Descriptions of paleoclimatic evidence; source of data</i> |
|--|--|
| ~1420 (¹⁴ C-dated) | Major flood event in San Francisco Bay estuary (Goman and Wells 2000) that seems to correlate with flood event in Sacramento Valley (Sullivan 1982). |
| ~1400-1480 (¹⁴ C-dated) | Wet interval in Owens Lake, California; Li and others 2000; Fig. 2C. |
| ~1400-1420 (¹⁴ C-dated) | Very abrupt and severe oxygen isotopic excursion in Mono Lake, California, suggesting increased freshwater recharge; Li 1995; Fig. 2B. |
| ~1400 (¹⁴ C-dated) | Rising water level at Mono Lake, California; Stine 1990; Fig. 2A. |
| ~1400 (¹⁴ C-dated) | Decrease in salinity in San Francisco Bay water, due to increased river inflow from California hinterland; Ingram and others 1996. |
| ~1413-1424 | Increased precipitation in Santa Barbara, California, based on tree-rings; Haston and Michaelsen 1994. |
| ~1410-1420 | Positive precipitation anomaly during growing season in southern Sierra Nevada; Graumlich 1993. |
| 1414-1425 | No low-growth years in Sierra Nevada sequoia tree-ring record, California, suggesting absence of drought; Hughes and Brown 1992. |

Table 1-2 Paleoclimatic evidence for 1418 ± 10 yr. Notes as in Table 1-1.

| <i>Time period (yr AD)</i> | <i>Descriptions of paleoclimatic evidence; source of data</i> |
|--|--|
| ~1400 | Arctic and Antarctic ice cores show most dramatic atmospheric change to increased meridional intensity in the last 4000 years; Kreutz and others 1997. |
| 1420s | Predominantly cold summer temperatures in the Northern Hemisphere (Jones and others 1998), but Sierra Nevada tree-ring records show regionally mild temperatures (Scuderi, 1987, 1993; Graumlich, 1993). |
| 1407-1408, 1422-1423 | Severe winters in Europe; Lamb 1982, p. 187. |
| 1420s, 1430s | Lamb (1982, p. 195) notes widespread European famines for the 1420s and 1430s, with cannibalism reported in eastern Europe. |
| 1423 | Adverse tree growth conditions, eastern Norway, based on tree-rings; Kalela-Brundin 1999. |
| ~1400 (¹⁴ C-dated) | Abrupt change from warm to cold sea surface temperature in Norwegian Sea; Jansen and Koç 2000. |
| 1421 | Catastrophic North Sea flood; Lamb 1982, p.181. |
| 1417 | Flooding in Spain; Barriendos Vallve and Martin-Vide 1998. |
| 1410, 1413, 1418, 1420, 1426 | Severe Mediterranean sea storms; Camuffo and others 2000. |
| ~1414-1417 | Relatively high conductivity in ice cores from Ellesmere Island, Canada; Zheng and others 1998. |
| ~1410-1417 | Relatively high acidity in Greenland ice core; Hammer and others 1980. |
| 1413 | Volcanic event recorded in Dye 3 ice core, Greenland; Fisher and others 1995. |
| 1408, 1427 | Years with low Nile flood occurrence, severity rank 3, suggesting El Niño conditions; Quinn 1999. |
| 1403 ± 72 yr (¹⁴ C-dated) | Coastal Peru, severe flood event #11; Wells 1990. |
| ~1420 (¹⁴ C-dated) | Abrupt wetting of Yucatan peninsula, end of drought; Hodell and others 2001. |
| ~1390-1400 | Drought on Peruvian altiplano; Thompson 1992; Fig. 2D. |
| Early 1400s (¹⁴ C-dated) | Cultural decline on Peruvian Southern Coast; beginning of the Inca Empire; Thompson and others 1994; Fig. 2F. |

Table 1-2 Paleoclimatic evidence for 1418 ± 10 yr. Notes as in Table 1-1.

| <i>Time period (yr AD)</i> | <i>Descriptions of paleoclimatic evidence; source of data</i> |
|----------------------------|---|
| ca. 1420s, early 1430s | Drought in Mali, Africa, causing the abandonment of Timbuktu in 1433 by the Mali empire to the Tuareg nomads. "Although it can never be safe to deduce climatic changes from human political history, in this extreme region the events described most probably confirm that drying out of the desert region was proceeding ..." (Lamb 1982, p. 197). |
| ~1400-1450 | Dramatic decrease in Scottish mean annual precipitation; Baker and others 2000; Fig. 2G. |
| ~1420 | Low salinity and wet climate in South China Sea; third phase of construction of Great Wall; Wang and others 1999. |
| ~1410 | Cold spell during growing season, New Zealand; D'Arrigo and others 1998. |
| ~1400 | Record winter warmth at Dome Summit South, Antarctica; Morgan and van Ommen 1997. |

Between Floods of ~1418 and ~1029. This interval without SBB flood evidence falls into Stine's (1994) "epic drought" period 1209-1350 that is documented by tree-stump evidence from California's mountain ranges. Drought in California's hinterland would not have affected coastal ecosystems to the same degree. Rapid cultural evolution of Native American cultures in Southern California is observed in the time period ~1150-1300, during relatively cool and dry coastal conditions, coinciding with the phase of coldest sea temperatures and the most unstable marine climatic interval of the Holocene, ~450-1300 (Kennett and Kennett 2000).

A.D. 1029 ± 20. Within the accuracy of dating of regional records from Mono Lake, Owens Lake (~990-1040), and flood evidence from elsewhere in the southwestern USA, the ~1029 SBB flood deposit seems to match with a generally wet period (Figure 2A, 2C; Table 1-3). In contrast, Stine (1994) reported evidence for a ~892-1112 "epic drought" in California, based on tree stumps around Mono Lake, Tenaya Lake, Walker River, and Osgood Swamp. The evidence for this regional drought is strong, but trees in the environments studied by Stine (1994) may not have recorded brief wet spells within an overall dry period. Drought would have reduced vegetation cover and thus prepared the soil in the Santa Barbara region for erosion, enabling intermittent severe storms to produce a mid-size SBB flood deposit. Graumlich's (1993) southern Sierra Nevada tree-ring study also does not indicate wetness ~1029 (and neither for ~1605), but trees are primarily recorders of environmental conditions during the growing season, and even then do not adequately register flooding. The Sierra Nevada tree-ring record might not reflect mid-winter and late-winter storms.

The flood during the early 11th century occurred during a period often referred to as the "Medieval Warm Period" (MWP). The period 1001-1100 was the second warmest century of the millennium in the Northern Hemisphere, surpassed only by the last century (Jones and others 1998). Although many parts of the Northern Hemisphere experienced unusual warmth, the expression "Medieval Climatic Anomaly" is more appropriate on a larger geographic scale (Bradley 2000; Bradley and

others 2001). Sierra Nevada tree-ring records show predominantly mild temperatures for the growing season during the first half of the 11th century (Scuderi 1987, 1993; Graumlich 1993). However, several references document significant cold spells with wide geographic distribution in the 1020s and 1030s (Table 1-3), linking some cooling to volcanic eruptions, possibly to that of Baitoushan in ~1025 (Zielinski 2000). A cold spell around the 1030s is recorded in Sierra Nevada tree rings (Graumlich 1993). An intermittent cold spell may have interrupted a relatively warm climate regime. This may have triggered the SBB flood event, by shifting mid-latitude storm tracks equatorward, either via expansion of the circumpolar vortex, or via persistent ridges of high pressure. The preponderance of the evidence in Table 1-3 points towards the late 1020s or early 1030s as a likely age for this SBB flood deposit.

Meggers (1994) suggested that a rare “mega El Niño event” was responsible for cataclysmic South American cultural changes around the turn of the first millennium. Along this line of thought, some workers cite obscure sources to cluster disastrous El Niño activity around 1050 (Chepstow-Lusty and others 1996), but Quinn’s (1999) last compilation of historic El Niño evidence lists nothing higher than rank 3 El Niño events from 1009 through 1095, while the closest extreme El Niño events are dated 967 (rank 5+) and 1096 (rank 5). Also, Eltahir and Wang’s (1999) nilometer-based El Niño reconstruction does not indicate higher El Niño frequency around 1050.

Table 1-3 Paleoclimatic evidence for 1029 ± 20 yr. Notes as in Table 1-1.

| <i>Time period (yr AD)</i> | <i>Descriptions of paleoclimatic evidence; source of data</i> |
|-------------------------------------|--|
| ~1050 (¹⁴ C-dated) | Rising water level at Mono Lake, California; Stine 1990; Fig. 2A. |
| ~990-1040 (¹⁴ C-dated) | Wet interval at Owens Lake, California; Li and others 2000; Fig. 2C. |
| ~1020-1050 | Negative precipitation anomaly during growing season in southern Sierra Nevada; Graumlich 1993. |
| ~1000-1200 (¹⁴ C-dated) | Increased flood occurrence in southwestern U.S.; Ely and others 1993. |
| ~950-1050 | Tree-ring records from northern “high” latitudes record distinct warmth on centennial time scale; Briffa 2000. |
| early 1030s | Global cold spell lasting 2-3 years; Jones and others 1998. |
| 1032 | Third coldest summer of the last millennium on the Northern Hemisphere; Jones and others 1998. |
| 1029 | Tree-ring evidence for volcanic-induced frost in California and Nevada; LaMarche and Hirschboeck 1984. |
| 1026-1036 | Transition from 20-year warm period to 50-year cold interval in Sierra Nevada; 1030s predominantly cold; Graumlich 1993. |

Table 1-3 Paleoclimatic evidence for 1029 ± 20 yr. Notes as in Table 1-1.

| <i>Time period (yr AD)</i> | <i>Descriptions of paleoclimatic evidence; source of data</i> |
|--------------------------------------|---|
| 1020 | Winter temperature below average in western central Europe; Pfister and others 1998. |
| ~1030s | Extreme cold spell in northern Patagonian Andes; Villalba 1990. |
| 1011-1020 | Fourth coldest decade of summer temperatures of the last millennium on the Southern Hemisphere; Jones and others 1998. |
| 1020 | Severe Adriatic sea storm; Camuffo and others 2000. |
| ~1025 | Volcanic eruption of Baitoushan recorded in Greenland ice core GISP2; Zielinski 2000. |
| ~1020 (¹⁴ C-dated) | Sedimentary evidence for severe drought on Yucatan peninsula that centered on 1020 and lasted until 1060 (Hodell and others 2001). Other evidence for aridity on Yucatan peninsula and in central Mexico 1000 listed by Metcalfe and others 2000. Yucatan drought ¹⁴ C-dated to 986 and 1051 by Curtis and others 1996. This drought is implicated as a destabilizing factor in the final Classic Maya collapse 1000 (Hodell and others 2001). |
| ~1000 (¹⁴ C-dated) | Cultural changes in Peru and Ecuador; Ecuador Santa Elena peninsula abandoned; discussed in Thompson (1992) and by Meggers (1994); Fig. 2F. |
| ~994, ~1050 (¹⁴ C-dated) | Mega-El Niño event affecting Amazonia and precolumbian populations in the Caribbean; Meggers 1994, 1996. |
| ~1040 (¹⁴ C-dated) | Onset of markedly drier conditions on the Bolivian-Peruvian altiplano causing the demise and eventual collapse of the Tiwanaku culture surrounding Lake Titicaca. The lake level dropped about 10m (deMenocal 2001; and references therein). |
| ~900-1050 (¹⁴ C-dated) | Dramatic environmental changes in Central Peruvian Andes; Ortlhoff and Kolata 1993; Chepstow-Lusty and others 1996. |
| ~1030-1040 | End of distinct wet period at Peruvian Quelccaya ice cap that had lasted since 760, followed by drought; Thompson 1992; Fig. 2D. |
| ~1025 | Dramatic decrease in Scottish mean annual precipitation; Baker and others 2000; Fig. 2G |
| 1010-1011 | Severe winter with ice on the Bosphorus Strait, Turkey, and on the Nile river; Lamb 1982, p. 157. |
| ~1030s (U, Th-dated) | South African stalagmite suggests cooling, drying; Holmgren and others 1999; with additional supporting regional evidence cited therein. |

Table 1-3 Paleoclimatic evidence for 1029 ± 20 yr. Notes as in Table 1-1.

| Time period (yr AD) | Descriptions of paleoclimatic evidence; source of data |
|---------------------|--|
| ~1047 | Volcanic signal in Antarctic ice core; Delmas and others 1992. |

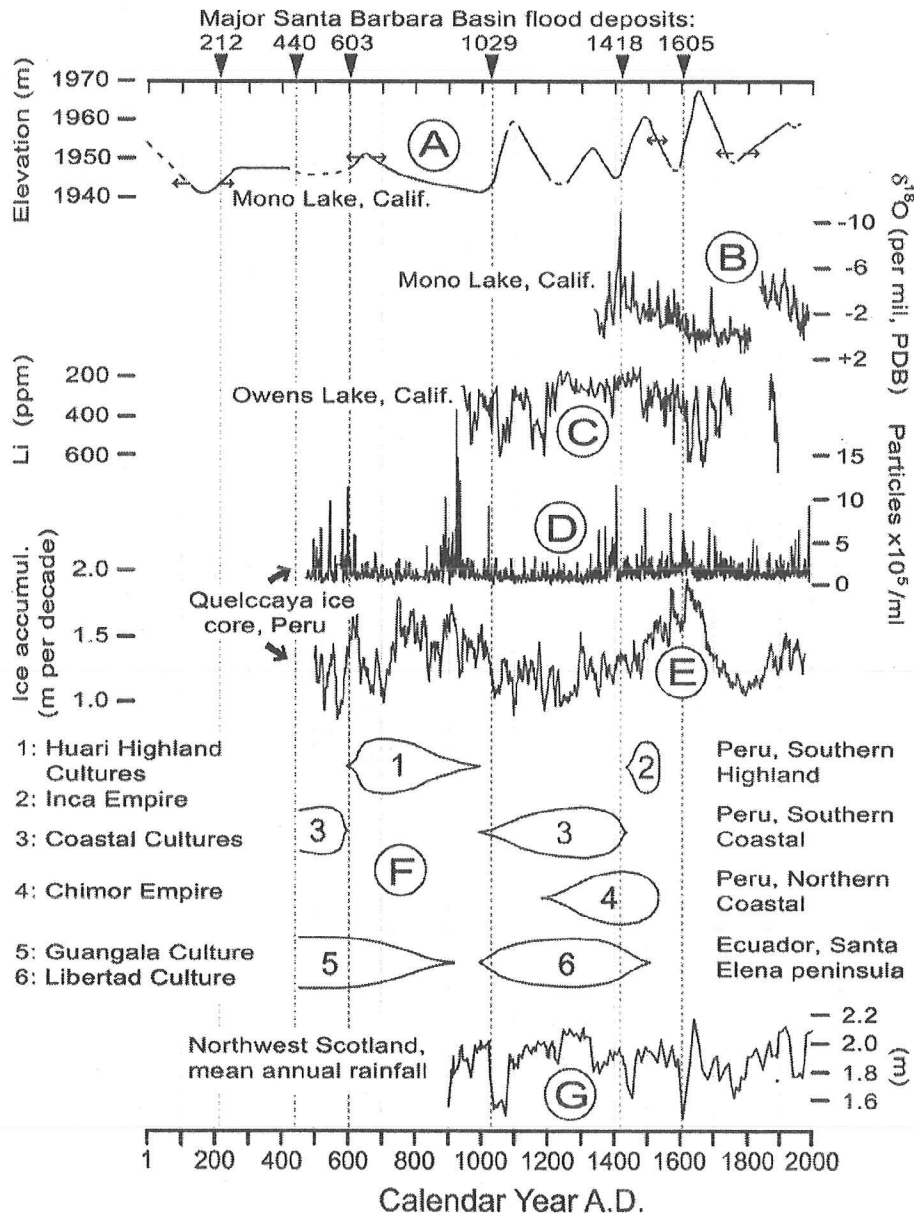


Figure 2 Correlation of the six major prehistoric flood deposits in Santa Barbara Basin over the past 2000 years with (A) Stine's (1990) record of Mono Lake level fluctuations, suggesting that Mono Lake was filling at times of SBB flood occurrence; (B) Mono Lake carbonate oxygen isotope ratios (Li 1995; more negative $\delta^{18}\text{O}$ -values suggest wet intervals); (C) lithium concentrations in Owens Lake sediment (Li and others 2000; lower lithium concentrations suggest wet intervals); (D) and (E) time series from the Peruvian Quelccaya ice core (Thompson

1992; dust from altiplano in ice shown in D, decadal ice accumulation in E as presented by deMenocal [2001]); (F) rise and fall of South American cultures (adapted from Thompson 1992); (G) Northwest Scotland mean annual rainfall (Baker and others 2000). The Quelccaya records (D) and (E) are anchored securely by the A.D. 1600 Huaynaputina eruption (Thompson 1992), with an estimated accuracy of ± 20 years at the A.D. 500 level (Shimada and others 1991). Records A, B, C, and F have typical radiocarbon dating uncertainty of no better than ± 50 years. Record G is based on counting of annual growth bands in a stalagmite without specified precision.

Between Floods of ~1029 and ~603. The period 699-823 had the highest drought frequency of the past 2000 years in the Sierra Nevada (Hughes and Brown 1992).

A.D. 603 \pm 35. Limited regional evidence from Mono Lake and the Sierra Nevada suggests wet conditions, or at least absence of drought (Table 1-4). Short-term volcanic-induced atmospheric cooling in the Northern Hemisphere is strongly supported by several studies for ~595-601 and for ~621-627. Cultural changes were observed in South America that were presumably linked to climatic changes (Thompson and others 1992). The limited evidence in Table 1-4 lets us speculate that the SBB flood deposit was deposited during the cold spell of ~595-601, possibly under El Niño conditions.

A.D. 440 \pm 40. This very thick SBB flood layer is varve-count-dated to a time-period when the Sierra Nevada was free of severe drought and the Pacific Ocean off Santa Barbara was entering the most unstable marine climatic interval of the Holocene (Table 1-5). Tree-ring evidence for a cold spell around 417-425 in the Sierra Nevada (Scuderi 1990) is not supported by a record from Colorado where no frost damage to tree-growth occurs from 393 until 470 (Brunstein 1996). Ample archeological and paleobotanical ^{14}C -dated evidence points towards dramatic climatic changes in South America and the Caribbean at around 450 (^{14}C -dated). The actual age of the SBB flood layer may be ca. 420 when a prominent cold spell occurred, possibly caused by the eruption of Mt. Etna 417-425.

Between Floods of ~440 and ~212. The period 236-377 was one of the three periods with the highest drought frequency of the past 2000 years in the Sierra Nevada (Hughes and Brown 1992).

A.D. 212 \pm 50. The relatively thin ~212 SBB flood layer was deposited at a time when the water level at Mono Lake was reportedly rising and the Sierra Nevada was not experiencing severe drought (Table 1-6). We speculate that either the eruption of Vesuvius ~202, or that of an unknown volcano ~176 (Scuderi 1990, 1993), was possibly instrumental for disturbing atmospheric circulation and steering heavy precipitation into southern California, although the Colorado tree-ring record (Brunstein 1996) offers no corroboration.

Table 1-4 Paleoclimatic evidence for 603 ± 35 yr. Notes as in Table 1-1.

| <i>Time period (yr AD)</i> | <i>Descriptions of paleoclimatic evidence; source of data</i> |
|--------------------------------|---|
| ~600 (^{14}C -dated) | Rising Mono Lake water level; Stine 1990, Fig. 2A. |
| 571-628 | No low-growth years in Sierra Nevada sequoia tree-ring record, California, suggesting absence of drought; Hughes and Brown 1992. |
| 622 | Strong Sierra Nevada tree-ring evidence for frost, presumably due to volcanic eruptions; Scuderi 1990. |
| 595, 601 | Tree-ring evidence for frost in California and Nevada; LaMarche and Hirschboeck 1984. |
| 626-627 | Notable frost-rings in Bristlecone Pines at Almagre Mountain, Colorado, likely due to volcanic eruption; Brunstein 1996. |
| ~600 (^{14}C -dated) | Glacially overrun trees, western Prince William Sound, Alaska; Wiles and others 1999. |
| 623 | Relatively high acidity in Greenland ice core; Hammer and others 1980. |
| 626 | Dry fog in Europe and Middle East, due to very large volcanic eruption; Stothers and Rampino, 1983; Stothers 1999. |
| ~600 (^{14}C -dated) | The largest adobe structure in the New World, the "Huaca del Sol" in the Moche capital in northern coastal Peru, was very abruptly abandoned, at the Moche IV-V transition. Regional drought had caused sand dunes to overrun irrigation channels (deMenocal, 2001; Shimada and others 1991). |
| ~600-620 | Drought in Peruvian altiplano regions causes dustiness on Quelccaya ice cap; dustiness peaks ~610, then drops abruptly; Thompson and others 1992, Fig. 2D. |
| ~600 | Severe drought ~562-594 recorded at Quelccaya ice cap (Shimada and others 1992) ends abruptly, followed by wet interval with maximum snow accumulation 610-620; Thompson and others 1992; Fig. 2E. |
| ~600 (^{14}C -dated) | End of drought on Yucatan; Hodell and others 1996; Curtis and others 1996. The drought centering ~580 coincides with a Maya building hiatus ~530-650 (deMenocal 2001). |
| ~600 (^{14}C -dated) | Cultural transition in South America; Shimada and others 1991; Thompson 1992; Thompson and others 1992; Fig. 2F. |

Table 1-5 Paleoclimatic evidence for 440 ± 40 yr. Notes as in Table 1-1.

| <i>Time period (yr AD)</i> | <i>Descriptions of paleoclimatic evidence; source of data</i> |
|--------------------------------------|--|
| 425-441 | No low-growth years in Sierra Nevada sequoia tree-ring record, California, suggesting absence of drought; Hughes and Brown 1992. |
| 425 | Sierra Nevada tree-ring evidence for frost damage, presumably due to volcanic eruption of Mt. Etna 417-425 (Scuderi 1990). The prominent low-growth signal occurs within good to excellent growth ~ 300 -500, where the period 408-427 has the second warmest 20-year mean value (Scuderi 1993). The 425 decreased ringwidth signal conflicts with Scuderi's (1993) report of 425 exhibiting the warmest mean late-season temperature in 1980-year long Sierra Nevada tree-ring record. |
| ~ 450 (^{14}C -dated) | Onset of the most unstable marine climatic interval of the Holocene, with coldest sea surface temperatures; Kennett and Kennett 2000. |
| 393-470 | No tree-ring evidence for frost damage at Almagre Mountain, Colorado; Brunstein 1996. |
| 417-425 | Mt. Etna eruption; Stothers and Rampino 1983. |
| 469-474 | Very large eruption of Vesuvius; Stothers and Rampino 1983. |
| ~ 350 (^{14}C -dated) | Peak of transgression in lakes on Yucatan peninsula and in central Mexico; Metcalfe and others 2000. |
| ~ 450 (^{14}C -dated) | Fragmentation of Amazonian rainforest due to drought (Meggers 1994), and cultural changes affecting precolumbian populations in the Caribbean (Meggers 1996), possibly in connection with "mega-El Niño" events. |

Climatic Implications for Transitions of Ancient Civilizations. Table 1 lists the evidence for ~ 1418 , ~ 1029 , ~ 603 , ~ 440 , and ~ 212 from studies advocating a climatic influence for the rise and fall of cultures in South America and the Caribbean. Thompson (1992) notes that coastal Ecuador and coastal Peru tend to be wet (for example, during El Niño events) when the highlands of southern Peru (including the Quelccaya ice cap; Figure 2D, 2E) and Bolivia experience drought. Consequently, coastal Peruvian cultures rise and fall in antiphase with highland (altiplano) cultures. The sketch of South American cultural successions (Figure 2F; adapted from Thompson 1992) indeed suggests a correlation between climatic and societal changes. These cultural responses to climate change, as well as corroborating evidence from other cultures, were reviewed by deMenocal (2001).

Table 1-6 Paleoclimatic evidence for 212 ± 50 yr. Notes as in Table 1-1.

| <i>Time period (yr AD)</i> | <i>Descriptions of paleoclimatic evidence; source of data</i> |
|------------------------------------|--|
| ~200 (^{14}C -dated) | Rising Mono Lake water level; Stine 1990, Fig. 2A. |
| 190-225 | No low-growth years in Sierra Nevada sequoia tree-ring record, California, suggesting absence of drought; Hughes and Brown 1992. |
| 176 | Sierra Nevada tree-ring evidence for very cold late-season temperature; 172-191 second coldest 20-year mean; Scuderi 1993. |
| 202 | Sierra Nevada tree-ring evidence for frost (Scuderi, 1990), probably due to large 202-203 volcanic eruption of Mt. Vesuvius (Stothers and Rampino 1983). |
| 230 | Several trees show frost-rings at Almagre Mountain, Colorado; Brunstein 1996. |
| 252 | Large eruption of Mt. Etna; Stothers and Rampino 1983. |
| ~125-210 (^{14}C -dated) | Sedimentological evidence (sulfur enrichment) for drought on Yucatan peninsula, consistent with pedological and archaeological evidence for a ^{14}C -dated drought in Guatemala, and coinciding with pervasive Preclassic Maya site abandonment; Hodell and others 2001. |
| ~220 | Second most negative reconstructed summer temperature excursion of the past millennium in southern Chile, based on tree-rings; Lara and Villalba 1993. |

The Sun as a Forcing Factor. A recent study by Hodell and others (2001) provides the strongest evidence yet for causal linkages between solar activity, large-scale changes in atmospheric circulation as expressed by the occurrence of droughts on the Yucatan peninsula, and societal changes in Maya cultures. Most SBB flood deposits seem to have occurred at times shortly following major droughts on the Yucatan peninsula. Yucatan droughts were reported to express a prominent ca. 208-year cycle, which in turn shows significant correlation with a ca. 208-year cycle of increased solar activity (shown via the atmospheric ^{14}C -budget, $\Delta^{14}\text{C}$ record; Figure 3; Hodell and others 2001). Although we do not subscribe to the view that SBB flood deposits are triggered via a fast-forcing mechanism in the wake of solar changes (van Geel and others 1999; with reply by Schimmelmann and others 1999), it now seems possible that fluctuations of solar activity at least prepare the stage for potential large-scale Southern California flooding every ca. 208 years. Flooding may occur when conditions are exacerbated by additional climatic factors like volcanic cooling and/or very strong El Niño events. In the past two millennia this SBB flood scenario skipped a beat only three times, and never skipped twice (Figure 3). If the past 2000 years of flood record have any forecasting value, our generation may have an opportunity to witness historically unprecedented flooding of Southern California.

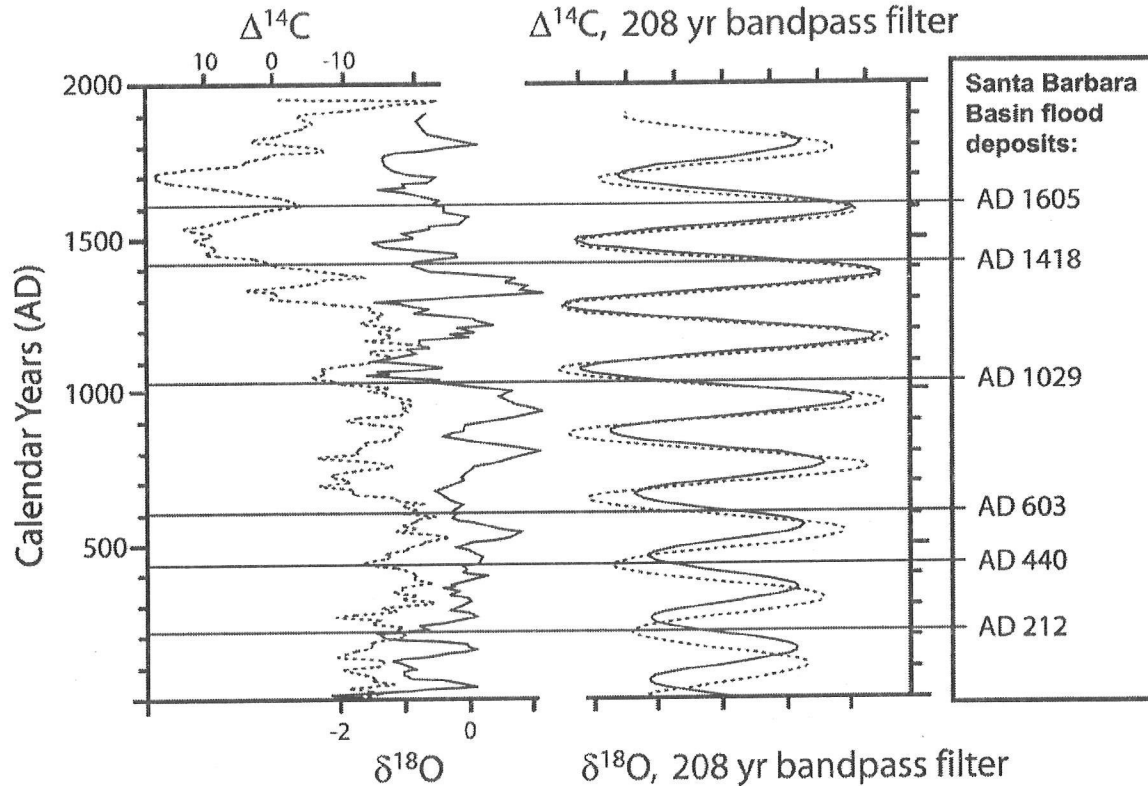


Figure 3 The global atmospheric $\Delta^{14}\text{C}$ record (dashed lines) and the $\delta^{18}\text{O}$ oxygen isotope record from Lake Punta Laguna (solid lines) from the Yucatan peninsula (adapted from Hodell and others 2001; an erroneous shift of plotted data by 50 years toward younger age in this published article was corrected). Both records exhibit strong ca. 208 year cyclicality that is displayed in the bandpass filter centered at 208 years. Santa Barbara Basin flood deposits (horizontal lines) occur in close proximity to peaks of $\delta^{18}\text{O}$, which coincide with drought conditions on Yucatan, and in most cases also with decreased $\Delta^{14}\text{C}$ associated with an increase in solar output (note the $\Delta^{14}\text{C}$ scales are inverted).

Conclusions

The six major flood deposits in the Santa Barbara Basin within the past two millennia are dated by varve-counting, characterized by their microscopic composition, and are interpreted via comparison with multidisciplinary paleoclimatic evidence:

- The ca. 1605 flood was caused primarily by short-term volcanic cooling that steered storm tracks southward of their usual landfall along the west coast of North America.
- The flood of ca. 1418 coincides with a global reorganization of atmospheric circulation at the onset of the Little Ice Age.
- While the evidence for a “cold storm” is overwhelming for ~1605, the more limited evidence for ~1029, ~603, ~440, and ~212 does not exclude the possibility of “warm storms.” The ~1029

flood occurred during the Medieval Climatic Anomaly when many regions on the Northern Hemisphere experienced warmth. However, a brief but intense cold spell ~1030, probably due to volcanism, seems to be superimposed on the Medieval Climatic Anomaly and may have triggered the SBB flood event.

- The floods of ~1418, ~1029, ~603, ~440, and ~212 are positioned at approximate times when archeological and paleobotanical evidence punctuates South American and Caribbean cultural and ecological transitions.
- The temporal spacing of Santa Barbara Basin flood deposits seem to correlate with a ca. 208-year cycle of solar activity and inferred changes in atmospheric circulation as suggested from a drought record on the Yucatan peninsula (Hodell and others 2001).
- Using the spacing of flood occurrence over the last 2000 years as a forecasting tool, we may expect the next window of opportunity for extreme flooding in Southern California for the early part of this century.

Acknowledgements

Funding was provided by National Science Foundation grants OCE 9807745 (to A.S.) and OCE 9815838 (to C.B.L.). We thank Brian Constantino for assistance with X-radiography, Colin Harvey for training in grain size analysis, and Maria Mastalerz for microscopic interpretation of plant debris. Gregg Garfin provided insight about the interpretation of tree-ring evidence.

References

- Baker A, Proctor C, Lauritzen S-E, Lundberg J. 2000. SPEP: high-resolution stalagmite records of NE Atlantic climate in the last millennium. *PAGES Newsletter* 8 (2000-2):14.
- Barriendos VM, Martin-Vide J. 1998. Secular climatic oscillations as indicated by catastrophic floods in the Spanish Mediterranean coastal area (14th–19th centuries). *Climatic Change* 38:473–91.
- Beer J, Mende W, Stellmacher R. 2000. The role of the sun in climate forcing. *Quat Sci Rev* 19:403–15.
- Biondi F, Perkins DL, Cayan DR, Hughes MK. 1999. July temperature during the second millennium reconstructed from Idaho tree rings. *Geophys Res Lett* 26:1445–8.
- Bradley RS. 2000. Climate paradigms for the last millennium. *PAGES: Past Global Changes* 8 (March):2-3.
- Bradley RS, Briffa KR, Crowley TJ, Hughes MK, Jones PD, Mann ME. 2001. The scope of medieval warming. *Science* 292:2011–2.
- Briffa KR. 2000. Annual climate variability in the Holocene: interpreting the message of ancient trees. *Quat Sci Rev* 19:87–105.
- Briffa KR, Jones PD, Vogel RB, Schweingruber FH, Baillie MGL, Shiyatov SG, Vaganov EA. 1999. European tree rings and climate in the 16th century. *Climatic Change* 43:151–68.

- Broecker WS. 2000. Abrupt climate change: causal constraints provided by the paleoclimate record. *Earth-Science Rev* 51:137–54.
- Brunstein FC. 1996. Climatic significance of the Bristlecone Pine latewood frost-ring record at Almagre Mountain, Colorado, U.S.A. *Arctic and Alpine Research* 28:65–76.
- Camuffo D, Secco C, Brimblecombe P, Martin-Vide J. 2000. Sea storms in the Adriatic Sea and the Western Mediterranean during the last millennium. *Climatic Change* 46:209–23.
- Chepstow-Lusty AJ, Bennett KD, Switsur VR, Kendall A. 1996. 4000 years of human impact and vegetation change in the central Peruvian Andes—with events paralleling the Maya record? *Antiquity* 70:824–33.
- Curtis JH, Hodell DA, Brenner M. 1996. Climate variability on the Yucatan Peninsula (Mexico) during the past 3500 years, and implications for Maya cultural evolution. *Quat Res* 46:37–47.
- Dahl-Jensen D, Mosegaard K, Gundestrup N, Clow GD, Johnsen SJ, Hansen AW, Balling N. 1998. Past temperatures directly from the Greenland ice sheet. *Science* 282:268–71.
- D'Arrigo RD, Cook ER, Salinger MJ, Palmer J, Krusic PJ, Buckley BM, Villalba R. 1998. Tree-ring records from New Zealand: long-term context for recent warming trend. *Climate Dynamics* 14:191–9.
- D'Arrigo R, Jacoby G, Frank D, Pederson N, Cook E, Buckley B, Nachin B, Mijiddorj R, Dugarjav C. 2001. 1738 years of Mongolian temperature variability inferred from a tree-ring width chronology of Siberian pine. *Geophys Res Lett* 28:543–6.
- Delmas RJ, Kirchner S, Palais JM, Petit J-R. 1992. 1000 years of explosive volcanism recorded at the South Pole. *Tellus* 44B:335–50.
- deMenocal PB. 2001. Cultural responses to climate change during the Late Holocene. *Science* 292:667–73.
- Eltahir EAB, Wang G. 1999. Nilometers, El Niño, and climate variability. *Geophys Res Lett* 26:489–92.
- Ely LL, Enzel Y, Baker VR, Cayan DR. 1993. A 5000-year record of extreme floods and climate change in the southwestern United States. *Science* 262:410–2.
- Field DB, Baumgartner TR. 2000. A 900 year stable isotope record of interdecadal and centennial change from the California Current. *Paleoceanography* 15:695–708.
- Fisher DA, Koerner RM, Reeh N. 1995. Holocene climatic records from Agassiz ice cap, Ellesmere Island, NWT, Canada. *The Holocene* 5:19–24.
- Fritz SC, Ito E, Yu Z, Laird KR, Engstrom DR. 2000. Hydrologic variation in the northern Great Plains during the last two millennia. *Quat Res* 53:175–84.
- Geirsdóttir Á, Hardardóttir J, Andrews JT. 2000. Late-Holocene terrestrial glacial history of Miki and I.C. Jacobsen Fjords, East Greenland. *The Holocene* 10:123–34.
- Gervais BR, MacDonald GM. 2001. Tree-ring and summer-temperature response to volcanic aerosol forcing at the northern tree-line, Kola Peninsula, Russia. *The Holocene* 11:499–505.

- Glaser R. 1995. Thermische Klimaentwicklung in Mitteleuropa seit dem Jahr 1000. *Geowissenschaften* 13: 302-312.
- Goman M, Wells L. 2000. Trends in river flow affecting the northeastern reach of the San Francisco Bay estuary over the past 7000 years. *Quat Res* 54:206-17.
- Graumlich LJ. 1993. A 1000-year-record of temperature and precipitation in the Sierra Nevada. *Quat Res* 39:249-55.
- Grove JM. 2001. The initiation of the "Little Ice Age" in regions round the North Atlantic. *Climatic Change* 48:53-82.
- Haston L, Michaelsen J. 1994. Long-term central coastal California precipitation variability and relationships to El Niño-Southern Oscillation. *Journal of Climate* 7: 1373-1387.
- Hammer CU, Clausen HB, Dansgaard W. 1980. Greenland ice sheet evidence of post-glacial volcanism and its climatic impact. *Nature* 288:230-5.
- Hodell DA, Benner M, Curtis JH, Guilderson T. 2001. Solar forcing of drought frequency in the Maya lowlands. *Science* 292:1367-70.
- Holmgren K, Karlén W, Lauritzen SE, Lee-Thorp JA, Partridge TC, Piketh S, Repinski P, Stevenson C, Svannered O, Tyson PD. 1999. A 3000-year high-resolution stalagmite-based record of palaeoclimate for northeastern South Africa. *The Holocene* 9:295-309.
- Hong YT, Jiang HB, Liu TS, Zhou LP, Beer J, Li HD, Leng XT, Hong B, Qin XG. 2000. Response of climate to solar forcing recorded in a 6000-year $\delta^{18}\text{O}$ time-series of Chinese peat cellulose. *The Holocene* 10:1-7.
- Hughes MK, Brown PM. 1992. Drought frequency in central California since 101 B.C. recorded in giant sequoia tree rings. *Climate Dynamics* 6:161-7.
- Ingram BL, Ingle JC, Conrad ME. 1996. Stable isotope record of late Holocene salinity and river discharge in San Francisco Bay, California. *Earth Planet Sci Lett* 141:237-47.
- Jansen E, Koç N. 2000. Century to decadal scale records of Norwegian Sea surface temperature variations of the past 2 Millennia. *PAGES, Past Global Changes* 8 (March):13-14.
- Jones PD, Briffa KR, Barnett TP, Tett SFB. 1998. High-resolution paleoclimatic records for the last millennium: interpretation, integration, and comparison with general circulation model control-run temperatures. *Holocene* 8:455-71.
- Kalela-Brundin M. 1999. Climatic information from tree-rings of *Pinus sylvestris* L. and a reconstruction of summer temperatures back to A.D. 1500 in Femundsmarka, eastern Norway, using partial least squares regression (PLS) analysis. *The Holocene* 9:59-77.
- Kennett DJ, Kennett JP. 2000. Competitive and cooperative responses to climatic instability in coastal Southern California. *American Antiquity* 65:379-95.

- Knox JC. 1993. Large increases in flood magnitude in response to modest changes in climate. *Nature* 361: 430-432.
- Kreutz KJ, Mayewski PA, Meeker LD, Twickler MS, Whitlow SI, Pittalwala II. 1997. Bipolar changes in atmospheric circulation during the Little Ice Age. *Science* 277:1294-6.
- LaMarche VC, Hirschboeck KK. 1984. Frost rings in trees as records of major volcanic eruptions. *Nature* 307:121-6.
- Lamb HH. 1982. *Climate, history and the modern world*. London: Methuen. 387 p.
- Lara A, Villalba R. 1993. A 3620-year temperature record from *Fitzroya cupressoides* tree rings in southern South America. *Science* 260:1104-6.
- Lean J. 2000. Evolution of the sun's spectral irradiance since the Maunder Minimum. *Geophys Res Lett* 27:2425-8.
- Li H-C. 1995. *Isotope Geochemistry of Mono Lake, California: applications to paleoclimate and paleohydrology* [PhD dissertation]. Available from University of Southern California, Los Angeles. 244 p.
- Li H-C, Bischoff JL, Ku T-L, Lund SP, Stott LD. 2000. Climate variability in east-central California during the past 1000 years reflected by high-resolution geochemical and isotopic records from Owens Lake sediments. *Quat Res* 54:189-97.
- Luckman BH. 1997. Developing a proxy climate record for the last 300 years in the Canadian Rockies—some problems and opportunities. *Climatic Change* 36:455-76.
- Luckman BH, Briffa KR, Jones PD, Schweingruber FH. 1997. Tree-ring based reconstruction of summer temperatures at the Columbia Icefield, Alberta, Canada, A.D. 1073-1983. *The Holocene* 7:375-89.
- Meggers BJ. 1994. Archeological evidence for the impact of mega-Niño events on Amazonia during the past two millennia. *Climatic Change* 28:321-38.
- Meggers BJ. 1996. Possible impact of the mega-Niño events on Precolumbian populations in the Caribbean area. In: Maggiolo MV, Fuentes AC, editors. *Ponencias. Primer Seminario de Arqueología del Caribe*. Museo Arqueológico Regional Altos de Chavon, Organización de Los Estados Americanos. p 156-176.
- Metcalf SE, O'Hara SL, Caballero M, Davies SJ. 2000. Records of late Pleistocene—Holocene climatic change in Mexico—a review. *Quat Sci Rev* 19:699-721.
- Moore JJ, Hughen KA, Miller GH, Overpeck JT. 2001. Little Ice Age recorded in summer temperature reconstruction from varved sediments of Donard Lake, Baffin Island, Canada. *J Paleolim* 25:503-17.
- Morgan V, van Ommen TD. 1997. Seasonality in late-Holocene climate from ice-core records. *The Holocene* 7:351-4.
- Ortloff CR, Kolata AL. 1993. Climate and collapse: agro-ecological perspectives on the decline of the Tiwanaku State. *J Archaeol Sci* 20:195-221.

2001 FACLIM Conference Proceedings

- Pfister C, Luterbacher J, Schwarz-Zanetti G, Wegmann M. 1998. Winter air temperature variations in western Europe during the early and high Middle Ages (A.D. 750-1300). *The Holocene* 8:535-52.
- Quinn WH. 1999. Climate variation in southern California over the past 2,000 years based on the El Niño/southern oscillation. In: Rose MR, Wigand PE, editors. *Proceedings of the Southern California Climate Symposium: trends and extremes of the past 2000 years*; 25 Oct 1991. Natural History Museum of Los Angeles County Technical Report nr. 11. p 213-238.
- Sadler JP, Grattan JP. 1999. Volcanoes as agents of past environmental change. *Global and Planetary Change* 21:181-96.
- Schimmelmann A, Zhao M, Harvey CC, Lange CB. 1998. A large California flood and correlative global climatic events 400 years ago. *Quat Res* 49:51-61.
- Schimmelmann A, Zhao M, Harvey CC, Lange CB. 1999. Reply to Van Geel et al.'s comment on "A large California flood and correlative global climatic events 400 years ago." *Quat Res* 51:111-2.
- Scuderi LA. 1987. Glacier variations in the Sierra Nevada, California, as related to a 1200-year tree-ring chronology. *Quat Res* 27:220-31.
- Scuderi LA. 1990. Tree-ring evidence for climatically effective volcanic eruptions. *Quat Res* 34:67-85.
- Scuderi LA. 1993. A 2000-year tree ring record of annual temperatures in the Sierra Nevada mountains. *Science* 259:1433-6.
- Shimada I, Schaaf CB, Thompson LG, Mosley-Thompson E. 1991. Cultural impacts of severe droughts in the prehistoric Andes: application of a 1,500-year ice core precipitation record. *World Archaeology* 22:247-70.
- Stahle DW, Cleaveland MK, Blanton DB, Therrell MD, Gay DA. 1998. The Lost Colony and Jamestown droughts. *Science* 280:564-7.
- Stine S. 1990. Late Holocene fluctuations of Mono Lake, eastern California. *Palaeogeography, Palaeoclimatology, Palaeoecology* 78:333-81.
- Stine S. 1994. Extreme and persistent drought in California and Patagonia during mediaeval time. *Nature* 369:546-9.
- Stothers RB. 1999. Volcanic dry fogs, climate cooling, and plague pandemics in Europe and the Middle East. *Climatic Change* 42:713-23.
- Stothers RB, Rampino MR. 1983. Volcanic eruptions from the Mediterranean before A.D. 630 from written and archaeological sources. *J Geophys Res* 88 (B8):6357-71.
- Sullivan DG. 1982. Prehistoric flooding in the Sacramento Valley: Stratigraphic Evidence from Little Packer Lake, Glenn County, California [MA thesis]. Available from University of California, Berkeley.
- Tarhule A, Woo MK. 1997. Towards an interpretation of historical droughts in Northern Nigeria. *Climatic Change* 37:601-16.

- Thompson LG. 1992. Ice core evidence from Peru and China. In: Bradley RS, Jones PD, editors. *Climate since A.D. 1500*. London: Routledge. p 517–48.
- Thompson LG, Mosley-Thompson E, Thompson PA. 1992. Reconstructing interannual climate variability from tropical and subtropical ice-core records. In: Diaz HF, Markgraf V, editors. *El Niño. Historical and paleoclimatic aspects of the Southern Oscillation*. Cambridge University Press. p 296–322.
- Thompson LG, Davis ME, Mosley-Thompson E. 1994. Glacial records of global climate: A 1500-year tropical ice core record of climate. *Human Ecology* 22:83–95.
- van Geel B, van der Plicht J, Renssen H. 1999. Comment on “A large California flood and correlative global climatic events 400 years ago” (Schimmelmans and others 1998). *Quat Res* 51:108–10.
- Villalba R. 1990. Climatic fluctuations in Northern Patagonia during the last 1000 years as inferred from tree-ring records. *Quat Res* 34:346–60.
- Wang L, Sarnthein M, Erlenkeuser H, Grootes PM, Grimalt JO, Pelejero C, Linck G. 1999. Holocene variations in Asian monsoon moisture: a bidecadal sediment record from the South China Sea. *Geophys Res Lett* 26:2889–92.
- Wang L, Payette S, Bégin Y. 2001. 1300-year tree-ring width and density series based on living, dead and sub-fossil black spruce at tree-line in Subarctic Québec, Canada. *The Holocene* 11:333–41.
- Wang N, Yao T, Thompson LG. 2000. Nitrate concentration in the Guliya ice core and solar activity. *PAGES, Past Global Changes* 8 (June):11.
- Wells LE. 1990. Holocene history of the El Niño phenomenon as recorded in flood sediments of northern coastal Peru. *Geology* 18:1134–7.
- Wiles GC, D'Arrigo RD, Jacoby GC. 1998. Gulf of Alaska atmosphere-ocean variability over recent centuries inferred from coastal tree-ring cores. *Climatic Change* 38:289–306.
- Wiles GC, Barclay DJ, Calkin PE. 1999. Tree-ring-dated “Little Ice Age” histories of maritime glaciers from western Prince William Sound, Alaska. *The Holocene* 9:163–73.
- Zheng J, Kudo A, Fisher DA, Blake EW, Gerasimoff M. 1998. Solid electrical conductivity (ECM) from four Agassiz ice cores, Ellesmere Island NWT, Canada: high-resolution signal and noise over the last millennium and low resolution over the Holocene. *The Holocene* 8:413–21.
- Zielinski GA. 2000. Use of paleo-records in determining variability within the volcanism-climate system. *Quat Sci Rev* 19:417–38.

The New Regimes: Fish Stories

Gary D. Sharp, James D. Goodridge, Leonid B. Klyashtorin, and Alexey V. Nikolaev

Natural Climate Variability

Our crusade is to have people stand back and look around themselves several times, slowly, as they try to attribute cause and effect in fisheries and societally relevant debates such as the recently emergent global warming topic. We have chosen to discuss three layers of such interpretations, each of which has benefited from “stepping back,” and re-examining possible linkages. First is a re-examination of the temperature trend data collected since 1947 in California, and arrayed by county size. The second is the definition of a “regime shift,” based on short-term measurements, compared to “smoothed” climate indices, and the third is the all important suggestion that some of the larger climate indices might be useful in fisheries management and agriculture “planning” in North America, if not over the globe.

Another Look at Natural Climate Variability in California

Goodridge (1996) published a graph suggesting that air temperature trends in California were related to the population sizes of the counties where the measurements were made (Figure 1). Missing from that study was the fact that our largest cities are generally close to the Pacific Ocean (Figure 2). The ocean has a great influence on air temperature. Urban heat islands are easily misjudged in a maritime setting. Urban and rural temperature differences however have been well known at least since 1812 when Luke Howard reported that the urban center of London was several degrees warmer than in the country. We still need to document urban island effects and separate urban and marine influences on weather trends.

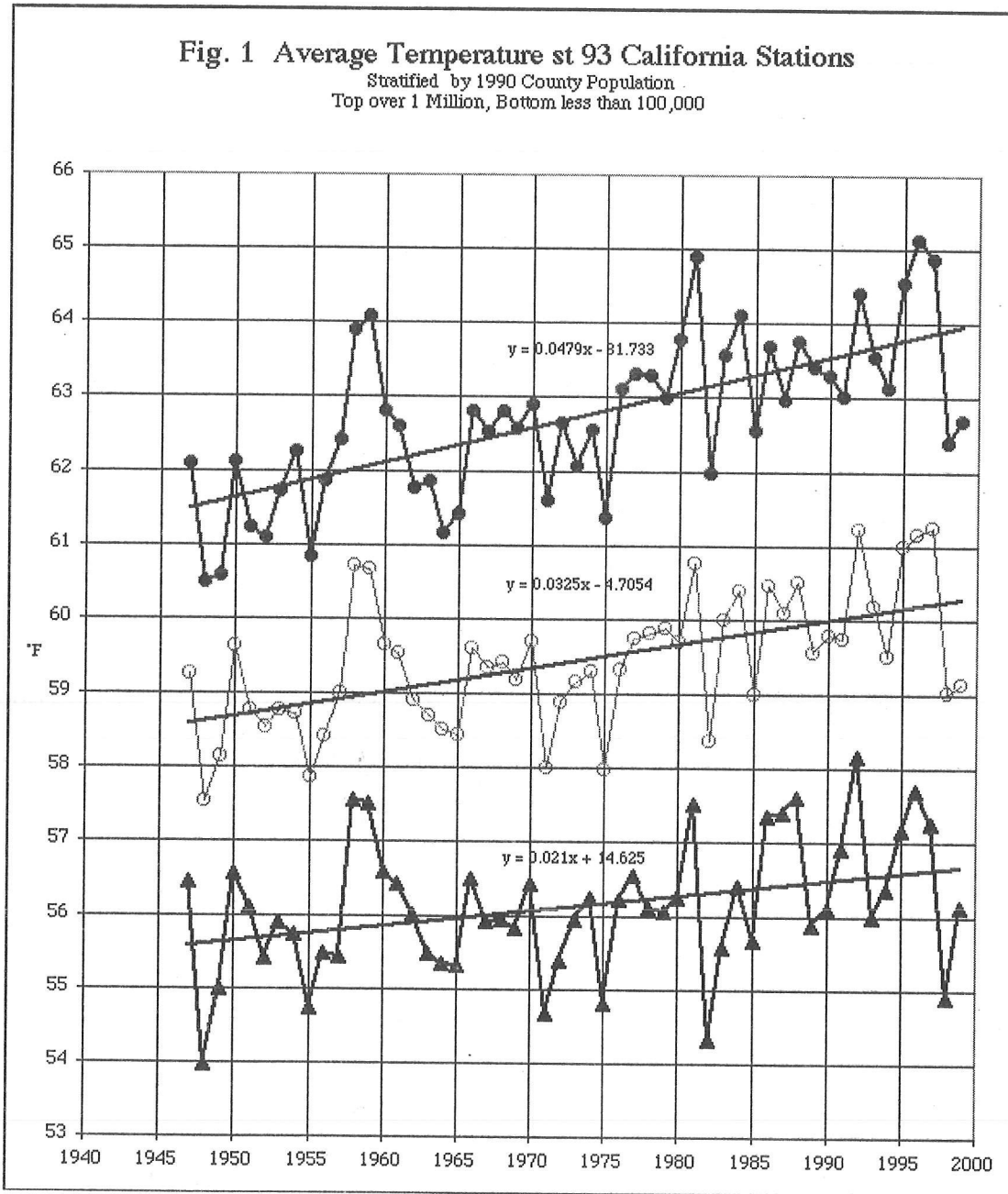


Figure 1 Average temperature st 93 California stations. Stratified by 1990 county population. Top over 1 million, bottom less than 100,000.

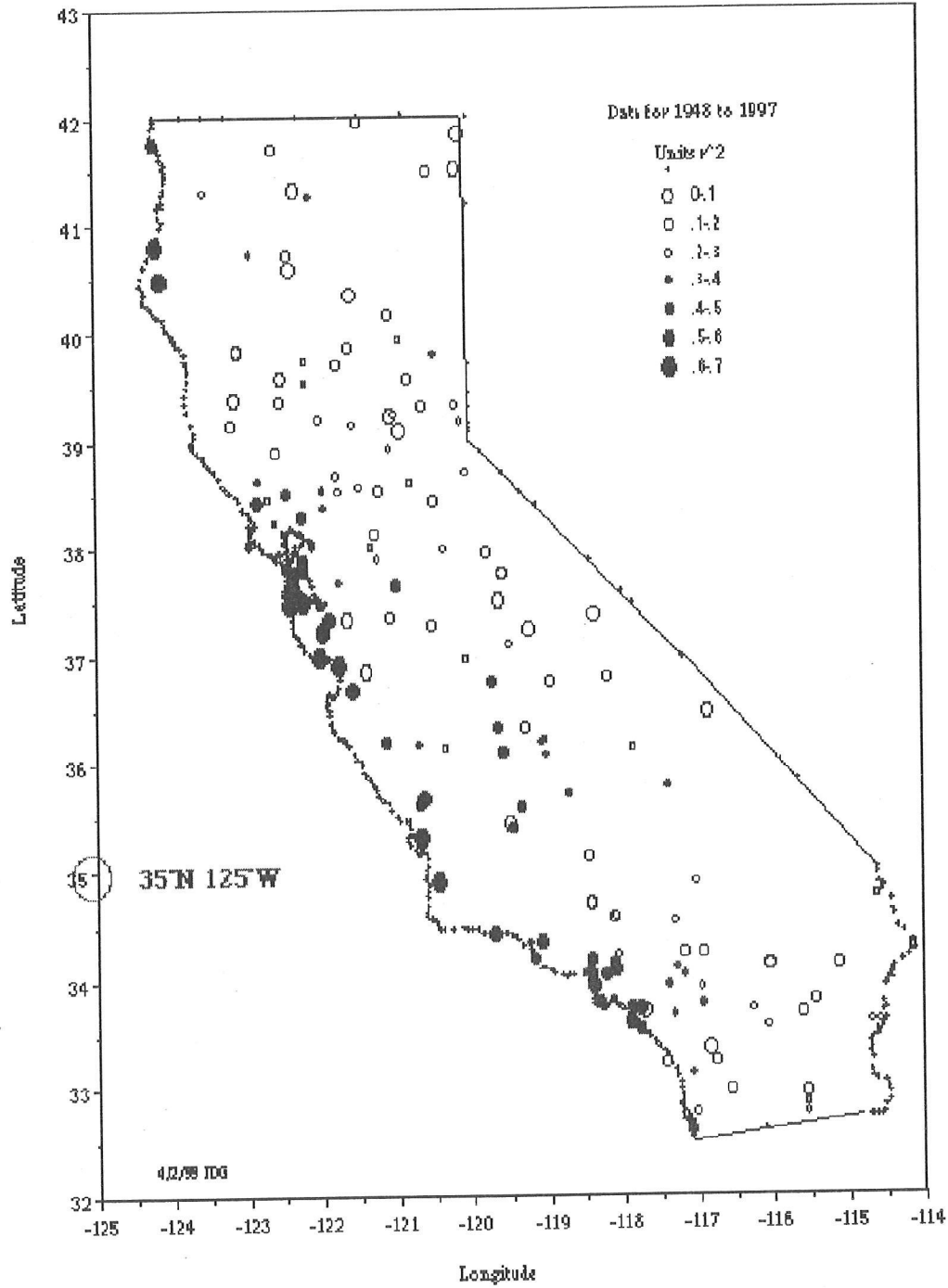


Figure 2 The ocean location at 35°N, 125°W was used as the reference point for an index of the regional ocean temperature, against which to reference the California temperature monitoring sites in a further examination of the basis for the state's recent sharp drop in measured temperatures at most coastal sites

Trends in air temperature at 68 California weather stations for 1947 to 1999 are compared with trends in the East-West differences in sea surface temperature for the 1947 to 2000 period. There are important similarities as can be seen in the relevant graphs described below. These similarities further verify the strong relationship with air temperature in California and sea surface temperature. These trends are also reflected in upwelling records in the Northeast Pacific Ocean.

Average monthly sea surface temperature records for the Pacific Ocean north of latitude 20° North for the years 1947 to 2000 were obtained from the Scripps Institution of Oceanography Web site. The 157 five-degree grid points were divided into eastern and western halves at the longitude 180°. The records were converted to departure from average for each half of the Ocean. The differences in the departures were plotted as accumulated departure from average on Figure 3. Notable features of this graph are the reversals in trend in 1975 and 1997.

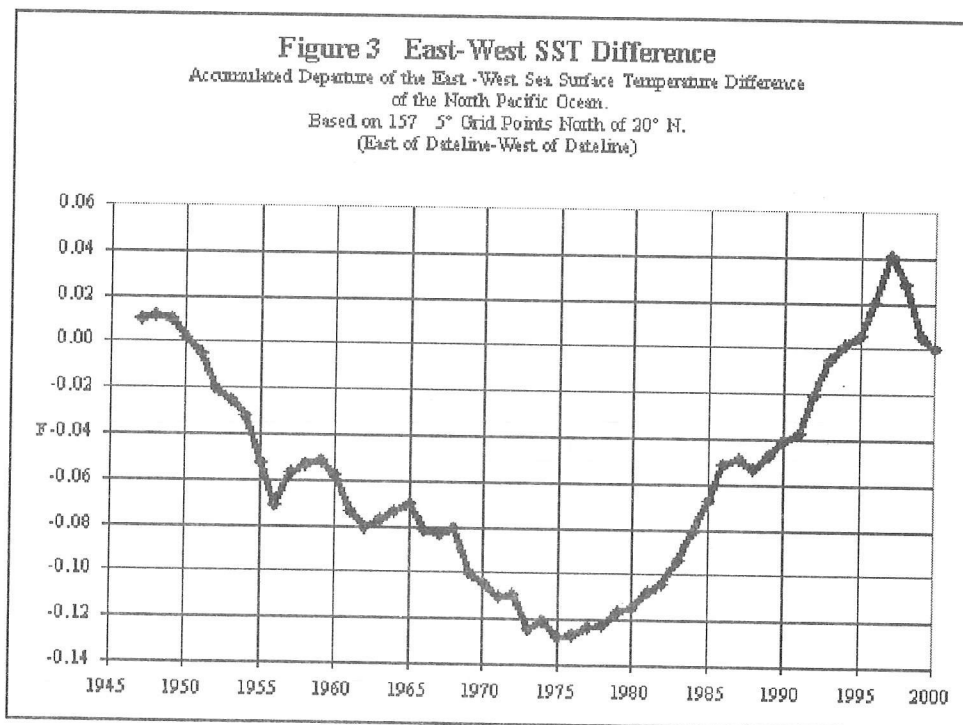


Figure 3 Yearly trends in sea surface temperature as departure from average are plotted for the East and West regions of the North Pacific Ocean.

California air temperature records from coastal areas are highly correlated with sea surface temperatures from the adjacent ocean. Ocean surface temperatures off California show a near-general north-south coherence between the 5° grid points. It was concluded that cool sea surface temperatures reflect regions of cold water upwelling.

This graph shows relatively lower temperatures in the Asia (West) Pacific during 1975 to 1997 and higher temperature on the North American (East) Pacific. This corresponds to the above average temperatures and increased rainfall variability for California for 1975 to 1997. In 1998 the trend was

reversed. California's mean sea levels decreased and upwelling resumed the pre -1975 values; California's air temperatures have decreased.

Air temperature records for California are published monthly in Climatological Data by the National Climatic Data Center. Sixty-eight of these records that were continuous for years 1947 to 1999 were averaged. The average was expressed as departures from average and plotted as Figure 3. Again, notable features of this graph are the reversals in trend in 1975 and 1997 as in Figure 4.

The temperature trend plotted on Figure 4 is consistent with the upwelling index calculated by the NOAA Fisheries Group in Monterey for 39°N, 125°W (70 miles west of Point Arena) shown below in Figure 6. The basic pattern of decreasing upwelling for the 1975 to 1997 years are illustrated as are the recent increase after 1998.

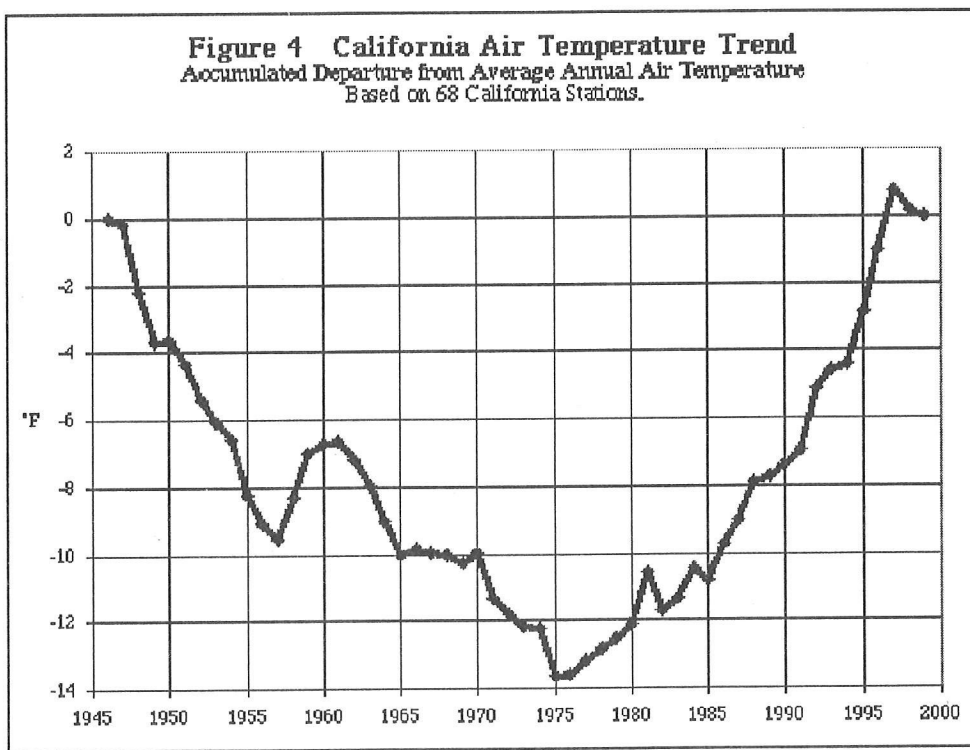


Figure 4 California air temperature trend. Accumulated departure from average annual air temperature based on 68 California stations.

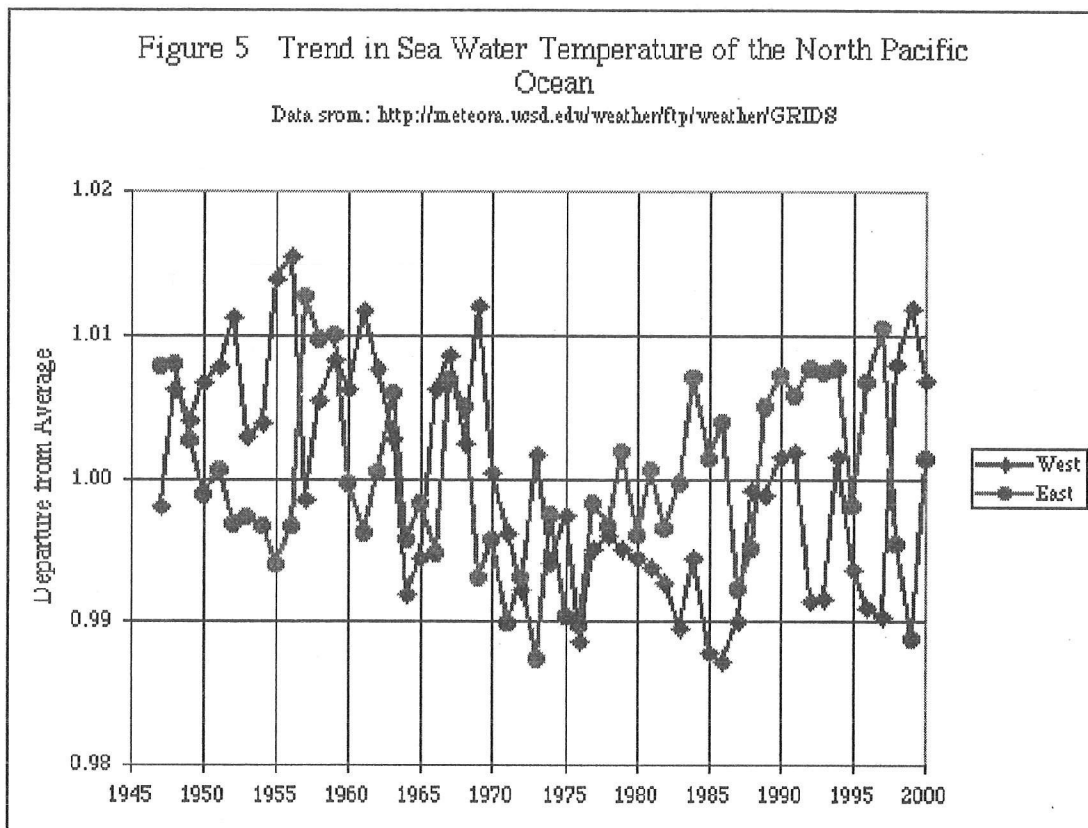


Figure 5 Trend in sea wter temperature of the North Pacific Ocean.

Source: <http://meteora.uscd.edu/weather/ftp/weather/GRIDS>.

Figure 5 is a graphic of the trends in ocean temperature (departure from the means) for the west and east North Pacific, showing their inverse relationship.

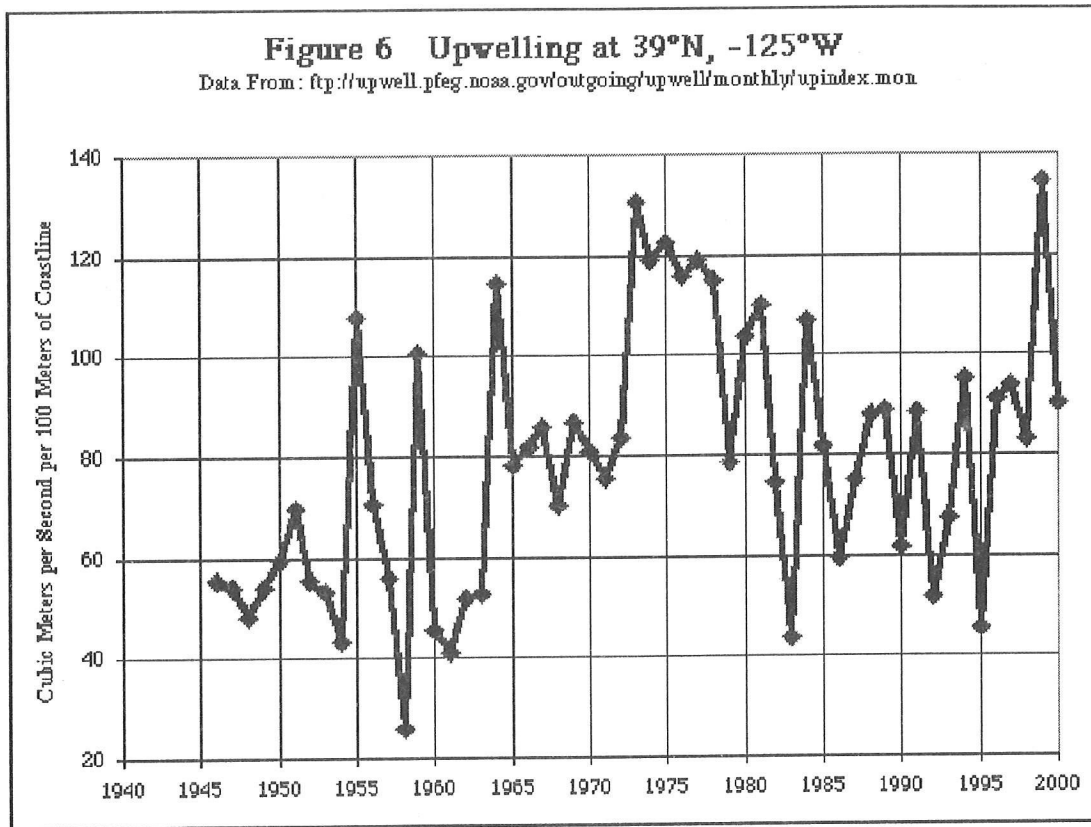


Figure 6 Upwelling at 39°N 125°W.

Source: <ftp://upwell.pfeg.noaa.gov/outgoing/upwell/monthly/upindex.mon>

High sea surface levels and low upwelling signify warmer ocean and air temperatures for coastal California. High sea surface suppresses upwelling and is associated with increased air temperature. The oceans are in a delicate hydrostatic balance responding easily to winds. It would be desirable to have wind records to compare with tide trends, upwelling, sea surface temperature, and rainfall trends. A San Francisco–Tokyo barometric pressure difference was examined as a proxy for an index of global wind circulation. A five-year running average was used to smooth the record as shown in Figure 7. Again, the trend reversal of the mid-1970s is evident.

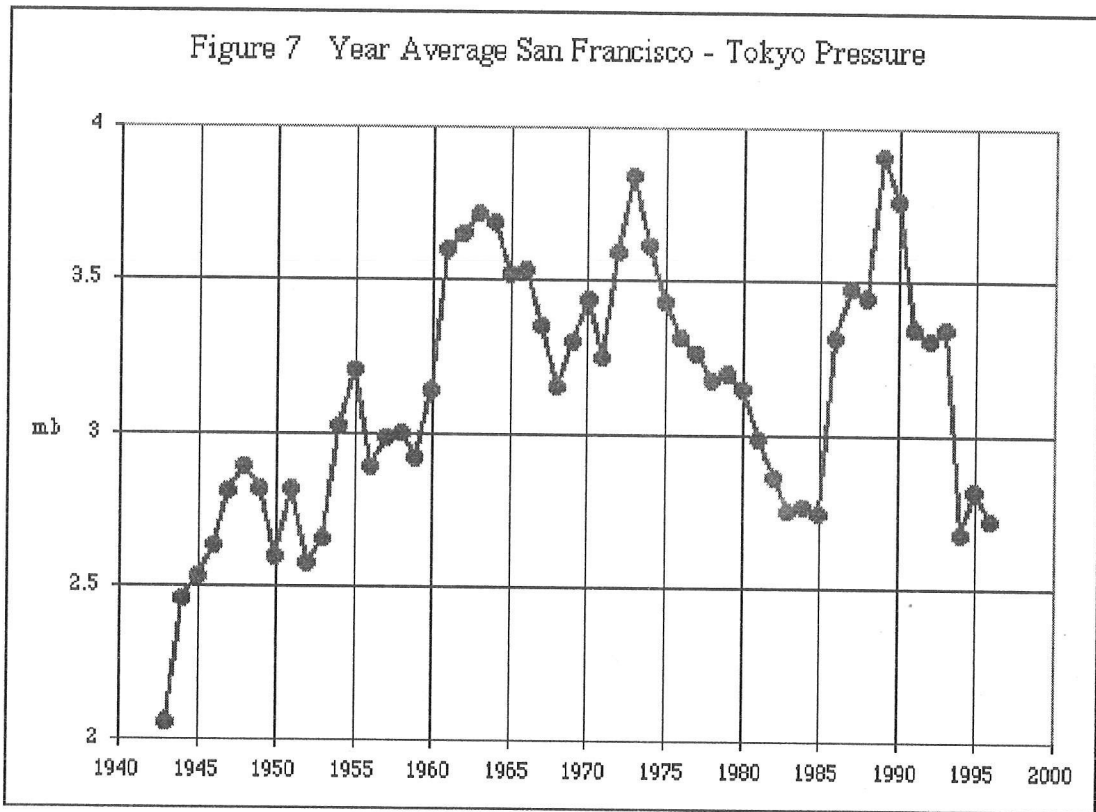


Figure 7 Year average San Francisco-Tokyo pressure

The Length-of-Day variation record (LOD) from the Naval Observatory was tested as an indicator of variation in atmospheric circulation as shown on Figure 8. The trend reversal of the mid-1970s was again evident.

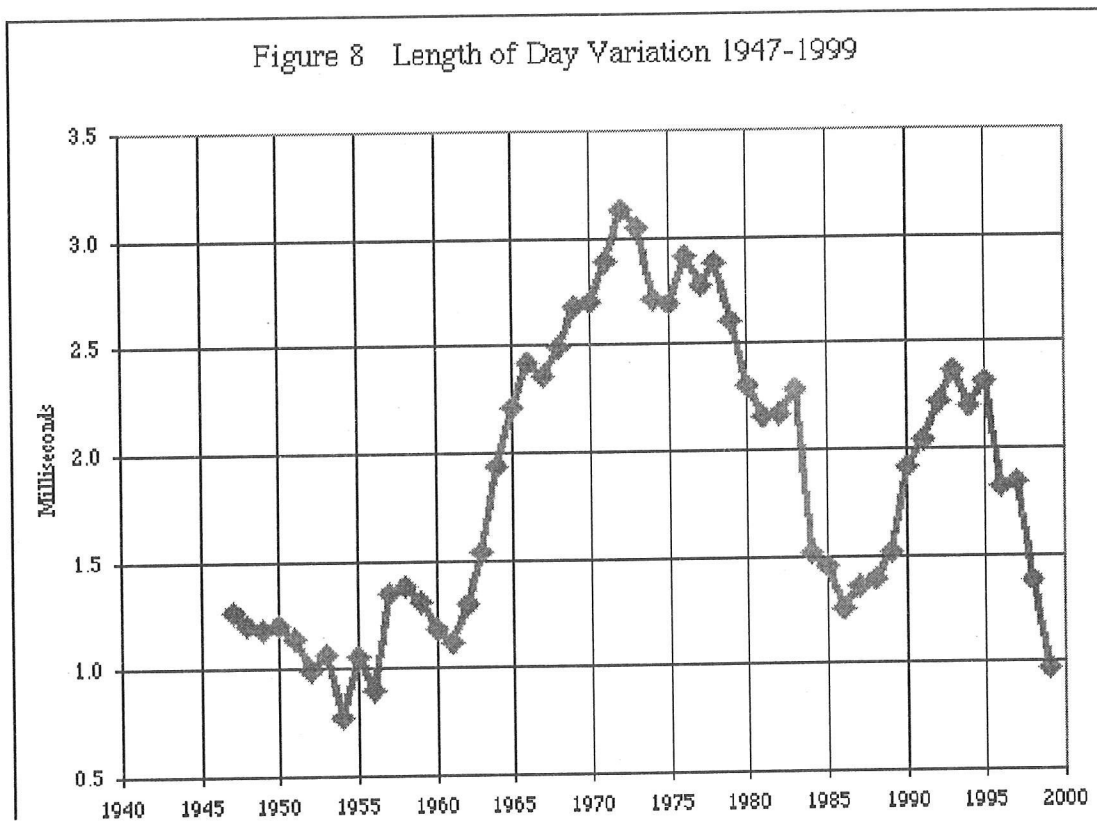


Figure 8 Length of day variation, 1947-1999

This LOD graph shares some resemblance to the graph of the accumulated departure from average rainfall in California in Figure 9.

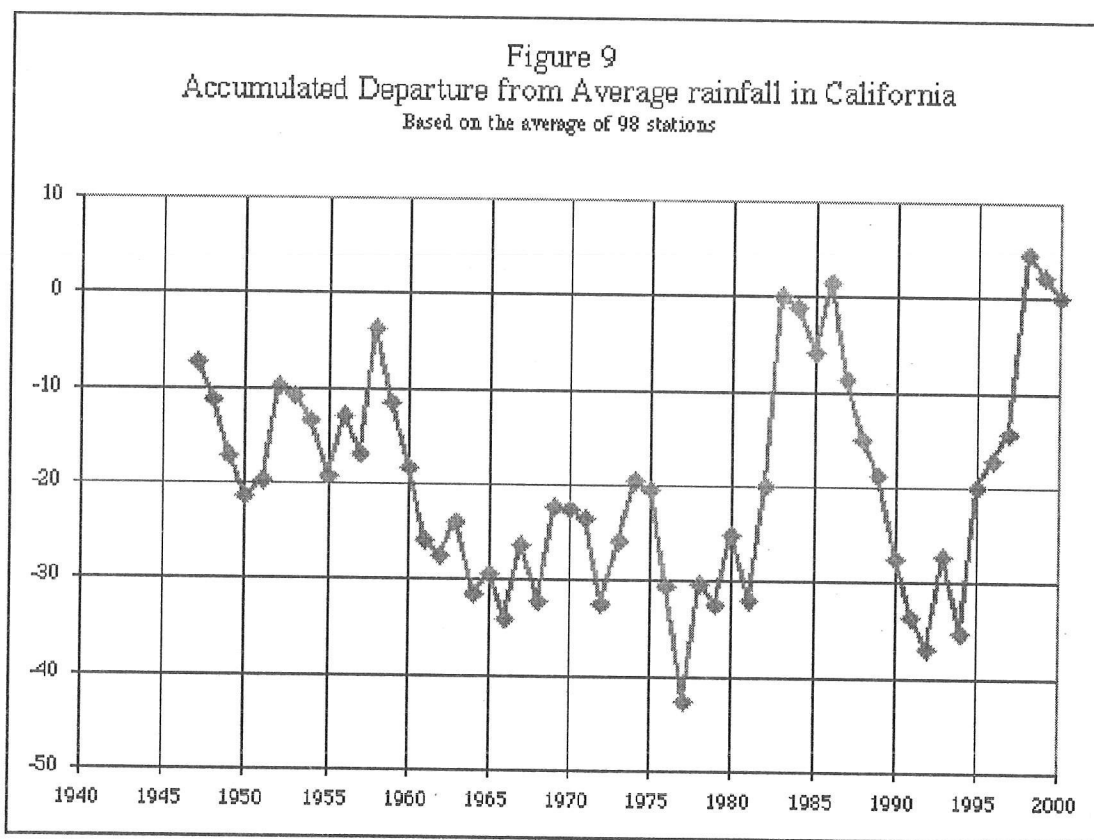


Figure 9 Accumulated departure from average rainfall in California based on the average of 98 stations

The variation in rainfall during the 1947 to 2000 period of sea surface temperature records was evaluated using a 9-year running ratio of the standard deviation over the average as shown in Figure 10.

Correlation coefficients of rainfall totals from adjacent years is near zero suggesting that inter-yearly rain totals are nearly random events, yet there are prolonged periods of persistent wet or dry and cold or warm years as shown on Figures 1, 4 and 9.

If 1975 to 1998 trends in sea surface temperature, air temperature, and rainfall variation are at a high value in 1998, then California may be in for a prolonged dry cooling spell as in the Dust Bowl Days of the 1930s. It is also notable that there are major changes in the climate regimes of much of the northern hemisphere.

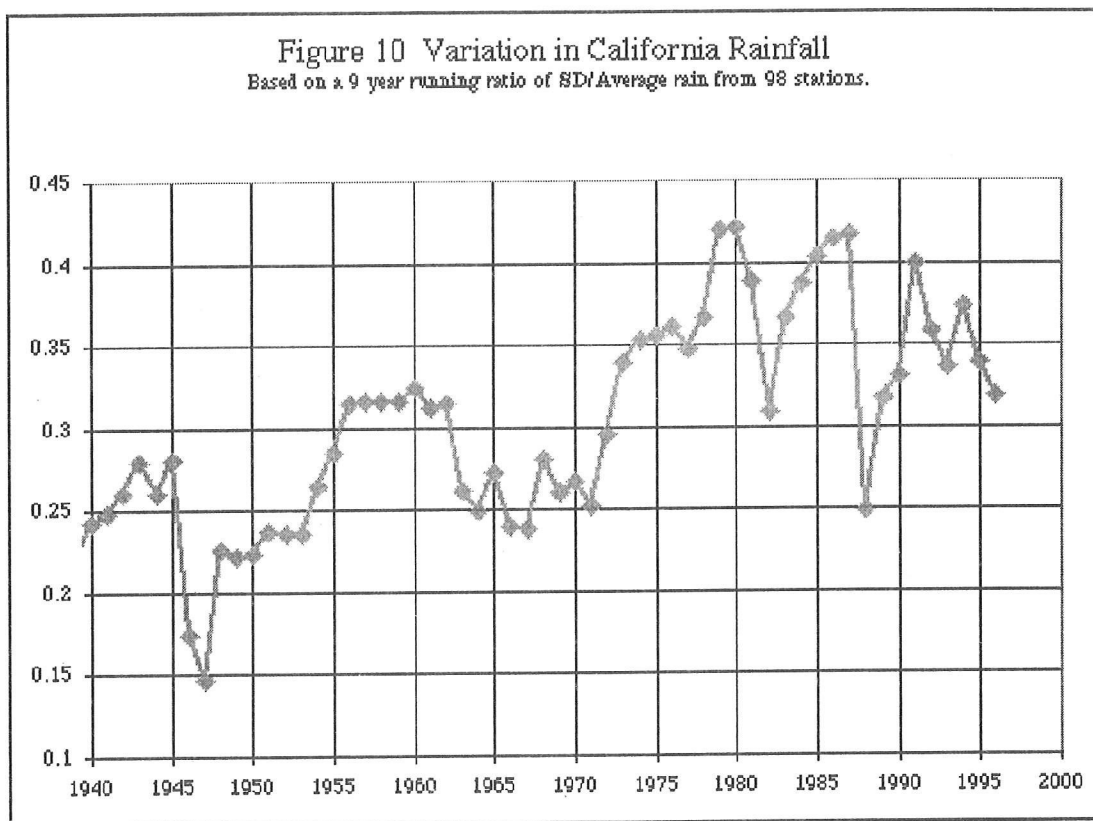


Figure 10 Variation in California rainfall. Based on a 9-year running ratio of SD' average rain from 98 stations.

Long-Term Fluctuations of the Earth Rotation Velocity and Some Global Climatic Indices

Our planet as a whole conserves its angular momentum except for the known effects of external torques associated with the lunar-solar tide, which induces a gradual decelerating of the earth's rotation velocity at a rate corresponding to increase in the astronomic length of day by about 1.4 millisecond per century (Munk and McDonald 1960). The full time series of LOD cover more than 350 years, with the most reliable data obtained in the last 150 years (Stephenson and Morrison 1995). It was noticed a while ago that this age-old trend in earth deceleration is accompanied with large-scale, multi-decadal irregularities in the earth rotation velocity.

Halpert and Bell (1997) and Song and Richards (1996) found that the multidecadal LOD fluctuations are in close correlation with the basic global climatic index, air-surface global temperature anomaly (dT). The causes of the multi-decadal fluctuations of LOD are not completely clear yet. It was shown that the sea level variation, continent drift, melting down of the Antarctic ice sheet, and variations in the ocean's largest Antarctic circumpolar current cannot induce significant changes to LOD (Munk and McDonald 1960; Hide and Dickey 1991). There are grounds to assume that motions in the

earth's liquid core (Hide and Dickey 1991) can excite the multi-decadal variations of negative LOD ($-$ LOD). For the recent quarter of century, however, the concepts of the structure and dynamics of the inner earth's spheres (in particular its liquid core) have substantially changed (Lambeck and Cazenave 1976), and new data were obtained on the LOD and dT dynamics. (Halpert and Bell 1997)

In the following we (1) compare in detail global geophysical (LOD) and climatic (dT) indices for the last 150 years and (2) evaluate the impacts of the processes running in inner earth's sphere on the long-term dynamics of LOD, according to new findings on the its structure and dynamics.

For more convenient visual comparison of the dT dynamics and earth rotation velocity, it is worthy to use $-$ LOD instead of direct LOD values. The dynamics of both $-$ LOD and dT for the last 140 years can be viewed as multi-decadal fluctuations against the background of its age-long trends (Figures 11a, 11b).

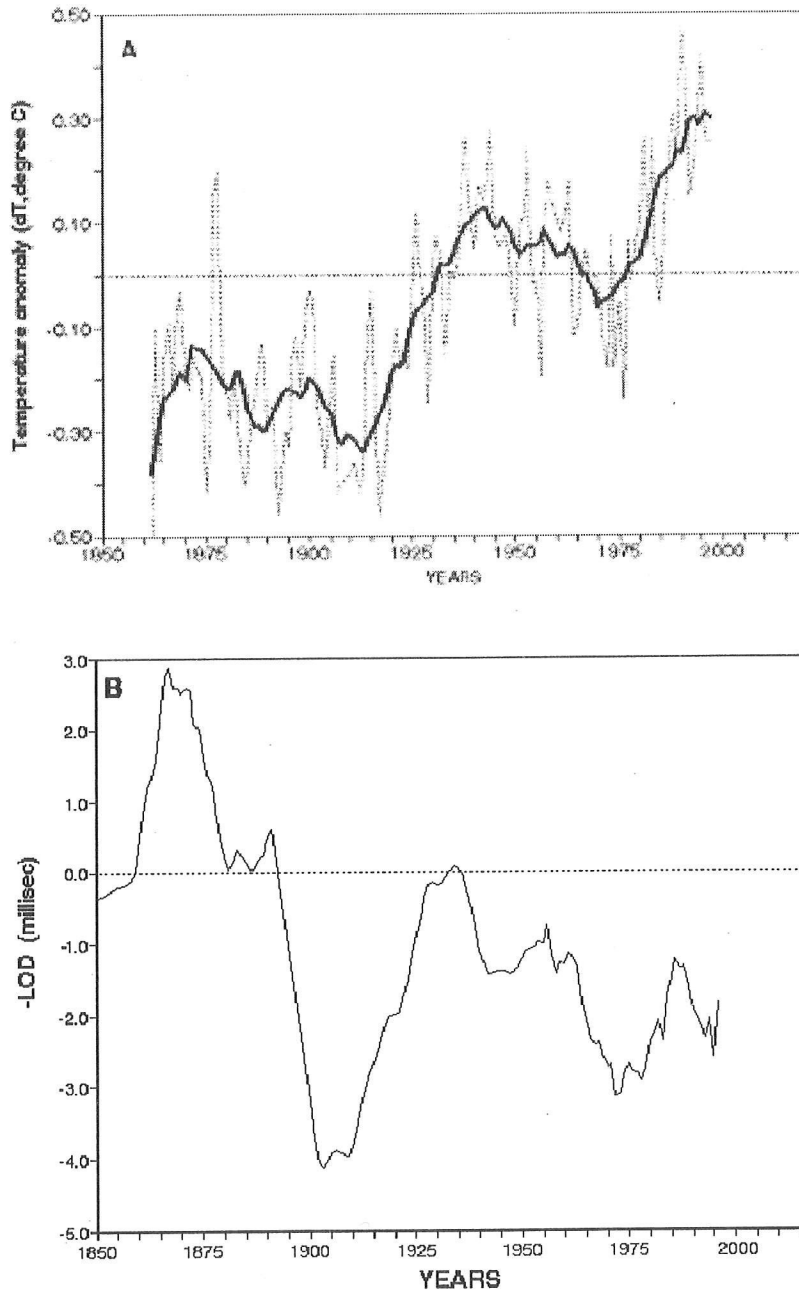


Figure 11 (a) Global dT is known to have ascending linear trend with the increment of $0.059\text{ }^{\circ}\text{C}$ per 10 years (Sonechkin 1998). As mentioned above, -LOD has the age-long descending linear trend with the increment about 0.14 ms per decade. (b) Different age-long linear trends of LOD and dT make it difficult to compare the dynamics of multi-decadal fluctuations of these indices.

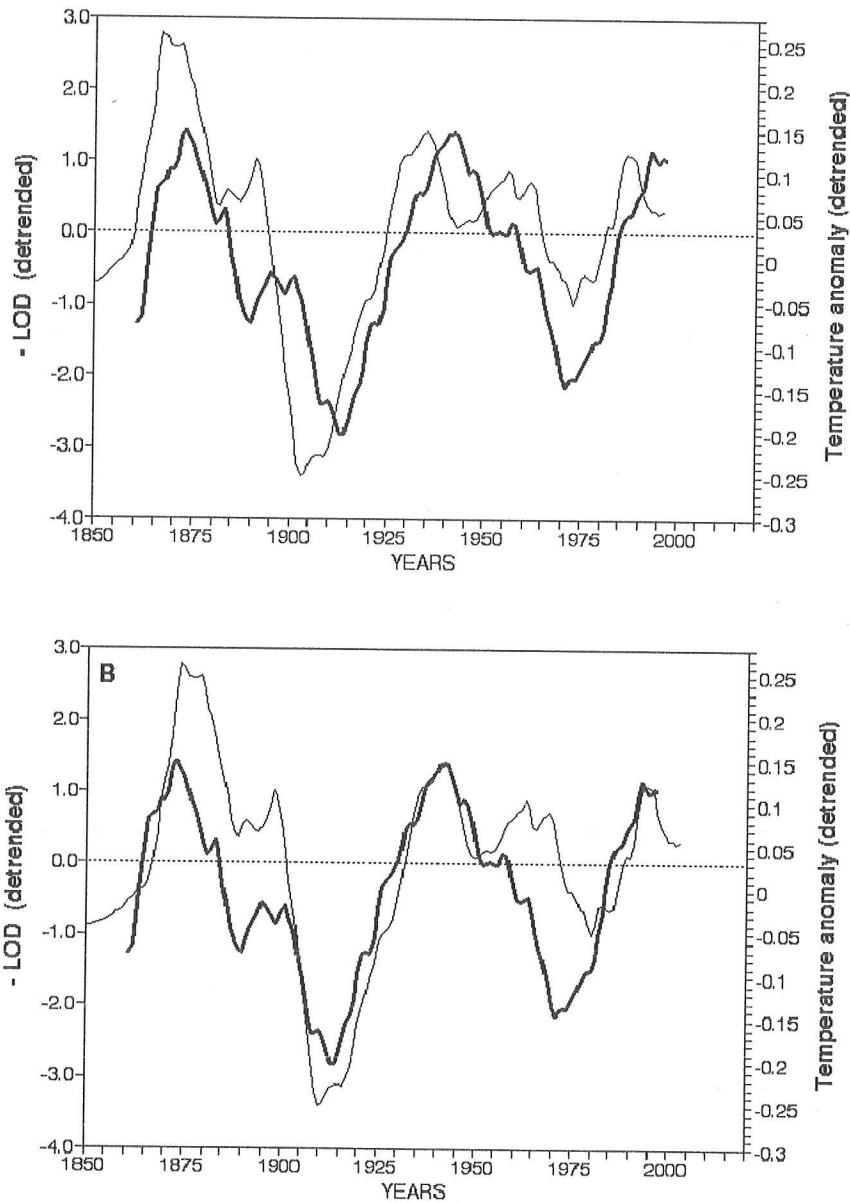


Figure 12 (a) Here, are both $-LOD$ and dT ranges, with the linear trends removed using the so-called “detrending” procedure (Statgraphics 1988). When detrended, the graphs are similar in shape, and it is clear that $-LOD$ runs several years ahead of dT , especially in its maximums. Shifting the $-LOD$ curve by 6 years to the right (Figure 12b) results in almost complete coincidence of the corresponding maximums of the early 1870s, late 1930s, and middle of the 1990s. (b) In general, the long-term dynamics of both dT and $-LOD$ are characterized by roughly 60-year periodicity. The global climate system was reported to oscillate with a period of 65-70 years (according to the time series since 1850) (Schlesinger and Ramankutty 1994). The same 60-70-year periodicity also was characteristic for the long-term dynamics of climatic and biological indices in the last 150 years (Klyashtorin 1998). See Figure 13.

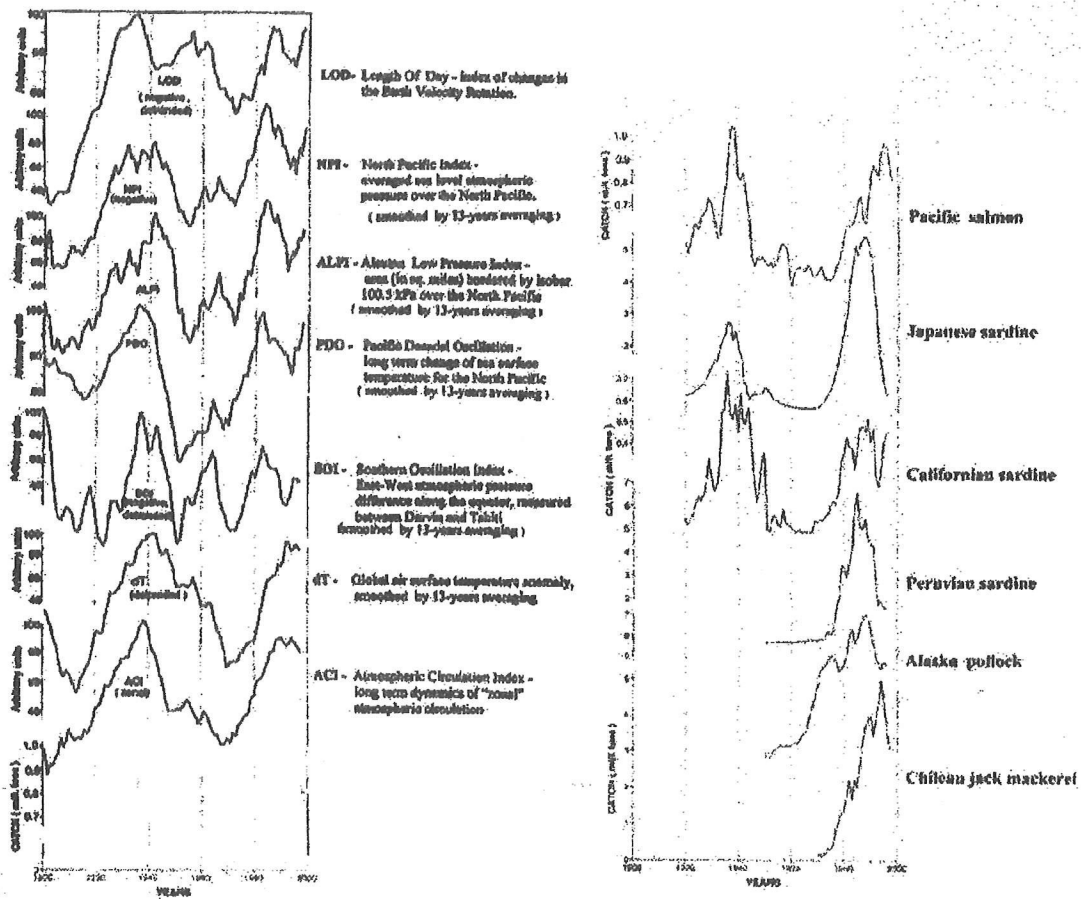


Figure 13 Several well-defined climate indices are amazingly similar to the catch records from six of the most productive fisheries in the Pacific Ocean, with peaks occurring in or about the same decades, 1940 and 1980–1990. Lows occur in the 1950–1970 period. Attribution of causality to the atmospheric indices is inappropriate. The identification of the forcing and interactions within each supporting ecosystem is the subject of intense studies around the world.

The similarity in the dynamics of detrended geophysical -LOD and climatic dT indices is clear: large fragments of the curves are much alike not only in general shape, but in detail as well. The resemblance is particularly manifested in the maximums and somewhat weakened in the minimums (The minimum of -LOD of 1970th is not ahead of the corresponding minimum of dT, but is lagged a bit behind it.)

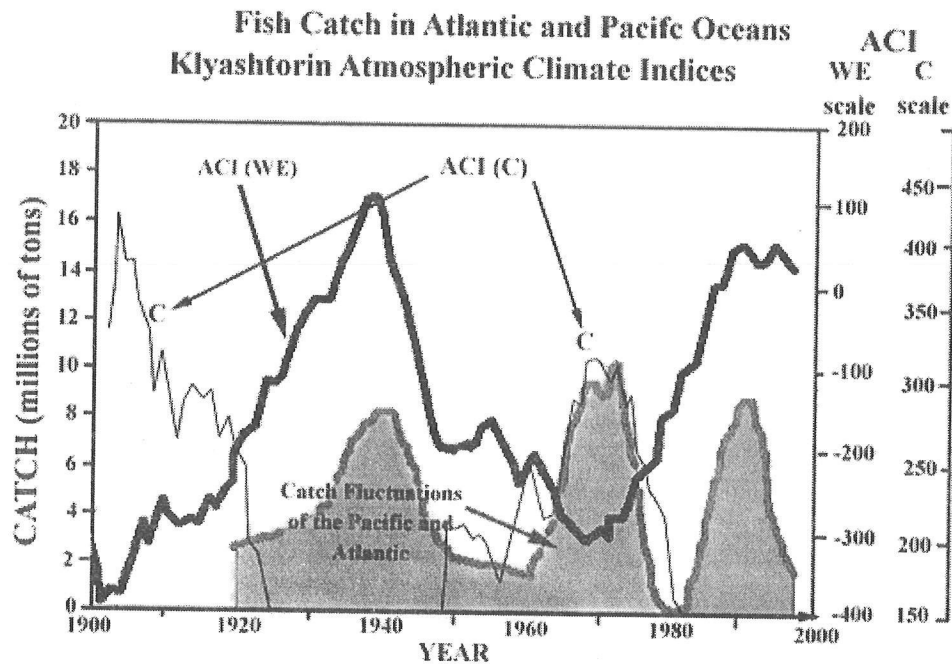


Figure 14 Fish catch in Atlantic and Pacific oceans. Klyashtorin atmospheric climate indices. Klyashtorin (1998) suggests that these two alternating dominance patterns underlie the 50-70 year patterns of alternating species production from the world's major ocean fisheries, including those found in the 2000 year paleosediment record from Santa Barbara Basin (Baumgartner and others 1992). Catch totals are for those species in Figure 13.

The similarity between the -LOD and dT dynamics makes it possible to assume the existence of some common causes inducing the observable synchrony in geophysical (LOD) and climatic (dT) indices variation. The atmospheric circulation as a whole is strongly driven by the so-called Equator-Pole Temperature Meridional Gradient. Greater warming in the polar region weakens this gradient in the lower troposphere, which leads to general weakening of surface winds (Boer 1990; Hsien and Boer 1992). The long-term dynamics of the atmospheric pressure fields over the North hemisphere during the last 90 years are characterized by alternating of roughly 30-year periods (the so-called "circulation epochs") with relative dominance of either zonal or meridional atmospheric circulation (Dzerdzeevski 1962, 1969; Girs 1971; Lambeck 1980).

The first type (zonal) is characterized by an increasing intensity of the zonal circulation at all latitudes and with a poleward migration of the belts of maximum wind intensities. The circulation is accompanied by a decrease in overall range of surface air temperature between the equator and poles and by overall increase in the mean global surface-air temperatures. Ocean-surface temperatures also tend to increase in high latitudes. The second type (meridional) is characterized by weaker zonal circulation, migration of the main streams toward lower latitudes, and overall decrease in temperature (Lamb 1972.) Both easterly and westerly winds increase with zonal type circulation and both decrease in the periods of meridional type of the circulation (Lambeck 1980).

Applications of Geophysical Indices in Forecasts and Proactive Fisheries Management and Agricultural Planning

These many indices represent forces ranging over various time-space scales (Sharp 1981a, 1981b, 1987, 1988). In the oceans, these range from wind-driven mixing, affecting small scale turbulence, hence enhanced localized food availability to the early life history stages of fishes (Owens 1981, 1989; Parrish and others 1981; Rothschild and Osborne 1988) onward to deep upwelling of nutrient rich water into the photic zone and local circulation patterns that enhance general production (Bakun and Parrish 1981, 1991), local iron limitations (Martin and others 1991), on to stimulation of deep-water currents that resuspend iron rich sediments, resulting in general system enhancements. However, we still do not have any realistic explanations for the high upper trophic level occupancy (tuna abundance) of the Sargasso Sea.

In the various examples in agriculture the stimuli for seasonal production are well represented in the pressure gradients ocean-atmosphere or earth-atmosphere transfers of energy (in the form of heat and moisture), that essentially define the seasonality, and provide the basis of plant production and waterway dynamics that can affect the sustainability of vast regions, and the resident insect, bird, and mammalian populations, humans included.

Given the generally hemispheric nature of the relationships, and somewhat coherent ocean basin-scale ecological responses, many are beginning to take serious looks into the use of geophysical indicators for all sorts of ecological and socioeconomic applications. Several indices have resulted, including the Aleutian Low Pressure Index (the area encompassed by the 100.5 kPa isobar) and the North Pacific Index (NPI), a measure of the average sea level atmospheric pressure over the North Pacific.

The recent focus on the North Pacific Decadal Oscillation (PDO), from studies initiated by Hare and Francis (1995), Hollowed and Wooster (1992, 1995a, 1995b) Mantua and others (1997), and most recently by Hare and Mantua (1999)—and similar efforts in the North Atlantic and Arctic—shows that none of these system responses is independent, and that the broader the scale examined, the more insights are yielded. There are also the much grander scale atmospheric and oceanographic processes and linkages needing to be identified, starting with the Southern Oscillation Index, and the Earth Rotation Rate, or its inverse, the LOD index, that seem to integrate far greater information that are likely to be useful over much larger venues.

Within these patterns lie the double patterned Atmospheric Circulation Indices (ACI-WE & ACI-C) of AA Girs (1971), that appear to relate more specifically the dominant directions of the atmospheric circulation, to the principal regional fisheries production. The fisheries see-saw resulting from two faunas with relatively distinct oceanographic and production patterns, is associated with colder upwelling dominated oceans (ACI-C) or the alternate state, where east-west winds tend to suppress coastal upwelling, and push warmer, more oceanic surface water onto coastal shelves. These warm vs. cold analogies are more indicative of the dominant oceanic processes, than absolute temperatures.

The atmosphere is the most variable component of the system exchanging relatively large proportions of its angular momentum with the solid earth below compared with other components (Salstein and others 1993). Numerous publications suggest that seasonal, inter-seasonal and inter-

annual variations of the earth's rotation velocity are in direct proportion to the relative angular momentum at the atmosphere that primarily depends on the velocity of zonal winds (Langley and others 1981; Rosen and Salstein 1983; Robertson 1991). On longer time scales, changes in LOD are in a correlation with the El Niño Southern Oscillation (ENSO) phenomenon and strong wind anomalies associated with ENSO events (Salstein and Rosen 1983; Dickey and others 1992a, 1992b; Barnes and others 1983).

A formal derivation of the dynamic relation between the atmosphere and solid earth (Bullen 1963) make it possible to calculate the changes in the earth's rotation velocity from the large-scale distribution of the atmospheric pressure and dynamics of the wind fields. These data are available from several world weather services (Salstein and others 1993).

Thus, on a wide range of time scales (from several days to years), there is an agreement between the dynamics of the angular momentum in the atmosphere and solid earth, which come into view as small but important changes in the rotation of the planet. By analogy, it is conceivable that the multi-decadal fluctuations of the earth's rotation velocity are likely to result from redistribution of the angular momentum between the atmosphere and solid earth due to the alternation of multidecadal epochs of zonal and meridional atmospheric circulation. Given the six-year lag, the LOD observations can be used as an indicator to predict the future climatic trends. Independently on real mechanism determining the correlation between the detrended climatic (dT) and geophysical (LOD) indices, the phenomenon of their close similarity for the recent 140 years makes LOD a convenient tool to predict general trend of the global temperature anomaly (dT) for at least six years ahead (Klyashtorin and others 1998). The fact that these and analogous species trends can be inferred from high resolution paleosediment records laid down over the recent two millennia or so, has stimulated discussion around the world, regarding the linkages (Sharp 1992; Kawasaki and others 1991; Schwartzlose and others 1998).

This information in hand, what can be said about the future dynamics from this index? According to A. Lubushin (senior scientist of Earth Physics Institute, Russian Academy of Science, personal communication), spectral density analysis of LOD time series for 1850-1998 revealed a manifested roughly 60-year maximum. The first and second multidecadal maximums of LOD took place in the early 1870s and middle 1930s, respectively, and the third maximum is likely to fall in the late 1990s to early 2000s. Based on this multidecadal periodicity of LOD, a gradual descending of dT may be expected in the middle of the first decade of the (21st) century. The trend of -LOD shown in Figure 12b also suggests that the global temperature anomaly (dT) will keep increasing until at least 2004.

The thesis that tied together the Sahel droughts, tropical cyclones and Atlantic hurricanes, (Gray 1990; Gray and Schaeffer 1991) and the coastal fisheries off west Africa and Central America, with ENSO, QBO, and other climate indices has led the way to more efforts to become proactive in climate forecasts. It takes a lot of self-confidence, and willingness to take on a barrage of nay-saying and nit-picking from peers, and wanna-be experts, to define the present conventions. Leonid Klyashtorin has opened the eyes of many to the near-lost knowledge from his Russian geophysical community's archives and "ivory towers." By the time this review becomes available, the FAO Fisheries Department will have published his technical report on the theory and applications of the AA Girs ACI in fisheries forecasts, and the next stages in the development of proactive rather than hindcast management procedures.

The historical global reviews of major upwelling system and ocean fisheries variabilities related to ocean and climate variations began with Dickson pulling David Cushing toward his (1982) review for the North Atlantic fisheries systems. The process of regional information integration progressed through the Sharp and Csirke (1983) global overview that spawned several regional efforts as participants returned home. Meanwhile, Wooster and Fluharty's (1984) focus on the southeastern sub-arctic Pacific region's response to El Niño shines brightly. As the North Pacific underwent major system-wide changes during the 1970-1980s, Ebbesmeyer and others (1991) documented, and, again, linked as many as possible, outward, into a larger scale phenomenon—the 1976 Pacific Ocean Climate Regime Shift. Over the ensuing years, the follow-up into the mechanisms and interactions needed the clarity finally arrived at by Bakun (1996), in which the myriad ocean production patterns were described, along with their linkages, potential and realized, to fish population dynamics. Today, many applied scientists in the realms of fisheries and agriculture are turning away from equilibrium-based and “stability” assumptions as a result of these efforts and facing the reality of continuous climate change, and the need to be prepared to cope with future transitions.

In the fisheries contexts described above, the obvious bi-modality is not symmetrical, as the initial fish population rises are sharper, and the collapses much more abrupt than the smoothed climate indices indicate should be the case. The transitions from one phase to another appear to be timed such that there are actually four stages, two for each Climate Phase. Given this now obvious insight, the real issue is how to minimize the impacts on the various exploited resource populations, once the fish population collapses begin. The Olde-Time equilibrium models presume that relief from fishing would allow the populations to once again increase their production—immediately bouncing back to higher levels. This is only rarely the case in this era of over-capitalization, and decision-making inertia. The reality is that if these populations' exploiters are to survive, they must be managed so that the maximum range extents and age structures for the populations are maintained once they begin to decline. Fishing impacts can be minimized over the twenty to thirty years until the next “bloom” for these populations. This will provide for long-term optimization, rather than the short-term over-exploitation that is rampant today with such devastating and extended consequences.

Similarly, the option to forecast fishery or rainfall patterns beyond the annual cycle, as a function of global climate trends, and particularly the all-important transition periods, provides an optimal planning environment. Fisheries operations as well as agricultural planning can be optimized, and waste and environmental or habitat damage minimized, securing ecosystems for the future generations. Clearly, these are worthy objectives, in comparison to the “business as usual” approach that only optimizes immediate rewards.

References

- Atomizdat. 1976. Tables of physical constants (in Russian). p. 620. Moscow, Russia.
- Bakun A. 1996. Patterns in the ocean. California Sea Grant/CIB 323 p.
- Bakun A, Parrish RH. 1981. Environmental inputs to fishery population models for eastern boundary current. In: G.D. Sharp, convenor, editor. Report and documentation of the workshop on the effects of environmental variation on the survival of larval pelagic fishes. IOC Workshop Report Series. No. 28. Paris, France: Unesco. p 68–79.

2001 PACLIM Conference Proceedings

- Bakun A, Parrish RH. 1991. Comparative studies of coastal pelagic fish reproductive habitats: the anchovy (*Engraulis anchoita*) of the southwestern Atlantic. *Journal de Conseil international pour la Exploration du Mer* 48:342-61.
- Barnes RTH, Hide R, White AA, Wilson CA. 1983. Atmospheric angular momentum fluctuations, length-of-day changes and polar motion. *Proceedings of the Royal Society of London* 334:55-92.
- Baumgartner TR, Soutar A, Ferreira-Bartrina V. 1992. Reconstruction of the history of Pacific sardine and northern anchovy populations over the past two millennia from sediments of the Santa Barbara Basin, California. *CalCOFI report* 33:24-40.
- Boer GI. 1990. Atmospheric exchange of angular momentum simulated in a general circulation model and implications for the length of day. *J Geophys Res* 95:5511-31.
- Bullen KE. 1963. *An introduction to the theory of seismology*. Cambridge University Press. 450 p.
- Buck KR, Chavez FP, Campbell L. 1996. Basin-wide distributions of living carbon components and the inverted trophic pyramid of the central gyre of the North Atlantic Ocean, summer 1993. *Aquatic Microbial Ecology* 10:283-98.
- Cushing DH. 1982. *Climate and fisheries*. London (UK): Academic Press. 373 p.
- Dickey JO, Marcus SL, Hide R. 1992. Global propagation of international fluctuations in atmospheric angular momentum. *Nature* 334:115-9.
- Dickey JO, Steppe JA, Hide R. 1992. The earth's angular momentum budget on seasonal time scales. *Science* 255:321-4.
- Dzerdziejewski BL. 1962. Fluctuations of climate and of general circulation of the atmosphere in extratropical latitudes of the Northern Hemisphere and some problems of dynamic climatology. *Tellus* 14(3):328-34.
- Dzerdziejewski BL. 1969. Climate epochs in the twentieth century and some comments on the analysis of past climates. In: Wright HW, editor. *Quaternary geology and climate*. 16:49-60. Washington: International Association for Quaternary Research.
- Ebbesmeyer CC, Cayan DR, McClain DR, Nichols FH, Peterson DH, Redmond KT. 1991. 1976 step in Pacific climate: forty environmental changes between 1968-1975 and 1977-1984. In: Betancourt JL, Tharp VL, editors. *Proceedings of the 7th Annual Pacific Climate (PACLIM) Workshop*; Apr 1990; Asilomar, California. Interagency Ecological Study Program Technical Report 26. Sacramento (CA): California Department of Water Resources. p 115-26.
- Girs AA. 1971. *Macrocirculation method for long-term meteorological prognosis (in Russian)*. Leningrad: Hydrometizdat Publ. 480 p.
- Goodridge JD. 1996. Comments on regional simulation of greenhouse warming including natural variability. *Bull Amer Met Soc* 77(7):1588-9.
- Gray WM. 1990. Strong association between west African rainfall and U.S. landfall of intense hurricanes. *Science* 249:1251-6.

- Gray WM, Sheaffer JD. 1991. El Niño and QBO influences on tropical cyclone activity. In: Glantz MH, Katz R, Nicholls N, editors. ENSO teleconnections linking worldwide climate anomalies: scientific basis and societal impacts. Cambridge (UK): Cambridge Univ. Press. p 257–84.
- Halpert MS, Bell GD. 1997. Climate assessment of 1996. *Bull Amer Met Soc* 78:1–49.
- Hare SR, Francis RC. 1995. Climate change and salmon production in the Northeast Pacific Ocean. In: Beamish RJ, editor. Climate change and northern fish populations. *Spec Publ Can Fish Aquatic Sci* 121:357–72.
- Hare SR, Mantua NJ, Francis RC. 1999. Inverse production regimes: Alaska and West Coast Pacific salmon. *Fisheries* 24:6–14.
- Hide R, Dickey JO. 1991. Earth's variable rotation. *Science* 253:629–37.
- Hollowed AB, Bailey KM, Wooster WS. 1995. Patterns of recruitment in the northeast Pacific Ocean. *Biol Oceanogr* 5:99–131.
- Hollowed AB, Wooster WS. 1992. Variability of winter ocean conditions and strong year classes of Northeast Pacific groundfish. *ICES Marine Science Symposia* 195:433–44.
- Hollowed AB, Wooster WS. 1995. Decadal-scale variations in the eastern subarctic Pacific: II. Response of Northeast Pacific fish stocks. In: Beamish RJ, editor. Climate change and northern fish populations. *Spec Publ Can Fish Aquatic Sci* 121:373–85.
- Hsien WW, Boer GJ. 1992. Global climate change and ocean upwelling. *Fish Oceanogr* 1(4):333–8.
- Kawasaki T, Tanaka S, Toba Y, Taniguchi A, editors. 1991. Long-term variability of pelagic fish populations and their environment. Tokyo, Japan: Pergamon Press.
- Klyashtorin LB. 1998. Long-term climate change and main commercial fish production in the Atlantic and Pacific. *Fish Res* 37:115–25.
- Klyashtorin L, Nikolaev A, Klige R. 1998. Variation of global climate indices and earth rotation velocity. In: Book of abstracts GLOBEC First Open Science Meeting, Paris, 17-20 March 1998, p 55. 10.
- Langley RB, King RW, Shapiro II, Rosen RO, Salstein DA. 1981. Atmospheric angular momentum and the length of day: a common fluctuation with a period near 50 days. *Nature* 294:730–2.
- Lamb HH. 1972. *Climate, present, past and future*. London (UK): Methuen and Co. 613 p.
- Lambeck K, Cazenave A. 1976. Long term variations in the length of day and climatic change. *Geophysical Journal of the Royal Astronomy Society* 46:555.
- Lambeck K. 1980. *The earth's variable rotation*. Cambridge (UK): Cambridge University Press.
- Mantua NJ, Hare SR, Zhang Y, Wallace JM, Francis RC. 1997. A Pacific decadal climate oscillation with impacts on salmon. *Bulle Amer Met Soc* 78:1069–79.

- Martin JH, Gordon RM, Fitzwater SE. 1991. Iron limitation? The case for iron. *Limnology and Oceanography* 36(8):1793–1802.
- Munk WH, McDonald GJF. 1960. *The rotation of the earth*. Cambridge (UK): Cambridge University Press. 323 p.
- Owen RW. 1981. Patterning of flow and organisms in the larval anchovy environment. In: Sharp GD, convenor, editor. Report and documentation of the workshop on the effects of environmental variation on the survival of larval pelagic fishes. IOC Workshop Report Series nr. 28. Paris, France: UNESCO. p 167-200.
- Owen RW. 1989. Microscale and finescale variations of small plankton in coastal and pelagic environments. *J Mar Res* 47:197–240.
- Parrish RH, Nelson CS, Bakun A. 1981. Transport mechanisms and reproductive success of fishes in the California Current. *Biol Oceanogr* 1(2):175–203.
- Robertson DS. 1991. Geophysical applications of very-long baseline interferometry. *Reviews in Modern Physics* 63:899–918.
- Rosen RD, Salstein DA. 1983. Variations in atmospheric angular momentum on global and regional scales and the length of day. *J Geophys Res* 88:5451–5470.
- Rothschild BJ, Osborne TR. 1988. Small-scale turbulence and plankton contact rates. *J Plankton Res* 10:465–74.
- Salstein DA, Rosen RD. 1983. Earth rotation as a proxy for internal variability in atmospheric circulation. *J Clim App Met* 25:1870–7.
- Salstein DA, Kann DM, Miller AJ, Rosen RD. 1993. The sub-bureau for Atmospheric Angular Momentum of the International Earth Rotation Service: a meteorological data center with geodetic applications. *Bull Amer Met Soc* 74(1):67–80.
- Schlesinger ME, Ramankutty N. 1994. An oscillation in the global climate system of period 65-70 years. *Nature* 367:723–6.
- Sharp GD. 1981a. Report of the workshop on effects of environmental variation on the survival of larval pelagic fishes. In: Sharp GD, convenor, editor. Report and documentation of the workshop on the effects of environmental variation on the survival of larval pelagic fishes. IOC Workshop Report Series nr. 28. Paris, France: UNESCO. p 6-62.
- Sharp GD. 1981b. Colonization: modes of opportunism in the ocean. In: Sharp GD, convenor, editor. Report and documentation of the workshop on the effects of environmental variation on the survival of larval pelagic fishes. IOC Workshop Report Series nr. 28. Paris, France: UNESCO. p 125–48.
- Sharp GD. 1987. Climate and fisheries: cause and effect or managing the long and short of it all. In: *The Benguela and Comparable Ecosystems*. South African Journal of Marine Science 5:811–38.
- Sharp GD. 1988. Fish oopulations and fisheries: their perturbations, natural and man induced. In: Postma H, Zijlstra JJ, editors. *Ecosystems of the world 27, continental shelves*. Amsterdam: Elsevier. p 155–202.

- Sharp GD. 1992. Fishery catch records, ENSO, and longer term climate change as inferred from fish remains from marine sediments. In: Diaz H, Markgraf V, editors. *Paleoclimatology of El Niño-Southern Oscillation*. Cambridge University Press. p 379-417.
- Sharp GD, Csirke J, editors. 1983. Proceedings of the expert consultation to examine the changes in abundance and species composition of Neritic fish resources; San Jose, Costa Rica; 18-29 April 1983. *FAO Fisheries Report Series 291*, volumes 2-3. 1294 p.
- Sharp GD, Csirke J, Garcia S. 1983. Modelling fisheries: what was the question? In: Sharp GD, Csirke J, editors. Proceedings of the expert consultation to examine the changes in abundance and species composition of Neritic fish resources; San Jose, Costa Rica; 18-29 April 1983. *FAO Fisheries Report series 291(3)*:1177-1224.
- Sonechkin DM. 1998. Climate dynamics as a nonlinear Brownian motion. *Int J Bifurc Chaos* 8(4):799-803.
- Song X, and P. Richards, 1996. Seismological evidence for differential rotation of the earth's inner core. *Nature*, 382:58-61.
- Statistical Graphic Corporation. 1988. *Statgraphics [statistic graphic system] user's guide*. STSK Inc. 440 p.
- Stephenson FR, Morrison LV. 1995. Long-term fluctuations in the earth's rotation: 700BC to AD1990. *Philos Trans Royal Society London*. A351:165-202.
- Wooster WS, Fluharty DL, editors. 1984. *El Niño North: Niño effects in the eastern subarctic Pacific ocean*. Seattle (WA): Washington Sea Grant, University of Washington. 312 p.

Diatoms as Indicators of Freshwater Flow Variation in Central California

Scott W. Starratt

Abstract

Diatoms from tidal marsh sediments collected from Rush Ranch, north of Suisun Bay, are used to reconstruct the history of salinity variability in the northern part of San Francisco Bay over the past 3,000 years. Evidence suggests that the primary factor controlling the distribution of diatoms is the salinity gradient within the estuary. The composition of modern diatom assemblages in freshwater (<2‰), brackish (2‰ to 30‰), and salt water (>30‰) marshes were used to calibrate the late Holocene assemblages. Variations in both individual taxa and ecological assemblages were then used in the analysis of salinity variations. Dominant taxa in each ecological assemblage vary downcore, indicating that variation in salinity is only one parameter in a complex set of factors that control the temporal and spatial distribution of diatoms in San Francisco Bay marshes.

At the Rush Ranch site there appears to be evidence of broad-scale salinity cycles. Prior to European contact about 150 years ago, there are two intervals dominated by freshwater taxa (2,500 cal yr B.P. to 1,750 cal yr B.P. and 750 cal yr B.P. to about A.D. 1850) and two intervals dominated by brackish water and marine taxa (3,000 cal yr B.P. to 2,500 cal yr B.P. and 1,750 cal yr B.P. to 750 cal yr B.P.) The upper cycle appears to be broadly related to the Medieval Warm Interval (upper brackish interval) and the Little Ice Age (upper freshwater interval). Minor fluctuations during the last 2,700 years occur in a pattern similar to the lake level record for Mono and Pyramid lakes, which lie east of the crest of the Sierra Nevada. An increase in the abundance of fresh water diatoms at Rush Ranch occurs at about the same time as high stands, implying contemporaneous increases in precipitation on both sides of the Sierra Nevada.

Introduction

The brackish marshes in the northern part of San Francisco Bay occur at the interface between freshwater flow from the rivers of interior California and the salt water entering through the Golden Gate. About 40% of the land area of California drains through the estuary (Conomos 1979). Prior to European occupation, brackish marshes were extensive in Suisun Bay, located between the Sacramento-San Joaquin Delta and San Pablo Bay (Figure 1). Brackish marshes can be identified by a diversity of macrophytes (Atwater and others 1977). Diatom diversity is also higher in brackish marshes than in either the normal marine environment of San Francisco Bay or the fresh water of the Sacramento-San Joaquin Delta (Starratt and Wan 1998).

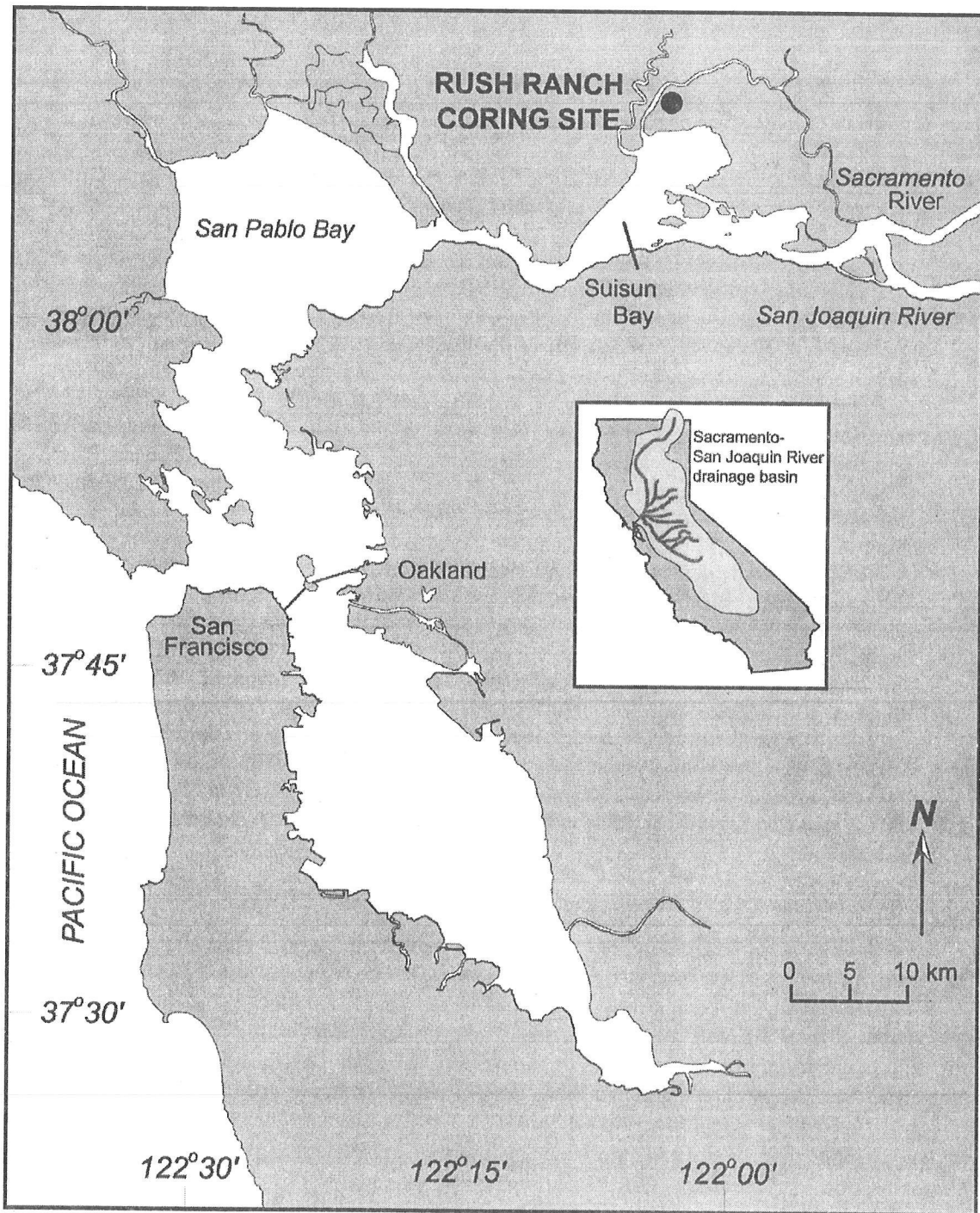


Figure 1 Map of San Francisco Bay showing the location of the Rush Ranch site and the drainage basin of the Sacramento and San Joaquin rivers

The mean annual salinity in San Francisco Bay ranges from 33‰ at the Golden Gate to 0-1‰ in the Sacramento-San Joaquin Delta (Byrne and others 2001). Salinity distribution is determined by the balance between the volume of river inflow and the strength of the tidal cycle. Of the two, the flow of fresh water dominates the environment, accounting for as much as 86% of the observed variability (Peterson and others 1989).

Both the volume and timing of fresh water flow affects the overall variations in annual salinity. The volume and timing of fresh water flow is largely determined by winter precipitation. During December, January, and February, about 55% of the annual precipitation falls. If winter precipitation values are high, then increased runoff from the Sierra Nevada will continue into the summer and the salinity in the estuary will be lower. If winter precipitation is low, then runoff tends to be low in the late spring and summer, and salinity will be high. The volume of runoff generated from winter precipitation is moderated to some extent by spring weather conditions. A wet, cloudy spring leads to a Sierra Nevada snowpack that persists into the summer. Peak river flow will be delayed until late spring or summer. If the spring is warm, peak runoff occurs earlier in the year, leaving little moisture available to moderate summer salinity.

Coastal oceanographic conditions also modify the estuarine response to spring runoff. Because variations in freshwater flow through the estuary far outweigh the marine effect, the role of seasonal upwelling is difficult to separate from the runoff effect.

The Role of the Atmosphere

California's climate is largely controlled by the interaction between the Pacific High and the Aleutian Low pressure systems. During the summer, the Pacific high strengthens over the northeast Pacific, driving storms to the north, into Washington and coastal Canada. In the winter, the high-pressure system weakens and moves southward, allowing the stronger Aleutian low to dominate the weather system. As the gradient between the two pressure systems increases, more storm systems develop and travel a more southerly track into California.

The El Niño-Southern Oscillation (ENSO) events are part of the central California weather system (Schonher and Nicholson 1989). A regional index that incorporates the effect of ENSO events on California weather in general, along with the timing and magnitude of streamflow, has been developed in an attempt to demonstrate the role of regional atmospheric pressure systems on local precipitation (Cayan and Peterson 1989; Dettinger and Cayan 1995).

These ENSO events generally result in increased precipitation in central California. In southern California, the intensity of an ENSO event is connected to the Southern Oscillation Index, but further north, the connection is somewhat tenuous. The Aleutian low is usually stronger during an ENSO event, and if it forms farther east than usual, high-volume precipitation falls in central California during the winter.

The Pacific Decadal Oscillation (PDO) is an ENSO-type pattern that exists across the Pacific basin. The PDO differs from the ENSO in both the length of each oscillation (20-30 years vs. 6-18 months) and region affected (North Pacific/North America vs. the tropics). The PDO appears to be linked to longer-term variability in precipitation and streamflow in the western U.S. (Cayan and others 1993,

1998; Dettinger and others 1998; Nigam and others 1999). The record of these atmospheric-precipitation connections exists for a period of about a century.

The Role of Biology

Both the amount of freshwater and the timing of its distribution affects the diatom floras in the marshes on northern San Francisco Bay. Lehman (1992, 1997, 2000a, 2000b) and Lehman and Smith (1991) noted substantial variations in the algal floras in the upper part of the San Francisco Bay estuary between wet and dry years. Because salinity is not the only variable that affects the composition of a diatom assemblage, the observed lack of consistency between several wet and dry intervals may be related to the timing of maximum freshwater flow and substantial variations in nutrient load between years of high and low freshwater flow (Peterson and others 1989).

Spring or summer runoff is the principle controlling factor in the nutrient budget in the northern part of San Francisco Bay. The combination of nutrient (nitrogen, phosphorous, silica) levels and insolation control both the diversity and taxonomic composition of the diatom flora at any given time.

The Late Holocene Record

Only a handful of studies have addressed the pre-1850 history of freshwater flow through the Sacramento-San Joaquin Delta and its significance in unraveling the complex history of late Holocene climate history in central California (Byrne and others 2001; Goman and Wells 2000; Ingram and DePaolo 1993; Ingram and others 1996a, 1996b; May 1999; Wells and Goman 1995). The purpose of this paper is to demonstrate the effectiveness of diatoms as indicators of centennial-scale climate change.

Methods

The brackish marsh at Rush Ranch (Solano County) was chosen because it lies midway between the normal marine environment of north San Francisco Bay and the freshwater environment of the Sacramento-San Joaquin Delta (Byrne and others 2001). Decadal to centennial-scale fluctuations in freshwater flow are difficult to identify in marshes in northern San Francisco Bay (Starratt, unpublished data) and further east in the Sacramento-San Joaquin Delta (Goman and Wells, 2000; May, 1999; Starratt, unpublished data; Wells and Goman, 1995) due to the lower variability at sites that lie at the marine and freshwater ends of the salinity spectrum. The Rush Ranch site is a small, unreclaimed relict of the tidal marshes that bordered Suisun Bay 150 years ago. During the 20th century the area was grazed by cattle and the hydrology was significantly influenced by water diversion (Nichols and others 1986).

The core (four sections, 3.5 m in total length) was collected using a modified Livingstone corer. The diatom assemblages from a total of 70 samples were tabulated. Samples were prepared using standard acid techniques and mounted using Naphrax. The counting method of Schrader and Gersonde (1978) was followed and, where possible, at least 300 individual frustules were counted.

Despite the available taxonomic literature, the diatom floras of the western U.S. freshwater and estuarine environments are poorly known. Many of the taxa are generally combined into groups of species, without detailed taxonomic differentiation. This method sometimes results in limited ecological and chronological resolution. It is also probable that some of the taxa are new to science.

The assignment of environmental preferences for particular taxa is tenuous at best. There is little agreement within the literature as to what physical and chemical parameters should be measured, as well as how those data should be presented. No such data set currently exists for the San Francisco Bay area. The ecological limits of some taxa (particularly the marine forms) is well established, while information on the brackish and freshwater taxa is more variable. The ecological preferences used in this paper are based on physical and chemical data taken from several recent lake and estuarine studies (Cumming and others 1995; Dixit and Smol 1994; Snoeijs 1993; Snoeijs and Balashova 1998; Snoeijs and Kasperovien 1996; Snoeijs and Potapova 1995; Snoeijs and Vilbaste 1994; Whitmore 1989).

Results

A detailed discussion of the chronology and stratigraphy of the Rush Ranch core can be found in Byrne and others (2001). A total of four AMS radiocarbon dates were obtained from seeds and rhizome material (Figure 2). The age of sediments at the base of the core is approximately 3,000 cal yr B.P. The sediment accretion rate ranges from 0.6 to 1.6 mm/yr. These values are generally consistent with data from other sites (Byrne and others 2001) in the northern part of San Francisco Bay which indicate that marshes in the region began to expand between 2,000 and 3,000 years ago.

To make a generalized interpretation of salinity variations downcore, most of the taxa were assigned to salinity categories (Figure 2):

- Freshwater: Taxa whose optimum population falls within the salinity range of $< 2\text{‰}$
- Freshwater and brackish water: Taxa whose optimum population falls within the salinity 0‰ to 30‰
- Brackish: Taxa whose optimum population falls within the salinity range of 2‰ to 30‰
- Brackish and normal marine: Taxa whose optimum population falls within the salinity range of 2‰ to $> 30\text{‰}$
- Normal marine: Taxa whose optimum population falls within the salinity range of $> 30\text{‰}$
- No salinity preference: Cosmopolitan taxa that demonstrate no salinity preference

Using these salinity categories, five intervals were identified: lower brackish, lower freshwater, upper brackish, upper freshwater, and post-1850 (Figure 2). The lower freshwater interval is characterized by a more diverse flora than the upper freshwater interval, which is dominated by only a few species (Figure 3). Both the brackish intervals contain a diverse flora.

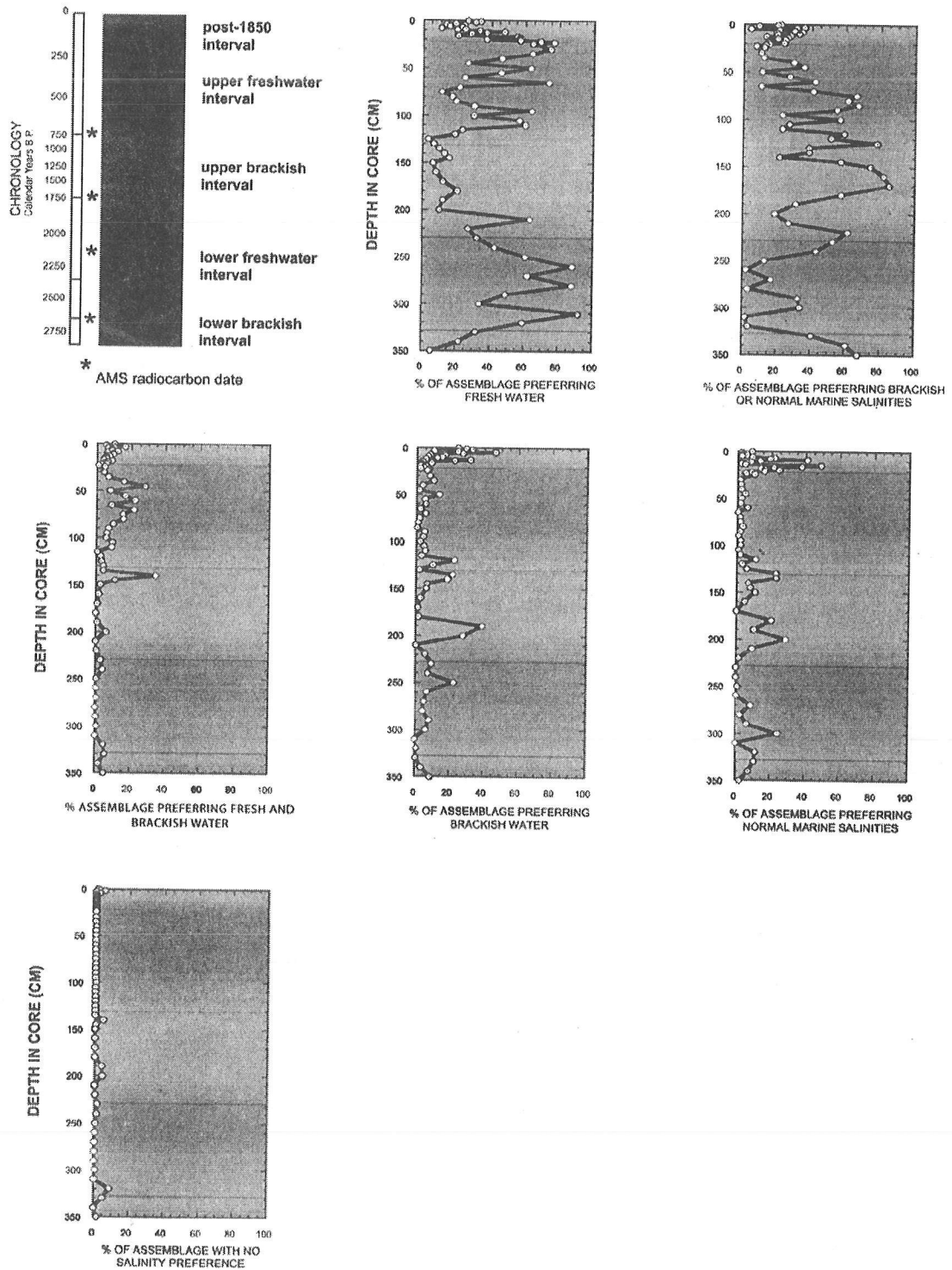


Figure 2 Five intervals representing variations in salinity at Rush Ranch. Diatom salinity preferences shown as percentage of total diatom assemblage. Chronology in calendar years B.P.

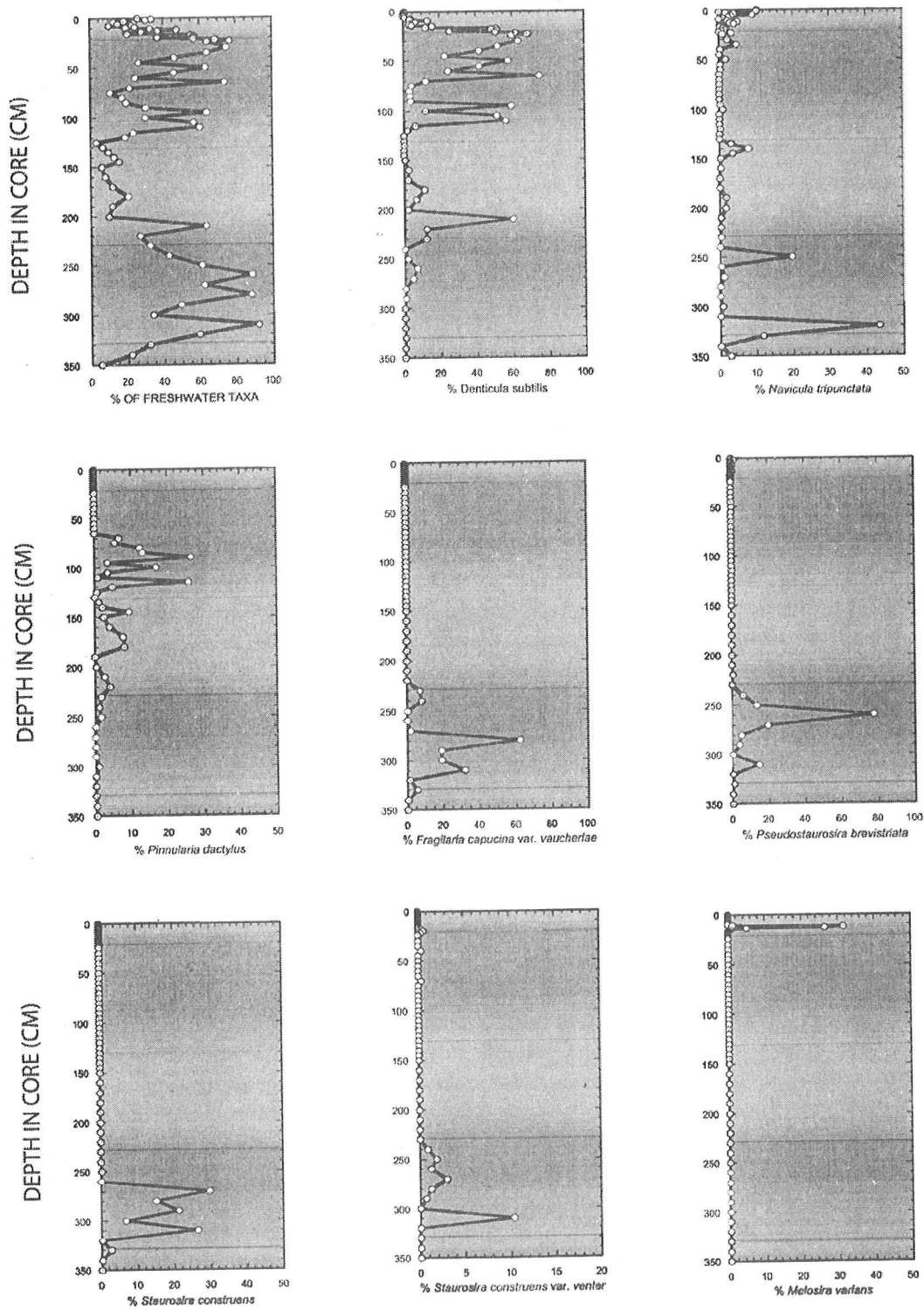


Figure 3 Freshwater assemblage abundance as a percentage of the total assemblage. Dominant taxa in the lower and upper freshwater intervals as a percentage of total flora. Percentage scale is variable.

Freshwater Taxa

A total of 74 taxa with a preference for freshwater have been identified in the samples. Of those taxa, 56 are associated with a benthic habitat, six in a planktonic habitat, and 12 are found in both habitats. In most samples, benthic taxa are the numerically dominant group. Taxonomic distribution within the assemblage is not equitable, with only 10 taxa constituting more than 10% of any one assemblage. In most cases, only one or two taxa dominate the assemblage. The remainder of the assemblage may include 25 to 30 taxa, many accounting for less than 1% of the flora. The majority of the taxa prefer a slightly alkaline environment.

Denticula subtilis is the dominant taxon in the upper freshwater interval, comprising more than 70% of the assemblage in several samples. In one sample in the lower freshwater interval, *D. subtilis* comprises more than 60% of the assemblage. This species is not present in any of the more brackish intervals. Members of this genus are commonly found in oligotrophic (low nutrient load) environments. *Pinnularia dactylus* is co-dominant with *D. subtilis* in the lower part of the upper freshwater interval; it is also the dominant freshwater taxon in the upper brackish interval. *Tryblionella gracilis* was the dominant benthic taxon at the time of European contact; over the past 150 years this dominance has been greatly reduced with increasing brackish water influence caused by increased diversion of water for agriculture. *Navicula tripunctata* and *Amphora ovalis* occur sporadically throughout the length of the core, but are significant in the lower part of the lower freshwater interval. Both these taxa are epilithic (attached to hard substrates), and are found in mesotrophic (moderate nutrient load) to eutrophic (high nutrient load) environments. Several other taxa, which occur in much smaller numbers, are also found in mesotrophic and eutrophic environments.

In the lower freshwater interval, the dominant taxa are obligate planktonic forms (*Fragilaria capucina* var. *vaucheriae*, *Pseudostaurosira brevistriata*, *Staurosira construens*, *Staurosira construens* var. *venter*). In single samples, these taxa comprise as much as 80% of the assemblage. *Melosira varians* briefly dominates the assemblage at the top of the upper freshwater interval. All of these taxa favor eutrophic environments. True planktonic freshwater taxa comprise only a few percent of the total assemblage in any sample.

Freshwater and Brackish Taxa

Taxa (7 benthonic; 2 planktonic) that favor both freshwater and brackish environments are a significant part of the assemblage only in the upper freshwater interval. *Tryblionella acuminata* accounts for more than 30% of the assemblage in the 140 cm sample, but only occurs sporadically elsewhere in the core, particularly below 140 cm. *Epithemia turgida* is a significant component of the flora in the upper freshwater interval, comprising between 10 and 15% of the assemblage in several samples between 40 and 100 cm. Planktonic taxa favoring both freshwater and brackish environments comprise as much as 15% of the assemblage in the upper freshwater interval. These taxa (*Cyclotella striata* and *C. menegheniana*) are also present in the post-1850 interval.

Brackish Taxa

Taxa characteristic of brackish water are distributed throughout the length of the core. The members of this group are most common at the top of the lower freshwater interval and in the post-1850 interval, where they comprise as much as 40% of the assemblage. *Rhopalodia gibberula* is present throughout the core and is a dominant member of the assemblage in samples from both the freshwater and brackish intervals. Short-term increases in the dominance of *R. gibberula* occur in the lower freshwater interval, upper brackish interval, and the post-1850 interval. This taxon also occurs in smaller numbers throughout the upper freshwater interval. *Achnanthes brevipes* var. *intermedia* occurs in small numbers throughout the length of the core, with one dominance peak at the top of the upper brackish interval. *Nitzschia obtusa* var. *scalpeliformis* and *N. sigma* are a significant part of the assemblage in the upper brackish and post-1850 intervals.

Brackish and Normal Marine Taxa

The overall abundance of the portion of the assemblage assigned to a brackish and marine salinity preference is due to varying abundances of *Navicula peregrina* and *Diploneis smithii*. *Navicula peregrina* reaches its greatest abundance (almost 80%) in the lower and upper brackish intervals. It is also a significant component of both freshwater intervals. The abundance of *N. peregrina* varies widely (0% to 30%) within a few centimeters of the core. *Diploneis smithii* is most abundant in the upper freshwater interval, where it comprises as much as 40% of the assemblage. Within this interval, the abundance of *D. smithii* varies from 0% to greater than 40% in the middle of the upper freshwater interval. In the upper part of the upper freshwater interval and the post-1850 interval, *D. smithii* is the dominant brackish and marine taxon, where as it is only a minor component of the lower brackish and lower freshwater intervals. The distribution of *Caloneis westii* somewhat mimics that of *N. peregrina*. *Paralia sulcata* (both large and small forms) do not comprise a significant part of the assemblage in any sample. This taxon is most common (up to 4%) in the upper part of the upper freshwater and post-1850 intervals.

Normal Marine Taxa

Marine taxa comprise a significant part of the assemblage in only a few samples. *Tryblionella granulata* and *T. granulata* var. 1 (Laws 1988) dominate the assemblage in the lower part of the post-1850 interval. Other abundance peaks occur in the lower and upper brackish intervals, as well as the lower part of the lower freshwater interval. Normal marine planktonic taxa never comprise more than 2% of the total assemblage.

Taxa Showing No Salinity Preference

Four taxa show no salinity preference. All occur in small numbers, generally within the brackish intervals and the post-1850 interval. In addition, 24 taxa have not been assigned to an environment based on salinity preference. In any one sample, these taxa rarely account for more than 1% of the assemblage.

Discussion

The downcore distribution of the diatom flora can be broadly separated into three intervals dominated by taxa that favor brackish and marine salinities, and two intervals dominated by freshwater taxa (Figure 2). These intervals correspond to intervals delineated using pollen and ^{13}C data (Byrne and others 2001). In addition to serving as an indicator of the salinity of the waters of the Sacramento River, and thereby, as a proxy for precipitation, diatoms also provide information on the trophic structure and pH of the river water.

Data on pH and trophic (nutrient) levels of individual taxa are generally limited to freshwater taxa (Stoermer and Smol 1999). Indicators of high nutrient levels in coastal marine environments (e.g. *Chaetoceros* spp.) are absent. The taxa present in the lower and upper freshwater intervals prefer a neutral to slightly alkaline environment. The exception is the acidophilic (preferring a slightly acidic environment) species *Eunotia monodon*, which comprises up to 1% of the assemblage in the upper freshwater interval. The freshwater taxa in the lower freshwater interval are dominated by the mesotrophic to hypereutrophic (very high nutrient load) taxa *Amphora ovalis*, *Fragilaria capucina* var. *vaucheriae*, *F. crotonensis*, *Navicula tripunctata*, *Nitzschia palea*, *Pseudostaurosira brevistriata*, *Staurosira construens*, and *S. construens* var. *venter*. The majority of these taxa are obligate planktonic taxa which begin their lives in the littoral zone and later form planktonic mats. The upper freshwater interval is dominated by marginally mesotrophic *Denticula subtilis*. The taxa in the post-1850 interval are a mix of oligotrophic to eutrophic taxa. The difference in the floras in the lower and upper freshwater intervals (Figure 3) may reflect variations in the rate of water exchange at Rush Ranch, with the more eutrophic taxa representing stagnant conditions. However, there is little information on diatom preferences for stagnant or flowing water. The few taxa common in the brackish intervals suggest that the water was slightly alkaline, whereas they provide little or no information on trophic structure.

The majority of the benthonic taxa are either epilithic or epipellic (attached to sediment), with a few epiphytic (attached to plants) species. Until studies of living distributions in San Francisco Bay are conducted, it will be difficult to determine whether the distribution patterns represent autochthonous or allochthonous taxa.

Comparison with other Long-Term Climate Records

The timing of the salinity variations at Rush Ranch can be placed both in the context of global climatic events and anthropogenic intervention within the Sacramento-San Joaquin watershed. The upper part of the upper brackish interval (A.D. 600-1250) corresponds with the Medieval Warm Period and the upper part of the upper freshwater interval (A.D. 1550-1850) corresponds to the Little Ice Age. The increase in salinity at the top of the core may be related to local human impact rather than global climate variations.

Ingram and DePaolo (1993) and Ingram and others (1996a, 1996b) developed a paleosalinity record for San Francisco Bay using strontium isotopes. Using paleosalinity values, a discharge record for the Sacramento-San Joaquin Delta was calculated for the past 700 years. This record broadly correlates with the variations in the abundance of freshwater taxa at Rush Ranch. Most noticeable in the discharge record is an abrupt increase in discharge corresponding to the onset of the Little Ice Age

(middle 16th century) and an abrupt decrease in discharge in the late 1800s, corresponding with increased agriculture in the Sacramento and San Joaquin valleys. Similar abrupt changes occur in the Rush Ranch diatom record.

Tree-ring records from the southern and central Sierra Nevada, White Mountains, and northern Sacramento Valley reflect similar patterns in precipitation as those observed at Rush Ranch. Scuderi (1987a) obtained a 4,000 year record from Cirque Peak in the southern Sierra Nevada and two sites in the neighboring White Mountains. Major decreases in timberline elevation centered at 2,400 and 400 years ago correspond with intervals that contain a high percentage of freshwater taxa (70% to 90%). A less significant downslope change in timberline centered at 600 years ago corresponds to an interval of increased freshwater influence within the upper brackish interval. Increases in the elevation of the treeline in the White Mountains during intervals centering on 900 and 600 years ago correspond with relatively low occurrences of freshwater taxa at Rush Ranch. More detailed records covering the last 1,200 years (Scuderi 1987b) demonstrate a correspondence between decreasing temperature and increasing abundance of freshwater taxa at Rush Ranch. Periods of decreased temperature derived from southern Sierra Nevada tree-ring records (Scuderi 1993) correspond to an increase in the abundance of freshwater taxa at Rush Ranch.

Hughes and Brown (1992) and Hughes and others (1990) utilized giant sequoias [*Sequoiadendron giganteum* (Lindl.) Bucholtz] at low elevation sites to calibrate the tree-ring record with the Palmer Drought Severity Index. This tree-ring analysis indicated that short intervals (2 to 4 years) of low growth were common throughout the 2089-year record (1127 BC to AD 1989). Periods of substantially longer drought corresponded to intervals of decreased freshwater flow at Rush Ranch. Several intervals of extended drought occurred during the upper brackish interval. These intervals may be related to slight variations in the abundance of freshwater taxa at Rush Ranch. However, these slight variations may also suggest that the dominant control on water volume flowing through the Sacramento-San Joaquin Delta at the time was the input from the northern part of the watershed. The longest period of extended drought corresponds with the increase in freshwater flow that occurs before the Little Ice Age.

Earle (1993) developed precipitation records from northern and central California and a discharge record for the Sacramento River based on tree-ring analysis. Positive and negative precipitation anomalies in northern California more closely correspond to river discharge variations which, in turn, correspond closely with variations in the abundance of freshwater diatoms at Rush Ranch. The reconstructed precipitation record for central California shows similar variations, although some of the shorter fluctuations are absent. In some cases the magnitude of the anomalies in central California precipitation is less than that in northern California, suggesting that the predominant source of moisture at this time was the upper Sacramento basin. Graumlich (1987) extended the tree-ring record from California to Washington. In her southern valley region, which includes several sites in northern California, the most notable correlation with the Rush Ranch record is a large positive precipitation anomaly during the later half of the 19th century, which corresponds to an increase in freshwater taxa and the large negative anomaly between 1910 and 1935, which corresponds with a low abundance of freshwater taxa. It should be noted, however, that this correspondence may be tainted by human manipulation of the Sacramento River watershed.

Benson and others (1999; personal communication 2001) demonstrated a strong correlation between fluctuations in historic lake levels in northern Nevada and surface-water supply to the Sacramento-San Joaquin Delta. Applying these correlations to a 2,700-year long ^{18}O record from Pyramid Lake, Nevada, they described 18 cycles of lake level variation. A similar pattern in freshwater flow variation may be reflected in the data from Rush Ranch.

The lake level record from Mono Lake (Stine 1990) provides a 1,800-year chronicle of precipitation in the west-central Great Basin. During that time, six or seven high lake level stands were identified (Figure 4). High and low stands correlate, respectively, with some of the high and low abundances of freshwater taxa at Rush Ranch. The Marina Low Stand and Lee-Vining Delta Low Stands correlate well with the beginning and end of the upper brackish interval, and the Mill Creek-East High Stand correlate well with the later of the two intervals with a higher abundance of freshwater taxa. The Marina Low and Lee-Vining Delta Low stands correspond to the intervals of lowest freshwater diatom abundance in the Rush Ranch record. During the past 1,000 years, the five high stands at Mono Lake are higher than those that occurred during the previous 800 years; during the same interval the abundance of freshwater diatoms is greater than during the previous 1,200 years. The low stands are not as low as either the Marina Low or Lee-Vining Delta Low stands. The Historic High and Historic Low stands are difficult to identify due to the effect of post contact alteration of the drainage.

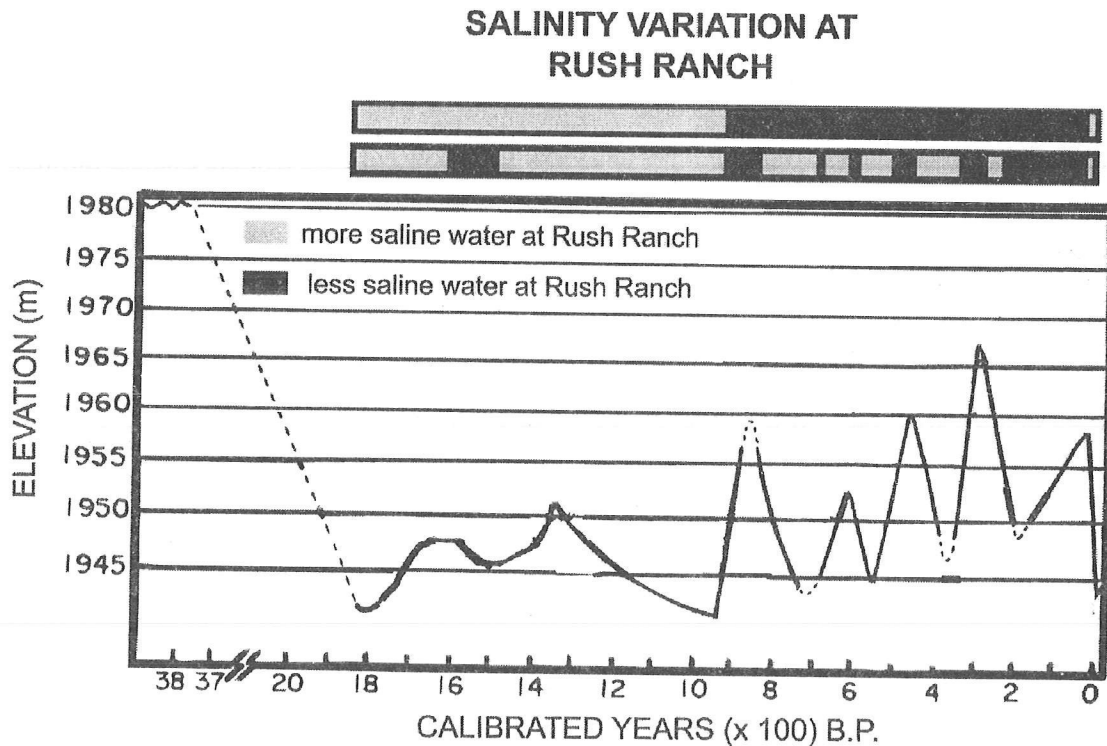


Figure 4 Variation in lake level at Mono Lake, California (modified from Stine 1990) compared with variation in fresh water diatom abundance at Rush Ranch

Conclusion

The diversity of the diatom flora at Rush Ranch is higher than previously reported for San Francisco Bay. There are two reasons for this: (1) previous studies were limited to marine and marginal marine environments which limited the number of taxa present and (2) one of the purposes of this study is to expand the knowledge of diatom diversity in San Francisco Bay. While it has been possible to increase the list of taxa found in San Francisco Bay, and most taxa can be assigned to a salinity preference based on the literature, the ecological significance of these taxa is not entirely clear. Detailed field information on present-day environmental preferences of these taxa, as well as determining what portion of the flora at each site is transported, will increase the value of environmental and climatic interpretations, enabling one to elucidate a possible climate record.

Comparison of the salinity-based discharge record for the Sacramento-San Joaquin river system indicates that diatoms are useful proxies for climate change in estuarine systems. High abundances of freshwater diatoms at Rush Ranch correspond to high lake levels at Mono Lake, and may also correspond to high lake levels at both Lake Tahoe and Pyramid Lake. There is also a strong correspondence between the tree-ring precipitation record and the discharge record. Discrepancies between the northern, southern, and coastal tree-ring records indicate that for the past 3,000 years most of the water flowing through the Sacramento-San Joaquin Delta originated in the Sacramento Basin.

At this stage, only a preliminary connection can be made between the fossils and regional-scale atmospheric processes. The two brackish intervals may represent intervals when the Aleutian low migrated further south and east, creating a wetter winter and spring. The opposite may be true during the more normal marine intervals when a stronger and more northerly Pacific high may have created relatively dry winter conditions.

Acknowledgments

I would like to thank John Barron for his continued support of my research in San Francisco Bay and Roger Byrne, Lynn Ingram, Frankie Malamud-Roam, and Mike May for their discussions on the vegetation and climate of the San Francisco Bay area. This scientific content and grammar of the manuscript were greatly improved as a result of reviews by John Barron and Mary McGann. This project is supported by the Earth Surface Dynamics Program of the U.S. Geological Survey.

References

- Atwater BF, Hedel CW, Helley EJ. 1977. Late Quaternary depositional history, Holocene sea-level changes, and vertical crustal movement, southern San Francisco Bay, California. U.S. Geological Survey Professional Paper 1014. 15 p.
- Benson L, Lund S, Paillet F, Kashgarian M, Smoot J, Mensing S, Dobb J. 1999. A 2800-year history of oscillations in surface-water supply to the central valley and to the bay area of northern California, and to the Reno-Sparks area of Nevada. EOS 80:F499-F500.

- Byrne R, Ingram BL, Starratt S, Malamud-Roam F, Collins JN, Conrad ME. 2001. Carbon-isotope, diatom, and pollen evidence for late Holocene salinity change in a brackish marsh in the San Francisco estuary. *Quaternary Research* 55:66–76.
- Cayan DR, Peterson DH. 1989. The influence of North Pacific atmospheric circulation on streamflow in the west. In: Peterson DH, editor. *Aspects of climate variability in the Pacific and the western Americas*. Geophysical Monograph 55. Washington, D.C.: American Geophysical Union. p 337–97.
- Cayan DR, Riddle LG, Aguado E. 1993. The influence of precipitation and temperature on seasonal streamflow in California. *Water Resources Research* 29:1127–40.
- Cayan DR, Dettinger MD, Diaz HF, Graham NE. 1998. Decadal variability of precipitation over western North America. *J Climate* 11:3148–66.
- Conomos TJ. 1979. Properties and circulation of San Francisco Bay waters. In: Conomos TJ, editor. *San Francisco Bay: the urbanized estuary*. San Francisco (CA): Pacific Division, AAAS. p 47–84.
- Cumming BF, Wilson SE, Hall RI, Smol JP. 1995. Diatoms from British Columbia (Canada) lakes and their relationship to salinity, nutrients and other limnological variables. *Bibliotheca Diatomologica* 31:1–207.
- Dettinger MD, Cayan DR. 1995. Large-scale atmospheric forcing of recent trends toward early snowmelt runoff in California. *J Climate* 8:606–23.
- Dettinger MD, Cayan DR, Diaz HF, Meko DM. 1998. North-South precipitation patterns in western North America on interannual-to-decadal timescales. *J Climate* 11:3095–3111.
- Dixit SS, Smol JP. 1994. Diatoms as indicators in the environmental monitoring and assessment program-surface waters (EMAP-SW). *Env Monit Assess* 31:275–306.
- Earle CJ. 1993. Asynchronous droughts in California streamflow as reconstructed from tree rings. *Quaternary Research* 39:290–9.
- Goman M, Wells L. 2000. Trends in river flow affecting the northeastern reach of the San Francisco Bay estuary over the past 7000 years. *Quaternary Research* 54:206–17.
- Graumlich LJ. 1987. Precipitation variation in the Pacific Northwest (1675–1975) as reconstructed from tree rings. *Ann Assoc Amer Geo* 77:19–29.
- Hughes MK, Brown PM. 1992. Drought frequency in central California since 101 B.C. recorded in giant sequoia tree rings. *Climate Dynamics* 6:161–7.
- Hughes MK, Richards BJ, Swetnam TW, Baisan CH. 1990. Can a climate record be extracted from giant sequoia tree rings? In: Betancourt JL, MacKay AM, editors. *Proceedings of the Sixth Annual Pacific Climate (PACLIM) Workshop*; 5–8 Mar 1989; Asilomar, California. Interagency Ecological Studies Program Technical Report 23. Sacramento (CA): California Department of Water Resources. p 111–4.
- Ingram BL, DePaolo DJ. 1993. A 4300-year strontium isotope record of estuarine paleosalinity in San Francisco Bay, California. *Earth Planet Sci Lett* 119:103–19.

- Ingram BL, Ingle JC, Conrad ME. 1996a. A 2000 yr record of Sacramento-San Joaquin River inflow to San Francisco Bay estuary, California. *Geology* 24:331-4.
- Ingram BL, Ingle JC, Conrad ME. 1996b. Stable isotope record of late Holocene salinity and river discharge in San Francisco Bay, California. *Earth Planet Sci Lett* 141:237-47.
- Laws RA. 1988. Diatoms (Bacillariophyceae) from surface sediments in the San Francisco Bay estuary. *Proc Cal Acad Sci* 45:133-254.
- Lehman PW. 1992. Environmental factors associated with long-term changes in chlorophyll concentration in the Sacramento-San Joaquin Delta and Suisun Bay, California. *Estuaries* 15:335-48.
- Lehman PW. 1997. The influence of climate on phytoplankton communities in the upper San Francisco estuary. In: Isaacs CM, Tharp VL, editors. *Proceedings of the Thirteenth Annual Pacific Climate (PACCLIM) Workshop*; 15-18 Apr 1996; Asilomar, California. *Interagency Ecological Program Technical Report 53*. Sacramento (CA): California Department of Water Resources. p 105-120.
- Lehman PW. 2000a. Phytoplankton biomass, cell diameter, and species composition in the low salinity zone of northern San Francisco Bay estuary. *Estuaries* 23:216-30.
- Lehman PW. 2000b. The influence of climate on phytoplankton community biomass in San Francisco Bay estuary. *Limnol Oceanog* 45:580-90.
- Lehman PW, Smith RW. 1991. Environmental factors associated with phytoplankton succession for the Sacramento-San Joaquin Delta and Suisun Bay estuary, California. *Estuarine, Coastal and Shelf Science* 32:105-128.
- May MD. 1999. Vegetation and salinity changes over the last 2000 years at two islands in the northern San Francisco estuary, California [MA thesis]. Available from the University of California, Berkeley. 54 p.
- Nichols FH, Cloern JE, Luoma SN, Peterson DH. 1986. The modification of an estuary. *Science* 231:567-73.
- Nigam S, Barlow M, Berbery EH. 1999. Analysis links Pacific decadal variability to drought and streamflow in United States. *EOS* 80:61.
- Peterson DH, Cayan DR, Festa JF, Nichols FH, Walters RA, Slack JV, Hager SE, Schemel LE. 1989. Climatic variability in an estuary: effects of river flow on San Francisco Bay. In: Peterson DH, editor. *Aspects of climate variability in the Pacific and the western Americas*. *Geophysical Monograph* 55. Washington, D.C.: American Geophysical Union. p 419-442.
- Schonher T, Nicholson SE. 1989. The relationship between California rainfall and ENSO events. *J Climate* 2:1258-69.
- Schrader H, Gersonde R. 1978. Diatoms and silicoflagellates. In: Zachariasse WJ and others, editors. *Micropaleontological counting methods and techniques—an exercise on an eight meter section of the lower Pliocene of Capo Rosselo, Sicily*. *Utrecht Micropaleontology Bulletin* 17. Utrecht, The Netherlands: University of Utrecht. p 129-76.
- Scuderi LA. 1987a. Late-Holocene upper timberline variation in the southern Sierra Nevada. *Nature* 325:242-4.

2001 PACLIM Conference Proceedings

- Scuderi LA. 1987b. Glacier variations in the Sierra Nevada, California, as related to a 1200-year tree-ring chronology. *Quat Res* 27:220–31.
- Scuderi LA. 1993. A 2000-year tree ring record of annual temperatures in the Sierra Nevada mountains. *Science* 259:1433–6.
- Snoeijs P, editor. 1993. Intercalibration and distribution of diatom species in the Baltic Sea, volume 1. The Baltic Marine Biologists Publication nr. 16a. Uppsala: Opulus Press. 130 p.
- Snoeijs P, Balashova N, editors. 1998. Intercalibration and distribution of diatom species in the Baltic Sea, volume 5. The Baltic Marine Biologists Publication nr. 16e. Uppsala: Opulus Press. 144 p.
- Snoeijs P, Kasperovičienė J, editors. 1996. Intercalibration and distribution of diatom species in the Baltic Sea, volume 4. The Baltic Marine Biologists Publication nr. 16d. Uppsala: Opulus Press. 126 p.
- Snoeijs P, Potapova M, editors. 1995. Intercalibration and distribution of diatom species in the Baltic Sea, volume 3. The Baltic Marine Biologists Publication nr. 16c. Uppsala: Opulus Press. 126 p.
- Snoeijs P, Vilbaste S, editors. 1994. Intercalibration and distribution of diatom species in the Baltic Sea, volume 2. The Baltic Marine Biologists Publication nr. 16b. Uppsala: Opulus Press. 126 p.
- Starratt SW, Wan E. 1998. Diatom evidence for fluctuations in the freshwater budget of northern San Francisco Bay, CA: a 3,000 year record. *Geological Society of America Abstracts with Programs* 30:A–285.
- Stine S. 1990. Late Holocene fluctuations of Mono Lake, eastern California. *Palaeogeography, Palaeoclimatology, Palaeoecology* 78:333–81.
- Stoermer EF, Smol JP, editors. 1999. *The diatoms: applications for the environmental and earth sciences*. Cambridge (UK): Cambridge University Press. 469 p.
- Wells LE, Goman M. 1995. Late Holocene environmental variability in the upper San Francisco estuary as reconstructed from tidal marsh sediments. In: Isaacs CM, Tharp VL, editors. *Proceedings of the Eleventh Annual Pacific Climate (PACLIM) Workshop; 19-22 Apr 1994; Asilomar, California*. Interagency Ecological Program Technical Report 40. Sacramento (CA): California Department of Water Resources. p 185–98.
- Whitmore TJ. 1989. Florida diatom assemblages as indicators of trophic state and pH. *Limnol Oceanogr* 34:882–95.

Abstracts

Abstracts for PACLIM 2001
Asilomar Conference Grounds
Pacific Grove, California
March 18–21, 2001

Holocene Evolution of the Coastal Upwelling System in the Northern California Region

John A. Barron¹, Linda Heusser², Timothy Herbert³, and Mitch Lyle⁴

¹U.S. Geological Survey, Menlo Park, California

²100 Clinton Road, Tuxedo, New York

³Dept. Geological Sciences, Brown University, Providence, Rhode Island

⁴CGISS, Boise State University, Boise, Idaho

Ocean Drilling Program Site 1019 (41.682°N, 124.930°W, 980 m water depth), located 70 km off Eureka, California, contains an excellent Holocene record of wind-driven coastal upwelling near the boundary between the subtropical and subpolar gyres of the northeastern Pacific. Six AMS dates on benthic foraminifers recovered from ODP 1019 establish a Holocene sedimentation rate of ca. 41 cm/kyr, making it an excellent section for studying Holocene climatic variation.

Alkenone-based SST data and relative abundance data of the gyre-related diatom *Pseudoennotia doliolus* together suggest that the mid Holocene interval between ca. 8000 and 3200 cal yr B.P. was characterized by cooler and less variable fall and wintertime SSTs than the earlier and later parts of the Holocene. An abrupt 3-fold increase in percent *P. doliolus* and a permanent ca. 1 °C increase in proxy alkenone SSTs are evidence that a warming of fall and winter SSTs occurred at ca. 3200 cal yr B.P. Proxy opal data indicates that diatom productivity may have increased by as much as 50% also at ca. 3200 cal yr B.P., signaling an increase in spring-summer coastal upwelling. Although pollen from redwood (*Sequoia sempervirens*), which is indicative of the fog associated with coastal upwelling, displays an earlier initial increase in relative abundance beginning at ca. 5000 cal yr B.P., peak abundances (25%-30%) of redwood alternating in high amplitude cycles with pine only occur after ca. 3300 cal yr B.P. The modern maritime climate of the northern California coastal region with cool, coastal upwelling-dominated summers and relatively warm, wet winters evolved during the late Holocene (between ca. 5000 and 3200 cal yr B.P.), presumably in response to insolation-driven atmospheric changes. The onset of modern oceanographic conditions with steep east-west SST gradient developing during the late summer and early fall would have made the region increasingly sensitive to ENSO and related Pacific Decadal Oscillations.

Multidecadal and Multicentennial Droughts Affecting Northern California and Nevada: Implications for the Future of the West

Larry Benson¹, Michael Kashgarian², Steve Lund³, and Fred Paillet⁴

¹U.S. Geological Survey, Boulder, Colorado

²Lawrence Livermore National Laboratory, Livermore, California

³Dept. of Earth Sciences, University of Southern California, Los Angeles

⁴U.S. Geological Survey, Lakewood, Colorado

Continuous, high-resolution $\delta^{18}\text{O}$ records from cored sediments of Pyramid Lake, Nevada, indicate that oscillations in the hydrologic balance occurred, on average, about every 150 yr during the past 7630 calendar years (cal yr). The records are not stationary; e.g., during the past 2740 yr, drought durations ranged from 20 to 100 yr and intervals between droughts ranged from 80 to 230 yr. Comparison of tree-ring-based reconstructions of climate change for the past 1200 yr from the Sierra Nevada and the El Malpais region of northwest New Mexico indicates that severe droughts associated with Anasazi withdrawal from Chaco Canyon at 820 B.P. and final abandonment of Chaco Canyon, Mesa Verde, and the Kayenta area at 650 B.P. may have impacted much of the western United States.

Between $\sim 6,300$ and $\sim 3,430$ cal yr B.P., the mean $\delta^{18}\text{O}$ value of CaCO_3 precipitated from Pyramid Lake was 1.6 ‰ less than the mean $\delta^{18}\text{O}$ value of CaCO_3 precipitated after that time. Calculations show that a $\geq 30\%$ reduction in “wetness” of the Sierra Nevada during the mid Holocene would have caused Lake Tahoe to fall below its sill depth, eliminating a source of ^{18}O -enriched water to the Truckee River. Numerical simulations of the response of Pyramid Lake $\delta^{18}\text{O}$ to hydrologic closure of Lake Tahoe indicate a 0.6 ‰ decrease in the steady state $\delta^{18}\text{O}$ value of Pyramid Lake water relative to the results of calculations using pristine mean-historical hydrologic inputs. The 1.0‰ residual can be accounted for if the late-Holocene period was, on average, somewhat drier than the last 100 yr and/or if 6,300 and 3,430 cal yr B.P. period autumns were $\sim 5^\circ\text{C}$ warmer than autumns during the past 2,740 yr. The most probable cause of the shift in $\delta^{18}\text{O}$ was a transition to a wetter and cooler climate.

Tropical Treelines and Tree Rings in the North American Monsoon Region

Franco Biondi and Rebecca Van Lieshout

Dept. of Geography, University of Nevada, Reno, Nevada

Instrumental records for the American Tropics are limited to the last century and are continuous only at few selected locations. Proxy climatic records of longer duration with annual resolution and exact dating are rare, mostly because tropical tree species often form either unclear or undatable growth rings. However, trees at the highest elevations experience much stronger seasonality and form clear growth layers. We provide here an update on the tree-ring chronology for *Pinus hartwegii* from Nevado de Colima, at the western end of the Mexican Neovolcanic Belt. Out of 128 specimens collected from 49 trees, a total of 79 segments from 30 trees have been visually and numerically crossdated. The

Nevado de Colima tree-ring chronology is well replicated from 1600 to 1997. From 1949 to 1997, the main dendroclimatic signal is June precipitation, which marks the beginning of the monsoon season. Additional investigations on densitometric parameters has been recently completed, and stable isotopic studies are underway. This presentation will describe ongoing activities and future plans for expanding tropical treeline dendrochronology in North America.

Climatic Influences on TMDL Measures of Suspended Sediment Loading in Tributaries of Lake Tahoe

Douglas P. Boyle and John C. Tracy
Div. of Hydrologic Sciences, Desert Research Institute, Reno, Nevada

Measures such as the Total Maximum Daily Load (TMDL) are used, or proposed for use, throughout the country to implement existing or proposed water quality improvements. In this study, we investigate the impact of climate on the efficacy of TMDL measures of daily-suspended sediment loadings in several tributaries of Lake Tahoe. Specifically, relationships between the daily streamflow, daily-suspended sediment loading, and seasonal/annual precipitation (rain and snow) are developed for characteristic periods of watershed behavior (e.g., spring snowmelt, summer base flow, fall and winter precipitation events, etc.). Finally, different TMDL measures are evaluated in terms of the characteristic periods for different climate scenarios (e.g., wet year, dry year, etc.).

Differing Effects of Holocene Insolation Change Across a Climatic Boundary in the Northern Rocky Mountains

Andrea Brunelle-Daines and Cathy Whitlock
Dept. of Geography, University of Oregon, Eugene

Pollen and charcoal records from the northern Rocky Mountains (NRM) of Idaho and Montana provide an opportunity to study the vegetation, fire, and climate history of the last 16,000 years. The NRM are characterized by steep topographic and climatic gradients. One of the most distinctive climatic gradients is the boundary between summer-wet and summer-dry precipitation regimes. Sites west of the Bitterroot crest generally experience drier summers than those to the east, due to the strong influence of the northeast Pacific subtropical high. Eastern sites receive more summer precipitation from recirculated monsoonal moisture. The vegetation and fire history of Burnt Knob Lake (BKL) (summer-dry), Lost Trail Pass Bog (LTPB) (Mehring and others 1977) (summer-wet), and Baker Lake (BL) (summer-dry) were compared to determine the effects of changing summer insolation on regional climate patterns in the Holocene. Preliminary analysis of the data from LTPB and BKL suggest that the vegetation and fire histories are generally similar. However, the timing of the vegetation/fire frequency shifts in the early Holocene is slightly different. High percentages of xerothermic taxa and elevated fire frequencies at BKL ca. 9,000 cal yr B.P. are probably a result of the intensified subtropical high during the summer insolation maximum. At LTPB, a warm and wet early Holocene (ca. 9000 cal yr B.P.) may be a result of a stronger-than-present monsoonal precipitation. These Holocene variations in climate history may result from the trade-off between the two

precipitation regimes and their registration on a complex landscape. The results, which are similar to those described in Yellowstone by Whitlock and Bartlein (1993), suggest that spatial heterogeneity is an important component of Holocene climate records of the western U.S. The addition of data from BL, a spatially and climatically intermediate site, will better define the response of climate to changing Holocene insolation.

Establishing High-Resolution Holocene Climate Records in the Sierra Nevada, California

Douglas H. Clark

Geology Dept., Western Washington University, Bellingham, Washington

Studies that integrate alpine glacier reconstructions and lake sedimentation, paleomagnetism, geochemistry, and palynology provide new opportunities to test concepts in regional paleoclimate change in the Sierra Nevada and throughout the mountains of western North America. In particular, new correlation tools for these records may help establish high-resolution linkages with other records in the region, and perhaps with some global records.

Whereas moraines alone preserve only "snapshots in time" of climate extremes, alpine lake sediments preserve continuous sedimentologic, geochemical, and ecological records of past climate change. Variations in moisture delivery and temperature affect the size (and consequent sediment output) of adjacent glaciers, the rates of soil formation and erosion, and the vegetation communities existing in these alpine settings. Clastic sediments in alpine lake cores from below modern glaciers in the Sierra Nevada suggest that the range was dominated by warm, non-glacial conditions for the early and middle Holocene. Starting about 3600-3200 ^{14}C yr B.P. (~3900-3400 cal yr B.P.), increases in fine clastic silt indicate onset of glacier growth. Glaciers appear to have advanced episodically for the remainder of the Holocene. However, they did not reach their Holocene maxima until the late Little Ice Age (i.e., the last 200-300 yrs). These cores do not show evidence during the last millennium for the extreme droughts documented elsewhere in the range (e.g., Stine 1994). Several planned coring sites should yield higher-resolution records of Holocene climate change in the Sierra Nevada.

It is important to note that recent advances in paleomagnetic analytic techniques allow measurement of past changes in geomagnetic field strength, inclination, and declination (secular variation) recorded in alpine lake sediments. These records offer a promising means to establish continuous, high-resolution chronologies and regional correlations between climatic events preserved in lake sediments. Such correlations are crucial to test linkages, leads and lags between regionally mapped glacial advances and other proxy records related to regional climate patterns. Preliminary analyses of secular variation in lake cores from the North Cascades show strong promise for using this approach elsewhere in western North America.

Experimental Seasonal Forecast of Monsoon Precipitation in Arizona

Andrew C. Comrie and Tereza Cavazos

Dept. of Geography and Regional Development, University of Arizona, Tucson Arizona

Stepwise regression and artificial neural networks are used to produce experimental forecasts of an index of all Arizona precipitation for the monsoon season (Jul-Sep). Predictor variables consist of 3-month, moving cool-season (Nov-Apr) precipitation, sea surface temperature (SST) indices from the eastern and north Pacific and the western and North Atlantic ocean, and two teleconnection indices: the Pacific/North America (PNA) and the Pacific decadal oscillation (PDO). The results indicate that a strong meridional SST gradient in the western Pacific (cold to the north, warm to the south, similar to a positive PDO) and positive SST anomalies over the North Atlantic ocean during winter (especially if they persist into the spring season) tend to be associated with wet monsoons in Arizona. The forecast for the 2000 monsoon season was close to average precipitation, which was better than the above normal precipitation forecast issued by the Climate Prediction Center (CPC), whose forecast for the Southwest may rely too heavily on ENSO conditions.

Vegetation and Climate Change in Central Mexico During the Last 2,000 Years: Implications for Understanding Meso-American Prehistory

Maria Elena Conserva and Roger Byrne

Dept. of Geography, University of California, Berkeley, California

Analysis of a 1700 year core from Laguna Atezca, near Molango, Hidalgo provides new insight into the environmental and cultural history of the eastern central highlands of Mexico. In particular, the record provides support for Pedro Armillas' 1969 hypothesis that the position of the northern frontier of Mesoamerica (the interface between nomadic hunter-gatherers and sedentary farmers) was more controlled by climate than by cultural dynamics. Pollen, microscopic charcoal, sediment chemistry, loss on ignition, and magnetic susceptibility were analyzed. Four conventional ^{14}C dates provide chronological control. Three phases of human occupation, deforestation, and erosion alternate with two phases of abandonment. Changes in forest composition during the abandonment phases provide climatic information. Humid conditions between A.D. 900-1075 are indicated by the dominance of the cloud forest taxa (*Liquidambar*, *Ostrya/Carpinus*, *Ulmus*, etc.). After A.D. 1075, conditions were drier as evidenced by the increased importance of pine and oak.

Glacial/Interglacial Contrasts in Productivity and Oxygen Deficiency on the Margins of the Californias

Walter E. Dean
U.S. Geological Survey, Denver, Colorado

The production and accumulation of organic matter on the continental shelf and upper continental slope (200-2700 m) off southern Oregon, California, and Baja California was markedly different during the last glacial interval (ca. 24-10 ka) than either the Holocene or last interstadial (oxygen-isotope stage 3, ca. 60-24 ka). In general, organic productivity on these margins was higher during the Holocene and stage 3 than during the last glacial interval, and this contrast is greatest off southern California and Baja California. This glacial/interglacial pattern in productivity is in contrast to the commonly held view that productivity in the world ocean was higher during the last glacial interval (e.g. Sarthstein and others 1988). However, this latter conclusion is based mainly on data from the eastern equatorial Pacific and off northwest Africa. Highest productivity on the margins of the Californias over the last 60 ky occurred during certain intervals within oxygen-isotope stage 3 when organic-rich, laminated sediments accumulated within the present oxygen-minimum zone on the upper continental slope from as far north as the Oregon-California border to as far south as the tip of Baja California and the adjacent margin of NW Mexico. These upper Pleistocene laminated sediments, interbedded with bioturbated sediments, contain more abundant hydrogen-rich (type II), marine algal organic matter than even surface sediments with large amounts of labile, marine organic matter. The stable carbon-isotopic composition of the organic matter does not change with time between bioturbated and laminated sediments, indicating that the greater abundance of type II organic matter in the laminated sediments is not due to a change in source but rather represents a greater degree of production and preservation of marine organic matter. The laminated, and even some non-laminated, stage-3 sediments contain high concentrations of molybdenum (Mo) and other redox-sensitive trace elements, suggesting that bottom waters were sulfidic. The presence of organic- and Mo-rich, laminated sediments indicates that the oxygen minimum zone in the northeastern Pacific Ocean was more intense and probably anoxic during the late Pleistocene as a result of increased coastal upwelling that enhanced algal productivity.

Seasonal, Interannual, and Trending Pattern of Global Atmospheric Water-Vapor Transport, 1948-2000

Michael Dettinger
U.S. Geological Survey, San Diego, California

The global hydrologic influences of the climatic seasonal cycle, interannual variations, and trends are transmitted, in part, by changes in the directions and intensities of atmospheric transports of water vapor from regions of net evaporation to regions of net precipitation. Average variations of the vertically integrated vapor transport associated with the seasonal cycle, the El Niño-Southern Oscillation (ENSO), North Pacific climate variations [e.g., the Pacific Decadal Oscillation (PDO)], and net climate trends since 1948 are illustrated in this poster. Atmospheric water-vapor transports

were computed by vertically integrating, and then seasonally averaging, the products of daily (vector) winds and water-vapor mixing ratios between eight levels in the atmosphere from the surface to the 300-hPa pressure level, using $2.5^\circ \times 2.5^\circ$ gridded fields from the National Centers for Environmental Prediction's (NCEP) reanalysis project. Monthly evaporation-minus-precipitation values also were computed from the Reanalysis dataset and plotted beneath the transport vectors to delineate the changing regions of net evaporation (from which vapor transports emerge) and regions of net precipitation (to which transports converge) associated with the seasonal cycle, interannual variations, and trends.

Considering the long-term average seasonal cycle, large changes in vapor transport over the Asian monsoon regions are perhaps the most notable feature. On interannual and longer time scales, the average northern winter and spring vapor-transport changes associated with the warm (El Niño) phase of ENSO and the El Niño-like phase of PDO are characterized by pronounced anomalous cyclonic vapor transport around the Aleutian Low over the central North Pacific (amounting to about $\pm 10\%$ of the average vapor transports). Also during the El Niño phases of ENSO and PDO, vapor transports out of the tropics into the Northern Hemisphere are enhanced over the South China Sea and the Caribbean. Elsewhere transports between the tropics and extratropics are either little changed or exhibit enhancements of the transports from the extratropics into the tropics (especially from the Southern Hemisphere) towards the zones of anomalous convective precipitation over the warm waters of the El Niño region and equatorial Indian Ocean. For El Niño conditions, during northern summer, enhanced vapor transports out of the tropics into the continental monsoon regions are a notable feature. The most notable trends during the last 50 years are increasing vapor transport out of the Sahel, out of southern and eastern Asia (associated with the Indian monsoon), and less so into the North American monsoon region, with possible increases in the westerly circulation of vapor over the Antarctic Ocean.

Teleconnectivity of Monsoon Rainfall in Mexico During Positive and Negative Phases of the Pacific Decadal Oscillation

Arthur V. Douglas and Phillip J. Englehart

Environmental and Atmospheric Sciences Dept., Creighton University, Omaha, Nebraska

A 71-year record of monthly precipitation data for Mexico has been assembled. Five separate regions of coherent summer rainfall have been identified using an oblique principal component analysis. Long-term decadal scale variations and trends in the rainfall data are noted. Because of these long-term fluctuations, we decided to explore the possibility that the Pacific Decadal Oscillation (PDO) may be contributing to the observed decadal scale fluctuations in rainfall. The regional rainfall data sets were partitioned according to the phase of the PDO: positive phase 1927-46 and 1977-97 and negative phase 1947-76. We performed a series of parallel correlation experiments between the PDO partitioned rainfall and key ocean-atmosphere variables. Correlations are strongest during the positive phase of the PDO. Specific variables that show high connectivity include ENSO (-0.56) and a Western Hemisphere Subtropical Anticyclone Index (0.64). In contrast, during the negative phase of the PDO local climate indices become prominently correlated with Mexican region rainfall. Variables with significant correlation with Mexican rainfall during the negative phase of the PDO include SST's in the Caribbean (0.50), Gulf of Mexico (-0.38) and Baja California (0.39). ENSO and SLP in the

South Pacific High show minimal correlation with regional rainfall during the negative phase of the PDO. Given the potential phase-locking of El Niño with the positive phase of the PDO, it is not too surprising that large-scale teleconnection points are prominent predictors of rainfall during the positive phase of the PDO. In contrast, during the negative phase of the PDO, local forcing mechanisms begin to play a role in the modulation of summer rainfall in Mexico.

Late Holocene Ocean-Climate Variations in Alfonso Basin, Gulf of California, Baja California Sur, Mexico

Robert G. Douglas, Donn S. Gorsline, and Alessandro Grippo
Dept. of Earth Sciences, University of Southern California, Los Angeles, California

Laminated hemipelagic sediments in Alfonso Basin, a small silled depression located near La Paz in the Gulf of California, were analyzed using sediment microfibrils, carbonate content, microfossils and stable isotopes to examine high-resolution ocean-climate variations of the past 8000 yr B.P. The record suggests small but important variations in surface productivity and climate related to shifts in the intensity of the monsoonal system in the Gulf.

A period of strong upwelling and a cooler and drier climate occurred between about 140 to 4000 (radiocarbon) yrs B.P. Sediments are well laminated (types 2 and 3A) with a higher organic-carbon (6%-8% total organic carbon, TOC) and variable but low carbonate content (0%-15%). Microfossil preservation is generally poor but when preserved fossil plankton are dominated by upwelling species (e.g. *Globigerina bulloides* and radiolaria indicative of nutrient-rich subsurface waters; Perez-Cruz 1999). Sediment microfibrils, horizontal microburrows and benthic foraminifera indicate dysoxic (< 0.2 ml O_2/L) bottom waters filled the basin. Accumulation rates vary between 0.5 to 0.8 mm/yr except for a short interval of intense lamination (type 2) about 2500 yr B.P. when rates reached 1.0 mm/yr. This event appears correlative with the rapid increase in biogenic silica and spring upwelling in the Guaymas basin (Barron 2000). The frequency of turbidite/flood layers is low throughout the period. About 140 yr B.P., roughly at the end of the Little Ice Age, surface productivity appears to have slackened. Bottom water oxygen increases, sediments become bioturbated, accumulation rates decrease significantly, and carbonate content and preservation increases.

Between 4500 yr B.P. and about 8000 yr B.P., the sediment and microfossil record suggests warmer and wetter conditions with less intense upwelling and/or lower surface productivity. Sediments have a lower TOC (4%-6%) and higher carbonate content (5%-25%) with significantly better microfossil preservation. Benthic foraminifera and sediment microfibrils with vertical microburrows indicate bottom waters were generally suboxic (> 0.2 ml O_2/L). Tropical plankton (diatoms, radiolaria and foraminifera) is common and frequently abundant. Except for two intervals (3800-4500 and 5000-5500 yr B.P.), sediments are poorly laminated or bioturbated (types 3B and 4). Turbidite/flood layers are common and increase in frequency prior to about 6000 yr B.P.

Spectral analysis of lamination patterns based on sediment X-rays and carbonate content reveal common frequencies at 300, 750, and 900 yr. Within the most intensely laminated sequences at 2500 and 4000 yr B.P., strong frequencies occur at 300 yr, a cluster of frequencies around 100 and 30 yr and low power but recurrent frequencies at 9-11 yr and 4-7 yr.

Support for Tropically Driven Pacific Decadal Variability Based on Paleoproxy Evidence

Michael N. Evans¹, Mark A. Cane², Daniel P. Schrag¹, Alexey Kaplan², Braddock K. Linsley³, Ricardo Villalba⁴, and Gerald M. Wellington⁵

¹Dept. of Earth and Planetary Sciences, Harvard University, Cambridge, Massachusetts

²Lamont Doherty Earth Observatory, Palisades, New York

³Dept. of Earth and Atmospheric Sciences, State University of New York, Albany

⁴Laboratorio de Dendrochronologia e Historia Ambiental, IANIGLA, Mendoza, Argentina

⁵Dept. of Biology and Biochemistry, University of Houston, Texas

The causes of Pacific decadal climate variability (termed here PDV) are the subject of much debate. Is PDV generated in the North Pacific? Or is PDV a basin-wide pattern of variability, originating in tropical phenomena? Resolving the processes controlling PDV is important for predicting socially important downstream effects on Pacific fisheries and water resources in the arid western states.

Two independent paleoproxy estimates of the basin-scale phenomenon—one oceanographic and from the south Pacific, the other terrestrial and from both hemispheres—confirm a statistically significant link between tropical and extratropical Pacific decadal SST variability over two centuries. An ENSO-like pattern of SST anomalies, symmetric about the equator, explains the simultaneous coherency of the proxy data. The result supports the idea that Pacific decadal variability is a basin-wide phenomenon originating in the tropics.

Tree-Ring Records of Drought and Temperature Spanning the Last 1000 Years from the Bighorn Basin Region, Wyoming

C. L. Fastie¹, S. T. Gray², J. L. Betancourt³, and S. T. Jackson²

¹Dept. of Biology, Middlebury College, Middlebury, Vermont

²Dept. of Botany, University of Wyoming, Laramie

³U.S. Geological Survey Desert Laboratory, Tucson, Arizona

Ring-width chronologies from three tree species (*Pinus flexilis*, *P. ponderosa*, *Pseudotsuga menziesii*) at three sites at the lower forest border on the western flanks of the Bighorn Mountains provide 500-1000 year proxy records of regional drought. An additional chronology from *Picea engelmannii* at upper treeline in the Bighorn Range records regional temperature. The lower-treeline records indicate multiple severe droughts spanning several decades; most of these droughts correspond to droughts documented from the northern Great Plains region. A spectral peak at 51 years indicates quasiperiodic nature of droughts in the region. Together, the upper and lower treeline records indicate extended (multidecade) cool, wet episodes during the late 18th and early 19th centuries.

The Impacts of Current and Past Climate on Pacific Gas & Electric's 2001 Hydroelectric Outlook

Gary J. Freeman

Pacific Gas & Electric Company, San Francisco, California

California is currently experiencing the impact of daily energy shortages. Both the lack of normal precipitation this year to date and the low elevation freezing levels associated with this year's December and January storms have left PG&E's reservoirs at or below their normal minimum winter operating levels. There is increased impact and risk of energy shortages in California during years when the northwest's Columbia River Basin and California experience unusually dry conditions together. That is the case this year. The northwest is experiencing below normal precipitation with very limited energy available for California. For PG&E, available water from surface reservoirs for hydro generation is near-zero while we wait for rain and spring snowmelt runoff to begin. During late December, January, and early February, approximately 65% of PG&E's daily hydro generation, which averaged about 22 GWh/day in January from all PG&E hydro sources, was from springs in the Pit/McCloud, Cow/Battle, and Lake Almanor watersheds. The remaining approximately 35% hydrogeneration was mostly from surface storage drawdown. Since more than 40% of PG&E's normal year hydro generation comes from watersheds with significant aquifer outflow, the state of the aquifers as a reflection of past climatic variation is an important part of California's energy picture. These springs are anticipated to provide a relatively "firm" annual output this year in excess of 5,400 GWh, about 1,400 MW daily peaking capability, and nearly 3 million acre-feet of "firm" water regardless of current climatic dryness. The springs in northern California have increased in sustained outflow during the past several wet years, beginning with 1995. However they may now be about to begin a multiyear decline, possibly the result of piezometric head dropping up slope of their surface outlets. The outflows from these aquifers reveal both short term cycling and longer term trending. During very dry years, this contribution of past wetness assumes a greater relative contribution in both sustained energy production and water availability into the Sacramento River.

Multi-Decadal Variability of Precipitation in the Greater Yellowstone Region as Inferred from Tree Rings

Lisa J. Graumlich and Jeremy Littell

Mountain Research Center, Montana State University, Bozeman Montana

Recently discovered long (1000+ years) tree-ring records from the Greater Yellowstone Region (GYR) are relevant to the larger effort to understand the patterns and causes of Pacific climate variability. The GYR is one of the few places in the world where we can develop a strongly replicated, multi-species network of long tree-ring series that are sensitive to winter precipitation. Interannual and decadal-scale variation in winter precipitation and snowpack in the GYR exhibits patterns that are strongly coherent with variability in the Pacific Northwest. The regional snowpack anomaly patterns are, in turn, associated with regional- to hemispheric-scaled atmospheric circulation patterns. As such, a strong potential exists for using the GYR data to reconstruct 1000+ year histories of key

multi-decadal atmospheric circulation patterns such as the Pacific Decadal Oscillation. Our preliminary analyses provide evidence for a shift from predominantly decadal-scale variability in GYR precipitation prior to A.D. 1200 to predominance of century-scale variability in earlier centuries.

Wind Stress Curl and Ocean Conditions in the Northeast Pacific: A Mechanism for Ocean Climate Change

P. Green^{1,2}; F. Schwing¹; and T. Murphree^{1,3}

¹PFEL, NOAA, NMFS, Pacific Grove, California

²Joint Institute of Marine and Atmospheric Research, Honolulu, Hawaii

³The Naval Postgraduate School, Monterey, California

Wind stress and wind stress curl strongly shape upper ocean conditions in the North Pacific on a full range of time scales. The NCEP reanalysis of surface daily winds has been processed to define climatologies and monthly values and anomalies of wind stress curl over the Pacific Basin. Prior work by Bakun and Nelson have shown that cyclonic wind stress in coastal regions coupled with alongshore equatorward flow can affect upwelling and therefore coastal temperatures, stratification, and productivity. By comparing the evolution of wind stress and curl to SST and subsurface temperature we are able to investigate the impact of Ekman processes and the seasonal progression of ocean conditions.

Climatologies show zonal bands of positive curl from the equator to 20N (20S) in winter (summer) and from 20N (20S) to 35N (35S) in summer (winter). From climatologies, the time of maximum annual wind curl occurs later in the season with distance from the equator along the West Coast of North America from spring to fall and for South America summer to winter. Isotherms shoal seasonally in response to the annual wind curl cycles. The relationships between wind curl stress and SST in an El Niño phase appear to be opposite those of a La Niña phase. Because the ocean response to atmospheric forcing is “dynamically similar” on annual and longer periods, the seasonal evolution of the wind field and the ocean’s response will provide insight on the development of ocean anomalies during extreme events such as El Niño and decadal oscillations.

A Process Model of Tree-Ring $\delta^{13}\text{C}$, $\delta^{18}\text{O}$, and δD Applied to 20th Century Ponderosa Pine Growth in Southern Arizona

Debbie Hemming¹, Harold Fritts¹, Steven Leavitt¹, William Wright¹, Alexander Shashkin², and Austin Long³

¹Laboratory of Tree-Ring Research, University of Arizona, Tucson

²Institute of Forest, Russian Academy of Science, Krasnoyarsk, Russia

³Dept. of Geosciences, University of Arizona, Tucson

Theoretical equations of $\delta^{13}\text{C}$, $\delta^{18}\text{O}$ and δD fractionation in C3 plants have been integrated with the TreeRing3 process model to better understand the biological processes that link daily climatic fluctuations with tree-ring growth and isotope composition. In particular, the aim of including isotopes was to provide insight into the timing and rate of partitioning of photosynthate and starch among storage or growth sinks.

The model has been tuned and parameterized using data from *Pinus ponderosa* trees growing in the Santa Catalina Mountains, just north of Tucson, Arizona, for 1900-1999. These trees were chosen because their ring structure exhibits a marked growth reduction ("false latewood" band) caused by pronounced dry conditions prior to summer monsoonal precipitation. As the timing of monsoon initiation is reasonably consistent (first week in July) this is a good time marker for intra-ring analyses. Daily meteorological data for a station approximately 3 km northwest of the study site are used to drive equations that regulate tree functional processes, including soil moisture, transpiration, photosynthesis, carbohydrate allocation, and cambial activity.

Observed inter and intra-annual variations in the $\delta^{13}\text{C}$, $\delta^{18}\text{O}$ and δD compositions of leaf and tree-ring material are compared with modeled compositions. In particular, the reason why theoretical estimates of the isotopic composition of presently formed photosynthate do not adequately explain the actual measured observations is examined. During the growth season the modeled $\delta^{13}\text{C}$, $\delta^{18}\text{O}$ and δD compositions of presently formed photosynthate are typically more enriched in the heavier isotopes than the equivalent compositions of stored starch. This is because the starch pool is dominantly accumulated during the autumn when moisture stress is at a minimum and fractionation by carboxylation reactions is close to maximum. When account is taken of differential intra-annual use of starch or present photosynthate in the model, isotopic results compare better with actual measurements from the study trees. These results indicate that remobilization of starch is a key component of tree structural formation, especially during the early growth season.

Holocene Patterns of Climate Change in Coastal Northern California

Linda Heusser¹, and John A. Barron²

¹100 Clinton Road, Tuxedo, New York

²U.S. Geological Survey, Menlo Park, California

Pollen analyses of 7 cores from northern California and offshore marine waters (between 37 to 44°N and 122° to 125°W) document regional Holocene evolution of the unique, temperate evergreen conifer forests of coastal northwestern North America (closed forests characterized by trees such as coastal redwood, western hemlock, and Douglas fir). Unlike these closed forests, early Holocene communities apparently combined remnants of full-glacial open, pine woodlands, chaparral, and grasslands with components of communities that later developed along the coast (e.g., coastal redwood-western hemlock, and mixed evergreen oak-Douglas fir forests).

In mid-Holocene assemblages, pine, herbs, and oak increase as redwood and cedar decrease, implying enhanced seasonality, particularly warm, dry summers. Greater summer drought is also reflected in the drying out of aquatic sites, and may also be related to the significant amount of charcoal occurring in sediments deposited in Rice Lake, between about 9000-4000 cal yr B.P.

During the last 4000 cal yr B.P., detailed in high resolution records (average sampling interval of about 40 years in cores from Schelling's Bog and W77-10A-26K, and about 200 years from ODP core 1019C) show millennial- and sub-millennial-scale oscillations overlying the general rise of conifer-dominated assemblages. The implied overall increase in effective moisture shows a decline between about 1300-700 cal yr B.P., when a decrease in redwood and alder, along with an increase in pine suggests warmer drier summers.

Systematic changes in Holocene climate variation on the northwest coast of California are correlative with changes in marine conditions (e.g., sea surface temperature, upwelling, and planktonic communities) reconstructed from the same cores (ODP 1019C, EW9504-17, and W8709-13). Particularly striking is the late Holocene establishment of coastal upwelling and redwood-dominated forests, a relationship that occurred in previous interglacials as well.

Synoptic Climatology at Decadal and Longer Time Scales: Interpreting Short-Term Processes from a Wide-Angle Lens

Katherine K. Hirschboek

Laboratory of Tree-Ring Research, University of Arizona, Tucson

Synoptic climatology can be defined as "the study of climate from the viewpoint of its constituent weather components or events and the way in which these components are related to atmospheric circulation at all scales" (Harman and Winkler 1991). While "circulation at all scales" has a definitive upper bound in space that is defined by planetary-scale circulation features, the existence of a

corresponding upper limit for the temporal scale over which synoptic climatology is viable is less clear. According to Yarnal (1993), all synoptic-climatological studies involve some classification of the circulation. To understand multi-decadal and longer climatic variability, parameterizations, averages, composites, correlations, indices, and eigenvectors are some of the many ways that short-term weather components are subsumed into classifications or patterns that (hopefully) imply mechanistic meaning at decadal and longer time scales. To compound matters, superimposed on this long-term perspective of short-term weather events are processes that operate naturally at decadal and longer time-scales, e.g., deep ocean circulation. Examples drawn from studies linking circulation patterns and western United States tree-ring variations over different time scales will be presented to illustrate some of the issues involved. The various temporal scales at which different synoptic climatological approaches are effective indicators of "constituent weather components" can provide a basis for assessing the value and interpreting the meaning of the "wide-angle perspective" of multi-decadal synoptic patterns.

Integrating Millennial Tree-Ring Records

Malcolm K. Hughes

Laboratory of Tree-Ring Research, University of Arizona, Tucson

There is a great abundance of high-quality natural archives of annual or near-decadal resolution in western North America and its coastal margin. These range from marine and lacustrine deposits and geomorphological features to more than 100 millennial tree-ring chronologies. I will discuss the integration of these tree-ring data with one another and with the other natural archives, with particular emphasis on their strengths and weaknesses as records of decade- to century-scale climate variability over the last several thousand years. Evidence for certain decadal departures on large geographic scales is strong, including dry-wet reversals around 1100, 1600, 1900 and 1976, and sustained periods of cool summers in the mid-14th, late 15th and early 19th centuries.

Winter (DJF) 1901–2001 PAPA Trajectory Index (PTI) Time-Series, Computed with the OSCURS Model, Is Updated and Examined for Decadal North-South Oscillation Patterns of Surface Water Drift in the Gulf of Alaska

W. James Ingraham, Jr.

Alaska Fisheries Science Center-NMFS-NOAA, Seattle, Washington

Surface water (mixed layer) 90-day drift trajectories with start-points from Ocean Weather Station PAPA (50°N, 145°W) were simulated using the OSCURS (Ocean Surface Current Simulations) model for each winter (Dec. 1- Feb. 28) for 1901-2001. The interannual time series of oceanic surface currents was smoothed in time with a 5-year running boxcar filter to reveal decadal variability patterns. The drift from Ocean Weather Station PAPA has fluctuated between north and south modes about every 20 years over the last century. The time-series has been updated with year 2001 calculations. Development of OSCURS was motivated by the need in fisheries research for indices

that describe variability in ocean surface currents. These synthetic data, although derived through empirical modeling and calibration with satellite-tracked drifters, provide insight which far exceeds their accuracy limitations. OSCURS daily surface current vector fields are computed using empirical functions on a 90 km ocean-wide grid of monthly mean sea level pressures (1900-1945) and daily sea level pressures (1946-2001); long-term-mean geostrophic currents (0/2000 db) were added. The model was tuned to reproduce trajectories of satellite-tracked drifters with shallow drogues from the eastern North Pacific. Additional start-points were selected in the Bering Sea and the California Current and their time series examined for variability patterns. Sea level pressure fields (December 1999) provided evidence for pinpointing the location of the second major Nike[®] sneaker spill this decade from a container ship.

Holocene Cycles: Relation to Southwest Climate and Longer Climatic Trends

Thor Karlstrom
U.S. Geological Survey (retired), Seattle, Washington

Early analyses of radiometrically and varve-dated marine and terrestrial paleoclimatic records (Karlstrom 1961) suggested longer term climatic trends latitudinal controlled by Obliquity and Precessional Solar Insolation (Milankovitch 1941). The records also suggested the presence of superposed shorter term cycles modulated by changing tidal forces generated by earth, moon and sun (Petterson 1911). Subsequent field work in Alaska and the Southwest and analyses of numerous published glacial, alluvial, lacustrine, eolian, colluvial, pollen, speleothem, grade-size, isotope, compositional and tree-ring records provide many more records that phase with these insolation and tidal resonance trends (Karlstrom 1972 cf.). The applied analytical procedures include time frequency diagrams of dated basal contacts (Point Boundaries) to determine temporal clustering of nondepositional intervals; half-cycle smoothing to define those primary and secondary climatic patterns that phase with turning points of solar insolation and tidal resonance; and differencing (derivatives) to amplify secondary oscillatory tendencies dampened by smoothing. The evidence for cyclical climate includes proxy records dated by radiocarbon, Thorium/Uranium, varves and tree rings along with some marine records that are further adjusted by fine-tuning to the theoretical insolation curves. The focus of this paper is to provide examples of Holocene paleoclimate records showing decadal, centennial, and millennial cycles that extend into the preceding colder period of the Pleistocene Ice Ages, and to demonstrate that similar harmonically related cycles occur as well in the American Southwest's alluvial, pollen, archaeological and tree-ring records of late Holocene (5,500 yr B.P. to present) age.

Correlative Evidence of an Externally Forced Link of Decadal and Centennial Variability in Climate from Ice-Core, Tree-Ring, and Direct Temperature Records

Charles D. Keeling and Timothy P. Whorf
Scripps Institution of Oceanography, The University of California, La Jolla

Global surface temperature data show spectral power near 6, 9, 10, and 20 years and some proxy paleo-records show spectral power near 70 and 180 years. All of these periods are close to astronomical periods derivable from three gravitational interactions of the sun and moon with the earth: two relating to respective distances from the earth and the other to the degree of mutual alignment of the three bodies. An hypothesis that episodes of strong oceanic tidal forcing cause temporary cooling of surface seawater leads to a prediction that the earth's surface on global average should have been cool near 1900, warm near 1940, and cool again near 1970, suggesting an ~70-year oscillation. Although there is no direct proof that oceanic tidal forcing contributes to climate variability, correlative evidence is at least as convincing as that of forcing from volcanic eruptions and variable solar irradiance, the two most widely accepted explanations for possible external forcing of climate. We propose that oceanic tidal forcing may explain why the earth's surface cooled off from 1940 to 1970 in spite of a general long-term warming trend possibly caused by an enhanced greenhouse effect.

A Multivariate Drought Index Applied to California

John Keyantash¹, and John A. Dracup²
Civil and Environmental Engineering Depts.
University of California, ¹Los Angeles; ²Berkeley

A multivariate, principal component-based index is proposed as a way to assess the aggregate severity of drought at the climate divisional level. The approach considers monthly records for precipitation, streamflow, soil moisture, evaporation and other drought-relevant processes. Data are subjected to principal components analysis; the selection and weighing of geophysical variables is performed by calibrating PCA-derived variables against the Vegetation Condition Index, an NDVI-based benchmark of vegetation health. Temporal comparisons will be made between the multivariate drought index and the PDSI for California climate divisions. It is hoped that the index will provide a regional-scale methodology to objectively quantify drought severity.

Stable Isotopes, Tree Rings, and the Southwestern Monsoon

Steven W. Leavitt¹, William E. Wright¹, and Austin Long²
¹Laboratory of Tree-Ring Research; ²Dept. of Geosciences
University of Arizona, Tucson

Ponderosa pine was sampled at 8 sites in 7 mountain ranges extending from the Santa Catalina Mts. in southern Arizona to the Sacramento Mts. in southern New Mexico to examine seasonal isotopic variability in tree rings over a common period from 1985-1995. A 100-yr chronology was developed at the site close to Tucson, Arizona. Replication was achieved by coring 4-7 trees at each site and subsequently pooling ring material for isotopic analysis of the cellulose component. Seasonal changes were revealed by subdivision of rings into three segments, two from the growth interval prior to and one after the onset of summer monsoon precipitation. The latter subdivision represents growth occurring after a "false latewood" band formed in response to the hyper-arid May/June period just before onset of the summer monsoon. Significant relationships were found between $\delta^{13}\text{C}$ and drought index (negative), with the three subdivisions respectively correlating most strongly with drought indices progressively later in the growing season. The second and third ring subdivisions are thus informing us about moisture conditions immediately before and after the summer monsoon. Correlation analysis using Tucson precipitation $\delta^{18}\text{O}$ time series from 1982-1999 and NCEP-NCAR reanalyzed specific humidity at 850 mb clearly indicates a subtropical Eastern Pacific moisture source fueling the North American Monsoon in southeastern Arizona (Wright and others 2001). Similar correlation analysis using seasonal tree-ring $\delta^{18}\text{O}$ time series from the ponderosa site near Tucson likewise revealed the same spatial patterns for 1958-1998 with possible PDO-related influence.

Difference in Climate Between Eastern China and Western Great Basin During the Past 1000 Years

Hong-Chun Li, Teh-Lung Ku, and Dorte E. Paulsen
Dept. of Earth Sciences, University of Southern California, Los Angeles

Precipitation over eastern China is mainly controlled by summer monsoons associated with the migration of ITCZ, whereas over central California it is dominated by the polar front related to the westerlies. To study the climate teleconnection between two sides of the Pacific, we have compared records from the two regions. The climate variability in eastern China has been reconstructed from the high-resolution stable isotope records of a stalagmite collected from Buddha Cave (109°10'E, 33°45'N), south of Xian. The $\delta^{18}\text{O}$ and $\delta^{13}\text{C}$ records show four intervals of major climatic shift during the past 1100 years. The first interval (A.D. 900-1250) was characterized by cool/dry climate during the first half and cool/wet climate during the second half. The climate became warm and dry during the second interval (A.D. 1250-1510), especially around A.D. 1400. The third interval, A.D. 1520-1820, corresponding to the Little Ice Age, was cold and wet. And the last interval since A.D. 1820 has been warm. However, the corresponding climatic variability in central California as represented by the geochemical records in core OL-97A retrieved from Owens Lake (117°50'W, 36°25'N), California, shows contrasting patterns. Effectively dry climate occurred between A.D. 950 and 1220, during which Owens Lake approached a playa situation. Wet climates prevailed during

A.D. 1220-1480, resulting in a relatively large and deep lake. Between A.D. 1480 and 1760, the climate turned dry, and Owens Lake became a playa during the later half of this interval. The record in OL-97A between A.D. 1760 and 1870 was disturbed by a tsunami event. Since approximately A.D. 1880, it shows that due mostly to human activity, the lake level has steadily dropped from its historic high stand.

The contrasting features of the two records may be related to the average positions of the ITCZ, Subtropical High, and Polar Jet. At the present, when the ITCZ migrates poleward during the summer months and brings abundant monsoonal rain over much of eastern China, northward migration of the Subtropical High and polar jet stream occurs and results in dry weather in central California. During winter months, as the ITCZ moves equatorward, dry winter monsoon prevails in eastern China whereas the southward shift of the polar jet stream associated with the westerlies brings storms to central California. On annual or longer time scales, if the position of ITCZ migrates further north than its present normal position and remains there for extended periods, the position of the polar jet stream may correspondingly shift further north as well. As a result, a wetter-than-normal climate could have prevailed in eastern China and a dryer-than-normal climate could have prevailed in California. The average positions of the ITCZ and the Polar Jet over long periods could be strongly influenced by the strength and position of the Subtropical High, which in turn could be controlled by the Pacific Warm Pool and ocean circulation. These are mere conjectures, of course. The cause for any long-term variations in the positions of ITCZ, Polar Jet, and Subtropical High remains to be understood.

Snowfall Occurrence at Two Lee-Side Mountain Locations, Comparing the Sierra Nevada, California, and Rocky Mountains, Colorado

Mark Losleben¹, Susan Burak², Robert E. Davis³, and Karla Adami¹

¹Mountain Research Station, INSTAAR, University of Colorado, Boulder

²Snow Survey Associates, Mammoth Lakes, California

³U.S. Army Engineering Research and Development Center, Cold Regions Research and Engineering Laboratory, Hanover, New Hampshire

The atmospheric conditions associated with snowfall occurrence on the lee (east) sides of the Sierra Nevada and Rocky Mountain ranges are compared in this study. These atmospheric conditions are defined in terms of general air flow patterns and by specific circulation indices, including force and vorticity. The two sites, Mammoth Mountain, California, and Niwot Ridge, Colorado, are at similar latitudes, and both are on the lee sides of their respective mountain ranges, but Mammoth is much closer to the Pacific Ocean, and Niwot is a more continental (inland) site. Data from three winter seasons (1996-1999) are used in this comparison. Differences and similarities in the circulation parameters and ENSO phase associated with snowfall occurrence, are described. Although only three seasons are used in this study, each occurs during a different ENSO phase; warm in 1997-98, cold in 1998-99, and neutral in 1996-97. The weather patterns associated with snowfall occurrence and maximum snowfall are slightly, but significantly, different between these phases.

Synoptic Influences on Seasons of Exceptional Winter Precipitation in the Rocky Mountain Region

Deborah Anne Luchsinger
University of Denver

The Rocky Mountain region presents a number of problems for climatologists and meteorologists seeking to analyze weather and climate trends. The complex terrain modifies atmospheric circulation patterns and can both initiate and alter storm systems. Frequency, intensity, and duration of storm events are in turn affected by upper atmospheric circulation patterns. This research examines relations between (1) the PNA teleconnection index, (2) upper atmospheric pressure patterns, (3) storm-track preferences, and (4) frequency of cyclonic activity during seasons of exceptional winter precipitation.

Map pattern analysis of standardized winter season precipitation indices calculated for each climate division in the Rocky Mountain region yield 6 anomalous winter patterns. Composite maps of the 500-mb surface are classified to determine modes of synoptic feature variability during the winter seasons analyzed. The significance of cyclone frequencies and the PNA index on precipitation anomaly patterns are determined through regression of the cyclone frequency and PNA indices against both divisional and regional precipitation indices. Finally, dominant storm track patterns are analyzed with respect to the anomalous precipitation patterns identified.

Do Ecosystem Restoration and Water Management Programs Require a Commitment to Science?

Samuel N. Luoma
CALFED Bay-Delta Program and U.S. Geological Survey, Menlo Park, California

The support for restoration and water bond issues in recent elections could provide unique opportunities for restoration and improved water management in California. The challenge is to generate effective programs. Where programs elsewhere have failed, insufficient incorporation of science was a factor. A coherent program of research, assessment, monitoring and adaptive management is critical to the success of policies and actions. New scientific knowledge is needed because environmental responses to human activities, whether stress or restoration, are not fully predictable. Case studies show that credibility is lost, resources are misallocated and, at worst, environmental disasters can occur when interconnections between environment and human activity are not recognized. Embedding continuous development of new knowledge and incorporating an adaptive management philosophy may help avoid management failures. Yet such programs are rare. Debates over scientific findings can paralyze policy; but methods exist to clarify debates and incorporate our ever-improving scientific understanding. Scientific progress and transparent elucidation of the status of scientific knowledge can, at least, reduce the intensity of policy conflicts and, at best, yield novel solutions. Peer review and technical evaluation must be built into every aspect of a water science program if science is to be credible. Credibility also means the technical

findings must be widely communicated and communications must be balanced in tone. The investment in science must also be substantial. A fixed proportion of the resources spent on managing and modifying an environment should be invested in learning about what we are managing. Water management in California is a daunting challenge; growth in knowledge must be a constant in the equation to meet that challenge.

Paleoclimatic Evidence for Late Holocene Reorganization of Atmospheric Circulation Patterns in the Western United States

Mark E. Lyford¹, Stephen T. Jackson¹, and Julie L. Betancourt²

¹Dept. of Botany, University of Wyoming, Laramie

²U.S. Geological Survey, Tucson, Arizona

Paleoclimatic inferences are often in conflict for the same general region. Such discrepancies can arise from poor chronology, from ambiguities between temperature and precipitation effects, or from different response times and sensitivities for the various kinds of climate proxies (e.g., lake, glacial and vegetation histories). However, divergent proxies, viewed synoptically, may reveal climatic changes more complex than generally assumed by paleoclimatologists, even though this complexity may be evident in the instrumental record. Recent advances in synoptic climatology indicate climatic variations on annual and decadal timescales that frequently consist of anti-phased precipitation and temperature anomalies in different geographic regions. For example, precipitation patterns in western North America vary systematically during positive and negative anomalies in the "Pacific/North American" teleconnection pattern (PNA). We identified millennial-scale anti-phasing of effective moisture on a continental scale through a review of mid- to late Holocene proxy records from central and western North America. The regional anti-phasing appears to conform to current climate patterns associated with the PNA. We hypothesize that changes in the frequency of occurrence of each mode of the PNA occurred during the mid- to late Holocene, with the positive mode dominating between ca. 6000 and 5000 ¹⁴C yr B.P., the negative mode between ca. 5000 and 2500 ¹⁴C yr B.P., and the positive mode again after 2500 ¹⁴C yr B.P.

Monthly Synoptic Patterns Associated with Very Wet and Very Dry Months of July in Arizona

Robert A. Maddox

Dept. of Atmospheric Science, University of Arizona, Tucson

During recent years there has been increasing interest in the summer precipitation regimes associated with the monsoon circulation of southwestern North America. The past two Julys provide an interesting contrast with respect to synoptic patterns and monthly precipitation over the southwestern United States. July 1999 was characterized by very heavy rainfall, while July 2000 was very dry. For example, basinwide rainfall over the Salt and Verde river basins in Arizona for July 1999 and 2000 were in the highest and lowest deciles, respectively, for the period of record. Past studies have indicated that dry Julys tend to occur in the Southwest when the over-land extension of the

Atlantic subtropical anticyclone, say at 500 mb, is suppressed unusually far south. Wet Julys tend to occur when the anticyclone position is shifted unusually far north. It is shown that the monthly mean synoptic conditions for the past two Julys were much different than the simple model described above. Comparison is also made with two other years, 1984 and 1993, which were also unusually wet and dry, respectively. However, in contrast, these two Julys fit the simple model well. The synoptic patterns for these four Julys illustrate well the large range of conditions that can produce extremely wet or dry conditions over the Southwest. Possible reasons for the large variance of precipitation during basically similar synoptic patterns are presented.

Relationship of Gulf of California Moisture Surges to Tropical and Subtropical Weather Features During Summer 2000

Robert A. Maddox¹, Vincent Holbrook², and Luis Farfan³

¹Dept. of Atmospheric Science, University of Arizona, Tucson

²National Weather Service Forecast Office, Tucson, Arizona

³Dept. of Geography, Arizona State University, Tempe

During the summer of 2000, data were gathered routinely at the Tucson NWS Forecast Office on the position and movement of features at low latitudes, i.e., tropical disturbances and storms, easterly waves, and inverted troughs. We have also monitored soundings and surface data over Arizona and the north end of the Gulf of California to document northward surges of cool and moist air into the state. Such "surge events" have been reported, in a number of papers in the formal literature, to be associated with increases in thunderstorm activity over Arizona. Two types of rapid movement of moist and unstable air into Arizona will be illustrated. One type of event occurs with an abrupt north and westward shift of the large-scale, subtropical air mass from northern Mexico into Arizona. The other type event is more mesoscale in nature and appears to be associated with flow, channeled by orography, north-northwestward up the Gulf of California. It is this second type event that has been previously documented in the literature. During summer 2000 important surges were associated with either named tropical storms that moved northwestward past the southern tip of Baja or middle to upper tropospheric inverted troughs that moved westward across central and northern Mexico. The synoptic relations among the important surges of summer 2000 and these low latitude features will be shown and discussed.

Primary Modes and Predictability of Year-to-Year Snowpack Variations in the Western United States from Teleconnections with Pacific Ocean Climate

Gregory J. McCabe¹ and Michael D. Dettinger²

¹U.S. Geological Survey, Denver Federal Center, Denver, Colorado

²U.S. Geological Survey, Scripps Institution of Oceanography, La Jolla, California

April 1 snowpack is the primary source of warm-season streamflow for most of the western United States (U.S.) and thus represents an important source of water supply. An understanding of climate factors that influence the variability of this water supply and thus predictability is important for water resource management. In this study, principal-component analysis is used to identify the primary modes of April 1 snowpack variability in the western U.S. Two components, the primary modes of April 1 snowpack variability, account for 61% of the total snowpack variability in the western U.S. Relations between these modes of variability and indices of Pacific Ocean climate [e.g. the Pacific Decadal Oscillation (PDO) and NINO3 sea-surface temperatures (SSTs)] are examined. The first mode of snowpack variability is closely associated with the Pacific Decadal Oscillation (PDO), whereas the second mode varies in concert with both the PDO and the NINO3 SSTs. Because these atmospheric-oceanic conditions change slowly from season to season, the teleconnections observed between the Pacific Ocean climate and April 1 snowpack suggest that April 1 snowpack can be forecasted beginning in the previous summer and fall seasons, especially in the northwestern U.S.

Latewood-Width Variations and Spatial Patterns of Monsoon Precipitation

D. M. Meko¹, C. H. Baisan¹, D. W. Stahle², M. K. Cleaveland², and M. K. Therrell²

¹Laboratory of Tree-Ring Research, University of Arizona, Tucson

²Dept. of Geography, University of Arkansas, Fayetteville

An expanding network of latewood-width tree-ring chronologies samples widely separated regions of influence of the North American Monsoon System (NAMS). Groups of chronologies with a signal for warm-season precipitation are now available for Mexico and scattered parts of the southern United States from California to Arkansas. A spatial correlation analysis of the latewood chronologies indicates regions of contrasting anomalies that may be related to modes of monsoon circulation. For example, negative correlation between the San Pedro Martir of northern Baja California and the mountain ranges of southern Arizona may reflect east-west displacement of the moisture tongue. Correlation patterns suggest an in-phase relationship between moisture anomalies in S. Arizona and most of mainland Mexico, with a weakening and possibly reversal of correlation to the south. Analysis of station precipitation records shows that latewood-width in southern Arizona tends to closely track summer precipitation; occasional breakdowns in the statistical relationship occur in periods of poorly organized summer precipitation anomalies and probably reflects inadequate sampling of precipitation near the trees by existing stations.

Low Frequency Variations in *Juniperus occidentalis* Tree-Ring Chronologies Over the past 1,000 Years

D. M. Meko, C. H. Baisan, and R. Touchan
Laboratory of Tree-Ring Research, University of Arizona, Tucson

Tree-ring data and the existence of relict stumps in lakes and rivers have been cited as evidence that more than 600 years ago the Sierra Nevada of California experienced droughts much more prolonged than any in the instrumental record. The intensity, duration, and spatial extent of these purported droughts is studied from newly developed *Juniperus occidentalis* (western juniper) chronologies from California, Oregon, and Nevada. Of the low-frequency variations synchronous across the California sites, the most prominent is a steep decline in growth from about A.D. 1020 to A.D. 1070, with recovery to previous high levels by about A.D. 1110. This feature, strong in chronologies 40 km NNW of Lake Tahoe, may reflect a northward extension of a drought thought to have reduced the inflow to Mono Lake at about the same time. The more arid of our sampled sites near Lake Tahoe also supports a major late-1500s drought and an excursion to extreme wetness near A.D. 1340 after a prolonged drought. Growth departures in chronologies farther north (southern Oregon) are out of phase with some of these major departures. The spatial contrasts might reflect persistent positioning of the storm track to the north or south.

Holocene Climate Change at Pyramid Lake, Nevada, Reconstructed from Fossil Pollen

Scott A. Mensing
Dept. of Geography, University of Nevada, Reno

Holocene climate records from the Sierra Nevada and western Great Basin appear to provide evidence of periodic extended droughts. Submerged stumps in Lake Tahoe dating to the mid-Holocene suggest this lake may have remained below its sill for centuries at a time. Pyramid Lake is fed by the Truckee River and is the terminal basin in the Lake Tahoe watershed. A recent ^{18}O record from Pyramid Lake supports the interpretation of an extended dry period during the mid-Holocene, and provides further evidence for droughts throughout the late Holocene. Evidence for recurrent droughts in the Sierra Nevada has significant potential consequences for water resources in California and Nevada. In this paper, I provide pollen evidence of vegetation and climate change, for comparison with the other proxy records. Three sediment cores were recovered from the deepest part of Pyramid Lake, a box core spanning about 300 years, and two piston cores spanning about 300 to 3000 cal yr B.P. and 3500 to 7500 cal yr B.P. Pollen analysis from the historic period records a reduction of Sierran pollen types and lowered lake levels as would be expected since water diversions during the last century significantly reduced flows to Pyramid Lake. Pollen data also suggest that the period of driest climate was centered around 7000 cal yr B.P. Other droughts identified in the ^{18}O record are generally confirmed by the pollen record; however, vegetation is less responsive to rapid climate shifts and the pollen record at this site is probably best suited to identification of periods of extended drought and large scale climate shifts.

Response of High-Elevation Conifers in the Sierra Nevada, California, to 20th Century Decadal Climate Variability

Constance I. Millar¹, Lisa J. Graumlich², Diane L. Delany¹, Robert D. Westfall¹, and John C. King³

¹U.S. Dept. of Agriculture Forest Service, Pacific Southwest Research Station, Albany

²Mountain Research Center, Montana State University, Bozeman

³Laboratory of Tree-Ring Research, University of Arizona, Tucson

Trees in high-elevation ecosystems of the central Sierra Nevada, California showed complementary 20th century responses in four independent studies of forest growth. Annual growth rates of horizontal branches in treeline *Pinus albicaulis* doubled from 0.9 cm/yr to 2.0 cm/yr between 1900-1996, with accelerated growth from 1920-1945 and 1984-1996. Since 1900, *P. albicaulis* has progressively invaded formerly persistent snow-covered slopes below treeline as snowfields melted earlier in summer. Invasion accelerated during 1920-1945 and 1976-1999. Vertical extension of branches ("flags") in otherwise shrubby, treeline *P. albicaulis* and invasion of montane meadows by *P. contorta* occurred in single dominant pulses from 1945-1976. These ecological responses, unassociated with local conditions or land-use, correlate with 20th century patterns of global warming and multidecadal phases of the Pacific Decadal Oscillation (PDO), corroborating that PDO is both detectable and has biotic effects in this region of California. Proper attribution of cause and effect to climate rather than human impacts of overgrazing and fire-suppression is important also to wildland management.

Teleconnections from Southeast Asia and the Western Tropical Pacific: Their Role in North Pacific and North American Climate Variations

Tom Murphree¹, Bruce Ford¹, Frank Schwing², and Phaedra Green²

¹Naval Postgraduate School, Monterey, California

²Pacific Fisheries Environmental Laboratory, Pacific Grove, California

The Southeast Asian (SA) and western tropical Pacific (WTP) regions experience large fluctuations in atmospheric heating on intraseasonal to decadal time scales. These fluctuations are often amplified and guided by the East Asian-North Pacific jet to produce large climate variations over the northeast Pacific (NEP) and North America (NA). The NEP-NA region is one of the most variable parts of the atmosphere, probably in large part because of its links to Southeast Asia and the western tropical Pacific. These links are revealed by strong correlations, or teleconnections, between climate variables in the SA-WTP and NEP-NA regions. The mechanisms for these links involve fluctuations of the Hadley-Walker circulation in the North Pacific region, and planetary wave trains that extend from East Asia into the NEP-NA region. These mechanisms appear to be important in explaining intraseasonal to decadal variations in the NEP-NA region (e.g., cool, wet conditions in the southwestern U.S. during October 2000; summer droughts and flooding in the Midwestern U.S.; many of the fall and early winter anomalies associated with El Niño and La Niña events; circulation anomalies associated with decadal regime shifts). Increased understanding of these teleconnections

should lead to improved monitoring of the factors that drive NEP-NA climate variations and, eventually, to improved predictions of these variations.

Tropical Forcing of Extratropical Variability on Decadal Timescales

Matthew Newman
NOAA-CIRES Climate Diagnostics Center, Boulder, Colorado

It is well known that tropical forcing impacts extratropical variability on weekly to sub-seasonal time scales. The ENSO phenomenon gives rise to anomalous tropical convection, which consequently forces anomalous extratropical atmospheric circulation. It is also understood that this atmospheric circulation forces extratropical SST anomalies; this mechanism has been referred to as the “atmospheric bridge” (e.g., Alexander, Lau).

ENSO is, to a good approximation, a red noise process. That is, its power spectrum can be well modeled as being the result of a multivariate first order Markov process. Such a spectrum has power at decadal (and longer) timescales, even though the decorrelation time is on the order of a few months. Atmospheric variability can similarly be thought of as red, although its characteristic decorrelation time is on the order of a few days in the extratropics and about a week in the tropics.

Additionally, although there is a strong correlation between anomalous SST and anomalous convection in the tropics, it is only about 0.5, far less than 1. That is, two different ENSO events with the same SST anomaly will in general produce different convection anomalies, which will give rise to different extratropical atmospheric responses. These anomalies will be further obscured by noise in the extratropics, leading to quite different extratropical SST anomalies. Thus, the effect of the bridge will be partly obscured by noise.

In this talk, the possible effect of this noisy bridge upon decadal variability will be presented. In particular, a “null hypothesis” for the Pacific Decadal Oscillation (PDO) will be discussed. Results from an atmospheric GCM forced by tropical SST and containing an interactive mixed layer in the extratropics will be presented, which suggest that a realistic PDO signal can be produced from the atmospheric bridge alone. Consequences of this viewpoint will be evaluated.

Circulation Indices Reconstructed from a Millennial Network of Western Tree Rings

Fenbiao Ni, Malcolm K. Hughes, and Gary Funkhouser
Laboratory of Tree-Ring Research, University of Arizona, Tucson

Time series of tree-ring width serve as proxy records of past weather and climate beyond the short period covered by instrumental data. Atmospheric-oceanic indices, such as the Pacific Decadal Oscillation (PDO) and the Southern Oscillation Index (SOI), are important features that directly influence local and regional climate variations. The purpose of this research is to link these indices with the long tree-ring chronologies in the American Southwest. The trees that make up these chronologies are relatively isolated and have limited interaction with their neighbors. Many exhibit particularly clean climatic signal. We compare 1000-year reconstructions of SOI and PDO, providing a decadal to multicentury perspective on circulation variability. Preliminary results indicate that these key atmospheric-oceanic indices have distinct patterns of variation over the last millennium.

Siberian Tree Rings Related to Climate and North Pacific Teleconnections

Irina P. Panyushkina¹ and Muhktar M. Naurzbaev²

¹Laboratory of Tree-Ring Research, University of Arizona, Tucson

²Laboratory of Dendrochronology, Sukachev Institute of Forest, Krasnoyarsk, Russia

Decadal and longer behavior of coupled atmosphere-ocean system is a considerable and unsolved problem in climatic studies. Periodicity of the Pacific atmosphere-ocean variations was derived from less than a 100-year period of climatic observations. Long-term climate proxies with annual resolution from mid-latitudes and tropics, which are used for reconstruction of circulation indices and precipitation patterns, demonstrate Pacific teleconnection. However, does spatial climatic variability at the longer time scales reflect variability on the shorter time scales? The main goal of the present study is to estimate changes in time-spatial patterns of low and high frequency variability of temperature-sensitive tree-ring chronologies of larch in the Siberian Arctic (600-1700 E) and the Altai Mountains, which belong to the highlands of Central Asia located near the Tibet Plateau. Most tree-ring chronologies were contributed by Vaganov and others (1998). The climate variability of Siberia is dominated by the North Atlantic Oscillation. The climate of the Russian Far East is controlled by the Asian Summer Monsoon and North Pacific Oscillation. Based on factor analysis of tree rings for the last 500 years related to climate, we focused on periodicity of chronologies from four regions: Yamal (West Siberia), Taymir (Central Siberia), Indigirka (East Siberia), Chukotka and Altai (South Siberia). The fluctuations of transformed tree-ring factors were estimated by cross-spectral analysis. Tree ring response to atmosphere circulation patterns was simulated by composite mapping based on NCEP/NCAR reanalysis. The result shows that frequency components around 62, 44, 18, and 6 years persist in overall periodic behavior of the Siberian series. But cross-periodogram spikes of the Indigirka region (1400-1500 E) are the most distinct from the others and concentrate on bandwidth 4.31-2.3

years. It seems likely that the Pacific teleconnections impact summer conditions among the outlying eastern Siberia region according to tree-ring records.

Possible Effects of Solar Irradiance on EL Niño/La Niña

Charles A. Perry
U.S. Geological Survey, Lawrence, Kansas

Variations in total solar irradiance have a statistically significant relation with decadal variations in the world's sea-surface temperatures (SSTs). There also is evidence of relations between annual and interannual variations in solar irradiance and annual and interannual fluctuations in SSTs in specific regions of the Pacific Ocean. These solar-forced variations in ocean temperatures are suspected to affect Northern Hemispheric jet stream characteristics and ultimately precipitation and runoff over North America. The El Niño/La Niña phenomena also effects precipitation and runoff over North America, and there is evidence that variations in solar-irradiance variations may be affecting SSTs in the eastern and central tropical Pacific Ocean.

Comparison of El Niño/La Niña indices (i.e., NINO1+2, NINO3, and NINO4) with annual solar-irradiance differences shows no significant relations. However, when the indices are stratified according to the phase of the Quasi-Biennial Oscillation (QBO), an interesting relation emerges. When the QBO is positive (west wind), there is a significant correlation between NINO4 and solar-irradiance differences lagged 2 years ($r = 0.51$). Water from the Pacific Warm Pool appears to move eastward with the equatorial countercurrent warming the NINO4 region 2 years after an irradiance increase. When the QBO is negative (east wind), there is a significant correlation between NINO1+2 and the solar irradiance lagged 4 years. The pathway for this connection with the Pacific Warm Pool may be around the South Pacific Gyre and up the west coast of South America (4 years travel time). For QBO values greater than -20 meters per second, NINO3 shows a graphical relation with irradiance lagged 2 years.

Visualization of the Dynamics of Natural Landscapes and Climate Systems

Jack G. Peterson
The Miracle of a Desert River and The Aurora Project

Throughout history, we have attempted to portray, understand and describe our natural surroundings—to ourselves and to others. Visually, we have progressed from pictographs and petroglyphs, oral folk tales, pen and ink maps and sketches, watercolor and oil landscapes, black and white large format landscape photography, film and video photography, and geographical information systems, to today's digital elevation models draped with the latest Landsat 7 color imagery. We have moved from the art of pen and ink renderings of landscapes, flora and fauna to the art of imaging complex structures ranging from mitochondria to distant galaxies through computational science.

We now describe the dynamics of landscapes, ecosystems, watersheds, climates, ocean and atmospheric systems, and distant galaxies through complex algorithms solved with massive computational power. From the handwritten field notes and drawings by naturalists on early voyages of exploration, and railroad and boundary surveys, to the current avalanche of scientific papers, the quantity of scientific information is increasing daily, almost exponentially, via multiple media forms including the World Wide Web.

Today, because of the volume and velocity of information, much of our scientific literature is targeted to an ever narrower, specialized, and therefore, more limited audience. While we in the science, public policy and management arena have made amazing progress in visually imaging our surroundings and natural phenomena, we have lagged in explaining "What does all of this information mean?" to a curious and intelligent public. I have attempted to address that question. The first result is "The Aurora Project" about community watersheds. Completed in 1998, Aurora is an interactive documentary on CD-ROM that visually describes six watersheds in the West.

In early 2000, we completed "The Miracle of a Desert River: Conservation of the San Pedro River of Sonora and Arizona." This is the story of the last free flowing river joining Mexico and the United States - and the people, communities and institutions of both Nations whose efforts have saved the river in Spanish and English on the same CD. We also have just completed the prototype of the first "Explore the Last Great Places" sites with Intel and The Nature Conservancy, www.lastgreatplaces.org—the first of 200 Last Great Places sites planned worldwide. El Milagro, Aurora, and Explore the Last Great Places have received amazing response from high schools, colleges and universities, museums, non governmental organizations, and individuals. They are proof of the principle that there is a demand.

The foregoing prototypes have catalyzed a small group of scientists and researchers from Scripps, USGS, SDSC, NOAA, and UCSD to share their work on the dynamics of climate, water and landscapes in California's Sierra Nevada, the San Joaquin Valley and the San Francisco Bay-Delta—and to propose a visualization production that would capture and explain the meaning of this region's complex dynamics.

The Modern Distribution of Chironomids (Insecta: Diptera) in Eastern Sierra Nevada California Lakes: Potential for Paleoclimatic Reconstruction

David F. Porinchu and Glen M. MacDonald
Dept. of Geography, University of California, Los Angeles

Chironomids are non-biting midge flies belonging to the order Diptera. They are ubiquitous and frequently the most abundant insects found in freshwater ecosystems. Midge flies have three characteristics that are useful in paleoecological studies; they have relatively short lifecycles, the adults are mobile and the larvae possess chitinous head capsules. The chitinized larval head capsules of midge flies are readily preserved in lake sediment and therefore are easily recovered and identified. The mobility of adult midge flies along with their short life cycle allow them to respond to climate

change very quickly and, as a result, midge flies are likely to have distributions in equilibrium with climate. The aim of this research is to use the remains of chironomids preserved within lake sediment in the Sierra Nevada to reconstruct a late-Quaternary record of paleotemperature for eastern California.

Surface lake sediment and water samples were collected from a suite of 50 lakes along an altitudinal transect in the eastern Sierra Nevada during the summer of 1999. The sediment recovered from these lakes was analyzed for fossil chironomid remains. Five environmental variables - surface-water temperature, salinity, lake depth, air-temperature and particulate organic nitrogen - were identified as having statistically significant effects on chironomid community composition along the altitudinal transect. We are in the process of constructing a model that relates chironomid distributions to surface water-temperature; preliminary results indicate that a robust model can be developed. The results from this work and its future application to the chironomid assemblages preserved in late-Quaternary lake sediment from the eastern Sierra Nevada will be discussed.

A 1,200-Year Record of Fire and Vegetation from Northwestern Montana

M. Power and C. Whitlock

Dept. of Geography, University of Oregon, Eugene

A 1.3 m laminated sediment core from Foy Lake, Montana, provides decadal-scale resolution for the past ca. 1,200 cal yr B.P. Sedimentary charcoal and pollen analyses were used to reconstruct the relationships among fire, vegetation, and climate in the Foy Lake watershed. Pollen percentage data indicate high percentages of fire-adapted species from ca. 1200 to 600 cal yr B.P., including *Larix* and *Pseudotsuga*-type and the diploxylon-type *Pinus*, (attributed to either *Pinus contorta* and *Pinus ponderosa*) and low percentages of fire-sensitive species, e.g., *Abies* and *Picea*. This period is also associated with a number of fire events, as inferred from the sedimentary charcoal record. Herbaceous and shrub pollen, including *Poaceae* and *Artemisia*, increased from ca. 600 cal yr B.P. to the present-day suggesting increased forest openings and development of the modern steppe along the northern and western borders of Foy Lake. The charcoal data indicate fewer fires from 600 to 200 cal yrs B.P. followed by increased fire activity after ca. 200 cal yr B.P. The Foy Lake record is consistent with late Holocene records from northwestern Yellowstone that suggest heightened fire activity, coinciding with the Medieval Warm Period, from 1000 to 800 cal yr B.P., and an increase in fire in the last 200 years. The last hundred years at Foy Lake shows an increase in disturbance-adapted taxa, including *Alnus*, *Populus* and *Poaceae*, and decreased sedimentary charcoal, reflecting the early Euro-American cattle grazing and timber harvesting activity and fire suppression.

Water Year 2001 in Northern California: Can a Second Dry Start Be Overcome?

Maurice Roos

California Dept. of Water Resources, Sacramento

For the second water season in a row precipitation and snowpack accumulation in the October through December period were far below normal in northern California. In 2000, the season was saved by a 60-day wet period from mid-January to mid-March. No two years are alike and although some recovery is likely during the second half of the wet season this year, it is unlikely that the 20% deficit on January 1, 2001 will be made up. The historical odds of doing so are only 15% to 20% and it appears likely that the dry look of the water year will continue. Reservoir carryover storage from the previous water year on October 1 was about 10% above average which will help cushion expected shortfalls in runoff and water supply in 2001.

The main portion of the paper will be a review of where California stands on water supply for year 2001 as of mid-March. Parameters to be presented and compared include precipitation, snowpack, runoff and runoff forecasts, and in-State reservoir storage. Since about one quarter of the average rainfall season occurs after the middle of March (which is the date of the PACLIM Workshop) there will still be significant uncertainty on the eventual water year outcome.

Fifteen Centuries of Reconstructed Temperature and Precipitation from Northern Arizona Tree Rings

Matthew W. Salzer

Laboratory of Tree-Ring Research, University of Arizona, Tucson

Two independent calibrated and verified climate reconstructions from ecologically contrasting tree-ring sites provide the opportunity to evaluate decadal-scale climatic trends in the context of fifteen centuries of change. Millennial-length temperature and precipitation reconstructions for the northern Arizona region are applied to questions regarding the role of explosive volcanism as a forcing mechanism in temperature variability, the cultural-environmental interface in the northern Southwest, and the state of late 20th century climate compared to the range of natural variability in the past. The juxtaposition of temperature and precipitation reconstructions yields paleoclimatic insights unobtainable from either record alone. Results include the identification of relatively wet, dry, cool, and warm intervals. Many of the reconstructed cool periods are linked to explosive volcanism. The role of climate, particularly temperature, in prehistoric population movements on the Colorado Plateau merits additional consideration in paleodemographic models. The second half of the 20th century is the warmest in the period of record, and extremely warm/wet conditions have persisted since 1976.

Major Flood Events of the Past 2,000 Years Recorded in Santa Barbara Basin Sediment

Arndt Schimmelmann¹ and Carina B. Lange²

¹Dept. of Geological Sciences, Indiana University, Bloomington

²Scripps Institution of Oceanography, Geosciences Research Div., La Jolla, California

Every few hundred years the culmination of extreme regional precipitation in Southern California produces extraordinary flooding that dramatically increases transport of fine-grained sediments into California's offshore basins. Conspicuous gray, clay-rich flood deposits in the predominantly olive, varved Holocene sediment record in the central Santa Barbara Basin offer a paleoclimatic record of these Southern California flood events. Gray flood deposits, with thickness ranging from several mm to cm, were distinguished from the more stochastic occurrence of "gray turbidites" using a multidisciplinary combination of analytical methods (X-radiography, thin-sectioning and light/SEM microscopy, particle size distribution, chemical and XRD clay mineral characterization). The last extreme flood occurred about A.D. 1605 and correlates surprisingly well with a multitude of other climatic anomalies worldwide, coinciding with a brief, sharp cooling that compressed the world's atmospheric circulation patterns towards the equator. Earlier thick flood layers of the last 2,000 years were dated via varve counting to ca. A.D. 1418, A.D. 440, and A.D. 212. We present a matrix of published regional and global evidence for climate change that likely coincided with the ca. A.D. 1418, A.D. 440, and A.D. 212 Southern California flood events.

Statistical Detection of Multiscale Abrupt Changes in Climate

Frank Schwing, Jianmin Jiang, and Roy Mendelssohn

PFEL, NOAA, NMFS, Pacific Grove, California

A scanning and coherency algorithm for detecting abrupt change points is applied to selected long time series representing climate change (e.g. SOI, PDO, Niño3.4 SST, Nile River floods). The method detects statistically significant change points in the series at multiple frequencies, and tests for coherence with other series. It is similar to wavelet analysis, but provides a threshold for statistical significance. The method is applicable to the variety of time series used by PACLIM participants.

Preliminary analyses of several familiar time series reveals change points consistent with those previously identified; for example El Niño events, the 1976 regime shift, and chronologies of famine. The method clearly identifies frequency bands associated with change points, and shows that change is not always a broadband phenomenon. In addition, the phase relationships between series are shown to change on occasion. These results may help us identify unique climate change events and understand why they vary from canonical events.

Intra-Annual Variability of North American Climate

Jacqueline J. Shinker, Patrick J. Bartlein, and Peter V. Killoran

Environmental Change Research Group, Dept. of Geography, University of Oregon, Eugene

The climate of North America is characterized by spatial heterogeneity of seasonal temperature and precipitation regimes related to latitudinal and elevational variations. In addition, variations in atmospheric circulation and surface energy- and water-balance across the continent play an important role in climate variability of North America. Using the GHCN and NCEP/NCAR reanalysis data sets, a climatology of month-to-month changes in temperature, precipitation, surface energy- and water-balance and atmospheric circulation variables illustrate the processes that explain the spatial distribution of precipitation in North America. Intermonthly changes highlight smaller-scale climatic controls that can be used to explain spatial variability. In particular, decomposition of continental-scale circulation features (500 mb heights) into secondary circulation features (500 mb vertical velocity and relative vorticity) provides a mechanistic approach for understanding spatially heterogeneous patterns of intra-annual variability of precipitation.

Megadrought and Megadeath in 16th Century Mexico

D. W. Stahle¹, R. Acuna-Soto², M. S. Therrell¹, and M. K. Cleaveland¹

¹Tree-Ring Lab, University of Arkansas, Fayetteville

²*Dept. de Microbiología y Parasitología, Universidad Autónoma de México, México*

Tree-ring data from western North America, the southeastern USA, and the Great Lakes region indicate that the most severe and prolonged continent-wide drought in the last 500 years occurred during the mid- to late-16th century. This epic drought persisted with little relief for up to 40 years, and extended at times from the Pacific to the Atlantic, and from Mexico to the boreal forest. The 16th century megadrought has been associated with the disappearance of Sir Walter Raleigh's Lost Colony on Roanoke Island, North Carolina, severe hardship and abandonment of Santa Elena Colony, South Carolina, the depopulation of the upper Ohio River region by the Monongahela Culture, severe drought in the province of the Casqui (lower Mississippi Valley) referenced by the DeSoto Entrada during the early 1540s, the abandonment of several Puebloan villages in New Mexico, and in the costly 40-year war between the Chichimeca and Spanish in Zacatecas and Durango, Mexico. Two of the worst episodes of epidemic disease in Mexican and world history also occurred during the 16th century megadrought. The epidemic of 1545 killed an estimated 12 to 15 million people, and the 1576 epidemic killed an additional 2 million people. These horrible 16th century "cocoliztli" epidemics are described in Nahuatl codices and in first hand accounts of Spanish physicians. Symptoms included great effusions of blood from the nose, ears, and other body openings, extreme fever, vertigo, black tongue, green urine and skin, abscesses, acute neurological disorders, and frequently death in three or four days. Based on recent epidemiological work by Acuna-Soto and others (2001) and by Marr and Kiracofe (2000), it now appears that both the 1545 and 1576 epidemics were indigenous hemorrhagic fevers similar to hemorrhagic forms of hantavirus, and were not caused by introduced European diseases. The tree-ring record of climate over Mexico indicates that both epidemics occurred during brief wet episodes that were preceded by multi-year

drought, which is similar to the ENSO-related sequence of drought-then-wetness which is believed to have initiated the explosion of infected rodents that caused the hantavirus outbreaks in the Four Corners region in 1993 and 1997-1998 (Hjelle and Glass 2000).

A 3,000-Year Record of Salinity Variation in a Brackish Marsh at Rush Ranch, Northern San Francisco Bay, California

Scott W. Starratt

U.S. Geological Survey, Menlo Park, California, and
Dept. of Geography, University of California, Berkeley

Diatoms from sediment cores collected at Rush Ranch, north of Suisun Bay, have been used to reconstruct the record of salinity variation over the past 3,000 years. The site was chosen because it is located midway between the normal marine environment of San Francisco Bay and the freshwater environment of the Sacramento and San Joaquin rivers. Variations in the discharge of the Sacramento and San Joaquin Rivers is an indication of both the volume and timing of precipitation over more than 40% of California.

The composition of modern diatom assemblages in freshwater, brackish, and saltwater tidal marshes is used to calibrate the late Holocene record. Variation in the taxonomic composition of the entire assemblage, as well as a simplified biometric which summarizes the relationship between salinity and individual taxa are used as proxies for salinity. Dominant taxa in each assemblage vary downcore, indicating that variation in salinity is only one parameter in a complex set of physical and chemical factors that control the temporal and spatial distribution of diatoms in northern San Francisco Bay marshes.

At the Rush Ranch site there appears to be evidence of broad-scale salinity cycles over the past 3,000 years. Prior to European contact about 150 years ago, there are two intervals dominated by freshwater taxa and two intervals dominated by more marine taxa. The intervals that indicate more saline conditions (3,000 cal yr B.P. to 2,500 cal yr B.P. and 1750 cal yr B.P. to 750 cal yr B.P.) may correspond to periods of lower precipitation suggested by other California climate records. Smaller-scale variations within the salinity cycles correspond with variations in the lake level record at Mono Lake, as well as shorter precipitation cycles in the Sierra Nevada. Carbon isotope ($^{13}\text{C}/^{12}\text{C}$) and pollen records from Rush Ranch corroborate the diatom evidence.

ENSO, Pacific Decadal Oscillation, and Drought Variability in Northwest Montana

Jeffery Robert Stone
University of Nebraska, Lincoln

Southern Oscillation Index ratios compared with normalized precipitation and temperature values for the winter season in northwestern Montana suggest that the Southern Oscillation may produce cooler, wetter winters during strong La Niña years and warmer, drier winters during El Niño years. Analyses of historical strong ENSO events during the winter season at the weather station in Kalispell, MT show that this teleconnectivity exists, regardless of drought or extremely moist conditions.

Little correlation appears to exist between drought and Southern Oscillation variability in the region. The recurrence of drought suggests that it is part of the climate variability and could have some predictable climatic controls. A comparison of Palmer Drought Severity Index (PDSI) for northwestern Montana and Pacific Decadal Oscillation (PDO) curves over the past century show a very strong correlation between warm water storage in the Pacific Ocean and drought conditions in northwestern Montana; cool water storage in the Pacific Ocean is likewise correlated to moist conditions in the same region.

Three small closed-basin lakes near the region of Kalispell, Montana, are currently being analyzed for long-term trends in climate variability using diatom, pollen, geochemistry, and other proxy. Preliminary results indicate that drought within the region may have had a direct impact on the climatic history of the lake systems and water budget in the past century. Lake sediments from this region may provide valuable insight into the impact of climate variability on local and regional scales over the past 6,000 years.

What Controls the Marine Record of Climate Variability?

Lowell Stott
Dept. of Earth Sciences, University of Southern California, Los Angeles

Prior to the Holocene, the Earth experienced rapid transitions between interstadial and stadial conditions. The mechanisms driving the rapid climate transitions are unknown, raising concerns about our ability to predict future climate variability. The jumps between cold stadials and warmer interstadial climates were rapid, ranging from several decades to several years. These abrupt climate changes have now been shown to have occurred over broad areas of the earth including the tropical Pacific warm pool. In an effort to understand the cause of these climate alternations a number of hypotheses are being considered, including tropical ocean-atmosphere interactions (Cane, 1998), ice sheet dynamics (van Kreveld and others 2000), and thermohaline circulation changes (Broecker 2000; Zheng and others 2000). However, perhaps none of the hypotheses are as controversial as that recently presented by Kennett and others (2000). Kennett and others have proposed that episodic releases of methane to the atmosphere from dissociated sedimentary gas hydrates triggered

interstadial warmings. They cite as evidence negative carbon isotope excursions in benthic foraminifera from the Santa Barbara Basin at precisely the same times as the interstadial/stadial transitions. In their hypothesis, changes in the temperature of upper Pacific Intermediate Water (PIW) caused clathrates to melt, releasing methane gas to the atmosphere (Kennett and others 2000b; Hendy and Kennett, submitted). The ice core records from Greenland do record higher methane concentrations during the warmer stadials but the conventional interpretation of these records attributes increased atmospheric methane to enhanced methanogenesis in tropical wetlands.

The Kennett (2000) hypothesis is highly controversial for several reasons: (1) Severinghaus and others (1998) and Severinghaus and Brook (1999) have estimated that the rise in atmospheric methane was synchronous or lagged behind the warmings, (2) methane has a short residence time in the atmosphere, (3) its contribution to radiative forcing is small compared to other greenhouse gases and extensive positive feedbacks would have to be invoked. Nevertheless, there is no question that the $\delta^{13}\text{C}$ record from Santa Barbara Basin exhibits distinct brief excursions as well as millennial-scale oscillations associated with stadial-interstadial changes.

We present an alternative interpretation of the Santa Barbara basin isotopic record that is based on our studies of modern environmental variability and modern biogeochemistry. We present evidence that the Santa Barbara Basin benthic $\delta^{13}\text{C}$ record does not reflect millennial-scale variations in the flux of methane from sedimentary gas hydrates but rather changes in upwelling and productivity that resulted from variations in the rain of organic matter and carbon oxidation within the basin (Stott and others 2000b). We believe that the Pleistocene events documented by Kennett and others (2000) are the manifestation of the same decadal to centennial length patterns of changing upwelling and productivity documented in the North Pacific for the latest Holocene.

Reconstructing Pacific Northwest Climate Using Growth Increments in the Shells of Geoduck Clams (*Panope abrupta*)

Are Strom¹, Peter Hagen², and Robert C. Francis¹

¹School of Aquatic and Fishery Sciences, University of Washington, Seattle

²Alaska Dept. of Fish and Game, Juneau

Geoducks are the largest burrowing clams in the world. They are native to coastal and estuarine waters ranging from California to Alaska, and are among the longest-lived bivalves known. Life spans of up to 146 years have been reported. Internal growth rings in geoduck shells are deposited annually, and shell accretion in samples obtained from several sites in the Straits of Juan de Fuca and SE Alaska appears to be limited by water temperatures. We are measuring growth increment widths present in thin-sections extracted from the hinge area of the shells. Images of the growth rings are being obtained using a combination of scanning electron and light microscopy. A growth chronology has been constructed for the Straits of Juan de Fuca sites spanning the last 160 years, and chronologies from both the Washington and SE Alaska sites indicate a strong relationship between geoduck growth and 20th century temperature records. While the present chronology is constructed entirely from the shells of recently living clams, much older shell material can be obtained from a variety of sources and could potentially be used to reconstruct ocean temperatures over several centuries.

The Tree-Ring Record of Early Summer Precipitation Over Mexico

M. D. Therrell¹, D. W. Stahle¹, M. K. Cleaveland¹, J. Villanueva-Diaz, and D. M. Meko³

¹Tree-Ring Laboratory, Dept. of Geosciences, University of Arkansas, Fayetteville

²INIFAP, San Luis Potosi, Mexico

³Laboratory of Tree-Ring Research, University of Arizona, Tucson

Eighteen new tree-ring chronologies of Douglas-fir latewood width and Montezuma baldcypress total ring width have been developed in Mexico and southwestern Texas (*Pseudotsuga menziesii* and *Taxodium mucronatum*, respectively). These chronologies cover the Sierra Madre Oriental, Sierra Madre Occidental, Sierra Madre del Sur, and extend as far south as Oaxaca (16°N). Most of these chronologies are not highly correlated with total summer precipitation (JAS), but all are significantly correlated with late spring-early summer precipitation and appear to reflect anomalies in the onset of the summer Monsoon. We used the 18 normalized tree-ring chronologies for a preliminary investigation of spatial-temporal anomalies in tree growth linked to early summer precipitation across Mexico. We find that the decade-scale droughts of the 1860s, 1890s, and 1950s were the most severe and prolonged droughts to impact early summer precipitation over Mexico in the past 230 years. These droughts appear to have been more severe across northwestern Mexico, in the region of the North American Monsoon System. We also note a tendency for early summer drought and wetness regimes to occur out-of-phase between northern and southern Mexico.

The North American Monsoon in West-Central Mexico

Rebecca J. Van Lieshout and Franco Biondi

Dept. of Geography, University of Nevada, Reno

The North American Monsoon is an annual weather phenomenon whose onset migrates north from Central America or southern Mexico across the Sierra Madre Occidental and into the Southwestern United States. In central and western Mexico it is characterized by a heavy rainy season beginning between May and July and lasting as long as November. The start and end date of the monsoon and proportion of rain that falls during the season are all analyzed for spatial and temporal trends and correlations to tree growth. The proportion of annual rainfall that comes within the monsoon season shows a correlation to the Nevado de Colima tree-ring chronology. The strength of the correlation changes over time, becoming stronger during the most recent twenty years.

Full Glacial to Recent Vegetation in the Klamath Mountains: Preliminary Pollen Record from Twin Lake, Humboldt County, California

Jim Wanket, Dept. of Geography, University of California, Berkeley, California

Relatively few continuous records of full glacial to recent local vegetation changes exist for California due to a lack of non-glacial depositional sites. A 7.5-meter long core from Twin Lake, a slump basin at 1200 meters elevation in the Klamath Mountains, yielded a basal radiocarbon age of $45,300 \pm 2400$ years. A preliminary coarse-resolution analysis of sedimentary pollen indicates a dramatic shift in vegetation occurred at the Pleistocene/Holocene transition, characterized by the replacement of subalpine forest species by temperate taxa. During the Pleistocene, the site was within an open-canopy forest dominated by *Tsuga mertensiana*. In the latter part of the Pleistocene, *T. heterophylla* and *Picea* were important forest constituents along with *T. mertensiana*. The early Holocene is marked by the replacement of the montane taxa by a closed-canopy forest of *Pinus*, Cupressaceae, and *Pseudotsuga*. The late Holocene has seen the increasing importance of *Pseudotsuga* and the arrival of *Lithocarpus/Chrysolepis* at Twin Lake. It is clear that glacial/interglacial vegetation and climatic changes are evident, and a higher-resolution study will likely yield an important century- to millennial-scale record of vegetation and climate since the full glacial.

Tree-Ring Records of Precipitation Variability in the Southern Canadian Cordillera

Emma Watson and Brian H. Luckman
Dept. of Geography, University of Western Ontario, London, Ontario, Canada

Fifty-three ring-width chronologies have been developed from open-grown, low-elevation stands of *Pseudotsuga menziesii* (Douglas fir) and *Pinus ponderosa* (Ponderosa pine) in the southern Canadian Cordillera. The sites are unevenly distributed across the interior valleys from east of the Coast Ranges to the eastern flanks of the Canadian Rockies and from the Canada-U.S. border to the northern limits of both species (54° N for Douglas fir). The chronologies range in length from 123-691 years (mean = 383 years) and, on average, have a strong within-chronology common signal (68% of the chronologies have an EPS > 0.85 with < 9 trees). Reconstructions of annual precipitation (p[July-June] or p[August-July]) were previously developed for 6 sites explaining 35-60% of the variability in the instrumental record used for calibration (Watson 1998). Climate calibration with precipitation and PSDI data is currently in progress for the remainder of the sites.

Rotated Principal Components Analysis (RPCA) from the 53 chronology network identifies three regions within which annual ring-width chronologies covary similarly. A preliminary assessment of regional chronologies and patterns of extreme narrow and wide marker rings suggest distinctive regional patterns of growth on both interannual and longer timescales that vary through time and are possibly linked to persistent larger scale climatic anomalies. When complete, these proxy precipitation and/or PSDI records will provide important information on the magnitude and duration of drought

at individual locations and across the southern Cordillera. They will also contribute to larger scale studies of the spatial extent and evolution of historical dry and wet events across North America. Precipitation patterns associated with large-scale circulation anomalies in southwestern Canada are typically out-of-phase with those in the southwestern United States and southern Alaska. Therefore records from the southern Canadian Cordillera will enhance the study of the pre-instrumental variability of large-scale climatic phenomenon in the northeast Pacific and may afford some insight into the historical behaviour of synoptic and larger scale phenomena operating at decadal timescales. Locally these precipitation records also complement the extensive collection of proxy temperature data that exists from treeline sites in this region. In combination these records will provide a more complete picture of the large-scale atmospheric and oceanic phenomena which influence precipitation and temperature patterns in the region and improve studies of phenomena which are controlled by both precipitation and temperature (e.g., glacier mass balance).

The Holocene History of Fire in the Pacific Northwest and Its Climatic Controls

Cathy Whitlock and Patrick J. Bartlein
Dept. of Geography, University of Oregon, Eugene

The incidence of fire is closely linked to variations and interactions among weather, climate, and vegetation conditions. However, the nature of climate-fire-vegetation linkages on different time scales and the mechanisms involved in linking climate variations and specific fire-weather conditions are poorly understood in many regions. Information on past fire frequency, severity, and area has become particularly important in light of both recent large fires in the western U.S. and climate model projections that suggest more frequent fires in the future. Knowledge of fire history comes from two sources: dendrochronological and historical data that span the last few centuries, and longer records based on charcoal and pollen data. Tree-ring records have high spatial and temporal resolution, but they are limited to the age of living trees and reconstruct fires that are generally non-lethal. Charcoal records, although of coarser resolution, disclose the frequency of stand-replacing fires and cover time spans of millennia. In the last decade, considerable effort has been made to develop decadal-resolution Holocene fire chronologies in the Pacific Northwest, northern California, northern Rockies and Yellowstone National Park, based on charcoal evidence. These records suggest that the early Holocene featured more-frequent fires than at present, except in regions under the influence of the stronger-than-present summer monsoons. The early-Holocene fire activity is attributed to the higher-than-present summer insolation which had a direct effect on surface energy- and water-balance components and hence on fuel moisture, and an indirect effect on atmospheric circulation resulting in a strengthened northeastern Pacific subtropical high-pressure system. Modern fire regimes were established in only the last 3000 years, but several records show a brief period of higher-than-present fire occurrence ca. 1000 years ago.

An examination of the large-scale controls on recent fire-climate variations offers plausible explanations for variations in the incidence of fire throughout the Holocene. During recent years of large fires in the PNW, for example, the normal zonal flow at 500mb over the eastern Pacific during the fire season is replaced by an upper-level ridge with an axis trending along 140W, while the ridge over the western states becomes weaker than normal. The attendant surface climate anomalies

produce lower-than-normal Palmer drought-severity indices. Similar circulation anomalies are apparent in climate-model simulations for the early Holocene, when fires were more frequent, suggesting that the specific patterns that promote fire (or that control fire climate) have remained similar, despite the change in the controls of large-scale circulation over time.

Spatial and Temporal Variations in Regional Rainfall Patterns in the San Francisco Bay Region

Raymond C. Wilson
U. S. Geological Survey, Menlo Park, California

In the San Francisco Bay region (SFBR) of California, spatial variations in rainfall largely reflect the interaction of North Pacific winter cyclones with the local topography—a series of long ridges, roughly normal to the storm track. On windward slopes, orographic lifting of the air mass produces a consistent, proportional, increase in the amount of rainfall, but no change in storm frequency. Upland stations report up to 50 inches of mean annual precipitation (MAP), compared to 20 inches at coastal stations. On the lee side, a rain shadow produces a constant decrement in storm rainfall amounts, with a consequent decrease in storm frequency. Stations in the lee of the ridges average as few as 65 rain-days/year, compared to 86 rain-days/year at the coast.

Similar effects may be seen in the temporal variations in SFBR rainfall. Wet years may have seasonal totals of up to 2.5 times the long-term MAP; dry years, totals of less than half the MAP. Yet, not all wet seasons, nor all dry, follow the same pattern. Some seasons have more (or less) frequent rainfall, but the size distribution of individual storms are close to the long-term average. Wet years with frequent rainfall include the El Niño seasons of 1983 and 1998; dry seasons with less frequent rainfall include 1959 and 1977. In other years, the rainfall frequency is close to the long-term normal, but with a higher proportion of large storms (e.g. 1862, 1982, and 1997) producing wet years, or a shift towards smaller storms producing dry years (e.g. 1972 and 1976).

While the causes of the inter-annual variations are less obvious than the spatial variations caused by topography, the inter-annual variations exhibit similar patterns, reflecting either a constant decrement (or increment), changing the rainfall frequency, or a consistent, proportional increase (or decrease), shifting the size distribution of individual storms. Inter-annual variations in the size and position of the perennial ridge of high barometric pressure in the northeast Pacific may account for most of the changes in rainfall frequency, but the causes of shifts in the size distribution of storms are more perplexing. Improving our understanding of both the spatial and temporal variations could improve our skill in forecasting (or at least hind-casting) floods and droughts, as well as improve our management of water resources.

Patterns of Temperature Variability for Western North America Over the Last 700–1000 Years

Connie A. Woodhouse¹, Peter M. Brown², Malcolm K. Hughes³, and Matthew W. Salzer³

¹NOAA Paleoclimatology Program, NGDC, Boulder, Colorado

²Rocky Mountain Tree-Ring Research, Ft. Collins, Colorado

³Laboratory of Tree-Ring Research, University of Arizona, Tucson

A set of new tree-ring chronologies enlarges a network of long (700-1000+ years), temperature-sensitive tree-ring chronologies in western North America. The new chronologies, from Colorado, Wyoming, Montana, and Idaho, fill a spatial gap between chronologies from the Great Basin and Sierra Nevada, and the Canadian Rockies. The goal of this expanded network is to provide a more complete understanding of spatial patterns of temperature variability over the past millennium. The new chronologies, from four sites and two species (*Larix lyalli* and *Picea engelmannii*), have been derived from ring width and density measurements. Climate/growth analyses indicate significant relationships between maximum latewood density and summer temperature, and ring widths and winter/spring temperature. Ring width series from several chronologies also correlate with the Pacific Decadal Oscillation (PDO).

In this study, we examine the relationships between these new chronologies and temperature reconstructions or temperature-sensitive chronologies from the Canadian Rockies, the Great Basin, and northern Arizona. A comparison of these records reveals several time periods characterized by widespread low growth/cool temperatures across the region, which may be related to strong or multiple volcanic eruptions. A principal components analysis (PCA) on 100-year periods, overlapped by 50 years, was used to investigate time periods when subsets of the chronologies exhibit similar low frequency variations. The results of the PCA suggest that there have been shifts in large scale summer temperature patterns over the past 700 years. During some periods, the chronology groupings suggest an east/west split, while others are characterized by a northeast/southwest split. A reconstructed record of PDO is investigated for possible links between variations in this circulation index and spatial patterns of temperature across western North America.

Possible Feedback Chain for Enhancing the Effects of Solar Variability on ENSO–PDO

Allen Hunt, Pacific Northwest National Laboratory, Richland, Washington

It can be shown that on time scales of up to a few years ENSO tends to enhance global temperature fluctuations, but on longer time scales the role of ENSO is to try to reverse such fluctuations. Consequently, persistent temperature rises, which are accompanied by more frequent El Niño events, are causing the more frequent events, rather than the other way around. On the other hand, it is possible for extratropical Pacific temperature variability to play a role of a positive feedback in El Niño occurrence frequency by increasing the occurrence of northwesterly winds in the northwestern Pacific and southwesterly winds in the northeastern Pacific. Such winds also reduce coastal upwelling,

particularly on the eastern margin. Given these results, plus the fact that the power spectrum of such extratropical Pacific SSTs is enhanced at 11 and 22 years, as well as the result that strong El Niño events over the last 400 years apparently occur more often at Gleissberg solar maxima, it is tempting to construct a hypothesis of how the Pacific Ocean can act as a feedback mechanism for effects of solar variability on climate. The mechanism is proposed to be related to a mismatch of time scales of adjustment to solar variability, with the tropical Pacific responding first, and the extratropical Pacific only later. The initial result of an increase in solar output should be an increase in the frequency of El Niños, with reduced upwelling, and a positive feedback through the extratropical wind anomalies. As a consequence of the reduced upwelling, the heat content of the upper layer should slowly increase. As the solar cycle approaches its maximum, then it should be expected that the chances of generation of a strong El Niño should be increased. Such a picture may help explain the modulation of upper layer heat content, and SSTs in phase with the solar cycle observed by White and others.

Western Weather and Climate Since PACLIM 2000

Kelly Redmond, Western Regional Climate Center, Desert Research Institute, Reno Nevada

For a third consecutive year, La Niña expressed its reluctance to exit the Pacific stage. After a very dry winter 1999-2000, the Southwest monsoon made its earliest appearance in history. Expectations of a wetter than usual summer there were not to be fulfilled, as most of the region received less than usual rainfall. Wholly unexpectedly, however, a portion of the Southwest experienced an extremely wet October, with some places receiving 50% more than any other month in history from a decidedly winterlike pattern. The November-December combination which followed was among the coldest ever in much of the eastern two-thirds of the U.S. Seemingly aligned with a near-zero Southern Oscillation Index, La Niña feigned an early autumn departure and then resumed at moderate strength. The ensuing winter precipitation distribution was just the opposite of the canonical La Niña pattern the West had become conditioned to. The Southwest received somewhat below to somewhat above average precipitation, while storms employed a variety of mechanisms to avoid the Pacific Northwest. By mid-March, the resulting deficit centered on the Columbia Basin was close to the lowest year on record, not even reaching the memorable 1976-77 winter above Grand Coulee Dam. A similar dry start in the Sierra was overcome to some extent by generous snows in February (120%), as splitting storms dived southward along the coastline, and lingered over the south coast.

Most unfortunately, a combination of additional circumstances produced huge increases in electricity prices in California. Hydroelectric producers in the Pacific Northwest were forced to sell power at a time when they most wanted to conserve their dwindling supply. This spectacular display of the importance of timing will continue to be played out all summer as salmon, hydropower, air quality, and other factors exert wildly different forces destined to test the resourcefulness of the most skilled resource managers up and down the West Coast. After one of the most active fire seasons in decades, the Pacific Northwest is gearing up for another potentially active summer. A small silver lining in the dry conditions could be found in the lessened liquefaction and landslides during a major earthquake near Olympia on February 28. Far to the north, a deeper Aleutian Low helped propel Cold Bay to an astounding 84 inches of rain during Calendar 2000, nearly 59% above any previous year. The warm air pumped northward into Alaska kept conditions very mild during the heart of winter all the way to the Arctic Ocean shoreline.

Appendix A: Agenda

Eighteenth Annual PACLIM Workshop
Asilomar Conference Grounds
Pacific Grove, California
March 18–21, 2001

PACLIM is a multidisciplinary workshop broadly focused on climate phenomena occurring in the eastern Pacific and western America. Its purpose is to understand climate effects in this region by bringing together specialists from diverse fields, including both physical and biological sciences. Time scales range from weather to paleoclimate.

Our theme sessions this year are equally diverse and deal with upcoming issues, like climate change, decadal changes in the North Pacific, and paleoclimatic reconstructions in the eastern Pacific and western North America. In addition, the future of the PACLIM Workshop itself will be discussed.

The atmosphere of the Workshop is intentionally informal, and room and board are provided for the participants. The Workshop is organized by a committee of representatives from several organizations, but historically it has been spearheaded by U.S. Geological Survey scientists. Held annually, the Workshop has benefited from funding and other forms of support from several agencies, public and private. This year's PACLIM Workshop is sponsored by:

| | |
|---|-------------------|
| CALFED Bay-Delta Science Program | Samuel N. Luoma |
| U.S. Geological Survey Water Resources Division | Bill Kirby |
| U.S. Geological Survey Geological Research Division | Eliot Spiker |
| NOAA Office of Global Programs | Roger Pulwarty |
| State of California Department of Water Resources | Barbara McDonnell |

Agenda

Sunday Evening, March 18

Current Events and Updates

- | | |
|--------------|--|
| 6:00–7:00 pm | Dinner |
| 7:00–7:30 pm | <i>Overview of Western Climate, Winter 2001</i> Kelly Redmond, Western Regional Climate Center |
| 7:30–8:00 pm | <i>Water Year 2001 in Northern California—Can a Dry Start Be Overcome?</i> Maury Roos, California Department of Water Resources |
| 8:00–8:30 pm | <i>Do Ecosystem Restoration and Water Management Programs Require a Commitment to Science?</i> Sam Luoma, USGS, Menlo Park; CALFED Lead Scientist |
| 8:30–9:00 pm | <i>The Impacts of Current and Past Climate on PG&E's 2001 Hydroelectric Outlook</i> Gary Freeman, PG&E |
| 9:00–9:15 pm | <i>State of the State's Energy Systems</i> Ross Miller, California Energy Commission |
| 9:15 pm on | Socializing |

Decadal to Centennial Variation in the Late Holocene

7:30–8:30 am Breakfast

**Records from the “Golden Triangle”
Moderator, Malcolm Hughes**

8:30–9:00 am *Multidecadal and Multicentennial Droughts Affecting Northern California and Nevada: Implication for the Future of the West*
Larry Benson (USGS, Boulder), M. Kashgarian, S. Lund, and F. Paillet

9:00–9:30 am *Evidence for Marine-Continental Climate Synchronicity in the Late Holocene of the American Southwest*
Doug Kennett (CSU, Long Beach), J. Kennett

9:30–10:00 am *Establishing High-Resolution Holocene Climate Records in the Sierra Nevada, California*
Douglas Clark, Western Washington University

10:00–10:30 am Break

10:30–11:00 am *Multi-Decadal Variability of Precipitation in the Greater Yellowstone Region as Inferred from Tree Rings*
Lisa Graumlich (Montana State University), J. Littel

11:00–11:30 am *Patterns of Temperature Variability for Western North America Over the Last 700–1000 Years*
Connie Woodhouse (NGDC, Boulder), P. Brown, M. Hughes, M. Salzer

11:30–12:00 pm *Integrating Millennial Tree-Ring Records*
Malcolm Hughes, LTRR, Univ. of Arizona

12:00–1:00 pm Lunch

Monday Afternoon, March 19

Decadal to Centennial Variation in the Late Holocene: Part II

- 1:30–2:00 pm *Response of High-Elevation Conifers in the Sierra Nevada, California, to 20th Century Decadal Climate Variability*
Connie Millar (NFS, Albany, Calif.), L. Graumlich, D. Delany, R. Westfall, J. King
- 2:00–2:30 pm *Decadal Precipitation in Western North America—Revisited*
Dan Cayan (SIO), M. Dettinger
- 2:30–3:00 pm Break

Decadal Teleconnections
Moderator, Robin Webb

- 3:00–3:30 pm *Synoptic Climatology at Decadal and Longer Time Scales: Interpreting Short-Term Processes from a Wide-Angle Lens*
Katie Hirschboeck, LTRR, Univ. of Arizona
- 3:30–4:00 pm *Possible Mechanisms, Tropical Links, and Forcing of Extratropical Pacific Decadal Oscillations*
Dave Pierce, SIO
- 4:00–4:30 pm *Support for Tropically Driven Pacific Decadal Variability Based on Paleoproxy Evidence*
Michael Evans (MIT), M. Cane, D. Schrag, A. Kaplan, B. Linsley, R. Villalba, G. Wellington
- 4:30–5:00 pm *Tropical Forcing of Extratropical Variability on Decadal Timescales*
Matt Newman, CDC
- 5:00–5:30 pm *Correlative Evidence of an Externally Forced Link of Decadal and Centennial Variability in Climate from Ice-Core, Tree-Ring, and Direct Temperature Records*
Charles Keeling (SIO), T. Whorf
- 6:00–7:00 pm Dinner

Monday Evening, March 19

Poster Sessions

- 7:30–9:00 pm Two-minute author's introductions, followed by two hours of gnoshing and poster discussions

Tuesday Morning, March 20

**North American Monsoon Variability
Moderator, Henry Diaz**

- 7:30–8:30 am Breakfast
- 8:30–9:00 am *Teleconnectivity of Monsoon Rainfall in Mexico During Positive and Negative Phases of the Pacific Decadal Oscillation*
Arthur Douglas (Creighton), P. Englehart
- 9:00–9:30 am *Relationship of Gulf of California Moisture Surges to Tropical and Subtropical Weather Features During Summer 2000*
Robert Maddox (Univ. of Arizona), V. Holbrook, L. Farfan
- 9:30–10:00 am *Latewood-Width Variations and Spatial Patterns of Monsoon Precipitation*
Dave Meko (LTRR, Univ. of Arizona), C. Baisan, D. Stahle, M. Cleaveland, M. Therrell
- 10:00–10:30 am Break
- 10:30–11:00 am *Tropical Tree Lines and Tree Rings in the North American Monsoon Region*
Franco Biondi (UNR), R. Van Lieshout
- 11:00–11:30 am *Stable Isotopes, Tree Rings, and the Southwestern Monsoon*
Steve Leavitt (LTRR, Univ. of Arizona), W. Wright, A. Long
- 11:30–12:00 noon *Experimental Seasonal Forecast of Monsoon Precipitation in Arizona*
Andrew Comrie (Univ. of Arizona), T. Cavazos
- 12:00–1:00 pm Lunch

Tuesday Afternoon, March 20

Back to the Holocene

- 1:00–1:30 pm *The Holocene History of Fire in the Pacific Northwest and Its Climatic Controls*
Cathy Whitlock (Univ. of Oregon), P. Bartlein
- 1:30–2:00 pm *Tree-Ring Records of Precipitation Variability in the Southern Canadian Cordillera*
Emma Watson (Univ. of West Ontario), B. Luckman
- 2:00–2:30 pm *Paleoclimatic Evidence for Late Holocene Reorganization of Atmospheric Circulation Patterns in the Western United States*
Mark Lyford (Univ. of Wyoming), S. Jackson, J. Betancourt
- 2:30–3:00 pm Break
- 3:00–3:30 pm *What Controls the Marine Record of Climate Variability?*
Lowell Stott, USC
- 3:30–4:00 pm *Holocene Evolution of the Coastal Upwelling System in the Northern California Region*
John Barron (USGS, Menlo Park), L. Heusser, T. Herbert, M. Lyle
- 4:00–4:30 pm *Major Flood Events of the Past 2000 Years Recorded in Santa Barbara Basin Sediment*
Arndt Schimmelmann (Indiana University), C. Lange
- 4:30–5:00 pm *Holocene Climate Change at Pyramid Lake, Nevada, Reconstructed from Fossil Pollen*
Scott Mensing, UNR
- 5:00–5:30 pm *Statistical Detection of Multiscale Abrupt Changes in Climate*
Frank Schwing (Pacific Fisheries Environmental Laboratory, Pacific Grove), J. Jiang, R. Mendelsson
- 6:00–7:00 pm Dinner

Tuesday Evening, March 20

Surviving this Variable World

- 7:00–7:30 pm *Multimedia Communication of Land and Watershed Management Objectives in the West*
Jack Peterson (DOI)
- 7:30–8:15 pm *Cultural Responses to Climatic Instabilities: Lessons from Prehistoric Native Populations of Coastal California*
Doug Kennett (CSU, Long Beach)

8:15–9:00 pm *Megadrought and Megadeath in 16th Century Mexico*
Dave Stahle (Univ. of Arkansas), R. Acuna-Soto, M. Therrell, M.
Cleaveland

9:00 pm on Additional socializing

Wednesday Morning, March 21

Potpourri of "Modern" Topics

7:30–8:30 am Breakfast

8:30–9:00 am *Intra-Seasonal Variability of North American Climate*
Jacqueline Shinker (Univ. of Oregon), P. Bartlein, P. Killoran

9:00–9:30 am *Teleconnections from Southeast Asia and the Western Tropical Pacific: Their Role in
North Pacific and North American Climate Variations*
Tom Murphree (Naval Postgraduate School), B. Ford, F. Schwing, P.
Green

9:30–10:00 am *Possible Feedback Chain for Enhancing the Effects of Solar Variability on ENSO-
PDO*
Allen Hunt, PNNL

10:00–10:30 am Break

9:30–10:00 am *Experimental Seasonal Forecast of Western Wildfire Activity*
Tony Westerling (SIO), D. Cayan, A. Gershunov

9:30–10:00 am *Synoptic Influences on Seasons of Exceptional Winter Precipitation in the Rocky
Mountain Region*
Deborah Luchsinger, Univ. of Denver

9:30–10:00 am *Spatial and Temporal Variations in Regional Rainfall Pattern in the San Francisco
Bay Region*
Ray Wilson, USGS, Menlo Park

12:00 noon Lunch and Exit

Appendix B: Poster Presentations

Climatic Influences on TMDL Measures of Suspended Sediment Loading in Tributaries of Lake Tahoe

Douglas Boyle (Desert Research Institute) and J. Tracy

Differing Effects of Holocene Insolation Change Across a Climatic Boundary in the Northern Rocky Mountains

Andrea Brunelle-Daines (University of Oregon) and Cathy Whitlock

Using Regression and Neural Networks to Reconstruct Cool-Season Precipitation in the Southwestern United States

Tereza Cavazos (CICESE), F. Ni, M. Hushes, G. Funkhouser, and A. Comrie

Use of ENSO Information in Improving Seasonal Water Supply Outlooks

Martyn Clark (CIRES, Boulder), M. Hoerling, K. Wolter, A. Ray, M. Serreze, and G. McCabe

Development of Short-term Streamflow Forecasts for Specific Management Applications: Case Study of Flow Requirements for the Maintenance of Endangered Fish Habitat

Martyn Clark (CIRES, Boulder), L. Hay, G. Leavesley, J. Pitlock, A. Ray, D. Cayan, M. Dettinger, and M. Meyer-Tyree

Vegetation and Climate Change in Central Mexico During the Last 2,000 Years: Implications for Understanding Mesoamerican Prehistory

Maria Elena Conserva (University of California, Berkeley) and R. Byrne

Glacial/Interglacial Contrasts in Productivity and Oxygen Deficiency on the Margins of the Californias

Walt Dean (U.S. Geological Survey, Denver)

Seasonal, Interannual, and Trending Patterns of Global Atmospheric Water-Vapor Transport, 1948–2000

Mike Dettinger (U.S. Geological Survey, La Jolla)

Late Holocene Ocean/Climate History in Alfonso Basin, Gulf of California, Mexico

Robert Douglas (University of Southern California) and D. Gorsline

Tree-Ring Records of Drought and Temperature Spanning the Last 1,000 Years from the Bighorn Basin Region, Wyoming

C. L. Fastie (Middlebury College), S. Gray, J. Betancourt, and S. Jackson

Estimating Basinwide Groundwater Recharge and Runoff Under Varying Climate Regimes in the Desert Southwest

Alan Flint (U.S. Geological Survey, Sacramento) and M. Dettinger

CLIMAS Climate and Fire Management Studies

Gregg Garfin (University of Arizona), B. Woodhouse, and T. Swetnam

Wind Stress Curl and Ocean Conditions in the Northeast Pacific: A Mechanism for Ocean Climate Change

Phaedra Green (PFEL, Pacific Grove), F. Schwing, and T. Murphree

A Process Model of Tree-Ring $\delta^{13}\text{C}$, $\delta^{18}\text{O}$, and δD Applied to 20th Century Ponderosa Pine Growth in Southern Arizona

Debbie Hemming (University of Arizona), H. Fritts, S. Leavitt, W. Wright, A. Shaskin, and A. Long

Holocene Patterns of Climate Change in Coastal Northern California

Linda Heusser (LDGO) and J. Barron

Winter (DJF) 1901–2001 PAPA Trajectory Index Time Series Computed with the OSCURS Model is Updated and Examined for Decadal North-South Oscillation Patterns of Surface Water Drift in the Gulf of Alaska

Jim Ingraham (NOAA Fisheries Science Center, Seattle)

Holocene Climatic Cyclicity: Relation to Southwest Climate and to Longer Climatic Trends

Thor Karlstrom (U.S. Geological Survey)

A Multivariate Drought Index Applied to California

John Keyantash (University of California, Los Angeles) and J. Dracup

Potential Impacts of Climate Change in San Francisco Bay

Noah Knowles (Scripps Institution of Oceanography)

The Influence of Climate on Production in Northern San Francisco Bay Estuary

Peggy Lehman (California Department of Water Resources)

Difference in Climate Between Eastern China and Western Great Basin During the Past 1,000 Years

Dave Meko (University of Arizona), M. Hughes, and G. Funkhouser

The Relationship of California Flooding to ENSO Events

Jan Null (Golden Gate Weather Service)

Siberian Tree Rings Related to Climate and North Pacific Teleconnections

Irina Panyushkina (University of Arizona) and M. Naurzbaev

Possible Effects of Solar Irradiance on El Niño/La Niña
Charles Perry (U.S. Geological Survey, Kansas)

The Modern Distribution of Chironomids (Insecta: Diptera) in Eastern Sierra Nevada, California, Lakes: Potential for Paleoclimatic Reconstruction
David Porinchu (University of California, Los Angeles) and G. MacDonald

A Late Holocene High-Resolution Record on Fire and Drought from Northwestern Montana
Mitchell Power (University of Oregon) and C. Whitlock

Spatial Analysis of Tree-Ring Chronologies from California's Black Oaks
Kelly Redmond (Western Regional Climate Center), D. Stahle, and D. Cayan

Fifteen Centuries of Reconstructed Temperature and Precipitation from Northern Arizona Tree Rings
Matthew Salzer (University of Arizona)

The New Regimes: Fish Stories
Gary Sharp (Center for Climate/Ocean Resources Study)

Climate Solutions for Southern California and Northern Baja California
John Snyder (Kent State University)

A 3000-Year Record of Salinity Variation in a Brackish Marsh at Rush Ranch, Northern San Francisco Bay, California
Scott Starratt (U.S. Geological Survey, Menlo Park)

ENSO, Pacific Decadal Oscillation, and Drought Variability in Northwest Montana
Jeff Stone (University of Nebraska, Lincoln)

Reconstructing Pacific Northwest Climate Using Growth Increments in the Shells of Geoduck Clams (*Panope abrupta*)
Are Strom (University of Washington), P. Hagen, and R. Francis

The Tree-Ring Record of Early Summer Precipitation Over Mexico
M. Therrell (University of Arkansas), D. Stahle, M. Cleaveland, J. Villanueva-Diaz, and D. Meko

The North American Monsoon in West-Central Mexico
Rebecca Van Lieshout (University of Nevada, Reno) and F. Biondi

Full Glacial to Recent Vegetation in the Klamath Mountains: Preliminary Pollen Record from Twin Lake, Humboldt County, California
Jim Wanket (University of California, Berkeley)

Appendix C: Participants

John Barron
U.S. Geological Survey
345 Middlefield Road, MS-910
Menlo Park, CA 94025

Larry Benson
Arid Regions Climate Project
U.S. Geological Survey
3215 Marine Street, Suite E-127
Boulder, CO 80303-1066

Franco Biondi
Dept. of Geography
University of Nevada, MS-154
Reno, NV 89557

Douglas Boyle
Division of Hydrologic Science
Desert Research Institute
2215 Raggio Parkway
Reno, NV 89512

Andrea Brunelle-Daines
Dept. of Geography
University of Oregon
1251 University of Oregon
Eugene, OR 97403

Dan Cayan
Scripps Institution of Oceanography
University of San Diego, Dept. 0224
9500 Gilman Drive
La Jolla, CA 92093

Douglas Clark
Geology Department
Western Washington University
Bellingham, WA 98225-9080

Andrew Comrie
Dept. of Geography
University of Arizona
409 Harvill
Tucson, AZ 85721-0076

Maria Elena Conserva
University of California, Berkeley
501 McCone Hall
Berkeley, CA 94720-4740

Walter Dean
U.S. Geological Survey
Federal Center Box 25046, MS-980
Denver, CO 80225

Michael Dettinger
U.S. Geological Survey
Scripps Institution of Oceanography
9500 Gilman Drive, Dept. 0224
La Jolla, CA 92093

Robert Douglas
Dept. of Earth Sciences
University of Southern California
Los Angeles, CA 90089-0740

Michael Evans
UCAR/HARVARD
Laboratory of Tree-Ring Research
University of Arizona
Tucson, AZ 85721

Gary J. Freeman
Pacific Gas & Electric Company
Room 1308, Mail Code N13C
245 Market Street
San Francisco, CA 94105-1702

Gregg Garfin
CLIMAS/University of Arizona
Institute for the Study of Planet Earth
715 North Park Avenue, 2nd Floor
Tucson, AZ 85721

Lisa Graumlich
Mountain Research Station
Montana State University
P.O. Box 173490
Bozeman, MT 59717-3490

Deborah Hemming
Laboratory of Tree-Ring Research
University of Arizona
105 West Stadium
Tucson, AZ 85721

Linda Heusser
Lamont-Doherty
100 Clinton Road
Tuxedo, NY 10987

Katie Hirschboeck
Laboratory of Tree-Ring Research
University of Arizona
105 West Stadium
Tucson, AZ 85721

Malcolm Hughes
Laboratory of Tree-Ring Research
University of Arizona
105 West Stadium
Tucson, AZ 85721

Allen G. Hunt
Pacific Northwest National Laboratory
MS K9-30, P.O. Box 999
Richland, WA 99352

Jim Ingraham, Jr.
NOAA-NMFS
Alaska Fisheries Science Center
Center Bin C15700
7600 Sand Point Way NE
Seattle, WA 98115-0070

Steve Jackson
University of Wyoming
Laramie, WY 82071

Thor Karlstrom
U.S. Geological Survey
4811 SW Brace Point Drive
Seattle, WA 98136

Charles Keeling
Scripps Institution of Oceanography
University of California, San Diego
1158 Culhara Drive
Del Mar, CA 92014

Douglas Kennett
Dept. of Anthropology
California State University, Long Beach
1250 Bellflower Blvd.
Long Beach, CA 90840-1003

John Keyantas
Dept. of Civil and Environmental
Engineering
University of California, Los Angeles
5731 Boelter Hall
P.O. Box 951593
Los Angeles, CA 90095-1593

Noah Knowles
Scripps Institution of Oceanography
University of San Diego, Dept. 0224
9500 Gilman Drive
La Jolla, CA 92093

Hong-Chun Li
Dept. of Earth Sciences
University of Southern California
3651 Trousdale Parkway
Los Angeles, CA 90089-0740

Steve Leavitt
Laboratory of Tree-Ring Research
University of Arizona
105 West Stadium
Tucson, AZ 85721

Peggy W. Lehman
California Dept. of Water Resources
3251 S Street
Sacramento, CA 95816

Mark Losleben
Mountain Research Station INSTAAR
University of Colorado
818 County Road 116
Nederland, CO 80466

Deborah Luchsinger
Dept. of Geography
University of Denver
2050 E. Iliff Avenue
Denver, CO 80208

Samuel N. Luoma
U.S. Geological Survey/CALFED
345 Middlefield Road, MS-465
Menlo Park, CA 94028

Mark Lyford
Dept. of Botany
University of Wyoming
P.O. Box 3165
Laramie, WY 82071

Greg McCabe
U.S. Geological Survey
Denver Federal Center, MS-412
Denver, CO 80225

Robert Maddox
University of Arizona
520 North Park Avenue, Suite 304
Tucson, AZ 85719

Scott Mensing
Dept. of Geography
University of Nevada
201 Mackay Science Hall
Reno, NV 89557

Dave Meko
Laboratory of Tree-Ring Research
University of Arizona
105 West Stadium
Tucson, AZ 85721

Connie Millar
U.S. Dept of Agriculture Forest Service
PSW Research Station Box 245
Berkeley, CA 94701-0245

Dave Miller
U.S. Geological Survey
345 Middlefield Road, MS-975
Menlo Park, CA 94025

Ross Miller
Electricity Analysis Office, MS-20
Energy Information and Analysis Division
California Energy Commission
Sacramento, CA 95814-5512

Tom Murphree
Navel Post-Graduate School
Monterey, CA 93943-5114

Matthew Newman
NOAA-CIRES
Climate Diagnostic Center
325 Broadway R/CDC
Boulder, CO 80303

Fenbiao Ni
Laboratory of Tree-Ring Research
University of Arizona
105 W. Stadium
Tucson, AZ 85721

Jan Null
San Francisco State University
480 Chardonnay Drive
Fremont, CA 94539

2001 FACLIM Conference Proceedings

Irina Panyushkina
Laboratory of Tree-Ring Research
University of Arizona
105 W. Stadium
Tucson, AZ 85721

Charles Perry
U.S. Geological Survey
Water Resources Division
4821 Quail Crest Place
Lawrence, KS 66049

David Pierce
Climate Research Division
Scripps Institution of Oceanography
9500 Gilman Drive, Dept. 0224
La Jolla, CA 92093-0224

Dave Porinchi
Dept. of Geography
University of California, Los Angeles
1255 Bunche Hall
Los Angeles, CA 90095

Mitchell Power
University of Oregon
230 West D Street
Springfield, OR 97477

Kelly Redmond
Western Regional Climate Center
Desert Research Institute
2215 Raggio Parkway
Reno, NV 89512-1095

Maurice Roos
California Dept. of Water Resources
1305 Lynette Way
Sacramento, CA 95831

Matthew Salzer
Laboratory of Tree-Ring Research
University of Arizona
105 W. Stadium
Tucson, AZ 85721

Frank Schwing
Pacific Fisheries Environmental Lab 1352
Lighthouse Avenue
Pacific Grove, CA 93950

Gary Sharp
Center for Climate/Ocean Resources Study
780 Harrison Road
Salinas, CA 93907

J. J. Shinker
Dept. of Geography
University of Oregon
107 Condon Hall
Eugene, OR 97403-1251

John Snyder
Kent State University
1756 25th Street #3
Cuyahoga Falls, OH 44223-1069

Dave Stahle
Dept. of Geosciences
University of Arkansas
Ozark Hall 113
Fayetteville, AR 72701

Scott Starratt
U.S. Geological Survey
345 Middlefield Road
Menlo Park, CA 94025

Lowell Stott
Dept. of Earth Sciences
University of Southern California
3651 Trousdale Parkway
Los Angeles, CA 90089-0740

Are Strom
University of Washington
Fishery Sciences Building
P.O. Box 355020
Seattle, WA 98195-5020

Matt Therrell
University of Arkansas
Dept. of Geosciences
Ozark Hall 113
Fayetteville, AR 72701

Rebecca Van Lieshout
Dept. of Geography, MS 154
University of Nevada, Reno
Reno, NV 89557-0025

James Wanket
Dept. of Geography
University of California, Berkeley
1108 6th Street
Albany, CA 94710

Emma Watson
Dept. of Geography
University of Western Ontario
131 Howland Avenue
Toronto Ontario, Canada, M5R 3B4

Anthony Westerling
Scripps Institution of Oceanography
Climate Research Division
9500 Gilman Drive
La Jolla, CA 92093-0224

Cathy Whitlock
Dept. of Geography
University of Oregon
Eugene, OR 97403-1251

Ray Wilson
U.S. Geological Survey
345 Middlefield Road
Menlo Park, CA 94025

Connie Woodhouse
NOAA Paleoclimatology
NGDC, 325 Broadway E/GL
Boulder, CO 80305

Printed By
DWR Printing Production
Services

